

Psycho Social Problems of Transgender in Salem District

D. Shanmugam, Research Scholar, Presidency College and

Dr. John Xavier, Associate Professor

sdbsamsonsd1979@gmail.com, xavier710@gmail.com

Abstract

According to Nolle, as per 2006 census, 33.2 percent of the transgender have attempted suicide because of the influence of gender based discrimination and victimization. According to National School Climate Survey, as per 2003 census, 55 percent of the transgender are reported being physically attacked. According to 2001 survey, 74 percent of transgender are reported being sexually harassed at school and 90 percent of transgender are reported feeling unsafe at school because of their gender expression. According to Wilchins, as per 1997 survey, 78 percent of the transgender reported having been verbally harassed and 48 percent reported having been victims of assault, including assault with a weapon, sexual assault or rape. The researcher is motivated to know the Psycho Social Problems of transgender. The above statistics shows the significance and need for under taking a scientific and out life situations of the transgender. The researcher believes that this research will be useful to transgender for their own development. The researcher hopes that this research will be useful to our Indian society to change the attitude toward the transgender. This research will surely inspire all the readers to render their services for the well-being of the neglected and discriminated transgender.

Key Words

Psycho- Social- Problems-Transgender

Introduction

According the Whittles (2000) Transgender is an umbrella term used to describe people whose gender identity (sense of them as male or female) or gender expression differs from that usually associated with their birth sex. Many transgender people live part-time or full-time as members of the other gender. Broadly speaking, anyone whose identity, appearance, or behaviour falls outside of conventional gender norms can be described as transgender. However, not everyone whose appearance or behaviour is gender-atypical will identify as a transgender person.

Transgender are not acknowledged by the relatives and society. The scientist needs to investigation of the family foundation and psycho - social issue of transgender. They include themselves in against social exercises like renting business sex work. They face part of physical just as financial issues throughout their life circle. The scientist needed to consider the Physical Social, Economic and Psychological status of transgender.

As per Indian law; all individuals are equivalent with no segregation dependent on religion, rank and sex, yet in our general public no one is eager to acknowledge transgender.

These individuals face more issues in day today life Transgender are not acknowledged by their relatives, so they don't have any chance to concentrate in a legitimate way. Thusly the analyst needs to contemplate the instructive status of the transgender. Transgender are not acknowledged by the general public; they are being disengaged man from the family so the analyst needs to know the mental issues that by the transgender because of the dismissal and separation of the general public and the relatives.

The specialist needs to recognize what are the desires and needs of transgender from the general public, relatives, and non-government offices and furthermore from the administration area. Through this, the analyst emphatically accepts that he can give the turn of events and government assistance measures for the transgender.

Review of Literature

Definition

Transgender is a term used to depict individuals who may act, feel, think, or appear to be unique from the sexual orientation that they were brought into the world with. The word transgender is utilized to incorporate numerous gatherings of individuals who share one significant "quality" (a method of feeling or acting) however may not be the equivalent in different manners.

Transgender:

An umbrella term for people whose gender identity, expression or behaviour is different from those typically associated with their assigned sex at birth, including but not limited to transgenders, cross-dressers, androgynous people, gender queers, and gender non-conforming people. Transgender is a broad term and is good for non-transgender people to use. "Trans" is shorthand for "transgender."

Transgender Man:

A term for a transgender individual who currently identifies as a man.

Transgender Women :

A term for a transgender individual who currently identifies as a woman.

Gender Identity:

An individual's internal sense of being male, female, or something else. Since gender Identity is internal; one's gender identity is not necessarily visible to others.

The basic quality for transgender individuals is that they call themselves "transgender" and feel that their given sex isn't exactly right. Once in a while "transgender" is additionally utilized by individuals who favor it to "transgender" (McMullen. M ,1995).

A transgender is an individual who has the inward and outer real highlights of one sex. Yet, has the evident conviction that the individual in question has a place with the other gender. For the most part, along with this conviction there is available a powerful urge to change their physical appearance so it adjusts to that of the ideal sex.

Transgender is much of the time used to depict a wide scope of characters and encounters that fall outside of the conventional comprehension of sexual orientation. Consequently, notwithstanding those individuals who wish to progress starting with one sexual orientation then onto the next or have done as such (who are frequently depicted by the clinical term "transgender"), transgender regularly is intended to envelop an enormous network that incorporates, for instance, drag queens and intersex people. Some transgender want to portray themselves as sexual orientation variation or sex nonconforming. (Francis, 2006)

Transgender incorporates both (MTF) Male to Female and (FTM) Female to Male. They are likewise some of the time alluded to as Trans, or Tranny or trannies. Transgender or TG is the right term. The others are unfavorable. More up to date phrasing replaces these terms with "Transwoman" or "Transman". Transgender individuals distinguish as an individual from the sex inverse to that allocated during childbirth, and want to live and be acknowledged all things considered.

Transgender individuals may go through sexual orientation change, the way toward adjusting one's sex articulation or introduction with their inward sex character. Individuals who have progressed could conceivably essentially distinguish as transgender or transgender any more, yet just as a man or a lady. The individuals who keep recognizing as transgender men or ladies might not have any desire to overlook their pre-progress life, and may proceed with solid binds with other Tran's kin and raising social cognizance.

The cycle of change may include some sort of clinical sexual orientation reassignment treatment and frequently (however not generally) incorporates hormone substitution treatment as well as sex reassignment medical procedure. References to "pre-usable", "post-employable" and "non-usable" transgender individuals show whether they have had, or are intending to have intercourse reassignment medical procedure, albeit some trans individuals

reject these terms as generalizing trans individuals dependent on their careful status and not their psychological sexual orientation character.

Transgender individuals are called Hijras in India and are frequently oppressed in occupations constraining them to depend on asking and prostitution. They meet in Koovagam, a town in the Ulundurpet taluk in Villupuram region, Tamil Nadu in the Tamil month of Chitrai (April/May) for a yearly celebration which happens for fifteen days.

Tamil Nadu has an expected populace of 30,000 transgender individuals. It has caused extraordinary steps in attempting to incorporate transgender individuals into society. This incorporates government assistance plans started by the Government and acknowledgment of transgender individuals into the traditional press and entertainment world.

Welfare Schemes in Tamilnadu

In a pioneering effort to solve the problems faced by transgender people, the government of Tamil Nadu (a state in South India) established a transgender welfare board in April 2008. Social welfare minister will serve as the president of the board. This effort is touted to be the first in India and even in the world. The government has also started issuing separate food ration cards for transgender people. In additional effort to improve the education of transgender people, Tamil Nadu government also issued an order on May 2008 to create a third gender for admissions to government colleges.

Research Methodology

Field of the Study and Selection of Sample

The study was conducted in Salem District. Salem is been surrounded by several small Taluk. The major occupation of the people is Business. Most of them are Professionals. There are nearly 350 transgenders in Salem District. All were from different areas. They have different type of problems. The researcher tries to analyse the physical and psycho social problems of the transgenders in Salem district. The researcher used descriptive design for this study. This design helps to describe the socio economic condition and also various problems of the transgender.

The researcher used non-probability sampling for this study. Because population of the research was unknown. The researcher used snow - ball sampling method,

to select 50 samples from Salem. The snow ball sampling is the method where one respondent refer another respondents.

Objectives of the study

- 1) To assess the physical problems of the transgender.
- 2) To point out the social and economic status as well as the problems of the transgender.
- 3) To examine the marital status and their internal feelings of the transgender.
- 4) To suggest the better government schemes for their wellbeing.

Working Definition

Transgender

A person who may like to act, feel, think or look different from their own gender they were born with is known as "Transgender". A transgender person is someone whose personal idea of gender does not correlate with his or her assigned gender role.

Gender Identity

An individual's internal sense of being male, female, or something else. Since gender Identity is internal; one's gender identity is not necessarily visible to others.

Psycho-Social

Psycho-Social refers to the aspects such as loneliness, shyness, anger, suicidal tendency, depression, tension, need for love, need for companion etc., experience and need transgender, Socio refers to the acceptance and support experienced from peer, family and society in general

Data Analysis and Intrepretation

Occupation of the Respondent

Table . 1

Occupation	Frequency	Percent
Begging	20	40.0
Commercial Sex Worker	14	28.0
Dancing	6	12.0
Others	10	20.0
Total	50	100.0

The above table shows that two-fifth (40%) of the respondents were begging and above one- fourth (28%) of the respondents were commercial sex workers and one-fifth (20%) of the respondents are doing other.

Respect from Government Officials and other Public Service Offices

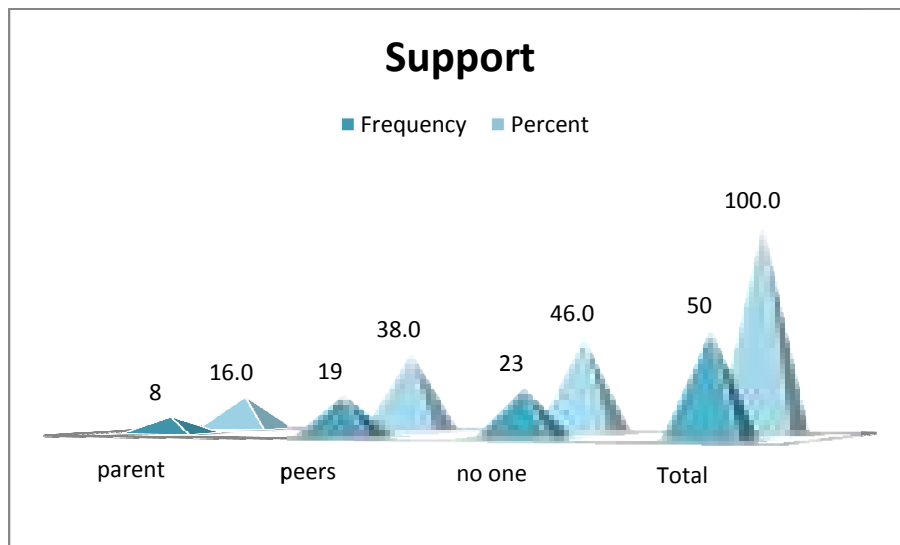
Table . 2

Government sector Treating Badly	Frequency	Percent
Police station	29	58.0
Ration shop	4	8.0
Hospital	17	34.0
Total	50	100.0

The above table shows that little less than three-fifth (58%) of the respondents were badly treated in police station while little above one-third (34%) of the respondents were badly treated in hospitals and below one-tenth (8%) of respondents were treated badly in ration shops.

Moral Support

Figure . 1



The above figure shows that below half (46%) of the respondents were have no one to support while below two-fifth (38%) of the respondents have their peers as their moral support and below one-fifth (16%) of the respondents have parents as their moral support.

Problems during Travel

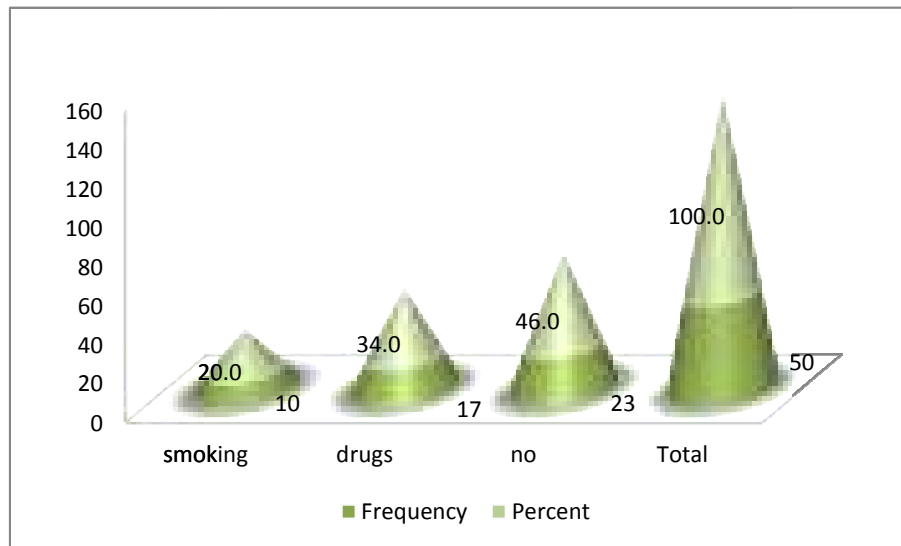
Table. 3

Problems during Travel	Frequency	Percent
Teasing	24	48.0
under estimation	10	20.0
Avoiding	16	32.0
Total	50	100.0

The above table shows that below half (48%) of the respondents were having teasing as the problem while below one-third (32%) of the respondents has avoiding as the problem.

Addiction to Habits

Figure. 2



The above figure shows that below half (46%) of the respondents are not addicted to drugs and above one-third (34%) of the respondents are addicted to drugs and one-fifth (20%) of the respondents have the habit of smoking.

Health Problem

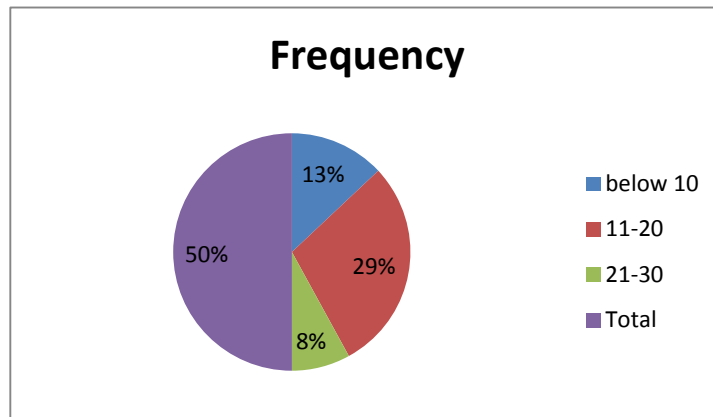
Table. 4

Health Problem	Frequency	Percent
Sugar	36	72.0
STD	14	28.0
Total	50	100.0

The above table shows that below four-fifth (72%) of the respondents have diabetes and above one-fourth (28%) of the respondents have Sexually transmitted diseases.

Age of transformation as Transgender

Figure. 3



The above figure shows that below three-fifth (58%) of the respondents become transgender between 11-20 years while above one-fourth (26%) of the respondents become below 10 years and below one-fifth (16%) of the respondents become transgender between 21-30 years.

Mental Status

Table. 5

Mental Status	Frequency	Percent
fear	19	38.0
anxiety	20	40.0
depressed	11	22.0
Total	50	100.0

The above table shows that two-fifth (40%) of the respondents felt anxiety while below two-fifth (38%) of the respondents felt fear and above one-fifth.

Chi-Square Tests

Age when they become Transgender * Occupation of the Respondent
Table.6

Age of the Respondent when they become Transgender	Occupation of the Respondent				Total
	begging	commercial sex worker	dancing	others	
below 10	0	5	3	5	13
11-20	16	7	2	4	29
21-30	4	2	1	1	8
Total	20	14	6	10	50

Chi-Square Tests

	Value	df	Asymp. Sig. (2-sided)
Pearson Chi-Square	12.717(a)	6	.048
Likelihood Ratio	17.136	6	.009
Linear-by-Linear Association	6.575	1	.010
N of Valid Cases	50		

H0- There is no significant relationship between age and occupation done by the transgender

H1- There is significant relationship between age and occupation done by the transgender

The above table shows that there is significant relationship between age and occupation done by the transgender because the table value is less than 0.05 null hypothesis is rejected. The age is very important to choose the profession.

SUGGESTIONS

Suggestions are proposed when certain action are need to change for betterment. The researcher believes that the following suggestions would enhance the development on the life of the transgender.

- ❖ The researcher found out that there were very few who finished degree. The government should provide special care in educating the transgender.
- ❖ Many of them do not have own house and they are living together in the house. Government should provide house for transgender for that the new schemes can be organized.
- ❖ The transgender do not have ration card and so they do not get any facility from the ration like, sugar, wheat, etc., therefore government should provide ration card for them and so they can get the benefits.
- ❖ Transgender do not have the voter identify card, which is very essential for any citizen who live in India. The government should give voter identify card.
- ❖ When the transgender go to any place, the people in the society are not respecting and they are ill-treated. The government should give awareness program to the people in the society.
- ❖ Transgender cannot fulfil the basic needs of day today life and if they go anywhere and they do not get any job at places. So, the NGO and Government have to come forward to give them training in skill development and so to leave prostitution.
- ❖ Transgender are not only treated very badly among the people but also treated very badly by the police. The police to treat them politely and give protection and security to those people.
- ❖ The government should have to give training program which are skill in making pickle, basket, embroiding, candle, mat, chalk, masala items etc.
- ❖ Transgender do not have the habit of saving habit in their old age there will not be many problems. For that government and NGO con motivate them to SHG and save money.
- ❖ Transgender even do not have facility for going to hospital. Government and private medical officer should not discriminate them instead the government should provide special medical officer and separate outpatient ward and inpatient ward for the transgender.
- ❖ Government and NGO should come forward to provide job facility and house facility and rehabilitation facility for them.
- ❖ Government and NGO's have to give sex education and adult education it may reduce third gender ratio.
- ❖ Third gender family members are to be consoled to realize these problems. So the government and NGOs give awareness for the society especially to third gender family members.

- ❖ Awareness towards defects of alcohol and other toxic substance must be provided by the Ngo and government.
- ❖ Government has to create separate laws and rights for transgender. Government should be taken Act of third gender leasing should have the implication of Eve teasing Act.
- ❖ Social relationship and social acceptance are to be improved by awareness about transgender.
- ❖ Government has advertise them in good manner, so as to get social relationship with others.
- ❖ Government and NGO should be given awareness and gender identify problem to public between 14 to 25 age group.
- ❖ Transgender do not like them because of the society. And for that government and NGO should provide psychological treatment and counselling and also they should be given sex education to teenagers. It may reduce transgender.
- ❖ Before going for castration, professional medical officers had to obtain consent from the particular Psychiatrist due to legal formalities.

CONCLUSIONS

God has created everyone equally, God wants that all are respected and treated equally with love, sympathy and kindness. If some are born or choose to be eunuchs, it is because they are made that way. It is in their biological system and nature.

The study was very helpful to the researcher to teach a lot about 'less know people' viz. the transgenders, it was also interesting to know of their life style and lives. It was difficult to collect the data, to establish report with them and to ask them some questions they were feeling shy and reluctant to answer.

Third genders were not given due attention in development plans of the government and development plants of the government and were stigmatized by the general public government and the NGO's have to work hard to liberate the third genders, recognize them legally, treat them with equal respect and provide facilities and opportunities like SHGs, ration cards. Voter identity cards, bank account facility, license, etc., adult education, literacy, night schools, awareness programmes, etc., would go a long way in helping them.

Third gender often faces multiple problems which include psychological, social, medical, and economical problems. Presently more NGOs and community base rehabilitation centre are working to create awareness about STD, HIV, and AIDS among this group but this

alone would not improve the quality of third gender. The psychosocial study of the third gender can only be improved by providing suitable jobs, training, rehabilitation and awareness.

They are in need of love and affection member of the society. But they are also isolated and negated by the society and government. In current situation there is an urgent need to form legislation for the welfare of the third gender. This research has enlightened the researcher on the problems of transgender faced in their families and society in general.

The researcher identified social problems, Economic problems. Psychological problems, educational aspiration and awareness level about transgender. This academic research will be useful and program for the well-being of transgender. The research believes that this research will be useful to those who will do research about transgender. The attitude of people in Indian society will be changed.

Limitations

- Respondents were not fully transparent with the details about occupation, income, savings, health problem and habits of the respondents.
- The research is done for academic purpose so the researcher took only forty seven questions, which may not have included other aspects.
- The respondents were reluctant to provide information to the researcher. They were asking the researcher to what the researcher would provide them or give them for their response.
- The sample size was only fifty and taken only in the Salem Town which cannot be generalized for other transgender in other place.
- The research believes that this research will be useful to those who will do research about transgender in the future.

Acknowledgement

I am indebted to God, and my guide Dr. John Xavier, Co-guide Dr. Francis for their constant support. Special thanks to Salem Thirunangaigal Nala Sangam (STNS) in Kurangusavadi in Salem to allow me to carry out my research.

BIBLIOGRAPHY

1. Bullough V.L. 1976, "Sexual Variance in Society and History", University of Chicago Press.
2. Chinnappa K, 2006 Third Gender Life and Festival of Koothandvar,
3. Galenter. M, Franco H, Kim And Metzgere. J, Third Gender Treatment for the dually diagnosed, New York.
4. Hennifer W. Jay, 1995, Third Gender under sincization in the Non-Longuest dynasties of China, China,
5. Magarasan, 2007, Aravanigal, Published by Thozhamai Veliyeedi, Chennai.
6. Marina Warner, 1996, The Organ Express, New York..
7. Mary M. Anderson, 1990, The Place of Imperical Chinese Cultureal Studies, China.
8. Samunthiram S.U, 2001, The Third Gender 2001 APAC-VHS-CHENNAI
9. Sineha A.P. 1967, Protection among the Third Gender, Eastern Anthropologist, P146.
10. Whittle S, 1994, The Margins Of The City: Gay Mens Urban Lives, Arena Press, Hampshire.
11. Whittle S, McMullen M 1995, The Transvestite, The Transsexual and The Law, Cavendish Publishing, London.
12. Whittle S, More K 1999, Reclaiming Genders: Transsexuals Grammers at the fin desiecle, Cassell Publishing.
13. Whittle S, 2002, Respect And Equality: Transsexual and Transgender Rights, Cavendish Publishing, London.
14. Whittle S, 2002, The Transgender Debate: The Crisis Surrounding Gender Identities, South Street Press.
15. Whittle, S., 2006, A Transgender Studies Reader, Taylor and Francis: Routledge New York and London.
16. Yogesh Shigala Vyas, 1987, The Life Style of the Third Gender, Anmol Publications New Delhi.
17. ZIA Jaffrey, 1990, The tale of the Third Gender of India, an Indian American Women, New York.

Website

1. <http://heartcorps.com/journey/everything/introduction.htm>retrived
2. <http://www.lawywescollective.org/hiv-aids/publications/articles-transgender-law>
3. <http://www.transgenderlaw.org.cases/>
4. <http://www.observer.gurdian.co.uk/>
5. <http://www.thehindu.com/2008/07/18/stories/2008071857850200.htm>
6. [http://www.livemint.com/articles/2007/07/29112654/Tamil-Nadu8217s transgender.html](http://www.livemint.com/articles/2007/07/29112654/Tamil-Nadu8217s%20transgender.html)
7. <http://malikatv.blogspot.com/>
8. <http://www.hinduonnet.com/thehindu/thscrip/rpint.pl?file=2008091852690300.htm&date=2008/09/18/&prd=th&>
9. <http://www.thingasian.com>
10. http://www.members.tripod.com/barry_stone/enuuchs.htm
11. http://transequality.org/Resources/NCTE_Trans_Terminology.pdf

See discussions, stats, and author profiles for this publication at: <https://www.researchgate.net/publication/348606301>

"A STUDY ON PSYCHOSOCIAL PROBLEMS FACED BY THE PARENTS OF CHILDREN WITH MULTIPLE DISABILITIES OF SALEM INSTITUTE OF REHABILITATION CENTER

Article · January 2021

CITATIONS

0

READS

1,018

4 authors, including:



[Shanmugam .D](#)

Sacred Heart College

13 PUBLICATIONS 1 CITATION

[SEE PROFILE](#)



[Robert Ramesh Babu Pushparaj](#)

Central University of Tamil Nadu

38 PUBLICATIONS 32 CITATIONS

[SEE PROFILE](#)

Some of the authors of this publication are also working on these related projects:



ENTREPRENEURIAL ATTITUDE AND LIFE COPING SKILLS OF RURAL WOMEN ENTREPRENEURS OF SELF-HELP GROUPS IN DHARMAPURI DISTRICT OF TAMILNADU, INDIA

[View project](#)



Safety Awareness [View project](#)

“A STUDY ON PSYCHOSOCIAL PROBLEMS FACED BY THE PARENTS OF CHILDREN WITH MULTIPLE DISABILITIES OF SALEM INSTITUTE OF REHABILITATION CENTER, SALEM, TAMILNADU.”

Shanmugam D, **Robert Ramesh Babu. P, ***Dr. John Xavier, **Selvaraj V**

**Research Scholar, Presidency College, Chennai.*

***Research Scholar, Central University of Tamilnadu, Tiruvarur.*

****Associate Professor*

******Research Scholar, University of Madras*

ABSTRACT

Background

The study focuses on psycho-social problems faced by the parents of children with multiple disabilities. The researcher is more interested in analyzing the problems of parents, especially on their personal, financial and social due to the multiple disabilities of their children in order to understand their feelings. The researcher underwent the study among the parents rehabilitation centre in Salem. Through this study, one can understand their own selves, responsibilities, duties, and identifying their actual psychosocial challenges

Aim

The aim of the study is to find out the psycho-social problems faced by the parents of children with multiple disabilities

Research method

This study has used non-experimental descriptive research design in order to recognize the types of problems care homes in Salem District. Primary data was collected from 100 respondents by using a structured questionnaire method administered among the randomly selected 100 Parents who come to the home for the treatment of their children. Hypotheses were tested with the application of descriptive and inferential statistics.

Findings

The overall stress levels of the parents are that High (24%), Average (52%) and low (24%). Most of the respondents have an average level of Stress.

Implications

Results of this study aptly suggests that it is one of good references for carrying out future studies and could be interrelated with other variables, which can be quoted as an apt and right reference to identify the causes of stress and the challenges of the problems they undergo. . This would suggest opt solutions to reduce the stress level and increase the coping mechanism of the parents.

The multiple disability children are the individuals, who have not been presented full participation in usual activities of their age because of the reason of their multiple disabilities. The effect of multiple disabilities can be more than the mixture of two individual disabilities. The multiple disabilities most in child may have a difficulty in learning, along with controlling their movements, hearing and vision. More serious effect on multiple disabilities damaging the confidence and ability to come out of their comfort zone and they are affected with more personal and social life.

Keywords – Psycho social Problems, Parents, Children with multiple disabilities

1. Introduction

It is quite natural that each and every child require assistance from their mothers to complete their day to day tasks especially children with multiple disabilities require even more support, attention and care to complete their daily routine activities; It is true that sometimes they are

completely dependent on their mothers. Either a single disability that creates a scenario like this or at times also multiple disabilities in combination too can create a situation like blindness, deafness, locomotors disability, autism, ADHD etc. Though, the mothers support these children in completing their tasks, also face more problems and challenges every day with lots of difficulties. But they take pains to care for their children to their best.

2. REVIEW OF LITERATURE

2.1 Multiple Disabilities

The combination of several disabilities in children makes them as “Multiple Disabled” personalities. It is not that so easy caring for multiple and severely disabled children and it requires enormous amount of time, patience and love in taking care of these children. An autonomous organization of the Ministry of Social Justice and Empowerment, Government of India, was set up under the “National Trust for the Welfare of Persons with Autism, Cerebral Palsy, Mental Retardation and Multiple Disabilities” (Act 44 of 1999) by understanding the need for advancement of administrations for such children with various incapacities. The concerns of guardians of such children are diminished now with the guide of this National Trust started by the Ministry of Social Justice and Empowerment.

2.1.1 Definition of Multiple Disabilities

As indicated by the demonstration "Different Disabilities" signifies a mix of at least two handicaps as characterized in proviso (1) of section 2 of the Persons with Disabilities (Equal Opportunities, Protection of Rights and Full Participation) Act, 1995 (1 of 1996) Disabilities under the National Trust Act are in fact Developmental Disabilities caused due to insult to the brain and damage to the central nervous system. These disabilities are Autism, Cerebral Palsy, Mental Retardation and Multiple Disabilities.

These kinds of multiple disabilities are not at all diseases nor contagious nor progressive. They are not curable with the help of drugs or even surgery. By early detection and training we can improve the performance of the child. Different approaches are applied to these kind of children using the services of Physic-Therapists, Occupational Therapists, and Speech Therapists, Community Based Rehabilitation Workers and Special Educators. The combination of disabilities and degree of severity may not be common in each child. The ‘age of onset’ is the term used to denote the time at which the disability occurs in the child and this time frame may also range from birth to a few days after birth, from early childhood till late teens.

Sometimes it becomes more pathetic condition when children are born with one disability but they acquire the second or third disabling conditions during childhood by various reasons. The nature of combination of the disabilities, the age of onset and the opportunities that have been available to a child in his environment, defines the characteristics and the needs of the children.

2.1.2 Multiple Disabilities Refers to

Multiple disabilities denotes to a mixture of two or more disabling conditions that have a combined effect on the child’s communication, mobility and performance of daily tasks. We can say that similarly as each child is unique, correspondingly every kid with MD is extraordinary. However there are some commonalities which can be observed in this type of children.

- It affects the holistic development of the child
- Communication with the external world is most severely affected
- Opportunities for interaction with the environment becomes very limited
- Movement of the child in its environment is restricted for lack of ability
- It needs someone to help regularly even in doing simple day-to-day activities like wearing a shirt, opening a door, finding a chair to sit down etc.
- So it requires a highly structured educational / rehabilitation programs to help in their training.
-

2.2 Different Types of Multiple Disabilities

Multiple disabilities in children will have a combination of various disabilities that may include: Speech, physical mobility, learning, mental retardation, visual, hearing, brain injury and possibly other types of disabilities. Sometimes there may be sensory losses and behavior and or social problems which they exhibit along with multiple disabilities. There are many educational implications for these students.

2.2.1 CEREBRAL PALSY (CP)

“Cerebral” denotes brain. “Palsy” is a kind of disorder of movement. This CP refers to a group of non-progressive neuromuscular problems with varying severity. CP is actually a damage to the brain, mainly to the part of the brain that controls motor functions. In such cases when other parts of the brain are also be affected the person is affected with more than one disability. The extent of the damage varies from person to person. For children with mild disability means fine motor skills with 3343`4t34, like using scissors or writing, becomes difficult. Children with severe disability is identified with poor movement of all four limbs, the trunk and neck. The child may even have difficulty in swallowing.

2.2.2 AUTISM

All children with ASD demonstrate deficits in

- 1) Social interaction,
- 2) Verbal and nonverbal Communication, and
- 3) Repetitive behaviors or interests.

In addition to all the above said, they will often have unusual responses to sensory experiences, such as certain sounds or the way objects look. Every one of these side effects runs the array from gentle to extreme. The symptoms will be present differently in each individual child. For instance, a child may have little trouble in learning to read but may exhibit extremely poor in social interaction. Each child will have their own kind of display of communication and social behavioral patterns that are individual but they fit into the overall diagnosis of ASD.

2.2.3 MENTAL RETARDATION

The characteristics of Intellectual disability is both by a score of significantly below-average on a test of Mental ability or intelligence and by showing limited ability to function in areas of day by day life, for example, correspondence, self-care and getting along in social circumstances and school exercises. Scholarly handicap is likewise here and there named as intellectual incapacity or mental hindrance.

Children with intellectual disability can learn new skills and also involve in that, but they develop comparatively slower than children with average intelligence and adaptive skills. The varying degrees of Intellectual disability are from mild to profound. An individual's degree of Intellectual inability can be characterized by their (IQ), or by the sorts and measure of help they need.

2.2.4 LOCOMOTOR DISABILITY

“Locomotors disability” is a kind of disability pertaining to the bones, joints or muscles leading to substantial restriction of the movement of the limbs or any form of cerebral palsy.

2.2.4.1. Spinal cord injuries

Usually, the result of a traumatic blow to the spine causes this type of injury. Some spinal cord injuries can completely heal; others will lead to paralysis.

2.2.4.2.Cerebral palsy

Cerebral palsy is a group of non-progressive conditions involving muscle control, posture and movement caused by brain damage.

2.2.4.3. Polio

Polio is a highly contagious infectious disease caused by poliovirus. It destructs the nervous system and also may cause paralysis.

2.2.4.4. Muscular Dystrophy

It is an inherited group of diseases that affects the muscles by weakening them and breaking them down over time.

2.2.4.5. Contractures

It is a severe and permanent tightening of muscles and joints

2.2.5 HEARING IMPAIRMENT

“Hearing impairment” is identified as the loss of sixty decibels or more as heard in the normal ear in the conversational range of frequencies.

2.2.6 DEAFNESS

A hearing loss greater than 90 dB in Individuals makes them deaf and they will have their vision as their primary input and it is impossible for them to understand speech through the ear. Deafness implies a conference debilitation that is serious to the point that the kid is disabled in preparing phonetic data through hearing, which antagonistically influences instructive execution (idea).

2.3 CHARACTERISTICS OF CHILDREN WITH MULTIPLE DISABILITIES

2.3.1 VISION PROBLEMS

When the children grow, some of them would always squeeze their eyes together when they look at something closely, or keep looking at their moving fingers/paper, bump into things while strolling, whine of an excess of light constantly. Their eyes may likewise appear to be unique from 'ordinary' eyes.

2.3.2 HEARING PROBLEMS

It is possible for a child with a hearing problem to respond to only particular sounds. It requires a long time and repeated training for such children to develop speech and mostly they can only repeat what they hear. They will also learn to adapt to their routine environment by ‘guessing’ the conversations going around, but it makes them actually face a lot of difficulty in new place with unknown people. Sometimes it is also noted that the deaf children also show difficulty in balancing their body or walking in a straight line.

2.3.3. LEARNING PROBLEMS

Since the children have the combined loss of two or more abilities, the rate and speed of learning of the children will always be very slow. For them learning often becomes repetitive and meaningless if not special care is taken to make the child feel safe about exploring the world around him. Multi impaired children likewise have exceptionally restricted plans to play with toys or things around them.

2.3.4 COMMUNICATION

Communication is one of the prominent areas that is most significantly affected in children with multiple disabilities. The children are not able to see or hear or follow the different ways in which their own brother and sister play with each other, how elders are greeted, standing in a queue to get a ticket or even passing a bottle of water around a dining table.

2.3.5. POSTURE AND MOBILITY

Normally for any human being our sight, hearing and body movements help us to move around, without bumping into things, remembering the way to reach places or even to use our own hands to hold and look at things. It becomes difficult for the child to manage his own body movements sometimes, because of Cerebral Palsy, loco motor disabilities and balance difficulties and makes it hard for the child to use his body to move from one place to another.

2.3.6 ODD BEHAVIORS

Different types of strange behaviors are observed in most of the children with multiple disabilities. Such behaviors are called ‘self-stimulating’ behaviors. Some of these behaviors are moving one’s body repeatedly, shaking head side to side, and moving fingers in front of eyes, hitting or slapping the ears, swinging in one place and so on. The children mostly do this since they are not

able to involve in any other task by themselves. Sometimes these kinds of movements or behaviors are important for them to continue doing it from time to time and it helps them get some information about the world around them in their own special way. These children also may show disturbed sleep patterns.

2.3.7 MEDICAL CONDITIONS

To worsen their condition, most of the multi-handicapped children also suffer from other medical conditions such as epilepsy, frequent eye and ear infections, respiratory disorders, muscular degeneration frequent surgeries and so on. Because of such frequent health disorders lead them to frequent hospitalizations and so the child again is deprived a lot of exposure and learning from the environment.

2.3.8 PREVALENCE

While analyzing the percentage of students who have severe multiple disabilities, is very low. It is quite consoling that if we take the statistics approximately 0.1 to 1 percent of the general school-age population and approximately 2 percent of the total population of school age students are affected by severe and multiple disabilities. It is not likely that more than one student with severe multiple disabilities would be enrolled in a general classroom at any given time.

2.4 Scholars view on Multiple Disabilities

Mash and Johnson, (2013) studied the parental perceptions of child behavior, parenting self-esteem and mothers reported stress of younger and older hyperactive and normal children. They took forty families with hyperactive children and fifty one families with normal children for their study. They used the following instruments for data collection and scaling their competence: Hyperactivity rating scale, child behavior checklist, parenting sense of competence scale, and parenting stress index. During their observation, results indicated that parenting self-esteem was much lower in parents of hyperactive children than in parents of normal children. The mothers of especially younger hyperactive children were noted markedly higher level of stress. Similarly backwards connection was found between parental confidence and impression of child problems, while rating of child disturbance and maternal stress were positively correlated.

Waisbren, Rones, Read, Marshal and Long, (2004) took for their study the predictors of parenting stress in parents whose children were diagnosed with a biochemical genetic disorders or through new born screening. The parents of two hundred and sixty three children with biochemical genetic disorders (139 identified by new born screening, 124 identified clinically) completed interviews by focusing on child health, medical services use, satisfaction with service, parenting stress and family functioning. Multiple regression analyses suggested that child adaptive functioning parental satisfaction with support, and difficulties parent experienced meeting their child's health care needs were associated with scores on parenting stress index.

Bailey, Golden, Roberts, and Ford, (2007) examined maternal depression in families having a child with disability. The examination resulted that mothers of children with disabilities generally exhibited a higher than average rate of depressive symptoms and were more at risk for clinical depression treatments. These kinds of depressive symptoms are caused by a complex relations formed by child behavior problems, maternal stress, coping style, and support.

3. Research Methodology

3.1 General Objectives:

- To study the socio-demographic details of the respondents
- To find out the social problems of respondents
- To find out the economic problems of the respondents
- To find out the psychological problems of the respondents

3.2 Hypothesis

- There is difference between the age group, educational groups, salary groups, Religion, occupation, castes, living places, family types, Problems faced, patients history and family history with the over all stress levels of the parents.
- There is association between the age groups, educational groups, salary groups, Religions, occupation, castes, living places, family types, Problems faced, patients history and family history with the over all stress levels of the parents.
- There is relationship between the age groups, educational groups, salary groups, Religions, occupation, castes, living places, family types, Problems faced, patients history and family history with the over- all stress levels of the parents.

3.3 RESEARCH DESIGN:

The researcher has adopted Descriptive research design for this study. This design describes about the psychosocial problems faced by the parents of children with multiple disabilities.

3.4 SAMPLING TECHNIQUE

The sampling technique used in the study is the non- probability sampling .The researcher adopted simple random sampling. The sample size is 100. The study consists of the parents of children with multiple disabilities at Salem rehabilitation centre. The researcher distributed the questioner to the respondent and explained in short, so then the respondents marked based on their problems choices and returned to the researcher.

4. Interpretation, Analysis and Findings

4.1 Demographic Characteristics

The age remains always an important independent variable in determining the characteristics of any social phenomena. According to this study the samples represents Age come under the age groups of : 22% of 20 to 25%, 58% of 26 to 30, 8% of 31 to 40, 10% of 40 to 50 and above and 2% of 51 and above.

Religion – Hindus 34% and Muslims 66%

Salary – Below 5000 40%, 5001 to 10,000 58% and Above 10,000 Rs 2%

Education: Primary 40%, Secondary 28%, Hr.Sec. 12% and Degree and Diploma 4%

Occupation : Home making 90%, Students 2%, Daily wages 2% and Buisness 6%

Living : Panchayat 76%, Corporation 16% and Municipality 8%

Family Type : Nuclear 80%, Joint 16% and Extended 4%

Marriage status: Married 58%, Unmarried 26%, Divorced 8% and Widow 8%

Married Type: Consanguine 32% and Non consanguine 68%

Problems : Economic 56%, Personal conflict 34%, Health 8% and other 2%

Patients history : Yes 82% and No 18%

Family history : Yes 66% and No 34%

Over all Stress :

	Low	Average	High
Stress Level	12 (24%)	26 (52%)	12 (24%)

The overall stress level of the parents is that High (24%), Average (52%) and low (24%). Most of the respondents have an average level of Stress.

S.No	Parental Stress Scale	Low	Percentage	Average	Percentage	High	Percentage
1	Reward	15	30%	26	52%	9	18%

2	Parental stressors	12	24%	28	56%	10	20%
3	Locus of control	23	46%	16	62%	11	22%
4	Parental satisfaction	29	58%	14	28%	7	14%
5	Care	12	24	30	60	8	16
6	Control	18	36	28	56	4	8

The following are the percentage levels of the components which make the parents in stress.

- Reward: 30% low, 52% Average and 18% as high. The level of Parental stressaors: 24% low, 56% average and 20% high. Locus of control : 46% low, 62% average and 22% high. Parental satisfaction : 58% low, 28% average and 14% high. Care : 24% low, 60% average and 16% high. And the control levels are : 36% low, 56% average and 8% high.
- Among them all the level of parental satisfaction is very low. 58% of the parents are not satisfied.

4.2 Annova :

Annova is a test to find the difference between the independent and dependent variables. These following independent variables have significant difference between the different groups of the Independent variables with the over all stress level of the parents.

Religion (0.000**), Education (0.002**), Marriage (0.003**) and Different problems (0.001**) all the independent variables significantly differ among themselves with 1% of difference.

Different occupations (0.020*) and Marriage type (0.020*) have significant difference among themselves with 5% level of difference with over all stress level

The Independent variables such as Salary (0.100), Living places (0.643), Family types (0.256), Patient history (0.728) and Family History (0.431) don't have any significant difference among themselves with the over all stress level.

4.3 Chi square Test.

Chi square is a test to find the association between the independent and dependent variables. These following independent variables have significant association with the over all stress level of the parents.

Religion (0.000**), Education (0.000**) and Different problems (0.002**) all the independent variables have 1% level of association with the over all stress level of the parents..

Marriage status (0.025*) and Marriage type (0.022*) all the independent variables have 5% level of association with the over all stress level of the parents.

The Independent variables such as Age, (.319,) Salary (0.164), Occupation (0.074), Living places (0.764), Family types (0.181), Patient history (0.715) and Family History (0.405) don't have any significant association with the over all stress level.

4.4 Co-relation

Co-relation is a test to find the relationship between the independent and dependent variables. These following independent variables have significant relationship with the over all stress level of the parents.

Marriage status (0.016*) and Living (0.013*), Education (0.038*) and Family history (0.039*) all the independent variables have 5% level of association with the over all stress level of the parents.

The Independent variables such as Age, (.180), Religion (0.148), Salary (0.059), Occupation (0.244), Family types (0.123), Marriage Type (0.241), Patient history (0.179) don't have any significant relationship with the over all stress level.

5. Suggestions

- The Parents undergo an average level of stress while dealing with their children of multiple disabilities.
- Periodical counseling, stress busters, coping mechanisms with meditation and knowledge over the behavior of the disabled children must be conducted.
- Marriages among the same sanguine must be avoided.
- Accidents and ill treatment of the children in the womb must be avoided by the parents and the family members.
- The level of parental satisfaction is very low. Proper sessions must be taken to all the parents how to accept and handle this stressful situations.
- Government assistance and social securities should be created to all these children and the parents.
- Day care centers and assistants to handle the each affected child would lesser the burden of the family members.

6. Conclusion

The result of this study provides some evidence that the parents are facing psychological problems because of having a multiple disabled child. This study suggest that if the organization provides some relaxation classes for the parents who are facing psychological problems it will be helpful for them to develop sound body and mind. The organization should provide some income generating program which will help the parents to cope up with their economic problems, if the organization provides some counselling session for the parents it will encourage them to be strong and to cope with social problems. They need support from various social systems like from their own family, community and government as well. In this field social worker have several important roles to play among the differently abled children as well as their family especially to their care givers. If more people involved in this field for helping affected children, they can bring changes to many lives as well as to many families.

References

1. Abosi O, 2007, 'Educating children with learning disabilities in Africa', *Learning Disabilities Research & Practice* 22(3), 196–201. <https://doi.org/10.1111/j.1540-5826.2007.00242.x>
2. Atkinson D, 2010, 'Narratives of people with disability', in Gordon G., Ramcharan P., Flynn M. & Richardson M. (eds.), *Learning disability: A life cycle approach*, pp. 7–27, Open University Press, London.
3. Bayat M, 2014, 'Understanding views of disability in Cote d'Ivoire', *Disability and Society* 52, 30–43. <https://doi.org/10.1080/09687599.2013.768954>
4. Booyens M., Van Pletzen E. & Lorenzo T, 2015, 'The complexity of rural contexts experienced by community disability workers in three southern African countries', *African Journal of Disability* 4(1), 1–9. <https://doi.org/10.4102/ajod.v4i1.167> [PMC free article] [PubMed]
5. Braun V. & Clarke V, 2006, 'Using thematic analysis in psychology', *Qualitative Research in Psychology* 3, 77–101. <https://doi.org/10.1191/1478088706qp063oa>
6. Burke P, 2008, *Disability and impairment: Working with children and families*, Jessica Kingsley, London.
7. Campbell J. & Oliver M, 1996, *Disability politics: Understanding our past, changing our future*, Routledge, London.
8. Chilwalo B.M, 2010, *A comparative analysis on the psychosocial factors that influence the parenting styles of single mothers among the Damara, Otjiherero and San people in Gobbabis, Omaheke region*, MA dissertation, University of Namibia, Windhoek.
9. Chiwara P, 2015, 'Social work's contribution in promoting social and economic equality. A Namibian case study', MSW Social Development and Policy, University of Pretoria, Pretoria.
10. Cortiella C, 2011, *The state of learning disabilities*, Centre for Learning Disabilities, New York.

11. Creswell J.W, 2007, *Qualitative enquiry and research design: Choosing among five approaches*, Sage, London.
12. Flack P, 2005, 'Towards new understandings of learning disability', *African Education, Review* 2(2), 318–328. <https://doi.org/10.1080/18146620508566308>
13. Fouché C.B. & Schurink W, 2011, 'Qualitative research designs', in De Vos A.S., Strydom H., Fouché C.B. & Delpont C.S.L. (eds.), *Research at grass roots for the social sciences and human science professions*, 4th edn., pp. 307–327, Van Schaik, Pretoria.
14. Freedman R. & Boyer N.C, 2000, 'The power to choose: Supports for families caring for individuals with developmental disabilities', *Health & Social Work* 25, 59–68. <https://doi.org/10.1093/hsw/25.1.59> [PubMed]
15. Gobrial E, 2009, *An exploration of management strategies for anxiety in children and young people with learning disabilities and autism*, University of Northumbria, Newcastle.]
16. Gona J.K., Mung'ala-Odera V., Newton C.R. & Hartley S, 2011, 'Caring for children with disabilities in Kilifi, Kenya: What is the carer's experience?', *Child: Care, Health and Development* 37(2), 175–183. <https://doi.org/10.1111/j.1365-2214.2010.01124.x> [PMC free article] [PubMed]
17. Greeff M, 2011, 'Information collection: Interviewing', in De Vos A.S., Strydom H., Fouché C.B. & Delpont C.S.L., *Research at grass roots for the social sciences and human science professions*, 4th edn., pp. 341–375, Van Schaik, Pretoria.
18. Grobler M.E, 2012, 'A paradigm of Namibian families', paper presented at the National Social Workers' Workshop on Parenting, 21–25 May.
19. Haihambo C. & Lightfoot E, 2010, 'Cultural beliefs regarding people with disabilities in Namibia: Implications for the inclusion of people with disabilities', *International Journal of Special Education* 25(3), 76–87.
20. Hailombe O, 2011, 'Education equity and quality in Namibia: A case study of mobile schools in the Kunene region', DPhil thesis, University of Pretoria, Pretoria.
21. Harper A., Dyches T.T., Harper J., Roper S.O. & South M, 2013, *Respite care, marital quality, and stress in parents of children with autism spectrum disorders*, Springer Science & Business Media, New York. [PubMed]
22. Harries A. & Enfield S, 2003, *Disability, equality & human rights: A training manual for development humanitarian organisations*, Oxfam, London.
23. Jackson K. & Abosi O, 2006, *South of the desert: A teacher's guide to child development in sub-Saharan Africa*, UNISA, Pretoria. [Google Scholar]
24. Kalek D, 2008, *The effectiveness of a family-centered early intervention program for parents of children with developmental delays ages 0 through 3*, Pepperdine University, Malibu, CA. [Google Scholar]
25. Kumar R, 2011, *Research methodology: A step-by-step guide for beginners*, Sage, London.
26. LaFont S. & Hubbard D, 2007, *Unravelling taboos: Gender and sexuality in Namibia*, Gender Research & Advocacy Project, Legal Assistance Centre, Windhoek.
27. Landman L. & Lombard A, 2006, 'Integration of community development and statutory social work services within the developmental approach', *Social Work/Maatskaplike Werk* 42(1), 1–15.
28. Lietz C.A., Langer C.L. & Furman R, 2006, 'Establishing trustworthiness in qualitative research in social work. Implications from a study regarding spirituality', *Qualitative Social Work* 5(4), 441–458. <https://doi.org/10.1177/1473325006070288>
29. Lukemeyer A., Meyers M.K. & Smeeding T, 2000, 'Expensive children in poor families: Out-of-pocket expenditures for the care of disabled and chronically ill children in welfare families', *Journal of Marriage and Family* 62(2), 399–415. <https://doi.org/10.1111/j.1741-3737.2000.00399.x>

WEB ADDRESS

- <https://www.ncbi.nlm.nih.gov/pmc/articles/PMC3999601/>
- <http://www.child-encyclopedia.com/parenting-skills/according-experts/parents-attitudes-and-beliefs-their-impact-childrens-development>
- <http://www.ncbi.nlm.nih.gov/pubmed/11923900>
- <https://www.specialeducationguide.com>

See discussions, stats, and author profiles for this publication at: <https://www.researchgate.net/publication/358346382>

ENTREPRENEURIAL ATTITUDE AND LIFE COPING SKILLS OF RURAL WOMEN ENTREPRENEURS OF SELF HELP GROUPS IN DHARMAPURI DISTRICT OF TAMILNADU, INDIA

Article · August 2021

CITATIONS

0

READS

90

3 authors, including:



[Shanmugam .D](#)

Sacred Heart College

13 PUBLICATIONS 2 CITATIONS

[SEE PROFILE](#)



[Robert Ramesh Babu Pushparaj](#)

Central University of Tamil Nadu

38 PUBLICATIONS 44 CITATIONS

[SEE PROFILE](#)

Some of the authors of this publication are also working on these related projects:



Entrepreneurial attitude and life coping skills of rural women entrepreneurs of self help groups in Dharmapuri district of Tamilnadu, India [View project](#)



Breast Cancer Awareness [View project](#)

ENTREPRENEURIAL ATTITUDE AND LIFE COPING SKILLS OF RURAL WOMEN ENTREPRENEURS OF SELF HELP GROUPS IN DHARMAPURI DISTRICT OF TAMILNADU, INDIA

SHANMUGAM. D, Research Scholar, Presidency College Chennai,
ROBERT RAMESH BABU P, Research Scholar, Central University of Tamilnadu, Tiruvarur,
Dr. JOHN XAVIER Ph.D, Associate Professor.

ABSTRACT

Background

Women self help groups have emerged as one of the greatest phenomena of this century in empowering the rural poor with self dignity and authority over their life situations. However, women entrepreneurs in rural areas undergo several problems due to different role they carry on in their homes as well as in the society. The demands of the new entrepreneurship without much experience and skill make them stressful and put them all into a dangerous position. This paper intends to identify the problems related to life coping strategies of women self help group members.

Aim

The aim of the study is to find out the entrepreneurial attitude and life coping skills of the rural women self help group members those who have emerged as entrepreneurs in rural areas.

Research method

This study has used non-experimental descriptive research design in order to recognize the types of problems and coping behavior of women rural entrepreneurs and their entrepreneurial attitude in Dharmapuri District. Primary data was collected from 200 respondents by using a structured questionnaire method administered among the randomly selected 200 women self help group entrepreneurs, who come under the age groups of 18 – 60 years. Hypothesis were tested with the application of descriptive and inferential statistics.

Findings

The overall entrepreneurial attitude of 200 respondents is that High (15%), Average (61%) and low (24%). Most of the respondents have an average level of life coping skills.

Implications

Results of this study aptly suggests that it is one of good references for carrying out future studies and could be interrelated with other variables, which can be quoted as a reference in terms of entrepreneurial attitude and also identifying the causes of stress and life coping strategies of women entrepreneurs in rural areas. This would suggest better solutions to reduce the stress level and increase the coping mechanism of the women entrepreneurs.

Keywords: Entrepreneurial attitude, women entrepreneurs, life coping skills, entrepreneurship, rural women, self-help groups.

1.1. Introduction

Women are the growing part of a present day human resources. The development would be imperfect if this section of the population is not given opportunities to prove their capabilities. It was in the ancient period women were recognized equally with men and in fact they were the head of the households and participated equally in decision making like men. The gender disparity prevailed in various areas including literacy, education, nutrition and health, employment, decision making, participation in politics and executive positions, property rights, etc.

This discrimination has been the outcome of the gender division of labour making the men to go out and market their services and so also act as the head of the household, decision-maker etc. On the other hand, making women to remain at home to continuously perform the domestic activities such as taking care of the children, cook and wash for the family which have not been recognized as work till 1981 Census in India. As a result of making the men as breadwinners of the family, the female members also started assigning themselves a secondary role next only to men and as such they are treated as secondary citizen in the society.

Women form a vital part of the Indian Economy, who constitute one third of the labour resource, and primary member contributing in the survival of the family. It is true that women form the backbone of agriculture sector, comprising the majority of agricultural labourers in India. Gender divisions in agriculture are stark with all activities involving manual labour assigned to women. While all operations involving machinery and drought animals generally performed by men.

Female agricultural laborers are among the poorest sections of Indian society. Agricultural wages for women are on an average 30-50 percent less than those for men. The greater is dependence on women's income. Despite several progresses made since independence in the lives of women, a gender analysis of most social and economic data demonstrates that women in India continue to be relatively disadvantaged in matters of survival, health, nutrition, literacy and productivity.

Review of literature

1.2. Micro Finance and Rural Poor

The micro finance and the micro credit and lending had been in practice since man started trade. The micro credit, which is claimed to be contributing to women through SHGs, was in existence prior to it in the name of IRDP, DWCRA etc. Finance has been the central focus in all these programmes. Given that finance is backbone of all economic activities, in alleviating poverty. They play a significant role in transferring funds from surplus to deficit sectors but hardly the formal banks concentrate on rural poor borrower particularly in backward areas.

It was felt by the women's associations and other organizations, that there is a need to mainstreaming of women. So that the human resource development would be complete and the economic development would be better with the contribution of the other half of the human resource and also the gender disparity will be reduced. However, till in year 1970 the organized efforts have not made to mainstream women by extending equal opportunities in education, nutrition and health, economic participation country right access to credit and decision-making practices both at the household and community.

Since 1975 with the United Nation's declarations of Women Empowerment Decade, every effort towards ensuring gender equality was recognized everywhere. In present days several approaches have been followed to empower women and address the gender disparities in the society. At the beginning stages in India the efforts taken to support women were related to welfare programmes in which the women were treated as beneficiaries. As a next stage equity approach was followed in which women were facilitated to be equal citizens in the field of economic participation.

Later the equity approach was replaced by empowerment approach, which emphasized that the women must be given equal power and must come to the mainstream to prove their capabilities. Then there is a paradigm shift in the development processes by incorporating the gender concerns as an important element of development strategy. Government of Andhra Pradesh has taken up women empowerment as

one of the two agenda items recognizing the importance and involvement of women to tackle rural poverty and socio-economic issues.

1.3.1 Indian Scenario

While accessing the credit, the women folk of the rural areas face myriad problems in the areas of collateral security, cultural distance between rural women and nationalized banks, high transaction cost, restricted and fixed banking hours, inflexibility in quantum and purpose of credit, inconvenient repayment schedule, cumbersome procedure and exploitation by the intermediaries. Dissatisfaction with the result of many provides affective financial service to the rural people, particularly to the rural women.

Taking a leaf out of the book of developing countries like Bangladesh, Indonesia, Bolivia and Philippines where the combination of the combine efforts of formal and informal finances provide sustainable and valuable services to the poor. Few NGOs in India have started experimenting on innovative schemes of Self Help Group.

The member's problems and satisfaction is the aside test for the success of efficiency of any women development programme. The "Member-Beneficiaries" of SHG groups are the key members of any rural development and women welfare network. The members who are enrolled in SHG programmes as members possess and came to equip with the given financial potency to invest on their income generating activities in order to keep away from the exploitation of the money lenders. Even though the government of India has been launching various schemes and providing subsidies, due to poor socio-economic background, these women are not able to generate sufficient income from various programmes.

The brief overview of the demand for micro-financial services suggests the huge challenges and the opportunities the Indian market presents. Protective financial services may be critical for poverty alleviation, but they do little for helping people out of poverty. Hence, promotional financial services are required, primarily for enhancing livelihood among poor people. It is said that micro-finance can also harm poor people.

The increase in income of micro-credit borrowers is directly proportional to their starting level of income – the poorer they were to start with, the less is the impact of the loan. Secondly, poor borrowers from Micro-financing organizations often do not graduate to higher and higher loans, and consequently to productive small enterprises. While credit may initially be the ruling constraint for micro enterprises, to grow beyond a certain size, other constraints come into play.

Livelihood promotion is complex, opening up multiple potential goals and interventions and demanding an understanding of individual household and enterprise as well as the economic systems or sub-sectors in which they operate. Intervening in livelihood promotion is far more challenging developing the efficient delivery of financial services.

The SHG has, in fact, moved away from livelihood Promotion. Using micro-credit to promote livelihood may not be feasible with such a strategy. As autonomous organization, SHG's share the challenges and dynamics of other small organizations. Forming new groups requires significant energy and the necessary group. Processes, Governments, donors, policy makers and resource providers need to be

aware of the dynamics involved in these small organizations. The institutional challenges in SHGs are three fold:

1.4.1. Life Coping or Adjustment Skills

Present study deals with Life Coping Skills otherwise known as Life Adjustment Skills. Coping skills refers to the behavioral process of balancing conflicting needs, or needs against obstacles the problems caused by environmental factors. Coping skills is otherwise called as specific psychological skills required to problem-solving.

Lazarus (2001)¹ defined that Coping skills or the Adjustment skills as a ways of managing and consists of coping with various demands and process of life. Good (1959)² state that adjustment is the process of finding and adopting modes of behavior suitable to the environment or the changes is the environment. Parameswaran & Beena (2004)³ defined adjustment is a process which a living organism acquires in a particular way of acting or behaving or changes an existing form of behavior or action. `

Coping is an important psychological activity of human being. Life is a process of life coping and adjustment. Coping is a persistent feature of human personality. If a person is not able to adjust himself to the environment he/she cannot develop his/her wholesome personality. A person with coping skills can lead a cheerful and wholesome life but a less adjusting person is prone to lead a depressed and unhealthy life. Adjustment is a process by which an individual learns certain ways of behavior to cope with the situation which he/she attains through harmony with his/her environment.

1.4.2. Areas of Coping (Adjustment) Skills

Emotional: Traditionally, women undergo various emotional changes due to varied responsibilities and roles they play in a family and in a society. Women as an entrepreneur from a rural areas even undergo more stressful situation due to lack of skills and experiences. The financial constrains, the business, the family demand and social ethos all contribute to the heightened level of stress and emotional imbalances.

Health: Good health contributes to good life-adjustment and in turn to good physical and mental health. Poor health and illness on the other hand, adversely affect personality through the unfavorable effects they have on social and personal adjustment. Poor adjustments often predispose the person.

Home: A certain degree of tension in the home life is normal during family life Furthermore, such feelings sometimes have strong motivating effects upon the individual and stimulate them into achieve something they do not have. It is only when these feelings become intense and persistent over a considerable period of time that they have seriously distressing influence on the overall adjustment.

Social: One of the most difficult developmental tasks women relates to social adjustments. These adjustments must be made with members of the opposite sex a relationship that never existed before and to adults outside the family and school environments. Early adults are a period of social expansion and development.

Educational: Young adolescents complain about school in general and about restriction, homework required courses, food in the cafeteria, and the way the school is run. They are critical of their teachers and the way they teach. This is the “thing to do.” A young adolescent who wants to be popular with their peers must avoid creating the impression that they are “brains.” This is even more important for girls

than for boys because less prestige is associated with academic achievement among girls than among boys.

1.4.3. Need of the study

Psychological problems faced by the members of the self help group members,

The rural women mostly undergo the following problems in their lives: Adjustment (53%), Jealousy (16%), Egoism (18%) and Self centeredness (11%).

Common Problems faced by the Self help group members

1. Lack of numerical skills (44%)
2. Income problems (83%)
3. Group conflict (43%)
4. Migration for employment (25%)
5. Lack of proper planning and management (35%)
6. High incident of defunct (16%)
7. Political inference (37%)
8. Unhealthy competition among the groups (42%)
9. Different attitude of banks (29%)
10. Lack of marketing of products (78%)

1.4.4. General Objectives:

The primary objective of the research is to study the Life coping skills of women entrepreneurs in Dharmapuri district of Tamil Nadu.

1.4.5. Specific Objectives:

1. To know the socio-economic conditions of women entrepreneurs.
2. To find out the entrepreneurial attitudes of women entrepreneurs
3. To explore the differences, association and correlations of selected independent variables of women entrepreneur with their overall life coping skills
4. To suggest measures for improving the development of women entrepreneurs in the study area based upon the findings of the present study.

1.4.6. HYPOTHESIS

1. There is significant relationship between the community and their life coping skills
2. There is significant difference between the educational qualification and their life coping skills
3. There is significant association between religion and their life coping skills
4. There is significant relationship between educational qualification and their life coping skills.
5. There is significant difference between the types of families and their life coping skills.
6. There is significant difference between different jobs of the women and their life coping skills.

1.4.7. FIELD OF STUDY

The women who have been doing entrepreneurship in rural areas of Dharmapuri district of Tamilnadu. India was studied. Dharmapuri is one of the drought affected district of Tamilnadu. The normal rainfall is very low. The people mainly depend on the agro based products for their living. The recent phenomenon of self help group movements has accelerated the rural poor to be self reliant and decision makers. This has given them varied opportunities to exercise their entrepreneurship skills with small amount.

1.4.8. RESEARCH DESIGN

The researcher has adopted a descriptive research design for this study. The researcher has explored the relationship between different variables like educational qualification, religion, community, type of family and life coping skills of women entrepreneurs. Moreover, this research explained the factors

responsible for the women becoming entrepreneurs; problems encountered by them and also described the psychological attitudes especially the home, educational, social, health and emotional status of women entrepreneurs.

Life Coping (Adjustment) Scale: The “Adjustment Inventory” is developed by A.K.P.SINHA and R.P.SINHA. This scale contains 102 items of which Home -16, Health -17, Social -22, Emotional -29 and Educational -18 items are randomly distributed on the scale. The scale gives a Holistic estimate of adjustment of an individual. The subjects can be classified into five categories in accordance with the raw scores obtained by them on the inventory. The five different categories of adjustment are: A = Excellent, B = Good, C =Average, D = Unsatisfactory, E = Very unsatisfactory adjustment.

1.4.9. FINDINGS

DEMOGRAPHIC CHARACTERISTICS

Independent variables:

Age is an important variable which determines the vigor of entrepreneurship. According to this study 44% of the respondents come under the age group between 26 to 40 and others as follows : Below 25 (36%) and 41 to 60 (20%). Almost half of the respondents belong to the middle age group.

The educational qualifications also contribute much to the entrepreneurship attitude. Nearly 59% of the respondents are illiterates and have done only under 10th standard. Illiterates (27%), Below 10th (32%), Higher secondary (10%), Graduation (15%), Post graduation (6%), Technical (3%) and other (4%)

In India, Religion plays a vital role in deciding ones character and their social actions.

Marriage status of the respondents has a very crucial in determining the entrepreneurial attitude. Married (68%), Unmarried (19%), Divorced (1%) and separated (2%)

The Monthly income of the respondents are : Below 1000 (25%), 1001 to 5000 (53.5 %), 5001 to 10,000 (14%), 10,000 to 15000 (7%). Caste is an inseparable factor to be studied in the Indian sociological context. According to this sample taken : FC (1%), MBC (79%), BC (11%) and SC (9%). Total number of years residing in one place : One year (20%), Two years (21%), 3Three years (47%), Four years (8%) and 5 years 4%). Studies on women entrepreneurs show that the single women are more successful in running their concerns. This study collected the samples from Nuclear (62%) Joint (38%) families.

The total number of family members : 1 to 5 (60%), 6 to 10 (38%) , 11 and above (2%). Family occupation : Entrepreneurial (80%) Non entrepreneurial (20%). The Yearly income of the family is : 1 to 5000 (37%), 5001 to 10,000 (28%), 10001 to 20,000 (26%), 20001 to 50,000 (8%) , 50001 and above (1%). Many of the women entrepreneurs run their operation as their family business . according to this sample 53% run this as their family business.

The Starting capital of the business varies from person to person: Below 5000 (28%), 5000 to 10,000 (24%), 10001 to 15,000 (12%), 150001 to 20,000 (5%), 20001 to 25,000 (7%), 25001 to 30,000 (4%), 30001 to 35,000 (7%), 40001 to 45 000 (9%), 45001 to 50,000 (1%) and 50001 and above (11%).

The most important factor of the SHS's are its savings : Below 5000 (5%), 5001 to 10000 (25%), 10001 to 20000 (58%), 20001 to 50000 (7%) and 50000 and above (5%). The duration of doing business : 1year (48%), 2 years (45%), 3 years (2%), 4 years (1%) and 5 years (4%).

The Persons behind the start of the business : Self interest (34%), Parents (22%), Both parents and self (9%), Friends and self (22%) and others (8%). The different reasons for starting the buisiness:

It is a family members business (32%), Inspired by the success of the friends and relatives (13%), Desire to become an entrepreneur (95%), Unemployment (11%), Realization of own ideas (11%), dissatisfaction with the previous employment (9%), To do self employed (12%), Availability of finance and technical aspects (4%), Let me try or accidental (5%) Flexibile working time and location (2%). Regarding the Entrepreneurial aspects of the respondents 18% posses the quality and 82% do not posses the entrepreneurial skill.

Duration of the trainings attended : IVDP (24%, Madhampatti (1%) and Velli santhai (1%). The Names of the business run by the respondents: Cool drinks shop (7%), Fancy shop (4%), Fruit shop (4%), Goat rearing (10%), Milk selling (30%), Petty shop (15%), vegetable shop (19%), Water business (4%)

The status of the business: Sole ownership (87%) and Informal (7%). The present condition of the business: Growth with good income (22%), Moderate (59%) and Critical (15%). The Number of hours devoted for the business: Less than 5 hours (25%), between 5 to 10 (62%), Between 11 hrs to 15 hrs (7%) and Over 15 hours (1%). The Method of marketing : Retail (94%), others (6%).

Regarding the Competitors for the business : 100% there is no one exist in this district. The Role model to their business: Friends (7%), Husband (30%), Relatives (10%), SHG Members (32%) and Villagers (15%).

The Present Business condition : Very good 98%), Good (46%), Satisfactory (46%). Regarding their Leisure time activities: Outdoor (43%) and Indoor (57%). Regarding their Social participation: Membership in an association (31%), SHG members (56%) and Any other (6%)

Family members opinion about the business: Very good (77%), Good (20%) satisfactory (2%) and Bad (1%). The Relatives opinion on the business : Very good (22%), Good (65%) satisfactory (8%) and Bad (5%). Friends opinion their buisiness: Very good (34%), Good (29%) satisfactory (29%),Bad (6%) and very bad (2%). The SHG group members opinion: Very good (47%), Good (35%) satisfactory (16%) and Bad (2%). The Opinion of the Youth group leaders : Very good (35%), Good (37%) satisfactory (17%) and Bad (6%) and very bad (5%). The Opinion of the Local association leaders: Very good (23%), Good (40%) satisfactory (21%) and Bad (13%) and very bad (3%). The Opinion of the Political leaders: Very good (17%), Good (28%) satisfactory (31%) and Bad (16%)and very bad (8%) and the Opinion of the other Entrepreneurs: Very good (22%), Good (28%) satisfactory (22%) and Bad (14%) and very bad 14%)

Customers satisfaction of the business they run: Very good (25%), Good (34%) satisfactory (30%) and Bad (7%)and very bad (4%). The opinions of the Financial institutions': Very good (25%), Good (22%) satisfactory (15%) and Bad (14%)and very bad (4%). The Mentors opinion Very good (34%), Good (26%) satisfactory (28%) and Bad (9%) and very bad (3%). The other community people's opinion on the business: Very good (21%), Good (43%) satisfactory (20%) and Bad (12%) and very bad (4%).

Participation of women in politics; especially from rural areas, considered to be one of the indicators of women development. 18% the respondents do participate in the politics, 38% don't involve themselves and 35% were Unable to commend.

Following are the habits practiced by the respondents:

Chewing the pawn: Always (12%), Occasionaly (9%), Never (79%)

Drinking habit : Always (2%), Occasionaly (14%), Never (83%)

Gambling: Always (2%), Occasionally (9%), Never (89%)

Dept and money lending: Always (15%), occasionally (26%), Never (59%)

Table : 1 Life Coping Skill

Factors of Life coping skill	High	Average	Low	Total
Emotional	25 (13%)	145 (73%)	30 (14%)	200 (100%)
Health	40 (20%)	130 (65%)	30 (15%)	200 (100%)
Home	20 (10%)	120 (60%)	60 (30%)	200 (100%)
Social	38 (19%)	106 (53%)	56 (28%)	200 (100%)
Educational	32 (16%)	105 (52%)	63 (32%)	200 (100%)
TOTAL	15%	61%	24%	100%

The overall entrepreneurial attitude of 200 respondents is that High (15%), Average (61%) and low (24%). The Life coping skills of the respondents trait wise: Emotional : High (13%), Average (73%) and Low (14%), Health : High (20%), Average (65%) and Low (15%), Home: High (10%), Average (60%) and Low (30%), Social : High (19%), Average (53%) and Low (28%) and Educational : High (16%), Average (61%) and low (32%).

The respondents have more of high level attitude in Health, more of average level in emotional, and more of low level in Educational attitudes.

The respondents have more of less level among the high level group is Home, Educational among average and emotional among the low level groups.

Anova

5% level of significant differences are observed among the independent variables with the overall life coping skills. Yearly income (0.019*), Religion (0.033*), Family occupation (0.042*) and year of residing in that place (0.29*)

No significant differences exists among the independent variables with the overall life coping skills such as method of marketing, Number of hours devoted for business, Present status of the business, Reasons for starting the business, Persons behind start of the business, Number of years doing the business, Personal savings, Operation as family business, Yearly income, Family type, Different castes, Monthly income, Religion, Educational qualifications and age groups. Marital status of the respondents, Family Income, Starting capital of the business and Loan sources

Chi square test

There is 5% level of association exist between the following independent variables with the overall entrepreneurial attitude.

The independent variable Religion (0.043*) has got 5% level of association with the overall life coping skill.

There is no association exists between the following independent variables with the overall life coping skills: Castes, sub-castes, Migratory status, Year of residing in a place, Family type, Total no of family members, Family occupations, Family income, Starting capital, sources of loans savings, Number of years involved in the business,, persons behind business, Reasons for starting, Marital status, Names of business, Monthly income, Number of hours devoted for work, Method of marketing, Role model.,

CORRELATIONS

1% level of correlation is observed between the following Independent variables with the overall life coping skill: Marital status (0.004**)

5% level of correlation is observed between the following Independent variables with the overall life coping skill. age (0.013*), Income (0.011*), Persons who inspired the business (0.033*) and Loan sources (0.021*)

There is no correlations established between these following independent variables with the overall entrepreneurship : Religions, age, Monthly income, castes, total number of years residing in one place, Family type, Educational qualification, , Business as family operation, starting capital, savings, Number of years involved in the business and reasons behind the business. Present status of business

1.4.10. SUGGESTIONS

Almost all the respondents have only the average levels of entrepreneurships. Therefore, it is very important to arrange trainings on life coping and life management skills. The respondents are more in low level of educational attitudes. It is very important to improve the educational knowledge. Formal and informal educational programs, skill training on life skill and stress coping skills are very essential.

REFERENCES

- Augustine, L. F., Vazir, S., Rao, S. F., Rao, M. V., Laxmaiah, A., & Nair, K. M. (2011). Perceived stress, life events & coping among higher secondary students of Hyderabad, India: A pilot study. *Indian Journal of Medical Research, 134*(1), 61-68.
- Chaudhary, S., & Joseph, P. M. (2010). Adolescents' Perceptions about Coping with Stress: A Qualitative View from India. *International Journal of the Humanities, 7*(11), 87-109.
- Deepshikha, & Bhanot, S. (2011). Role of Family Environment on Socio-emotional Adjustment of Adolescent Girls in Rural Areas of Eastern Uttar Pradesh. *Journal of Psychology, 2*(1), 53-56.
- Dhal, A., Bhatia, S., Sharma, V., & Gupta, P. (2007). Adolescent Self-Esteem, Attachment and Loneliness. *Journal of Indian Association for Child and Adolescent Mental Health, 3*(3), 61-63.
- Ganesh, K., & Vathsala, S. (2017). Pattern of Stress, Coping Strategies and Suicidal Ideation among women in Southern India. *Pattern of Stress, Coping Strategies and Suicidal Ideation among Adolescents in Southern India, 7*(1), 22-30.
- Lee, R. M., Jenny, S., & Yoshida, E. (2005). Coping with intergenerational family conflict among Asian American. *Journal of Counseling Psychology, 52*(3), 389-399.
- Mathew, A., & Nanoo, S. (2013, Jan-Mar). Psychosocial Stressors and Patterns of Coping in Adolescent Suicide Attempters. *Indian Journal of Psychological Medicine, 35*(1), 39-46.
- Parameswari, J. (2011, Jul-Dec). Self-Esteem and Life Coping among Adolescents. *Journal of Psychological Research, 6*(2), 257-264.
- Upadhayay, B. K., & Khokhar, C. P. (2006). Personality Traits And Feeling Of Loneliness In Unemployed Youths. *Europe's Journal of Psychology, 2*(4). Retrieved from Europe's Journal of Psychology: <https://ejop.psychopen.eu/article/view/288/html>

ROLE OF DISTRICT INDUSTRIAL CENTRE IN DEVELOPMENT OF MSME (WITH SPECIAL REFERENCE TO AUTOMOBILE ANCILLARY UNITS IN KRISHNAGIRI DISTRICT)

***K. Saritha¹**

**** Dr. R. Venkatesh²**

Abstract

The District Industries Centers (DICs) programme was started in 1978 with a view to providing integrated administrative framework at the district level for encouraging entrepreneurs in rural and urban areas. District Industries Centers (DICs) give full assistance to the entrepreneurs who are going to start the business on their own and in their regional places. District Industries Centers provided various schemes for promoting the development of rural and urban industries. This study focuses the role of DICs in development automobile ancillary units in Krishnagiri District. In this study the research were taken 120 automobile ancillary entrepreneurs from study area. Primary data were collected through mailed questionnaires.

Keywords: Role of District Industries Centers, Level of Satisfaction.

¹Research Scholar, PG and Research Department of Commerce, Don Bosco College, Dharmapuri

² Research Supervisor,PG and Research Department of Commerce, Don Bosco College, Dharmapuri

INTRODUCTION

The Micro, Small and Medium Enterprises (MSMEs) have been accepted as the engine of economic growth and for promoting equitable development. The MSME also play an important role in the development of the economy with their effective, efficient, flexible and innovative entrepreneurial spirit. MSMEs are the nursery where small existing businesses have the potential to become world beaters tomorrow. The organizational structure of DIC's consists of General Manager, Functional Managers and Project Managers to provide technical services in the areas relevant to the needs of the district concerned. Management of DIC is done by the state government. The DICs provide and arrange a package of assistance and facilities for credit guidance, raw materials, training, marketing etc. including the necessary help to unemployed educated young entrepreneurs in general. Thus it may be said that DIC extends promotional, technical, physical, financial, marketing and all other type of services required for growth and development of small scale industries.

Review of Literature

Singh et al, (2012)³ analysed the performance of small scale industry in India and focused on policy changed which have opened new opportunities for this sector. The study recommended the emergence of technology development and strengthening of financial infrastructure to boost ssi and to achieve growth target.

Anis Ali, Firoz Husain (2014)⁴ This study focuses upon the growth pattern of the MSMEs, number of units, investment, production and employment. The main objectives of this paper to study the present status of MSMEs in India. They researcher found that the MSMEs are providing more employment per unit.

³Singh, R, Verma, O.P., and Anjum, B. (2012), "Small Scale Industry: An Engine of Growth", *Zenith International Journal of Business Economics & Management Research*, Vol.2 Issue 5.

⁴Anis Ali, Firoz Husain (2014), *Msme's In India: Problems, Solutions And Prospectus In Present Scenario*", *International Journal of Engineering and Management Sciences*, Vol.No.5(2),2014 P-No. 109-115.

Dr. K. Kumaravel (2017)⁵,evaluated the development of entrepreneurs through small and medium enterprises. The study concluded that there are various opportunities available for the growth of MSME, but entrepreneurship is very good platform to promote and growth of this industry.

Seena P.P., Dr.Swarupa.R,(2018)⁶, they conducted a study to analyze the region wise growth and performance of MSME in Kerala. The study revealed that southern region good in industrialization and has showed a stable performance. Number of unit, employment generation production and investment are lowest in northern region but the compound growth rate is highest.

Objectives of the Study

- To trace the socio-economic status of the entrepreneur in Krishnagiri
- To identify and highlights the functions of DIC in Krishnagiri
- To analyze services offeredby DIC has fulfilled the requirements of entrepreneur and level satisfaction.

Research Methodology

The sample of the study was determined with the convenient sampling method and the sample size of this study defined as 120 repondents. Questionnaire were formed with two parts, part I determine demographic variables of the respondent and part II role of DIC in development of automobile ancillary units. The researcher was used for five point Likert scaling techniques. The data were analyzed by using frequency statistics and factor analysis and reliability. The researcher was used SPSS package to analyse and interpret the data.

Sample Unit

Sample unit defines the single unit of the sample, in the pre-decided sample which is to be drawn from the selected automobile ancillary units.

⁵*Dr. K. Kumaravel(2017), “ Growth and Performance of MSME Sector in India”, International Journal of Management and Humanities, Vol.No. 4 Issue No.2.*

⁶*Seena P.P., Dr.Swarupa.R.,(2018)⁶, Growth and performance of Small Scale Industries/Micro Small and Medium Enterprises in Kerala-Region Wise Analysis, International Journal of Management Studies, Vol-V Issue No 2(1), April 2018, p-no. 117 -122*

Table 1
Frequency and Percentage Regarding the Demographic Variables of Respondents

Demographic Profile		Frequency	%
Age in years	Below 20	9	8
	21-30	60	50
	31-40	39	32
	Above 41	12	10
Gender	Male	95	79
	Female	25	21
Educational Qualification	Primary	30	25
	Technical	45	37
	Graduates	18	15
	Professional	27	23
Marital status	Married	114	95
	Single	6	5
Experience(in Years)	Up to 5	60	50
	6-10	21	18
	11-15	27	22
	Above 15	12	10
Size of Company	Manufacturing	39	32
	Tooling	36	30
	Both	45	38
Total		120	100

Source: Primary Data

It is clear from the tables 1 that 8 % of the respondents belong to the age group of below 20 years, 50 % of them belong to the age group of 21 – 30 years, 32% of them are belong to the age group of 31-40 years and 10% of them belong to the age group of above 41 years. It shows that majority of the respondent are under the age group of 21-30 years

According to their gender, 79% of the respondents were Male and 21% of them are female. It is shows that majority of the respondents are male.

According to their educational qualification, 25% of the respondents have primary, 37% are Technical, 15 % of them are Graduates, and 23 % of them have Professional education. It shows that majority of the respondents are primary level.

According to their marital status, 95 % of the respondents are married and 5 % of them are Single. It shows that majority of the respondent are married.

According to their experience, 50 % of the respondents have up to 5 years, 18 % have 6-10 years, 22 % of them have 11-15 years and 10 % of the respondents have experience of above 15 years. It shows that majority of the respondent are having the experience of up to 5 years.

According to their Nature of Activity, 32% of the respondents are from Manufacturing, 30 % of them are from Tooling and 38 % of them are from Both. It reveals that majority of the respondent are both manufacturing and tooling of activity.

Table No 2

Opinion of the Entrepreneur about District Industrial Centre

Factors	SDA		DA		N		A		SA		Total
	N	%	N	%	N	%	N	%	N	%	N
Training enhance us to become efficient in a particular sector	6	5.0	3	2.5	39	32.5	15	12.5	57	47.5	120
DIC assistance generate numerous direct and indirect employment opportunities to backward areas of Krishnagiri	2	1.7	9	7.5	15	12.5	27	22.5	67	55.8	120
Granting financial and non-financial assistance to entrepreneurs	3	2.5	9	7.5	27	22.5	36	30.0	45	37.5	120
Liberal policies and procedures at DIC influence to become successful entrepreneur	6	5.0	15	12.5	18	15.0	15	12.5	66	55.0	120

Source: Primary Data

It is clear from the table 2 that only 5.0 % of the respondents were strongly disagreed, 2.5% of the respondents disagreed, 32.5 % of the respondents neutral, 12.5 % of the respondents were agreed and 47.5 % of the respondents were strongly agreed with the factor ‘Training enhance us to become efficient in a particular sector’.

Regarding the factor ‘DIC assistance generate numerous direct and indirect employment opportunities to backward areas of Krishnagiri’ 1.7 % of the respondents were strongly disagreed, 7.5 % of the respondents were disagreed, 12.5 % of the respondents were neutral, 22.5 % of the respondents were agreed and 55.8 % of the respondents were strongly agreed.

Regarding the factor ‘Granting financial and non-financial assistance to entrepreneurs’ 2.5 % of the respondents were Strongly disagreed, 7.5 % of the respondents were disagreed, 22.5 % of the respondents were neutral, 30.0 % of the respondents were agreed and 37.5 % of the respondents were strongly agreed.

Regarding the factor ‘Liberal policies and procedures at DIC influence to become successful entrepreneur’ 5.0 % of the respondents werestrongly disagreed, 12.5 % of the respondents were

disagreed, 15.0 % of the respondents were neutral, 12.5 % of the respondents were agreed and 55.0 % of the respondents were strongly agreed.

Table No. 3

Functions of District Industries Centre in Krishnagiri

Factors	SDA		DA		N		A		SA		Total
	N	%	N	%	N	%	N	%	N	%	
Provide Market Support	54	45.0	30	25.0	21	17.5	12	10.0	3	2.5	120
Facilitate credit linkages between Banks and Entrepreneurs	42	35.0	33	27.5	27	22.5	12	10.0	6	5.0	120
Counseling and guiding the entrepreneurs	12	10.0	21	17.5	39	32.5	36	30.0	12	10.0	120
Fairs and Exhibitions	9	7.5	18	15.0	21	17.5	18	15.0	54	45.0	120

Source: Primary Data

It is clear from the table 3 that only 45.0 % of the respondents strongly were disagreed, 25.0% of the respondents were disagreed, 17.5 % of the respondents were neutral, 10.0 % of the respondents were agreed and 2.5 % of the respondents were strongly agreed with the factor ‘Provide Market Support’.

Regarding the factor ‘Facilitate credit linkages between banks and entrepreneurs’ 35.0 % of the respondents strongly disagreed, 27.5 % of the respondents disagreed, 22.5 % of the respondents neutral, 10.0 % of the respondents agreed and 5.0 % of the respondents strongly agreed.

Regarding the factor ‘Counseling and guiding the entrepreneurs ’ 10.0 % of the respondents Strongly were disagreed, 17.5 % of the respondents weredisagreed, 32.5 % of the respondentswereneutral, 30.0 % of the respondents wereagreed and 10.0 % of the respondents werestrongly agreed.

Regarding the factor ‘Fairs and Exhibitions’ 7.5 % of the respondents werestrongly disagreed, 15.0 % of the respondents weredisagreed, 17.5 % of the respondents wereneutral, 15.5 % of the respondents agreed and 45.0 % of the respondents strongly agreed.

Table No 4**Different schemes and services of District Industries Centre**

Factors	SDA		DA		N		A		SA		Total
	N	%	N	%	N	%	N	%	N	%	N
Provide Training Programme to the Entrepreneurs	6	5.0	15	12.5	21	17.5	24	20.0	54	45.0	120
Promotional scheme for women	12	10.0	27	22.5	15	12.5	15	12.5	51	42.5	120
Schemes for weaker sections	15	12.5	21	17.5	45	37.5	27	22.5	12	10.0	120
Provide financial assistance and Subsidy to sick units	15	12.5	6	5.0	54	45.0	21	17.5	24	20.0	120

Source: Primary Data

It is clear from the table 4 that only 5.0 % of the respondents were strongly disagreed, 12.5% of the respondents weredisagreed, 17.5 % of the respondents neutral, 20.0 % of the respondents wereagreed and 45.0 % of the respondents werestrongly agreed with the factor ‘Provide Training Programme to the Entrepreneurs’.

Regarding the factor ‘Promotional scheme for women’ 10.0 % of the respondents werestrongly disagreed, 22.5 % of the respondents weredisagreed, 12.5 % of the respondents wereneutral, 12.5 % of the respondents wereagreed and 42.5 % of the respondents werestrongly agreed.

Regarding the factor ‘Schemes for weaker sections’ 12.5 % of the respondents wereStrongly disagreed, 17.5 % of the respondents weredisagreed, 37.5 % of the respondents wereneutral, 22.5 % of the respondents wereagreed and 10.0 % of the respondents werestrongly agreed.

Regarding the factor ‘Provide financial assistance and Subsidy to sick units’ 12.5 % of the respondents werestrongly disagreed, 5.0 % of the respondents weredisagreed, 45.0% of the respondents wereneutral, 17.5 % of the respondents wereagreed and 20.0 % of the respondentswere strongly agreed.

Table No. 5

KMO and Bartlett's Test		
Kaiser-Meyer-Olkin Measure of Sampling Adequacy.		.684
Bartlett's Test of Sphericity	Approx. Chi-Square	595.406
	df	66
	Sig.	.000

Bartlett's test of sphericity

Taking a 95 % level of significance $\alpha=0.05$ the p value (Sig.) of $.000 < 0.05$, therefore the Factor Analysis is valid.

If KMO greater than 0.5, the sample is adequate. Here, $KMO=.684$ which indicates that the sample is adequate and we may proceed with the factor analysis. Hence Factor Analysis is considered as an appropriate technique for further analysis of the data.

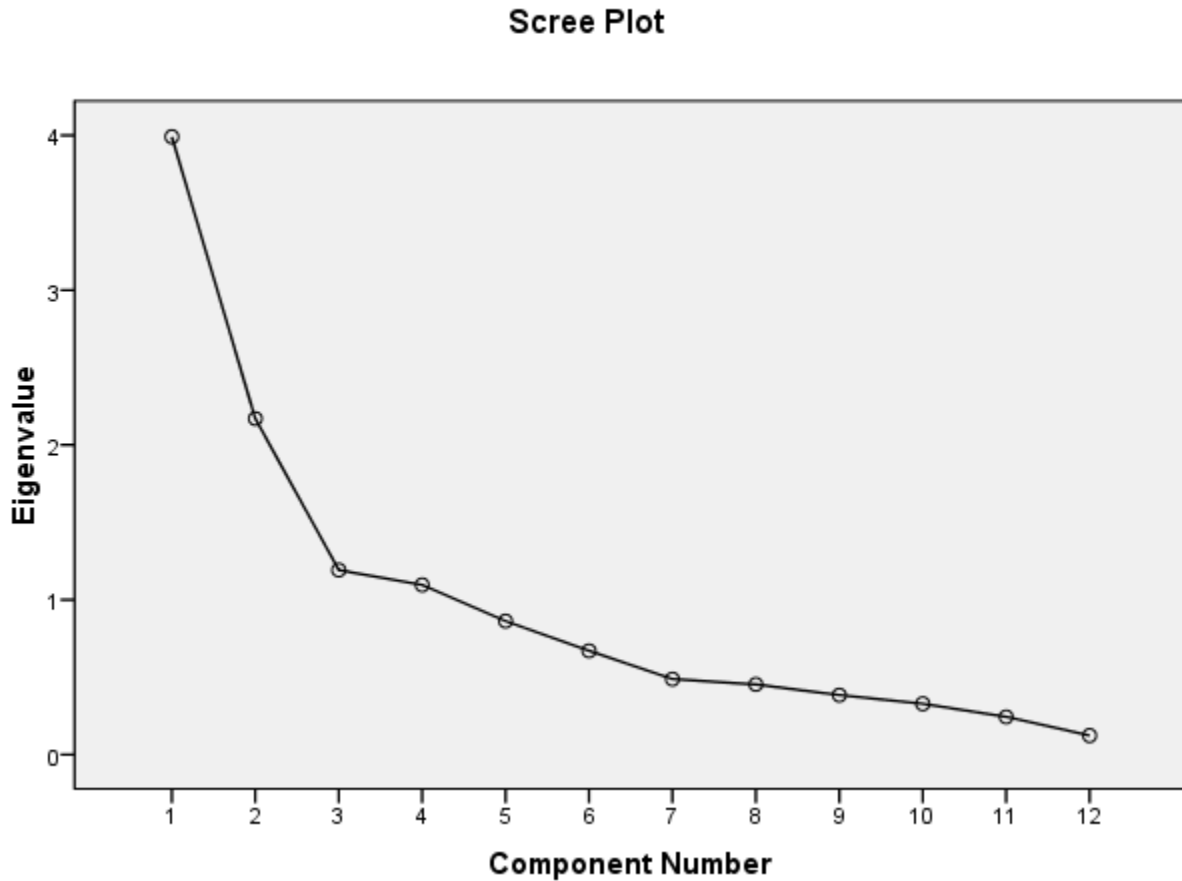
Factor Analysis**Table No 6**

Variables	Eigen Values	% of variance	N
Opinion of entrepreneur about DIC	3.991	33.259	120
Functions of DIC	2.170	18.084	120
DIC schemes and services	1.192	9.932	120
Satisfaction	1.096	9.132	120

Source: Primary Data

In order to evaluate factor analysis, we considered four variables which was segregated under the different titles like opinion of entrepreneur about DIC, functions, schemes and services and entrepreneur satisfaction. (Kaiser, 1960) stated that variables subjected to principal component

factor analysis with varimax rotation by using the criterion that factors with eigen value greater than 1.00 will be retained.



Findings:

- It shows that majority of the respondent are under the age group of 21-30 years
- It is shows that majority of the respondents are male.
- It shows that majority of the respondents are primary level.
- It shows that majority of the respondent are married.
- It shows that majority of the respondent are having the experience of up to 5 years.
- It reveals that majority of the respondent are both manufacturing and tooling of activity.

Suggestions

Female respondents showed lesser participation in DIC because they had a lesser awareness towards it. Huge number of respondents are facing capital deficiency to expand their business as well as lack of guidance in terms of how to develop automobile ancillary products. It is observed that many of them unaware about the functions of DIC.

Conclusions

The study concludes that the entrepreneurs of krisnagiri district showed positive response towards DIC because they get prospects in enhancing their skills through entrepreneurship development programme and utilize the schemes and services of DIC. These types of activities stimulate the entrepreneurs to perform well in Krishnagiri district and hence it upsurge the economy of Krishnagiri district in all over Tamilnadu.

Reference

1. Websites
2. Journals
3. Books
4. Singh, R, Verma, O.P., and Anjum, B. (2012), "Small Scale Industry: An Engine of Growth", *Zenith International Journal of Business Economics & Management Research*, Vol.2 Issue 5.
5. Dr. D.Paul Dhinakaran, "Community Relations Of Tamilnadu State Transport Corporation Ltd" *International Journal Of Research And Analytical Reviews* (E ISSN 2348-1269, print ISSN 2349-5138) Special Issue March 2019.
6. Anis Ali, FirozHusain(2014), *Msmes In India: Problems, Solutions And Prospectus In Present Scenario* ", *International Journal of Engineering and Management Sciences*, Vol.No.5(2),2014 P-No. 109-115.
7. Dr. K. Kumaravel(2017), " Growth and Performance of MSME Sector in India", *International Journal of Management and Humanities*, Vol.No. 4 Issue No.2.
8. Seena P.P., Dr.Swarupa.R.,(2018)¹, *Growth and performance of Small Scale Industries/Micro Small and Medium Enterprises in Kerala-Region Wise Analysis*, *International Journal of Management Studies*, Vol-V Issue No 2(1), April 2018, p-no. 117 -122
9. D.Paul Dhinakaran, "Passengers Satisfaction towards Tamil Nadu State Transport Corporation Bus Services *International Journal Marketing and Management Research*, (ISSN (online) 2229 - 6883, Volume 3, Issue 6-9, June-September, 2012

PROBLEM FACED BY MICRO SMALL MEDIUM ENTREPRENEURS IN HOSUR TALUK

*K. Saritha,

** Dr. R. Venkatesh

*Research Scholar, PG and Research Department of Commerce, Don Bosco College, Dharmapuri

** Research Guide, PG and Research Department of Commerce, Don Bosco College, Dharmapuri

Abstract

Micro, Small and Medium Enterprises (MSMEs) have played a crucial role in the economic development of a country and second largest workforce in the country after the agricultural sector. Today, small and medium industry occupies a position of strategic importance in the Indian economic structure due to its significant contribution in terms of output, exports and employment. MSMEs are complementary enormously to the socioeconomic development of the country and provide employment opportunities at lower capital cost than by the large industries. Small businesses often face a variety of problems related to their size. This study focuses the problems faced by micro, small and medium entrepreneurs in Krishnagiri District in Hosur Taluk. In this study, 100 MSME Entrepreneurs are taken from the study area were selected as the samples, through convenient sampling method. Primary data was collected with the help of interview schedule. This study used factor analysis for identifying the problems encountered by MSME Entrepreneurs. Factor analysis found that there are four factor components.

Keywords: *Business Start-ups, Problems faced by MSMEs Entrepreneurs.*

Introduction

The term “entrepreneurship” comes from the French verb “entreprendre” and the German word “unternehmen”, both means to “undertake”. Entrepreneur is a process where one person getting himself employed provides job to other. The persons are also called “entrepreneur”.

An Entrepreneur is an individual who, rather than working as an employee, finds and runs a small business, assuming all the risks and rewards of the enterprises. The entrepreneur is commonly seen as an innovator, a source of new ideas, goods, services and business or procedures. Entrepreneurs play a vital role in Indian economy. These are the people who have the skills and creativity necessary to expect current and future needs and bring about good new ideas to market. Entrepreneurs who prove to be successful in taking on the risks of a start-up are rewarded with profits, fame and continued growth opportunities. Those who fail suffer losses and become less prevalent in the markets.

This type of industry is to provide on various level of opportunity in our society like on various people are to getting on emplacement chance that way to developing on people standard living level and that improve on the economic level of the people.

Review of Literature

K. Suneetha and T.Sankaraiah (2014)¹, Problems of MSMEs and Entrepreneurs in Kadapa District, IOSR Journal of Economics and Finance: The study conducted a survey on 156 enterprises to study their problems. It was found that 103 enterprises were facing financial problems and among them 62.8 per cent are from Micro enterprises. Moreover 23 percent found as meager assistance from government agencies. In the study the divisions of Kadapa, Jammulamadugu and Rajampet were covered.

W.G Bonga (2014)² analyses the challenges faced by SMEs in the internationalization of their products and suggests some strategies which can be employed at both individual and national levels. It also suggests a simplified regulatory framework, good governance, accessible finance, proper infrastructure, and availability of foreign market information to help SMEs in the promotion of their exports. Some of the major challenges in the way of increased exportation are lack of adequate finance, inadequate market research and analysis, inability to understand competitive conditions, lack of expertise to enter a foreign market, unfamiliar export procedures, etc. government assistance, initial focus on few selected markets, realistic commitments, understanding employment policies and reduction of regulatory burden are few of the suggestions.

Meeravali Shaik, et. al. (2017)³ establishes that although MSME sector has shown a positive contribution to employment and fixed assets growth in recent years but it still faces a number of challenges such as lack of timely credit, high cost of credit, difficulty in procurement of raw material, problems in storage and designing, inadequate infrastructure, low technology levels, lack of skilled manpower, etc. it suggests the government to adopt integrated policy with efficient governance for the MSME to help the sector increase its productivity and contribution to economic growth.

Objectives of the Study

- To identify the problems faced by MSMEs in Hosur Taluk.

¹k. Suneetha and T.Sankaraiah, (Mar.-Apr. 2014) *Problems of MSMEs and Entrepreneurs in Kadapa District, IOSR Journal of Economics and Finance (IOSR-JEF)*, e-ISSN: 2321-5933, p-OSSN: 2321-5925, Vol.3, Issue 2. Ver.1, pp 31-37.

²Bonga, Wellington Garikai (2014). 'challenges faced by SMEs on exportation and possible strategies.' *Social Science Research Network*. Retrieved from: <https://ssrn.com/abstract=2399878>.

³Shaik, Meeravali and Kankipati, Ajay Kumar and Ramesh, KV and Babu, G. (2017). 'Performance of MSMEs sector in India.' *SSRG International Journal of Economics and Management Studies*. Vol. 4(3). pp 11-15.

Research Methodology

The study is conducted in Hosur Taluk in the district of Krishnagiri. The sample of the study was determined with the convenient sampling method and the population of this study defined as 100 respondents. The data were collected through questionnaire with two parts, part I demographic profile of the respondents and part II the problems faced by MSMEs Entrepreneurs.

Analytical Tools

Statistical techniques such as simple percentage, mean score and used factor analysis for identifying problems encountered by MSME Entrepreneurs.

Result and Discussion

Table 1: Demographic Distribution of Respondents

Demographic Details		Frequency	Percentage(%)
Gender	Male	87	87
	Female	13	13
Total		100	100
Age Group	Below 20 years	8	8
	21 – 30 Years	51	51
	31-40 Years	31	31
	Above 40 Years	10	10
Total		100	100
Marital Status	Married	95	95
	Unmarried	5	5
Total		100	100
Educational Qualification	Primary	24	24
	Secondary	40	40
	Degree	15	15
	Technical/Diploma	21	21
Total		100	100
Year of Previous Experience	Below 5 Years	49	49
	6-10 Years	21	21
	11-15 Years	20	20
	Above 15 Years	10	10
Total		100	100
Type of Experience	Machine Setting	21	21
	Machine Operator	28	28
	Supervisor	35	35
	Others	16	16
Total		100	100

Source: Primary Data

From the above table inferred that the demographical profile of the respondents which includes gender, age, marital status, educational qualification, year of previous experience and type of experience.

1. 87 respondents are male entrepreneurs out of 100 respondents and remaining 13 are female respondents has taken for the study.
2. 51 respondents are in the age group of 21-30 years, 31 respondents are in the age group of 31-40 years, 10 respondents are above 40 years and remaining 8 respondents are below 21 years.
3. Out of 100 respondents 95 respondents are married entrepreneurs and remaining unmarried respondents.
4. 40 respondents are qualified up to secondary, 24 respondents are qualified up to primary, 21 respondents are qualified only Technical/Diploma and other 15 respondent are Degree.
5. 49 respondents have less than 5 years of experience, 21 respondent have 6 -10 years of experience, 20 respondent have 11-15 years of experience and 10 respondent have above 16 years of experience.
6. Out of 100 respondents 28 respondent under the group of supervisor.

FACTOR ANALYSIS

Factor Analysis is a method used to transform a set of variables into a small number of linear composites, which have a maximum correlation with original variables. Factor analysis is used to study a complex product (or) services, in order to identify the major characteristics or factors considered important by the respondents. The purpose of factor analysis is to determine whether the responses of several statements favoured by the respondents are significantly correlated. If the responses to the several statements are significantly correlated, it is considered that the statement measures some factors common to all of them.

Factor analysis can only be applied to continuous variables (or) interval scaled variables. Factor analysis is like Regression analysis as it tries to 'best fit' the factors to a scatter diagram of data in such a way that the factors explain the variance associated with the responses to each statements. Factor analysis was conducted by the researcher in the present research in the following stages.

Table No: 2 KMO and Bartlett's Test^a

Kaiser-Meyer-Olkin Measure of Sampling Adequacy.		.703
Bartlett's Test of Sphericity	Approx. Chi-Square	1.120E3

	df	105
	Sig.	.000

a. Based on correlations

Table 4.50 indicates that the Kaiser-Meyer-Olkin (KMO) measures of sampling adequacy in the study are 0.703. This is a good result, as it exceeds 0.5. Bartlett's Test of Sphericity is 0.000, meaning that factors that form the variables are adequate.

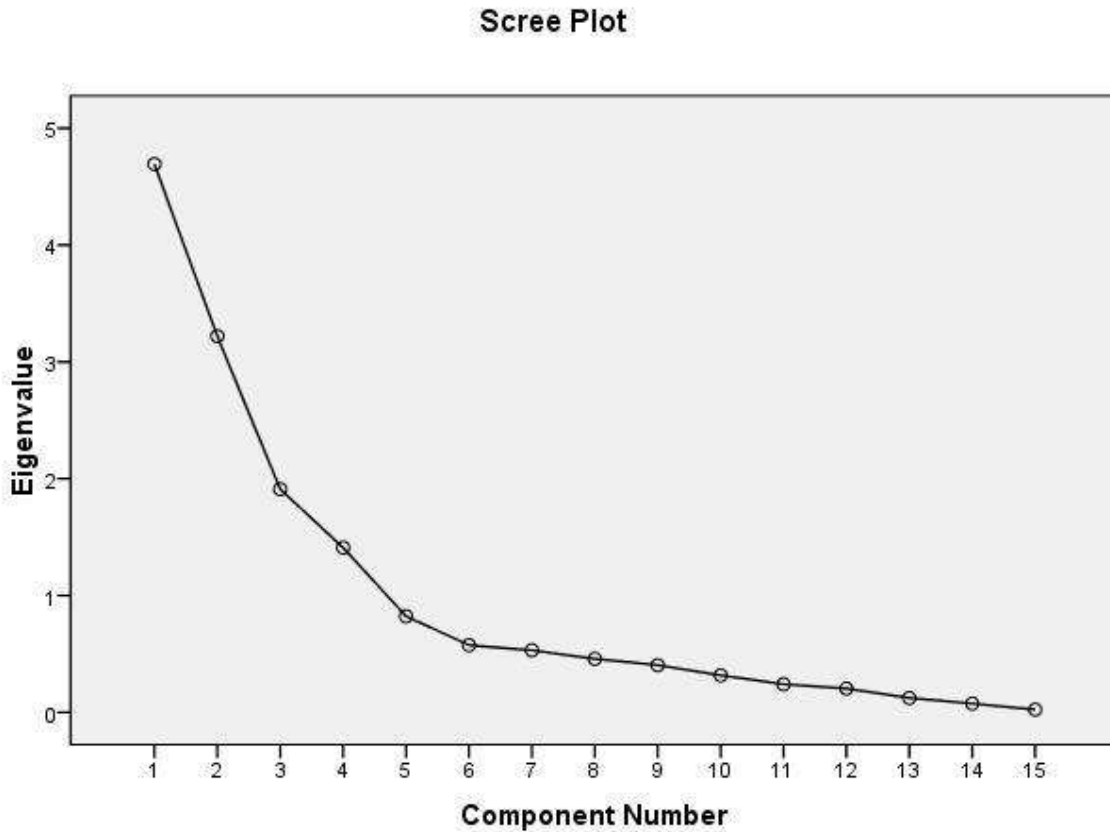
Table No. 3 Total Variance explained for Problem Factors

Component	Initial Eigenvalues			Rotation Sums of Squared Loadings		
	Total	% of Variance	Cumulative %	Total	% of Variance	Cumulative %
1	4.694	31.290	31.290	3.325	22.168	22.168

2	3.220	21.469	52.760	3.156	21.038	43.206
3	1.910	12.734	65.494	2.708	18.050	61.256
4	1.409	9.390	74.884	2.044	13.628	74.884
5	.822	5.482	80.366			
6	.575	3.832	84.198			
7	.531	3.539	87.737			
8	.457	3.049	90.786			
9	.403	2.690	93.476			
10	.316	2.106	95.582			
11	.240	1.602	97.184			
12	.203	1.352	98.537			
13	.122	.815	99.351			
14	.075	.498	99.849			
15	.023	.151	100.000			
Extraction Method: Principal Component Analysis.						

The factor analysis by principal component method with varimaxrotation has revealed four eigen values as 3.325, 3.156, 2.708 and 2.044 respectively. This indicated that the eigen values greater than 1 led to theexistence of four major factors with 74.884 percent of variance (Table - 4.18).These factors are subjected to continuous varimax rotation with respect to thecorrelation values and component-wise segregation which has been givenbelow:

Figure:1



The above Component number explains the trend of the 15 variables based on Initial Eigen value. The movement of trend from the left it is higher value and step downwards towards right. This is a good sign to apply Factor analysis techniques.

Table No. 4 Rotated Component Matrix for Problem Factors

Rotated Component Matrix ^a				
	Component			
	1	2	3	4
Factor I Raw Material Problems				
Scarcity of raw materials	.921			
Shortage of raw materials	.908			
Poor knowledge of alternative source	.866			
Troubling with raw materials and supplier	.773			
Factor II Financial Problems				
Legal or bureaucratic Problems		.863		
Low level risk taking attitude		.804		
Financial Problems		.730		
Lack of family support		.701		
Lack of investor's confidence		.649		
Factor III Production Problems				
Lack of skilled labour			.913	
Labour Absenteeism			.863	
Production Problems			.729	
Factor IV Marketing Problems				
Market-oriented risk				.830
Absence of organized marketing				.824
Competition from other small scale units				.754
Extraction Method: Principal Component Analysis.				
Rotation Method: Varimax with Kaiser Normalization.				
a. Rotation converged in 6 iterations.				

The rotated component matrix table indicated the variable loadings in each predominant factors of women entrepreneurial growth. The first factor consisted of three variables which were suitably named as '*Raw Material Problem*'. The second factor contained four variables which were suitably called as '*Financial Problem*'. The third factor included three variables which were

named as '**Production Problem**'. The fourth factor contained three variables which were named as '**Marketing Problem**'.(Table No. 4)

Friedman Test

Table No. 5 Ranking of Problems Factors

S. No	Factor Name	Mean	Rank
1	Raw Material	2.54	II
2	Financial problem	2.57	I
3	Production Problem	2.49	III
4	Marketing Problem	2.40	IV

Source: Primary Data

The above table shows that MSMEs Entrepreneurs are facing various problems identified that the mostly faced in on "**Financial Problem**" occupies first rank followed by "**Raw Material Problem**" second rank, "**Production Problem**" third rank and "**Marketing Problem**" fourth rank.

Findings

- The study reveals that the majority of the respondents are male (87%)
- The age group of the respondent falls in between 21-30 years (51%)
- The majority of the respondents are married (95%)
- 40% of the respondents are secondary level.

Conclusion

This study attempted to know about the problems faced by MSME Entrepreneurs in Hosur Taluk. Factor analysis found that there are four factor components. Legal or bureaucratic Problems, Low level risk taking attitude, Financial Problems, Lack of family support and troubling with raw materials and supplier are the second factor component which is ranked into one. Scarcity of raw materials, Shortage of raw materials, Poor knowledge of alternative source and Troubling with raw materials and supplier are the first factor component which is ranked into two. Lack of skilled labour, Labour absenteeism and production problems are the third factor component which is ranked into third. Marketing-oriented risk, absence of organized marketing and Competition from other small scale units are the fourth factor component which is ranked into four.

Suggestions

The MSMEs Entrepreneurs is mostly faced in on financial problems and then raw material problems, labour problems and also production problems of the MSMEs industry. When the

government is to reduce on financial problem and then to arrange on rawmaterial facilities in MSMEs sectors. The government is provide on this facility for developing on MSMEs Sectors.

Reference

1. *Gottlieb MJ, How to Ruin a Business without Really Trying, Morgan James Publishing, 2014.*
2. *Dr. D.Paul Dhinakaran, "Community Relations Of Tamilnadu State Transport Corporation Ltd" International Journal Of Research And Analytical Reviews (E ISSN 2348-1269, print ISSN 2349-5138) Special Issue March 2019.*
3. *Arun Mittal & Gupta, S.L., Entrepreneurship Development, International Book House Pvt., Ltd., Mumbai, 2011.*
4. *k. Suneetha and T.Sankaraiah, (Mar.-Apr. 2014) Problems of MSMEs and Entrepreneurs in Kadapa District, IOSR Journal of Economis and Finance (IOSR-JEF), e-ISSN: 2321-5933, p-OSSN: 2321-5925, Vol.3, Issue 2. Ver.I, pp 31-37.*
5. *Bonga, Wellington Garikai (2014). 'challenges faced by SMEs on exportation and possible strategies.' Social Science Research Network. Retrieved from: <https://ssrn.com/abstract=2399878>.*
6. *D.Paul Dhinakaran, "Training and Development Programmes in Tamilnadu State Transport Corporation Limited, Kumbakonam", international Journal of Research in Commerce, IT & Management, (ISSN (online):0976 -2183), Volume 3, Issue 12, Dec2013, P. 146-149.*
7. *Shaik, Meeravali and Kankipati, Ajay Kumar and Ramesh, KV and Babu, G. (2017). 'Performance of MSMEs sector in India.' SSRG International Journal of Economics and Management Studies. Vol. 4(3). pp 11-15.*



Contents lists available at ScienceDirect

Chemical Physics Letters

journal homepage: www.elsevier.com/locate/cplett

Perovskite type BaSnO₃-reduced graphene oxide nanocomposite for photocatalytic decolourization of organic dye pollutant

G. Venkatesh^{a,c,*}, R. Suganesh^a, J. Jayaprakash^b, M. Srinivasan^c, K.M. Prabu^{a,*}^a PG & Research Department of Physics, Sri Vidya Mandir Arts & Science College, Katteri, Uthangarai 636 902, India^b Department of Physics, Don Bosco College, Dharmapuri 636 809, India^c SSN Research Centre, Sri Sivasubramaniya Nadar College of Engineering, Kalavakkam 603 110, India

ARTICLE INFO

Keywords:
Surfactant-free
Perovskite
Hydrothermal
rGO

ABSTRACT

rGO-BaSnO₃ nanocomposite was prepared by hydrothermal route. The physicochemical properties were analyzed by spectroscopic analysis. From the results, the rod-like crumbled particles were well dispersed on rGO sheets. The optical bandgap was found to be 2.72 eV for BSG-10 which is comparatively lower than BS. The implementation of rGO makes an interfacial contact with BS facilitates e⁻ transfer from BS to rGO, effectively suppresses the e⁻/h⁺ pair recombination rate. The BSG-10 nanocomposite exhibits 94 % degradation efficiency under 180 min of visible light irradiation. The radical contributions involved in degradation process and the stability of the photocatalysts are also discussed.

1. Introduction

Over the past few years, potential degradable and nondegradable pollutants badly affect the water quality of the ecosystem due to industrial wastes, agricultural practises, mining activities, etc [1,2]. Researchers have discovered many technologies such as physical, chemical and biological treatments to remove organic pollutants as well as water contamination. Amongst all, heterogeneous photocatalysis attracted wide-scale attention owing to its low cost, being eco-friendly, good chemical stability, sustainability and high degradation efficiency [3,4]. Photocatalysis is a technique to degrade or remove the dye molecules present in organic and inorganic pollutants under light irradiation [5]. For this purpose, semiconductor-based photocatalysts such as metal oxides, (oxy) nitrides, selenides, sulphides, etc., have garnered attention to decontaminate the water by dye removal/degradation process [6–8]. However, these photocatalysts plagued with some drawbacks such as low UV–visible light response, unable to migrate the charge carriers on the material surface and highly possible for charge recombination process [9].

Based on the aforementioned drawbacks over semiconductor photocatalysts, an approach towards ABO₃ perovskite became a combating material for efficient photocatalyst. Moreover, it has unique applications like chemical and gas sensor, catalysis, energy storage, electrode materials in solid fuel cells, etc [10]. The attention on Sn based metal oxide

MSnO₃ (M=Ca, Sr, Ba, Zn) perovskites have been reported as an active photocatalyst for dye degradation [11–15]. BaSnO₃ (BS) is an *n*-type semiconductor with a wide bandgap, attracted attention towards optical and electrical properties [16,17]. The photocatalytic activity of this material limits only at UV irradiation. Based on reports there is a need for an approach to develop extend absorption of photocatalysts by UV or visible region. This is a common problem for many researchers in semiconductor-based materials. To overcome this problem a composite with this semiconductor may be alternative system to enhance the property towards specific field of application.

Perovskite-based barium stannate (BaSnO₃) is an *n*-type semiconducting material with perovskite structure. In recent years, it attracts attention due to its superior optical and electrical property towards a wide range of science and technological applications [18–21]. It is a well suitable material for design supercapacitors, light-emitting devices, fuel cells, dielectric ceramics, chemical sensors, and photocatalysts, etc [22,23]. Many researchers have synthesised through various methods like solid-state route [24], hydrothermal [25], sol–gel [26], self-heat-sustained (SHS) route [27], modified combustion [28] and reverse micelle method [29]. All these aforementioned methods are relatively similar thereby it needs to elevate higher temperature, long time reaction process, the necessity of capping agents and toxic compounds were used as a starting material. Moreover, these reports for the modification for the properties of BS need an effective process to become an efficient

* Corresponding authors at: PG & Research Department of Physics, Sri Vidya Mandir Arts & Science College, Katteri, Uthangarai 636 902, India.
E-mail addresses: gvphy2019@gmail.com (G. Venkatesh), kmprabuphys@gmail.com (K.M. Prabu).

<https://doi.org/10.1016/j.cplett.2021.139237>

Received 24 September 2021; Received in revised form 13 November 2021; Accepted 17 November 2021

Available online 20 November 2021

material. The energy consumption for heating is an integral part of any chemical synthetic process. So, the researchers have adopted the microwave irradiation method. It is one of the most desirable sources of energy to resolve the problem. It could be able to rapid volumetric heating without the process of heat conduction, uniform heating can be accomplished in a short duration of time [30–35]. So, the researchers have concentrated their efforts on the conventional hydrothermal method. This method provides a high level of thermal energy and a high level of temperature, which could ease the reduction process and make it faster and more effective [36]. This approach is well suitable for designing an intercalated hybrid nanostructure by maintaining superior optical property, well crystalline, and controlled morphology with size and shape [37]. Moreover, it affords with low temperature, moderate price, large scalability, and relatively simple fabrication procedure [38]. Several workers have utilized wide bandgap material of BaSnO₃ for photocatalytic applications. Moshtagi et al. [39] evaluated the photocatalytic degradation of anionic eriochrome black T dye in UV irradiation. Moshtagi et al. [40] investigated the barium stannate by erythrosine degradation was about 82 % of efficiency after 120 min irradiation in UV light. Zhong et al. [13] reported BaSnO₃ nanoparticles were studied the photocatalytic activity in UV light. Ye and co-workers [41] evaluated the photocatalytic properties of BaSnO₃ with the case of sacrificial reagents under UV light illumination. However, the attempt towards enhancement in photocatalytic activity by use of visible light was not a sense of achievement. So, the modification or implementation of other materials coupled barium stannate photocatalyst is necessary.

In recent years, composite materials have attracted attention because of its numerous advantages and enhanced characteristics compared to other constituent materials. So, the researchers have turned up to carbon-based semiconductor nanocomposites for making and utilizing the properties in a wide field of applications [42]. Due to the outstanding property of graphene with 2-D layered structure by anchoring under the surface layer of the materials [43–45]. The reports on composites with graphene shows the high surface area, porous composition and fast e⁻ transfer technology [46,47]. Graphene-based photocatalysts have been ultimately pursued to be an active material due to efficient charge flexibility, enormous surface area, slow down the electron-hole (e⁻/h⁺) pair recombination and high rate of e⁻ transfer [48,49]. The enhancement in the catalytic activity of the photocatalyst can be occurred by diminishes the e⁻/h⁺ pair recombination by graphene and it works as an e⁻ acceptor for photogenerated e⁻ [50]. Based on the above discussions, we decided to modify the property of BaSnO₃ by implementing rGO in BaSnO₃ to tune the optical bandgap and to improve the light harvesting property for large scale application with carbon based photocatalyst for environmental applications. Moreover, to the best of our knowledge very rare reports are available at present on the use of BaSnO₃ as electron transport promoters under visible light, and its application in photocatalysis by coupling rGO in BaSnO₃ has not yet been studied.

In this work, BaSnO₃-rGO composite was successfully synthesised by facile hydrothermal method. The as-prepared BS and BSG-10 nanocomposite heterostructure formations are systematically characterized and correlated with photocatalytic activity measurement. The photocatalytic performance of the prepared catalysts were investigated over cationic MB dye under visible light irradiation. Furthermore, the role of reactive radicals, photocatalytic mechanism, stability and reusability of the photocatalyst is also determined.

2. Experimental section

2.1. Materials

All the chemicals/precursors were commercially purchased and used without further purification. Tin (IV) chloride (SnCl₄·5H₂O – 97%), Barium hydroxide octahydrate (Ba(OH)₂·8H₂O – 99.99%), Sodium Hydroxide (NaOH – 97%), Graphite powder (99.5%), Hydrogen

peroxide (H₂O₂ – 30% purity), Sulfuric acid (H₂SO₄ – 97%), Hydrochloric acid (HCl – 38.0%), Potassium permanganate (KMnO₄ – 99.0%), Sodium nitrate (NaNO₃ – 99.0%), Methylene Blue (MB), Benzoquinone (BQ – 98%), Isopropyl alcohol (IPA – 99.8%) and Ammonium oxalate ((NH₄)₂C₂O₄ – 99.0%) were used. And de-ionized (DI) water was used for all the experiment processes.

2.2. Synthesis of BS and rGO-BaSnO₃ nanocomposite

The BS photocatalyst was prepared by conventional microwave irradiation method. A stoichiometric quantity of Ba(NO₃)₂ and SnCl₄·5H₂O were added to distilled water and stirred for 30 min at room temperature. The mixture was then added with NaOH for the suspension to get precipitation. The precipitated mixture was transferred to a silica crucible and placed in a microwave oven. The mixture was approved and processed for 20 min with 700 W of microwave irradiation. The solution was first irradiated by microwaves and then the compositions began to boil and dehydrated as part of the mixtures with continuous radiation. Finally, a centrifugation process was performed to eliminate unreacted ions by carefully washing the product with ethanol and DI water. Finally, the resultant products were annealed at 700 °C for 3 h in a muffle furnace.

The preparation of GO was prepared by same procedure reported in our previous work [51]. The synthesis of rGO-BaSnO₃ was obtained by facile hydrothermal method. The schematic representation of the synthesis procedure shown in Fig. 1. A suitable amount of GO was initially dispersed in the mixture containing 50 mL DI water, 25 mL ethanol in an aluminium foil closed 100 mL beaker to avoid evaporation of liquid molecules. Then it was thoroughly dispersed by ultrasonication for 2 h. After the dispersion of GO in the mixed solution, 0.4 g of synthesised BS was added and stirred for 3 h to get homogenous suspension. Then the mixture was transferred into 100 mL Teflon-lined stainless-steel autoclave and placed in a hot-air oven with 120 °C of reaction temperature for overnight to obtain the formation of the BSG-10 nanocomposite. The resultants were then finally, centrifuged and washed with ethanol and DI water several times and dried at 80 °C for 12 h. Then the prepared pure BS and GO-BaSnO₃ nanocomposite samples were labelled as BS and BSG-10.

2.3. Photocatalytic experiments

The investigation of photocatalytic activity for the synthesized photocatalysts over MB dye was done under visible irradiation. To exhibit the dye degradation effect 100 mg of photocatalyst was initially dissolved into MB aqueous solution. Prior to the reaction and illumination, the solution was kept under the dark condition for 30 min to attain absorption/desorption equilibrium. During the photocatalytic process, 1 mL of aliquots was pipetted out for every 30 min up to 180 min to measure the dye concentration. Then the absorption of the dye solution was measured by UV–vis. spectroscopy. The degradation efficiency of the photocatalysts were calculated by empirical equation [51].

The radical trapping experiment was carried out to detect the active species involved in the degradation reaction process. The addition of scavengers was 1 mM of benzoquinone (BQ) for superoxide radicals (O₂⁻), 1 mM of isopropyl alcohol (IPA) for hydroxyl radicals (·OH) and 1 mM of ammonium oxalate (AO) for holes (h⁺) radicals was established by typical degradation experiment.

3. Results and discussion

3.1. Structural analysis

The crystalline phase and purity of GO, BS and BSG-10 nanocomposite was recorded using powder X-ray diffractometer. From Fig. 2, the observed diffraction peaks of BSG-10 composite show obviously similar to BS. The indexed characteristic peaks detected at an angle 2θ =

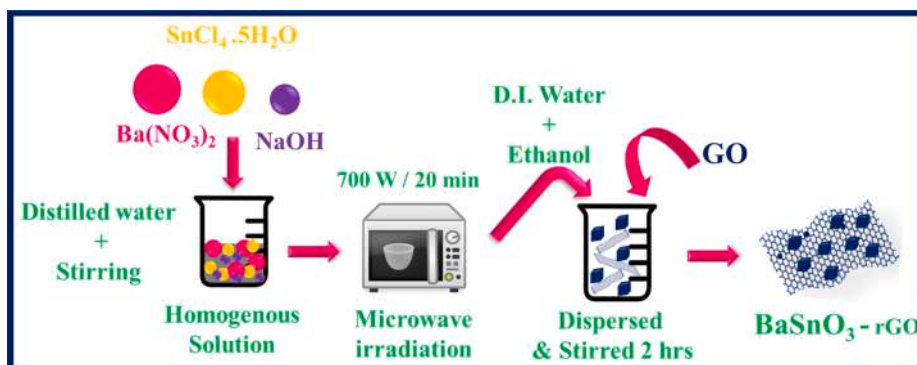


Fig. 1. Schematic representation of the synthesis procedure for BS and BSG-10 nanocomposite.

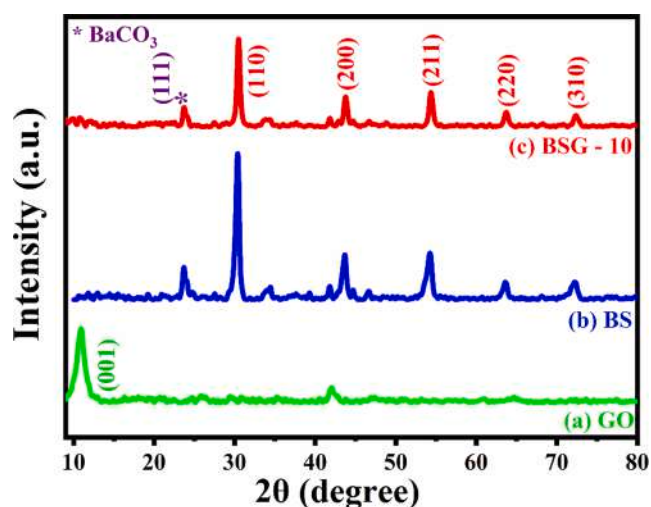


Fig. 2. XRD patterns for (a) GO, (b) BS and (c) BSG-10 nanocomposite.

30.68°, 43.95°, 54.56°, 63.90° and 72.55° which corresponds to (1 1 0), (2 0 0), (2 1 1), (2 2 0) and (3 1 0) crystal planes. The recorded peaks were agreed well with JCPDS No. 15–0780 and the synthesized sample corresponds to cubic structure. The indexed XRD peaks of (1 1 1) plane at 23.89° matched with JCPDS No. 45–1741 of BaCO₃. The presence of BaCO₃ does not involve in the preparation process of BS. However, it exhibits only due to Ba²⁺ ions directly reacted with atmospheric CO₂ [52]. While the addition of GO to BS no diffraction peaks of rGO exhibited in BSG-10 composite peaks but it partially varies the intensity of the composite compared to pure BS. This unveiled the successful formation of composite in the rGO assisted sample. Therefore, the synthesized BS would be surrounded by dispersed rGO sheets that can exhibit in the BSG-10 nanocomposite.

3.2. FTIR analysis

The investigated FTIR spectra of BS and BSG-10 shown in Fig. 3. The spectra recorded in the wavenumber range of 4000–470 cm⁻¹. The strong respective characteristic peak observed at 520 and 630 cm⁻¹ ascribed to Sn–O stretching mode of vibration that contributes uniform regular SnO₆ octahedra metal stannates [53]. The observable characteristic peaks of graphene lie between 4000 and 900 cm⁻¹. As like the functional group of O–H stretching bond vibration present at 3500 and 3000 cm⁻¹ [54]. The band observed at 854 and 1063 cm⁻¹ are due to the presence of carbonates in the synthesized sample. Furthermore, three peaks observed at 1442, 1204 and 854 cm⁻¹ are attributed to C–O and C=O stretching modes [28]. The stretching mode of the observed peaks at 1350 and 987 cm⁻¹ shows a difference in intensity and full-width half

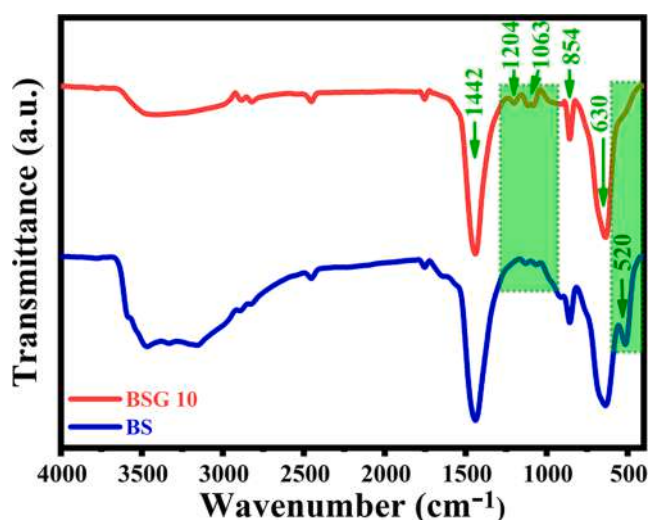


Fig. 3. FT-IR spectra for BS and BSG-10 nanocomposite.

maximum confirms the oxygen-containing functional groups were dramatically reduced and exhibits the formation of graphene oxide into reduced graphene oxide.

3.3. Morphological and elemental analysis

The internal structure and surface morphology of the prepared BS and BSG-10 composite were studied by FESEM and HRTEM as shown in Fig. 4. The recorded FESEM image for rGO sheets as shown in Fig. 4(a). It reveals that rGO sheets were well dispersed with some folds on the surface layer. From Fig. 4(b), the synthesized BS has crumbled particles with an agglomerated rod-like morphology. Moreover, these particles were monodispersed on the surface of the rGO sheets shown in Fig. 4(c). These results indicate the bonding between BS and the specific sites of GO successfully formed during hydrothermal treatment. The nanocomposite with interfacial connect between BS and rGO could improve the charge transfer property and the current collector. Moreover, the elemental composition of the BSG-10 nanocomposite was analyzed by using EDX as shown in inset of Fig. 4(c). The presence of Ba, Sn, O and C elements was confirmed by EDX spectra shown in inset of Fig. 4(c). Moreover, the Cu element arose from the copper grid used for analysis. The mass and atomic percentage of the elements depicted in the inset of EDX spectra.

From the HRTEM image, as shown in Fig. 4(d) crumbled particles of BS with rods were surrounded by rGO sheets, which reveals the efficacious formation of the composite. From Fig. 4(e) the rGO sheet isolated and the interplanar space distance of the nanoparticles appeared. The obtained lattice fringes with an interplanar distance of the BSG-10

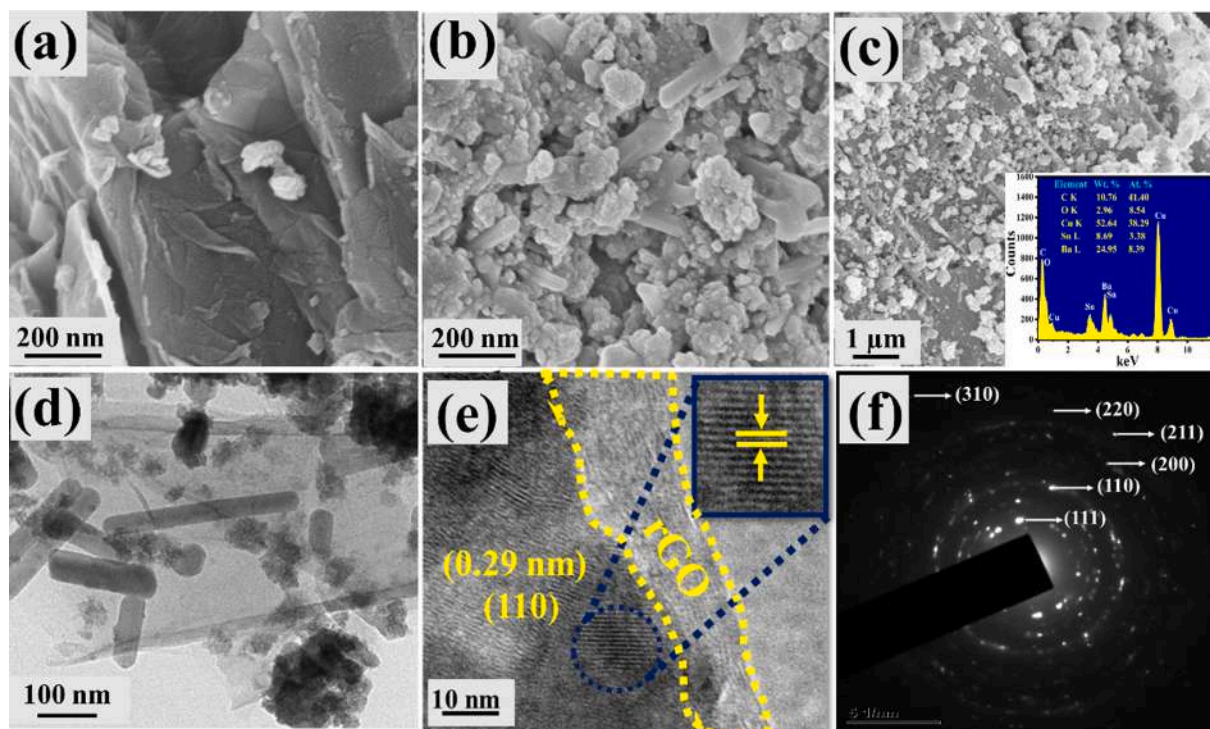


Fig. 4. FESEM image of (a) rGO sheet, (b) BS, (c) BSG-10 nanocomposite (inset shows EDX spectra), (d & e) TEM & HRTEM images and (f) SAED pattern of BSG-10 nanocomposite.

nanocomposite was measured and calculated as 0.29 nm, which can be well indexed to the (110) crystal plane and coordinated with XRD peaks. Furthermore, from inset Fig. 4(e) the lattice fringes with different orientation confirm the synthesized product could be polycrystalline material. The selected area diffraction pattern of BSG-10 nanocomposite is depicted in the inset of Fig. 4(e), the obtained bright spots with rings were well accordance with the crystal planes of synthesised sample.

3.4. Optical property analysis

The optical properties of the synthesized samples were examined by UV-vis. absorption spectroscopy. The absorption spectra of the synthesized sample were recorded in the range of 200 to 800 nm shown in Fig. 5. As shown in Fig. 5, the recorded spectra for BS and BSG-10

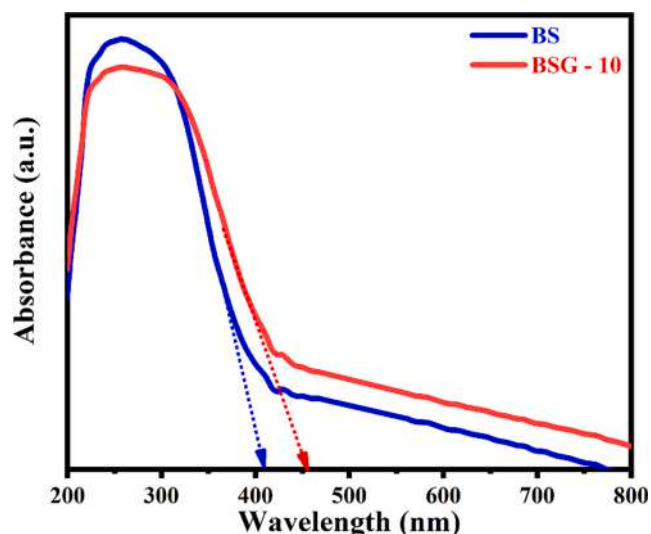


Fig. 5. UV-vis. absorption Spectra for BS and BSG-10 nanocomposite.

samples heavily absorbs and predominantly rising at ~ 330 nm in the nearer to the visible region. Moreover, BSG-10 nanocomposite's absorption ability shows its response in the visible region. It is only due to the implementation of rGO and ascribes to create high-mobility π (π) electrons, which is placed upper and under of the graphene sheet. Generally, these π (π) orbitals tend to overlap could be enhanced by the presence of carbon-carbon bonding in graphene oxide sheet [55]. Furthermore, the bandgap of the samples were determined by using Tauc's equation based on absorption spectra are shown in Fig. 5. The obtained band gap value (absorption edge) for BS and BSG-10 were 3.06 eV (405 nm) and 2.72 eV (455 nm), respectively. The absorption band edge positions possess UV-vis. region with strong absorption peak at ~ 400 nm to ~ 460 nm is due to π - π^* transition [56]. The strong absorption bands associated with the wavelength 405 nm is mainly by optical transitions from valence band (VB) to conduction band (CB) involving Sn^{4+} : 5s and O_2^{2-} : 2p orbitals [57]. After the reduction of GO to rGO, the generation of electronic transfer including π and π^* orbitals in sp² remains in the graphene structure [58]. Thus, the rGO incorporated BaSnO₃ showed its increased absorption edge at 455 nm. The shift in absorption edge occurred due to electronic coupling between rGO and BS [59]. Therefore, the strong coupling between these heterostructures leads to enhances the light harvesting efficiency of BSG 10 nanocomposite. Based on the above results, it reveals that both the synthesized samples could respond to visible light spectrum. Therefore, rGO plays a major role in modifying the optical properties of perovskites towards the visible light region.

3.5. Photoluminescence analysis (PL)

The PL spectra of BS and BSG-10 nanocomposite obtained with an excitation wavelength of 400 nm shown in Fig. 6. The recorded spectra attribute to the green emission region which commonly refers to the trapping state region of emission [60]. Specifically, the green emission transition was due to the individual ionized oxygen vacancy in BS and emission results from a photogenerated h^+ radiation recombination with an e^- which occupies the oxygen vacancy [61]. Moreover, the

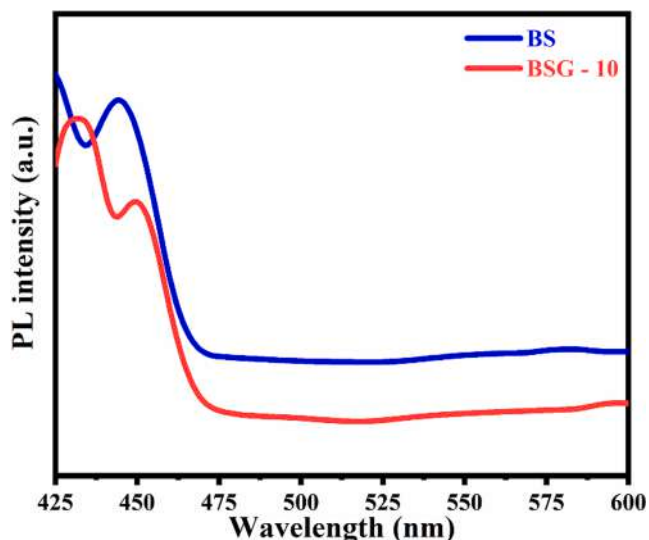


Fig. 6. PL spectra of pure BS and BSG-10 nanocomposite.

introduction of rGO into BS the intensity of the spectra decreases while compared with pure BS, which suggests that the photogenerated charge carriers are separated effectively and affect the recombination process. Therefore, it suggests that the synthesized nanocomposite could enhance the photocatalytic efficiency.

3.6. Photocatalytic activity

The photocatalytic activity of the synthesized BS, BSG-10 photocatalysts were estimated by the degradation of MB dye by employing visible light irradiation as a source. The evaluation of photocatalytic efficiency was carried out by the UV-vis. absorption spectra of the illuminated samples with different time intervals. The recorded UV-vis. absorption spectra for BS and BSG-10 photocatalysts were shown in Fig. 7(a & b). It can be seen that the comparison of before and after the illumination of light at samples shown extraordinary changes in their absorption peak. Before the illumination, the suspension was stirred for several min and kept under the dark condition to ensure the absorption-desorption equilibrium. The MB dye with the presence of photocatalysts was not degraded in the dark condition. Both the MB dye absorption spectra observed at 664 nm and the respective spectra were collected from 0 min to 30 min of regular time interval until the decolourization occurs. The absorption intensity of MB dye gradually decreased its intensity by increasing the irradiation time of visible light and the obtained spectra shown in Fig. 7(a & b). The decolourization

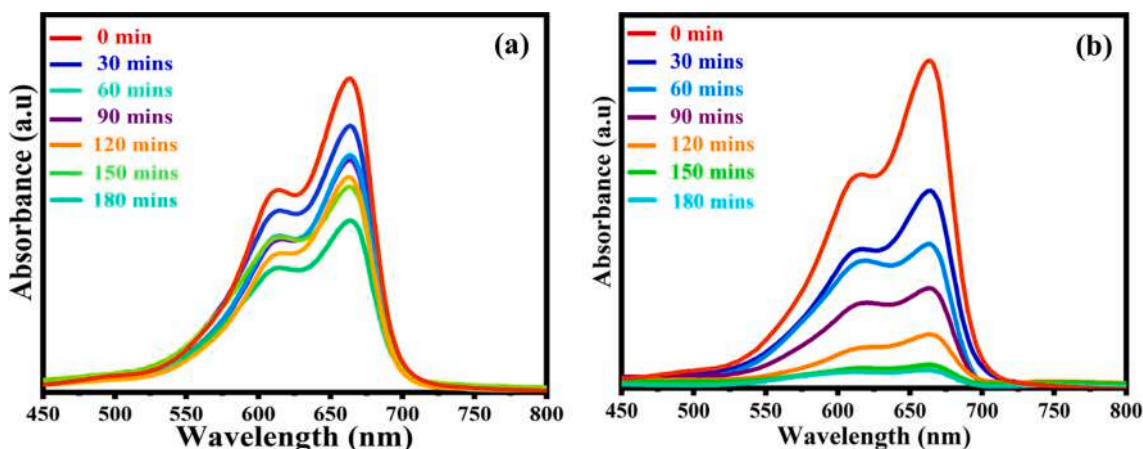


Fig. 7. UV-vis. absorption spectra for the degradation of MB dye under visible light irradiation of (a) BS and (b) BSG-10 photocatalyst.

spectra recorded up to 180 min for BS and BSG-10 photocatalyst. BS and BSG-10 photocatalysts degrade 46 % and 94 % of MB dye respectively for 180 min of visible light irradiation and the degradation percentage was calculated, visualized in Fig. 8. All the photocatalytic reaction process was carefully monitored by using UV-vis. spectrophotometer.

Notably, the degradation efficiency of BSG-10 shows superior photocatalytic activity compared to BS. This may due to the presence of rGO in the nanocomposite that enhances the improvement of its structural and electronic properties. Moreover, its photocatalytic efficiency is suppressed by a high charge recombination process that causes a reduction in photodegradation efficacy against MB. During the hydrothermal process, the specific sites of GO and pure BS ascribed to chemical bonding between them. The approximated bandgap of pure BS is 3.06 eV and the BSG-10 nanocomposite existed with -0.34 eV of 2.72 eV. Thus, the synthesized BSG-10 could be easily photoexcited and generates more e^-/h^+ pairs leads to higher photocatalytic activity.

i) Scavenger Test

The investigation of various reactive species responsible for the photocatalytic process has been detected by radical experiments. The scavengers BQ ($O_2^{\cdot -}$ superoxide), AO (h^+ holes) and IPA ($\cdot OH$ super hydroxyl) respectively were used for respective experiments under visible irradiation. As shown in Fig. 9, the addition of IPA as a scavenger the degradation of MB dye was not affected and it was almost close to the

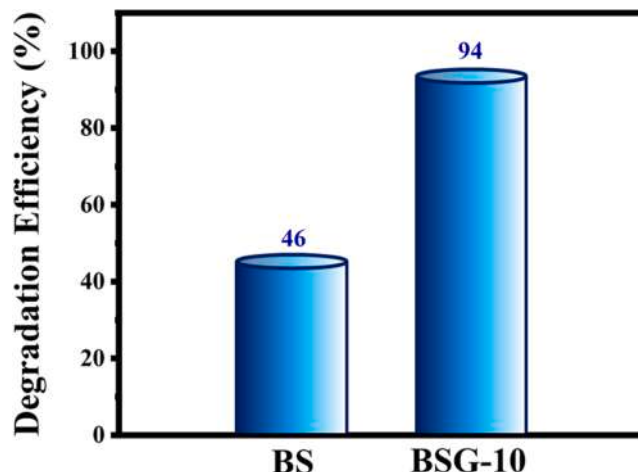


Fig. 8. Photodegradation efficiency of MB dye for BS and BSG-10 nanocomposite.

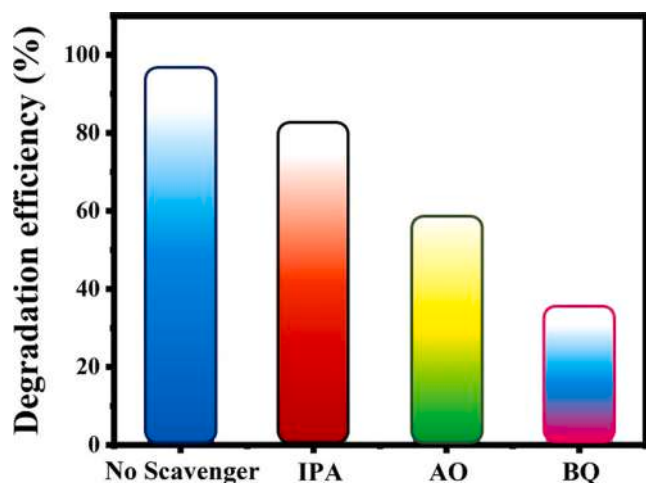


Fig. 9. Effect of various scavenging agents on the MB photodegradation for BSG-10 nanocomposite under visible light irradiation.

bare BGN photocatalyst. While adding AO and BQ as a scavenger the radicals of h^+ scavenger and $O_2^{\cdot-}$ scavenger obviously decrease the degradation efficiency and the photocatalytic activity was greatly suppressed. Furthermore, the h^+ radical also drastically quenches degradation. Therefore, the dominating active species in the radical experiment utilized in BGN photocatalyst was superoxide radical ($O_2^{\cdot-}$). These results suggesting the main active species involved in the degradation was identified and the series of radicals affecting the degradation in the order ' $OH > h^+ > O_2^{\cdot-}$ '.

ii) Reusability and Stability Measurement

As known, the superior photocatalytic ability could expect by recycling the photocatalysts under the same reaction conditions of degradation experiment. To evaluate the stability and reusability of the photocatalyst is one of the most vital parameters. So, the synthesized photocatalyst of BSG-10 was subjected to the experiment. As depicted in Fig. 10(a), the BSG-10 photocatalyst exhibits with slightly little loss of photodegradation efficiency in each cycle of recycle experiment up to 4 cycles. Moreover, the photocatalysts showed comparatively higher photocatalytic degradation ability. As observed in Fig. 10(b), after 4 successive runs of the photocatalyst it could be actively maintained the degradation efficiency indicates the good stability of the photocatalyst.

The drawn XRD patterns are also unaffected which confirms that the BSG-10 photocatalyst undoubtedly a stable, efficient and non-photo corrosion material for photocatalytic based practical applications. Comparison of degradation efficiency of the prepared BSG-10 photocatalyst with earlier reports is shown in Table 1.

iii) Possible photocatalytic mechanism

The photocatalytic ability of the photocatalyst can be determined by a crucial role played by an optical energy bandgap of the material. Based on experiments results, the photocatalytic mechanism efficiently described and proposed in Fig. 11. The potentials of the VB and CB plays a significant role in promoting the charge carrier process in the electrolytic reaction system. The absorption of photon energy is larger than or equal to the bandgap of a material that excites an e^- from the VB to CB, which means the production of e^-/h^+ pairs. The halving reaction begins as the photogenerated e^- has a potential which exceeds the redox couple's reduction potential. The photogenerated h^+ also needs to have a potential that reaches the oxidation half-reaction of redox potential. The band edge alignments of CB and VB of the semiconductor photocatalyst can be calculated by using the equation [67],

$$E_{CB} = \chi - E_C + 0.5E_g \quad (1)$$

$$E_{VB} = E_{CB} - E_g \quad (2)$$

where, χ is the geometric mean of absolute electronegativity of the

Table 1

Comparison study of dye degradation efficiencies by previously reported photocatalysts.

S. No.	Photocatalyst	Degradation efficiency (%)	Reaction time (min)	Pollutant	References
1.	Bi_2O_3 -RGO	96	240	MB	[62]
2.	PANI/graphite oxide	89	180	MB	[63]
3.	$g-C_3N_4/BaTiO_3$	76	360	MB	[64]
4.	SnO_2	82	180	MB	[65]
5.	$CoFe_2O_4$ - graphene	100	240	MB	[66]
6.	10 wt% rGO/ $BaSnO_3$ (BSG-10)	94	180	MB	This work

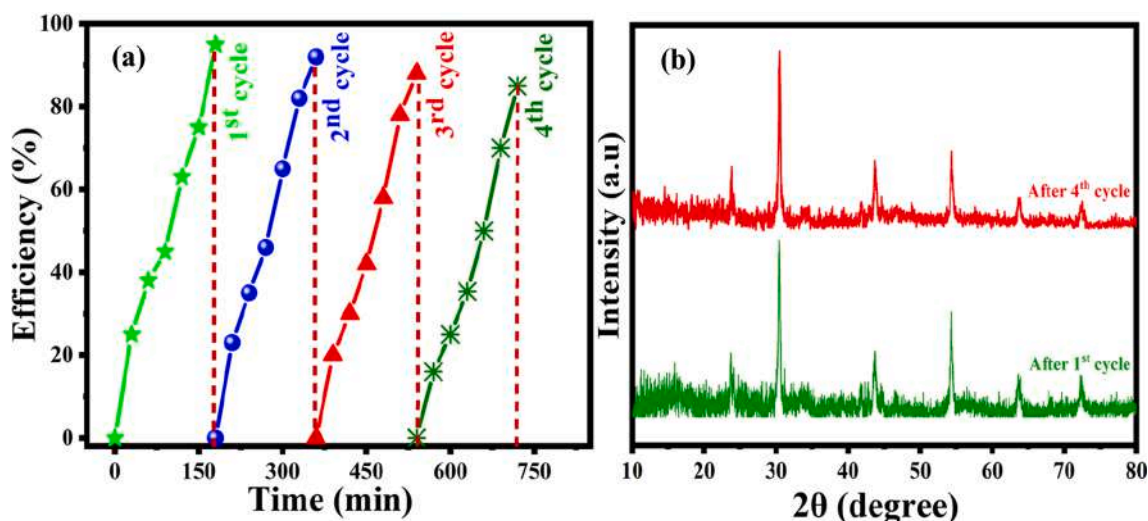


Fig. 10. (a) Recyclability and (b) reusability test for BSG-10 photocatalyst.

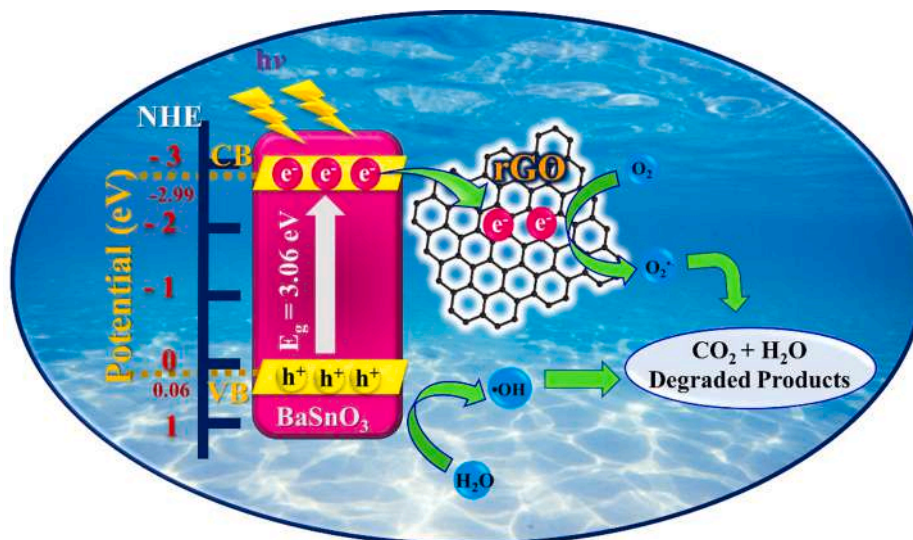
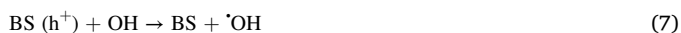


Fig. 11. Possible photocatalytic degradation mechanism.

semiconductor, E_C is the free electron energy on hydrogen scale (~ 4.5 eV), E_{VB} is the VB edge potential and E_g is the bandgap of semiconductor [68]. The values obtained from the calculation for BS band edge potential value of E_{VB} is 0.061 eV/NHE and the E_{CB} value is -2.99 eV/NHE. Moreover, the energy bandgap (E_g) of the synthesized material is 3.06 eV. From these obtained band edge potential values of CB and VB is well suited with the calculated optical energy bandgap of BS as $E_g = 3.06$ eV. So, the synthesized sample is definitely suitable for e^-/h^+ separation with an increased lifetime. Moreover, the implementation of rGO as a composite, can easily be contacted with BS makes the charge transfer process easier. Though rGO has oxygen-containing groups that act as a capturing medium between them and accelerating the charge transfer across the heterostructure of the nanocomposite. Therefore, the synthesized nanocomposite could be attributed to enhancement in photocatalytic activity compared to pure BS.

In the photocatalytic experiment, throughout the process, visible light irradiation has used the e^- and h^+ are generated from CB and VB of BS respectively. The e^- from CB of BS are accelerated towards rGO which makes solid–solid contact between BS and rGO. Graphene with its excellent e^- export ability leads to induce the photogenerated e^- quickly from BS to rGO network. Then rGO (e^-) reacts with absorbed O_2 to produce superoxide radicals $O_2^{\bullet -}$. While some unreacted radicals of $O_2^{\bullet -}$ could react with H_2O to generate hydroxy radical $\cdot OH$. The solid–solid contact between BS and rGO the e^- from BS may be trapped by rGO network and it extends the lifetime of charge carriers and suppress the recombination rate. Furthermore, the photoinduced e^- from the surface of BS and the trapped e^- of rGO tempt the redox reaction to the targeted pollutant of MB dye. Though reduced GO serves as a backbone (accelerating the e^-) of e^- , h^+ separation mechanism. The possible photocatalytic chemical reaction as follows,



4. Conclusion

The $BaSnO_3$ -rGO nanocomposite was successfully synthesized by a simple hydrothermal method. The prepared nanocomposites were characterized by XRD, FTIR, FESEM, HRTEM, UV, PL analysis and photocatalytic experiments. Based on the results, the effective formation between rGO and $BaSnO_3$ as a nanocomposite enhances the photocatalytic efficiency with shrinkages in the charge recombination process. The synthesized BS and BSG-10 nanocomposite reveal cubic crystalline structure. The optical bandgap was tuned and it is partially decreased with BSG-10 nanocomposite compared to BS. The prepared nanocomposite shows that the rGO sheets were well dispersed and exfoliated over pure BS. The photocatalytic performance of the synthesized photocatalyst achieved with 94 % of degradation efficiency over MB dye as a model pollutant under 180 min of visible light irradiation. Furthermore, the catalysts were reused for 4 consecutive runs that shows good photocatalytic stability and reusability.

CRediT authorship contribution statement

G. Venkatesh: Conceptualization, Supervision, Methodology, Writing – review & editing, Project administration, Investigation, Writing – original draft, Visualization. **R. Suganesh:** Methodology, Data curation, Validation, Formal analysis. **J. Jayaprakash:** Data curation, Validation, Formal analysis. **M. Srinivasan:** Data curation, Validation, Formal analysis. **K.M. Prabu:** Supervision, Visualization, Resources, Formal analysis.

Declaration of Competing Interest

The authors declare that they have no known competing financial interests or personal relationships that could have appeared to influence the work reported in this paper.

References

- [1] M. Ikram, T. Inayat, A. Haider, A. Ul-Hamid, J. Haider, W. Nabgan, A. Saeed, A. Shahbaz, S. Hayat, K. Ul-Ain, A.R. Butt, Graphene Oxide-Doped MgO Nanostructures for Highly Efficient Dye Degradation and Bactericidal Action, *Nanoscale Res. Lett.* 16 (2021) 56, <https://doi.org/10.1186/s11671-021-03516-z>.
- [2] M. Ikram, J. Hassan, M. Imran, J. Haider, A. Ul-Hamid, I. Shahzadi, M. Ikram, A. Raza, U. Qumar, S. Ali, 2D chemically exfoliated hexagonal boron nitride (hBN) nanosheets doped with Ni: synthesis, properties and catalytic application for the treatment of industrial wastewater, *Appl. Nanosci.* 10 (9) (2020) 3525–3528, <https://doi.org/10.1007/s13204-020-01439-2>.

- [3] M. Ikram, A. Raza, M. Imran, A. Ul-Hamid, A. Shahbaz, S. Ali, Hydrothermal Synthesis of Silver Decorated Reduced Graphene Oxide (rGO) Nanoflakes with Effective Photocatalytic Activity for Wastewater Treatment, *Nanoscale Res. Lett.* 15 (2020) 95, <https://doi.org/10.1186/s11671-020-03323-y>.
- [4] A. Ibhaddon, P. Fitzpatrick, Heterogeneous Photocatalysis: Recent Advances and Applications, *Catalysts*. 3 (2013) 189–218, <https://doi.org/10.3390/catal3010189>.
- [5] S. Megala, S. Prabhu, S. Harish, M. Navaneethan, S. Sohila, R. Ramesh, Enhanced photocatalytic dye degradation activity of carbonate intercalated layered Zn, ZnNi and ZnCu hydroxides, *Appl. Surf. Sci.* 481 (2019) 385–393, <https://doi.org/10.1016/j.apsusc.2019.03.091>.
- [6] R. Narayanan, M. Deepa, A.K. Srivastava, Nanoscale connectivity in a TiO₂/CdSe quantum dots/functionalized graphene oxide nanosheets/Au nanoparticles composite for enhanced photoelectrochemical solar cell performance, *Phys. Chem. Chem. Phys.* 14 (2) (2012) 767–778, <https://doi.org/10.1039/C1CP22548K>.
- [7] R. Nakamura, T. Tanaka, Y. Nakato, Oxygen Photoevolution on a Tantalum Oxynitride Photocatalyst under Visible-Light Irradiation: How Does Water Photooxidation Proceed on a Metal–Oxynitride Surface? *J. Phys. Chem. B*. 109 (2005) 8920–8927, <https://doi.org/10.1021/jp0501289>.
- [8] C. Le Paven-Thivet, A. Ishikawa, A. Ziani, L. Le Gendre, M. Yoshida, J. Kubota, F. Tessier, K. Domen, Photoelectrochemical Properties of Crystalline Perovskite Lanthanum Titanium Oxynitride Films under Visible Light, *J. Phys. Chem. C*. 113 (15) (2009) 6156–6162, <https://doi.org/10.1021/jp811100r>.
- [9] M. Rastogi, H.S. Kushwaha, R. Vaish, Highly efficient visible light mediated azo dye degradation through barium titanate decorated reduced graphene oxide sheets, *Electron. Mater. Lett.* 12 (2) (2016) 281–289, <https://doi.org/10.1007/s13391-015-5274-8>.
- [10] R. Sarvari, S. Agbolaghi, B. Massoumi, Engineered organic halide perovskite solar cells by incorporation of surface-manipulated graphenic nanosheets, *J. Mater. Sci. Mater. Electron.* 30 (10) (2019) 9281–9288, <https://doi.org/10.1007/s10854-019-01258-4>.
- [11] Z. Song, J. Zhao, Q. Liu, Luminescent perovskites: recent advances in theory and experiments, *Inorg. Chem. Front.* 6 (11) (2019) 2969–3011, <https://doi.org/10.1039/C9QI00777F>.
- [12] Z. Lu, L. Chen, Y. Tang, Y. Li, Preparation and luminescence properties of Eu³⁺-doped MSnO₃ (M = Ca, Sr and Ba) perovskite materials, *J. Alloys Compd.* 387 (1–2) (2005) L1–L4, <https://doi.org/10.1016/j.jallcom.2004.06.036>.
- [13] F. Zhong, H. Zhuang, Q. Gu, J. Long, Structural evolution of alkaline earth metal stannates MSnO₃ (M = Ca, Sr, and Ba) photocatalysts for hydrogen production, *RSC Adv.* 6 (48) (2016) 42474–42481, <https://doi.org/10.1039/C6RA05614H>.
- [14] S.K. Gupta, B. Modak, D. Das, P. Modak, A.K. Yadav, K. Sudarshan, Multiphoton light emission in barium stannate perovskites driven by oxygen vacancies, *Eu 3+ and La 3+ : accessing the role of defects and local structures*, *Phys. Chem. Chem. Phys.* 23 (2021) 17479–17492, <https://doi.org/10.1039/D1CP02349G>.
- [15] Q. Chen, Y. Wang, M. Wang, S. Ma, P. Wang, G. Zhang, W. Chen, H. Jiao, L. Liu, X. Xu, Enhanced acetone sensor based on Au functionalized In-doped ZnSnO₃ nanofibers synthesized by electrospinning method, *J. Colloid Interface Sci.* 543 (2019) 285–299, <https://doi.org/10.1016/j.jcis.2019.02.055>.
- [16] M.J. Schafer, T.A. White, K. Iijima, A.J. Haak, G. Ligresti, E.J. Atkinson, A.L. Oberg, J. Birch, H. Salmonowicz, Y. Zhu, D.L. Mazula, R.W. Brooks, H. Fuhrmann-Stroissnigg, T. Pirtskhalava, Y.S. Prakash, T. Tchkonina, P.D. Robbins, M.C. Aubry, J.F. Passos, J.L. Kirkland, D.J. Tschumperlin, H. Kita, N.K. LeBrasseur, Cellular senescence mediates fibrotic pulmonary disease, *Nat. Commun.* 8 (2017) 14532, <https://doi.org/10.1038/ncomms14532>.
- [17] Y. Zhang, M.P.K. Sahoo, J. Wang, Tuning the band gap and polarization of BaSnO₃/SrSnO₃ superlattices for photovoltaic applications, *Phys. Chem. Chem. Phys.* 19 (10) (2017) 7032–7039, <https://doi.org/10.1039/C6CP06042K>.
- [18] H. Mizoguchi, P.M. Woodward, C.-H. Park, D.A. Keszler, Strong Near-Infrared Luminescence in BaSnO₃, *J. Am. Chem. Soc.* 126 (31) (2004) 9796–9800, <https://doi.org/10.1021/ja048866i10.1021/ja048866i.s001>.
- [19] D.W. Kim, S.S. Shin, S. Lee, I.S. Cho, D.H. Kim, C.W. Lee, H.S. Jung, K.S. Hong, BaSnO₃ Perovskite Nanoparticles for High Efficiency Dye-Sensitized Solar Cells, *ChemSusChem* 6 (3) (2013) 449–454, <https://doi.org/10.1002/cssc.201200769>.
- [20] Y. Yuan, Z. Zhao, J. Zheng, M. Yang, L. Qiu, Z. Li, Z. Zou, Polymerizable complex synthesis of BaZr_{1-x}Sn_xO₃ photocatalysts: Role of Sn⁴⁺ in the band structure and their photocatalytic water splitting activities, *J. Mater. Chem.* 20 (32) (2010) 6772, <https://doi.org/10.1039/c0jm00455c>.
- [21] X. Han, X. Li, X. Long, H. He, Y. Cao, A dielectric and ferroelectric solid solution of (1-x)BaSnO₃-xPbTiO₃ with morphotropic phase boundary, *J. Mater. Chem.* 19 (34) (2009) 6132, <https://doi.org/10.1039/b820229j>.
- [22] W.F. Zhang, J. Tang, J. Ye, Photoluminescence and photocatalytic properties of SrSnO₃ perovskite, *Chem. Phys. Lett.* 418 (1–3) (2006) 174–178, <https://doi.org/10.1016/j.cplett.2005.10.122>.
- [23] C. Udawatte, Low temperature synthesis of pure SrSnO₃ and the (Ba_xSr_{1-x}) SnO₃ solid solution by the polymerized complex method, *Solid State Ionics*. 128 (2000) 217–226, [https://doi.org/10.1016/S0167-2738\(99\)00306-9](https://doi.org/10.1016/S0167-2738(99)00306-9).
- [24] T. Huang, T. Nakamura, M. Itoh, Y. Inaguma, O. Ishiyama, Electrical properties of BaSnO₃ in substitution of antimony for tin and lanthanum for barium, *J. Mater. Sci.* 30 (6) (1995) 1556–1560, <https://doi.org/10.1007/BF00375264>.
- [25] H.J. Gulley-Stahl, W.L. Schmidt, H.A. Bullen, Characterization and reactivity of chromia nanoparticles prepared by urea forced hydrolysis, *J. Mater. Sci.* 43 (22) (2008) 7066–7072, <https://doi.org/10.1007/s10853-008-3056-5>.
- [26] W. Lu, H. Schmidt, Synthesis of nanosized BaSnO₃ powders from metal isopropoxides, *J. Sol-Gel Sci. Technol.* 42 (1) (2007) 55–64, <https://doi.org/10.1007/s10971-006-1508-4>.
- [27] A.-M. Azad, L.L.W. Shyan, T.Y. Pang, C.H. Nee, Microstructural evolution in MSnO₃ ceramics derived via self-heat-sustained (SHS) reaction technique, *Ceram. Int.* 26 (7) (2000) 685–692, [https://doi.org/10.1016/S0272-8842\(00\)00005-5](https://doi.org/10.1016/S0272-8842(00)00005-5).
- [28] A.S. Deepa, S. Vidya, P.C. Manu, S. Solomon, A. John, J.K. Thomas, Structural and optical characterization of BaSnO₃ nanopowder synthesized through a novel combustion technique, *J. Alloys Compd.* 509 (5) (2011) 1830–1835, <https://doi.org/10.1016/j.jallcom.2010.10.056>.
- [29] J. Ahmed, C.K. Blakely, S.R. Bruno, V.V. Poltavets, Synthesis of MSnO₃ (M=Ba, Sr) nanoparticles by reverse micelle method and particle size distribution analysis by whole powder pattern modeling, *Mater. Res. Bull.* 47 (9) (2012) 2282–2287, <https://doi.org/10.1016/j.materresbull.2012.05.044>.
- [30] L.-Y. Meng, B. Wang, M.-G. Ma, K.-L. Lin, The progress of microwave-assisted hydrothermal method in the synthesis of functional nanomaterials, *Mater. Today Chem.* 1–2 (2016) 63–83, <https://doi.org/10.1016/j.mtchem.2016.11.003>.
- [31] A. de la Hoz, Á. Díaz-Ortiz, A. Moreno, Microwaves in organic synthesis. Thermal and non-thermal microwave effects, *Chem. Soc. Rev.* 34 (2) (2005) 164–178, <https://doi.org/10.1039/B411438H>.
- [32] F. Wiesbrock, R. Hoogenboom, U.S. Schubert, Microwave-Assisted Polymer Synthesis: State-of-the-Art and Future Perspectives, *Macromol. Rapid Commun.* 25 (20) (2004) 1739–1764, [https://doi.org/10.1002/\(ISSN\)1521-392710.1002/marc.v25:2010.1002/marc.200400313](https://doi.org/10.1002/(ISSN)1521-392710.1002/marc.v25:2010.1002/marc.200400313).
- [33] A.R. Hajipour, F. Rafiee, A.E. Ruoho, A rapid and convenient method for the synthesis of aldoximes under microwave irradiation using in situ generated ionic liquids, *J. Iran. Chem. Soc.* 7 (1) (2010) 114–118, <https://doi.org/10.1007/BF03245867>.
- [34] C. Zhang, L. Liao, S. (Sarah) Gong, Recent developments in microwave-assisted polymerization with a focus on ring-opening polymerization, *Green Chem.* 9 (2007) 303, <https://doi.org/10.1039/b608891k>.
- [35] L. Li, Y.-J. Zhu, M.-G. Ma, Microwave-assisted preparation of calcium sulfate nanowires, *Mater. Lett.* 62 (30) (2008) 4552–4554, <https://doi.org/10.1016/j.matlet.2008.08.040>.
- [36] M.A. Basith, R. Ahsan, I. Zarin, M.A. Jalil, Enhanced photocatalytic dye degradation and hydrogen production ability of Bi₂₅FeO₄₀-rGO nanocomposite and mechanism insight, *Sci. Rep.* 8 (2018) 11090, <https://doi.org/10.1038/s41598-018-29402-w>.
- [37] Y.M. Rangel-Hernandez, J.C. Rendón-Angeles, Z. Matamoros-Veloza, M.I. Pech-Canul, S. Diaz-de la Torre, K. Yanagisawa, One-step synthesis of fine SrTiO₃ particles using SrSO₄ ore under alkaline hydrothermal conditions, *Chem. Eng. J.* 155 (1–2) (2009) 483–492, <https://doi.org/10.1016/j.cej.2009.07.024>.
- [38] S.S. Patil, M.G. Mali, M.A. Hassan, D.R. Patil, S.S. Kolekar, S.-W. Ryu, One-Pot in Situ Hydrothermal Growth of BiVO₄/Ag-rGO Hybrid Architectures for Solar Water Splitting and Environmental Remediation, *Sci. Rep.* 7 (2017) 8404, <https://doi.org/10.1038/s41598-017-08912-z>.
- [39] S. Moshtaghi, S. Zinatloo-Ajabshir, M. Salavati-Niasari, Preparation and characterization of BaSnO₃ nanostructures via a new simple surfactant-free route, *J. Mater. Sci. Mater. Electron.* 27 (1) (2016) 425–435, <https://doi.org/10.1007/s10854-015-3770-0>.
- [40] S. Moshtaghi, S. Zinatloo-Ajabshir, M. Salavati-Niasari, Nanocrystalline barium stannate: facile morphology-controlled preparation, characterization and investigation of optical and photocatalytic properties, *J. Mater. Sci. Mater. Electron.* 27 (1) (2016) 834–842, <https://doi.org/10.1007/s10854-015-3824-3>.
- [41] L.M.C. Honorio, M.V.B. Santos, E.C. da Silva Filho, J.A. Osajima, A.S. Maia, I.M. G. dos Santos, Alkaline earth stannates applied in photocatalysis: prospection and review of literature, *Cerâmica*. 64 (2018) 559–569, <https://doi.org/10.1590/0366-69132018643722480>.
- [42] M. Ikram, R. Tabassum, U. Qumar, S. Ali, A. Ul-Hamid, A. Haider, A. Raza, M. Imran, S. Ali, Promising performance of chemically exfoliated Zr-doped MoS₂ nanosheets for catalytic and antibacterial applications, *RSC Adv.* 10 (35) (2020) 20559–20571, <https://doi.org/10.1039/D0RA02458A>.
- [43] M. Ikram, S. Ali, M. Aqeel, A. Ul-Hamid, M. Imran, J. Haider, A. Haider, A. Shahbaz, S. Ali, Reduced graphene oxide nanosheets doped by Cu with highly efficient visible light photocatalytic behavior, *J. Alloys Compd.* 837 (2020) 155588, <https://doi.org/10.1016/j.jallcom.2020.155588>.
- [44] H. Moussa, E. Giro, K. Mozet, H. Alem, G. Medjahdi, R. Schneider, ZnO rods/reduced graphene oxide composites prepared via a solvothermal reaction for efficient sunlight-driven photocatalysis, *Appl. Catal. B Environ.* 185 (2016) 11–21, <https://doi.org/10.1016/j.apcatb.2015.12.007>.
- [45] H. Afzal, M. Ikram, S. Ali, A. Shahzadi, M. Aqeel, A. Haider, M. Imran, S. Ali, Enhanced drug efficiency of doped ZnO-GO (graphene oxide) nanocomposites, a new gateway in drug delivery systems (DDSs), *Mater. Res. Express.* 7 (2020) 15405, <https://doi.org/10.1088/2053-1591/ab61ae>.
- [46] S. Agbolaghi, S. Aghapour, S. Charoughchi, F. Abbasi, R. Sarvari, High-performance photovoltaics by double-charge transporters using graphenic nanosheets and triisopropylsilyl ethynyl/naphthothiadiazole moieties, *J. Ind. Eng. Chem.* 68 (2018) 293–300, <https://doi.org/10.1016/j.jiec.2018.07.056>.
- [47] L. Xiao, D. Wu, S. Han, Y. Huang, S. Li, M. He, F. Zhang, X. Feng, Self-Assembled Fe₂O₃/Graphene Aerogel with High Lithium Storage Performance, *ACS Appl. Mater. Interfaces*. 5 (9) (2013) 3764–3769, <https://doi.org/10.1021/am400387i>.
- [48] M. Zeighami, S. Agbolaghi, A. Hamdast, R. Sarvari, Graphenic nanosheets sandwiched between crystalline cakes of poly(3-hexylthiophene) via simultaneous grafting/crystallization and their applications in active photovoltaic layers, *J. Mater. Sci. Mater. Electron.* 30 (7) (2019) 7018–7030, <https://doi.org/10.1007/s10854-019-01019-3>.
- [49] M.M.J. Sadiq, U.S. Shenoy, D.K. Bhat, Novel RGO-ZnWO₄-Fe₃O₄ nanocomposite as high performance visible light photocatalyst, *RSC Adv.* 6 (66) (2016) 61821–61829, <https://doi.org/10.1039/C6RA13002J>.

- [50] M.J.S. Mohamed, U.S. Shenoy, D.K. Bhat, High Performance Dual Catalytic Activity of Novel Zinc Tungstate—Reduced Graphene Oxide Nanocomposites, *Adv. Sci. Eng. Med.* 9 (2) (2017) 115–121, <https://doi.org/10.1166/ asem.2017.1977>.
- [51] G. Venkatesh, M. Geerthana, S. Prabhu, R. Ramesh, K.M. Prabu, Enhanced photocatalytic activity of reduced graphene oxide/SrSnO₃ nanocomposite for aqueous organic pollutant degradation, *Optik (Stuttg.)* 206 (2020) 164055, <https://doi.org/10.1016/j.ijleo.2019.164055>.
- [52] J. Cerdà, J. Arbiol, G. Dezanneau, R. Díaz, J.R. Morante, Perovskite-type BaSnO₃ powders for high temperature gas sensor applications, *Sensors Actuators B Chem.* 84 (1) (2002) 21–25, [https://doi.org/10.1016/S0925-4005\(02\)00005-9](https://doi.org/10.1016/S0925-4005(02)00005-9).
- [53] Jörg Bohneemann, R. Libanori, Mário.L. Moreira, E. Longo, High-efficient microwave synthesis and characterisation of SrSnO₃, *Chem. Eng. J.* 155 (3) (2009) 905–909, <https://doi.org/10.1016/j.cej.2009.09.004>.
- [54] M. Stürzel, Y. Thomann, M. Enders, R. Mülhaupt, Graphene-Supported Dual-Site Catalysts for Preparing Self-Reinforcing Polyethylene Reactor Blends Containing UHMWPE Nanoplatelets and in Situ UHMWPE Shish-Kebab Nanofibers, *Macromolecules* 47 (15) (2014) 4979–4986, <https://doi.org/10.1021/ma500769g>.
- [55] V. Etacheri, G. Michlits, M.K. Seery, S.J. Hinder, S.C. Pillai, A Highly Efficient TiO₂-x C x Nano-heterojunction Photocatalyst for Visible Light Induced Antibacterial Applications, *ACS Appl. Mater. Interfaces.* 5 (5) (2013) 1663–1672, <https://doi.org/10.1021/am302676a>.
- [56] X. Li, J. Bai, J. Li, C. Li, X. Zhong, S. Deng, The effect of n-π* electronic transitions on the N₂ photofixation ability of carbon self-doped honeycomb-like g-C₃N₄ prepared via microwave treatment, *RSC Adv.* 10 (12) (2020) 7019–7025, <https://doi.org/10.1039/D0RA00101E>.
- [57] R. Kurre, S. Bajpai, P.K. Bajpai, Synthesis, Characterization, Optical and Transport Properties of BaSnO₃ Synthesized by Wet Chemical Route, *Mater. Sci. Appl.* 09 (01) (2018) 92–110, <https://doi.org/10.4236/msa.2018.91007>.
- [58] J.-A. Yan, L. Xian, M.Y. Chou, Structural and Electronic Properties of Oxidized Graphene, *Phys. Rev. Lett.* 103 (2009) 86802, <https://doi.org/10.1103/PhysRevLett.103.086802>.
- [59] D. Li, M.B. Müller, S. Gilje, R.B. Kaner, G.G. Wallace, Processable aqueous dispersions of graphene nanosheets, *Nat. Nanotechnol.* 3 (2) (2008) 101–105, <https://doi.org/10.1038/nnano.2007.451>.
- [60] S. Sarkar, A. Makhil, T. Bora, S. Baruah, J. Dutta, S.K. Pal, Photoselective excited state dynamics in ZnO–Au nanocomposites and their implications in photocatalysis and dye-sensitized solar cells, *Phys. Chem. Chem. Phys.* 13 (27) (2011) 12488, <https://doi.org/10.1039/c1cp20892f>.
- [61] A. van Dijken, E.A. Meulenkaamp, D. Vanmaekelbergh, A. Meijerink, The Kinetics of the Radiative and Nonradiative Processes in Nanocrystalline ZnO Particles upon Photoexcitation, *J. Phys. Chem. B.* 104 (8) (2000) 1715–1723, <https://doi.org/10.1021/jp993327z>.
- [62] X. Liu, L. Pan, T. Lv, Z. Sun, C.Q. Sun, Visible light photocatalytic degradation of dyes by bismuth oxide-reduced graphene oxide composites prepared via microwave-assisted method, *J. Colloid Interface Sci.* 408 (2013) 145–150, <https://doi.org/10.1016/j.jcis.2013.07.045>.
- [63] R. Thekkayil, P. Gopinath, H. John, Enhanced photocatalytic activity of polyaniline through noncovalent functionalization with graphite oxide, *Mater. Res. Express.* 1 (2014) 45602, <https://doi.org/10.1088/2053-1591/1/4/045602>.
- [64] T. Xian, H. Yang, L.J. Di, J.F. Dai, Enhanced photocatalytic activity of BaTiO₃@g-C₃N₄ for the degradation of methyl orange under simulated sunlight irradiation, *J. Alloys Compd.* 622 (2015) 1098–1104, <https://doi.org/10.1016/j.jallcom.2014.11.051>.
- [65] A. Sadeghzadeh-Attar, Efficient photocatalytic degradation of methylene blue dye by SnO₂ nanotubes synthesized at different calcination temperatures, *Sol. Energy Mater. Sol. Cells.* 183 (2018) 16–24, <https://doi.org/10.1016/j.solmat.2018.03.046>.
- [66] Y. Fu, H. Chen, X. Sun, X. Wang, Combination of cobalt ferrite and graphene: High-performance and recyclable visible-light photocatalysis, *Appl. Catal. B Environ.* 111–112 (2012) 280–287, <https://doi.org/10.1016/j.apcatb.2011.10.009>.
- [67] M.M.J. Sadiq, U.S. Shenoy, D.K. Bhat, Synthesis of BaWO₄/NRGO-g-C₃N₄ nanocomposites with excellent multifunctional catalytic performance via microwave approach, *Front. Mater. Sci.* 12 (3) (2018) 247–263, <https://doi.org/10.1007/s11706-018-0433-0>.
- [68] Y. Yan, H. Yang, X. Zhao, R. Li, X. Wang, Enhanced photocatalytic activity of surface disorder-engineered CaTiO₃, *Mater. Res. Bull.* 105 (2018) 286–290, <https://doi.org/10.1016/j.materresbull.2018.05.008>.



Lightweight Feistel structure based hybrid-crypto model for multimedia data security over uncertain cloud environment

Denis Rayappan¹ · Madhubala Pandiyan²

Accepted: 23 October 2020
© Springer Science+Business Media, LLC, part of Springer Nature 2020

Abstract

The exponential rise in software computing and internet technologies have broadened the horizon of cloud computing applications serving numerous purposes like business processes, healthcare, finance, socialization, etc. In the last few years the increase in security breaches and unauthorized data access has forced industry to achieve computationally efficient and robust security system. The increase in multimedia data communication over different cloud applications too demands an efficient security model, which is expected to have low computational complexity, negligible quality-compromise and higher security robustness. Major conventional security-systems like cryptography and steganography undergo high computational overhead, thus limiting their potential towards cloud-communication where each data input used to be of large size and a gigantic amount of multimedia data is shared across the network. To alleviate above stated problems and enable a potential solution, in this paper a highly robust Lightweight Feistel Structure based Substitution Permutation Crypto Model is developed for multimedia data security over uncertain cloud environment. Our proposed model applies substitution permutation crypto concept with Feistel structure which performs substitution-permutation over five rounds to achieve higher confusion and diffusion. To retain higher security with low computation, we applied merely 64-bit block cipher and equal key-size. MATLAB based simulation revealed that the proposed lightweight security model achieves better attack-resilience even maintaining low entropy, high-correlation, and satisfactory computation time for multimedia data encryption. Such robustness enables our proposed security model to be applied for real-world cloud data security.

Keywords Multimedia data security · Cloud computing · Hybrid cryptosystem · Feistel structure · Substitution and permutation network

1 Introduction

The exponential rise in software technologies and sophisticated hardware platforms has broadened the horizon for highly integrated services and solutions to serve varied socio-industrial demands. In the last few decades, multimedia communication and allied information exchange has

gained wide-spread attention. Similarly, the fast-increasing internet technologies too have broadened the horizon for new computing environment like cloud computing, internet-of-things (IoTs), etc. Undeniably, the large numbers of internet enabled applications or the communication systems are generating huge data everyday to provide corresponding solutions such as social networking sites, healthcare purposes, e-commerce, scientific communities, financial sectors and other industrial demands like surveillance and security systems. Social media and entertainment, surveillance footages [1–3], consumer multimedia data, IoT assisted communication environment [2, 4–7] demand potential security solution and policies to protect their data from unauthorized access. Similarly, enterprise software has also witnessed significant growth across the industries, government agencies, banks and other organizations, which generates and communicates data

✉ Denis Rayappan
denisatshc@gmail.com

Madhubala Pandiyan
madhubalasivaji@gmail.com

¹ Department of Computer Science, Periyar University, Salem, Tamil Nadu, India

² Department of Computer Science, Don Bosco College (Affiliated to Periyar University), Dharmapuri, Tamil Nadu, India

(including multimedia data) in large volume. On the contrary, in the last few years, the adversarial efforts have increased significantly forcing industries to achieve secure data communication over the different ecosystems including IoT and cloud-infrastructures [1–5, 8–10]. Functionally, the amalgamation of the different data sources and allied voluminous data aggregation has given rise to the technology named cloud computing. Cloud computing enables different stakeholders to access data, making real-time computation and decision using cloud infrastructure irrespective of location or geographical boundaries. The prominent concern in cloud computing is the data security [2, 8]. More importantly, ensuring data security with low computational complexity, high time-efficiency with uncompromised multimedia data quality has been the key driving force for research communities [1, 2, 5, 6]. To avoid security breaches a number of efforts have been made; however, the major at-hand approaches function either by introducing data-access security models or infrastructure security or by implementing certain on-data security features [8]. Researchers have proposed security models in which the user requires getting authenticated before accessing the data (access-control), or the data itself is processed in such manner that it is communicated as a hidden content without revealing to the unauthorized users (Ex. Steganography).

Towards major multimedia data security approaches, steganography and cryptosystems are the most used methods [9, 10]; however, their robustness as standalone solution has remained questionable. Majority of the classical cryptosystems like RSA, AES, ECC, homomorphic models etc., consume significantly high computation due to higher key size. Though, higher key size hypothesizes to have higher attack-resiliency; however, at the cost of increased computational overhead. On the other hand, the recent events of the attacks like brute-force attack, impersonation attack etc., have put question on their robustness. Though, a few researches have suggested applying high bit-size to confuse the attacker, the computational cost of such approaches can't be denied. These facts alarms requirement of a more robust and computationally-efficient (say, lightweight) security system. With this motive, in this paper a highly robust and lightweight cryptosystem is developed which amalgamates the robustness of substitution-permutation (SP) concept and Feistel structure. The use of Feistel structure enables better confusion and diffusion while maintaining equivalent encryption and decryption which eventually helps retaining lower computational cost with higher attack-resiliency. The proposed Lightweight Hybrid SP-Feistel Crypto-Model embodies symmetric key-block cipher constituting 64-bit key size, which makes it computationally more efficient even without compromising with the level of security. Additionally,

we introduced a novel Key-Expansion Block Function (KEBF) which helped in retrieving five distinct keys over five rounds to introduce higher level of confusion and diffusion towards higher attack-resilience. To process confusion and diffusion (CDF) our proposed model executed KEBF for five rounds where for each round 4-bit of data was processed at a time. It enabled computational efficiency to handle multimedia data even of the large size and volume. The overall proposed model was developed using MATLAB 2019b, where its efficiency was assessed over the multimedia data of the different sizes. The performance assessment was made in terms of histogram analysis, correlation assessment, entropy, computation-time, Number of Changing Pixel Rates (NPCR) and the Unified Average Channel Intensity (UACI). Additionally, we examined robustness of the proposed security model qualitatively, where it was found suitable to avoid attacks like weak-key combination attack, square attack, regular and singular attacks (say, steganalysis), etc.

The remaining sections of the presented manuscript are given as follows. Section II discusses the related work, which is followed by the discussion of problem formulation in Section III. Section IV presents the overall proposed system and its implementation, while the simulation results are discussed in Section V. Conclusion of the overall research is given in Section VI.

2 Related work

Xue et al. [11] proposed content adaptive steganography, where the secret data was embedded into the noisiest pixels. Vipula et al. [12] combined AES crypto-algorithm with steganography to hide secret data within the cover multimedia images. Unlike [11], Lokesh [13] used alteration component method to hide AES encrypted message within the cover image. Saleh [14] applied modified AES algorithm for encrypting the secret message to be hidden in the cover image. M.E. Saleh et al. [15] proposed a new image steganography enhancement method for the pixel value difference (PVD) method and achieved maximum hiding capacity and image quality. Duluta et al. [16] found that the classical encryption algorithms have numerous limitations which can confine its suitability for cloud computing environment. Pancha [17] encrypted the input image to retrieve cipher image by applying encryption key in conjugation with Chirikov mapping. Subsequently, they applied steganography to hide cipher image within the cover image. To introduce higher level of confusion, Leung et al. [18] applied multiple encryption techniques to encrypt different parts of the media for the best security protection subject to the given computing resources. Mukhedkar [19] too applied different cryptosystems such

as DES, 3DES, AES, Blowfish Algorithm to encrypt the secret data before embedding within cover image. Li et al. [20] applied region of interest identification and clustering concept for video fingerprinting-based multimedia security. Ahmed [21] applied elliptic curve cryptography (ECC) based (text) encryption, followed by LSB embedding to safeguard the data over uncertain channel. To further strengthen their approach, authors [21] transmitted data over the different channels to the same target. Undeniably, this approach could undergo significantly large computational overheads. To achieve non-perceptibility over steganography, Hajduk [22] performed secret message encryption using quick response code (QR). The embedding process was additionally protected by AES algorithm. Alam [23] applied McEliece cryptosystem for data encryption to improve the security and privacy. Kumar et al. [24] proposed a symmetric key cryptography algorithm for secure three-dimensional color image security. Sharma [25] performed speech-signal encryption followed by steganography to secure data over communication channels. Wang et al. [26] applied watermark concept for multimedia data transmission over unsecure channel transmission.

Zaher [27] enhanced classical chaotic shift keying (CSK) method where the secret data were hidden within the chaotic transmitter states that could change among four different chaotic attractors in such manner that the binary information could effectively diffused. Authors applied cryptography to change the transmitter parameters in such manner that they have a quadruple form and therefore breaking into the public communication channel using return map attacks will fail. Realizing time-exhaustion due to chaotic map-based encryption, Hossain et al. [28] proposed a non-linear 3D chaos based simple encryption technique by applying 3D chaos for position permutation and value transformation technique. Saxena et al. [29] combined encryption and digital watermarking to enhance the image security. Gupta [30] recommended using discrete wavelet transform (DWT) to split input image into four sub band, followed by data hiding within the splits. Hiding the text-data within the image, authors performed compression to achieve transmission efficiency. Authors [31–37] combined cryptography and steganography; however, it could not guarantee computational efficiency over cloud infrastructure. Torvi [38] proposed unique data security using text steganography (UDSTS) framework that can transmit and receive encrypted messages embedded in a rich text format. Sarairoh [35] used filter bank cipher to encrypt the secret text message, followed by DWT based steganography to hide the encrypted message within the cover image. Towards imperceptibility, Laskar et al. [37] applied discrete cosine transform (DCT) method to perform data hiding (in cover image) in frequency domain. Pleshkova

et al. [39] proposed a mathematical concept for public key infrastructure (PKI) to secure the audio-data transmission from unauthorized access. Pai [40] encrypted video data and generated video-ciphers in a time and space efficient approach. Authors found that region permutation followed by application of AES and DES can enhance security of video files. However, such systems were found computationally costly [13].

Cui et al. [41] developed encrypted data sharing environment for secure image service for mobile devices with privacy assurance over cloud environment. Usman et al. [42] developed a privacy preserving security model for internet of multimedia things (IoMT). Zheng et al. [43] developed an encrypted cloud model with secure de-duplication for secure video transmission. Authors exploited the concept of scalable video coding (SVC) and secure de-duplication to achieve multimedia security over Azure platform. However, it could not be assessed in terms of data reconstruction quality and computational overhead. Abdul et al. [44] developed biometric security model with visual encryption technique. Though the use of visual cryptography and Zero-watermarking helped protecting the ownership of multimedia content, it was found computationally exhaustive. X. Li et al. [45] assessed different security models for cloud computing, where he found that cloud computing requires maintaining a fair balance in between the computation as well as attack-resilience. It indicates towards the need of certain lightweight solution. Q. Li et al. [46] proposed privacy preserving access control concept for multimedia data security over cloud platform. Authors applied ciphertext-policy attribute-based encryption (CP-ABE) that enabled cloud-assisted mobile multimedia data sharing. Hamid et al. [47] developed privacy preserving model with pairing based cryptography for medical data security for cloud computing. To achieve computational efficiency authors applied a tri-party one-round authenticated key agreement model. Khedr et al. [48] developed SecureMed a GPU accelerated homomorphic encryption concept for medical data security.

Zhu et al. [49] developed image encryption technique using non-uniform sampling to introduce more attack-resilience. As standalone multimedia security, Zhang et al. [50] developed ECC based image encryption with Diffie-Hellman public key sharing concept. Tawalbeh et al. [51] applied two ECC-based encryption algorithms for secure multimedia communication. The first algorithm performed selective encryption on the transform coefficients during compression, whereas the second algorithm achieved perceptual encryption based on selective bit-plane encryption before compression. Guan et al. [52] developed frequency domain DNA coding based chaotic image encryption model for multimedia data security where both the amplitude and phase components in frequency-domain

were diffused and scrambled. J.He et al. [53] developed a bit stream-based JPEG image encryption. Hamza et al. [54] focused on key-frame confidentiality and developed hash-based encryption for key-frame of diagnosis hysteroscopy. Authors [54] designed local sensitive hash (LSH) to strengthen data security. Xia et al. [55] suggested a content-based image retrieval (CBIR) privacy-preserving scheme that enables the data owner to outsource the image database and CBIR service to the cloud, without exposing the actual database content to the cloud server. Xu et al. [56] applied hamming embedding algorithm to generate binary signatures for image security. This method achieved the balance between security, accuracy and efficiency of safe large-scale image retrieval in public clouds. Fawaz et al. [57] have suggested a scheme for image encryption based on two rounds of substitution—diffusion. They applied it in a block by block manner to attain the avalanche effect in overall image level, and ensured a high level of security and randomness.

Noura et al. [58] developed an effective image encryption scheme based on a dynamic structure. The proposed cipher structure consists of two distinct lightweight rounds (forward and backward chaining blocks) and a block permutation mechanism. Furthermore, the development of a dynamic key based on a secret key and a nonce was proposed as a key derivation feature. This key can be modified for each validate period (session), or for each new input image, depending on its configuration. Then the cipher layers were generated on the basis of this key, which were an integer or a binary diffusion matrix and an S-box substitute table, together with a P-box permutation table. The image was divided into blocks by Visalakshi et al. [59], and then transformed by moving the columns from left to right and right to left. After that, Blowfish algorithm was applied. A new lightweight secure cryptographic scheme for secure image communication was proposed by Mondal et al. [60]. In this scheme the plain image was permuted first using a sequence of pseudo random number (PRN) and encrypted by deoxyribonucleic acid (DNA) computation. The scheme was proposed for gray label images but the scheme can be extended for color images and text data. However, in order to make it applicable to the internet of things, there is potential for more developments in encryption techniques. In order to secure medical images, Noura et al. [61] proposed a cipher scheme with three variants (selective, middle-full and full). For each input image the scheme was based on primitive dynamic diffusion and/or confusion, which ensured good cryptographic efficiency with reduced rounds.

Belguith et al. [62] proposed a lightweight encryption algorithm consisting of a combination of symmetric algorithms to encrypt data and asymmetric ones to distribute keys. This work can be improved by proposing a new key

distribution system that aims to offer the encryption key to any approved user without the involvement of the cloud provider. Daniel et al. [63] combined hashing and symmetric encryption with improved distributed hash table data structure to reduce overhead communication and computation for integrity verification and also to allow efficient operations of the data. The storage cost was drastically decreased by deduplication using the combined techniques of convergent encryption and filters. Rad et al. [64] introduced the concept of extending the capabilities of cloud file storage from just storing images to also performing encryption and analytics by moving and executing user-defined programs close to the data within an object cloud. The proposed PFCC algorithm provides a new parallel scheme for image encryption for cloud file sharing environment. One of the main differences between the existing transform-based encryption schemes and the proposed algorithm was the dual encryption method, which introduces a large amount of encryption complexity. Jinbo Xiong et al. [65] proposed a role symmetric encryption (RSE) algorithm and an RSE-based Proof of Ownership (RSE-PoW) scheme for secure deduplication in hierarchical heterogeneous environments, based on the role of symmetric encryption, proof of ownership and bloom filter. Aljawarneh et al. [66] proposed a resource-efficient encryption method for encrypting multimedia big data in IoT. The proposed framework took advantage of Feistel Encryption Scheme, advanced encryption standard (AES) and genetic algorithms. Alassaf et al. [67] analyzed the efficiency of the SIMON cryptographic algorithm and suggested a SIMON-based lightweight cryptography algorithm to minimize encryption time and preserve the realistic trade-off between security and performance in an IoT-driven setup for its potential use. The modified SIMON with 32, 48, 64, 96-bit block sizes showed interesting speed-up compared to the original SIMON, where some of them were found to be slower than AES. A lightweight selective encryption scheme was introduced by Amna Shifa et al. [68] in which encoder syntax elements were encrypted with the revolutionary EXPer (extended permutation with exclusive OR). A hybrid encryption algorithm for lightweight data stored in a cloud has been proposed by Liang et al. [69]. By increasing the key size to produce large prime numbers, this hybrid algorithm strengthens the RSA algorithm and then combined it with the AES algorithm. The authors of [70] proposed a one-round cipher (implemented on static images) for IoMT (Internet of Multimedia Things) in which the substitution and permutation principles were selected for the encryption.

3 Problem formulation

Majority of the at-hand image security models apply classical cryptosystems or steganography concepts, whose limited attack-resiliency and increased computational overhead can't be denied [45]. As standalone solution, most of the cryptosystems propose encryption with higher key-size (Ex. AES-256, RSA-256, homomorphic computation, etc.). Though, increasing key-size can increase the level of security and complexity towards unauthorized decryption, it significantly increased large computational overheads and processing-time. Such limitations confine their efficacy to meet real-world cloud computing demands. Steganography as an alternate too is found computationally exhaustive due to overheads imposed by wavelet transform, cipher embedding, compression etc. Additionally, the major steganography concepts don't address imperceptibility objective, which is must in the contemporary cloud communication environment. This is because majority of the statistical assessment-based attackers like steganalysis with sophisticated decryption tools can sense the hidden data and can eventually retrieve the same.

Addressing above stated problems and to achieve a novel and robust multimedia data security model, in this paper a lightweight cryptosystem has been developed. Unlike classical cryptosystem, our proposed model intends to maintain lower bit size or key-size (here, only 64-bit key) and lower computational while maintaining higher level of confusion to avoid any attack over cloud network. Our proposed security system can be considered as a hybrid model which exploits robustness of block cipher technique like substitution and permutation network (SPN) and Feistel architecture (a type of symmetric block cipher technique) to inculcate higher level of attack-resiliency even with lower computational overheads. Functionally, our proposed model consists of three consecutive steps, key generation, encryption and decryption. Here, at first, we apply SPN block cipher with iterative and alternating rounds of substitution and permutation (say, transposition) while ensuring that it fulfills the demands of Shannon's Confusion and Diffusion characteristics. To achieve it, we have developed a novel key-expansion block function (KEBF) which intends to assure that the cipher has been manipulated in pseudo random manner. To introduce more level of confusion and security-structure KEBF has been applied over five rounds, where in each round it intends to fulfill above stated Shannon's confusion and diffusion conditions. In this manner the proposed model ensures maintaining higher confusion with lower computation (Note, unlike classical AES cryptosystem which applies 15 rounds of encryption with 256-bit key size, our proposed

model applies merely 5-round of computation with merely 64-bit key size. It can reduce overall computation to a great extent). The proposed model enables manipulating cipher text in such manner that it can avoid easy exposure of the original data to the intruder. To further strengthen the efficiency, we applied Feistel architecture with SPN to perform encryption and decryption of the input image data. Noticeably, the application of Feistel architecture enables decryption in the same way as encryption and hence reduces additional computational-exhaustion. Unlike other ciphers such as DES, Camelia, Blowfish etc., our proposed Feistel architecture can enable swift and more efficient encryption-decryption over large data size.

4 System model

As indicated in the previous section, the proposed security model can be stated as a hybrid cryptosystem functional on the basis of a symmetric key block cipher constituting 64-bit key and plain-text. In any symmetric key model, our proposed encryption method applies 5-rounds iterative mechanism which is also called encryption-rounds. In this process each round operates over certain predefined mathematical functions (here, KEBF) to generate confusion and diffusion matrix. Though, higher rounds assure better level-of-security; however, at the cost of increased computational overheads. The typical cryptographic methods apply an average of 10–20 rounds to encrypt the target data, which can cause significantly huge computational overhead and time-exhaustion. To avoid such complexity and time-exhaustion we performed KEBF merely for five rounds (Fig. 1) so as to enhance computational time, resource, redundancy etc. without compromising with the level-of-security. In other words, we performed only five-round of encryption where each encryption round processes over a 4-bit of input data. When encrypting the input data, the encryption function is executed in such manner that it creates sufficient confusion and diffusion to avoid any possible attack. To achieve it, we applied Feistel architecture to perform substitution and diffusion. The detailed discussion of the key-generation and expansion unit is given as follows. Some notations used in the explanation are shown in Table 1.

4.1 Key-generation and expansion

Considering the fact that in cloud computing environment each node behaves like a key generator as well as decoder, it is vital to maintain minimum possible computations. To achieve it, we designed a mathematical model by using XOR and XNOR logical function and data concatenation. The key task during encryption and decryption is the key

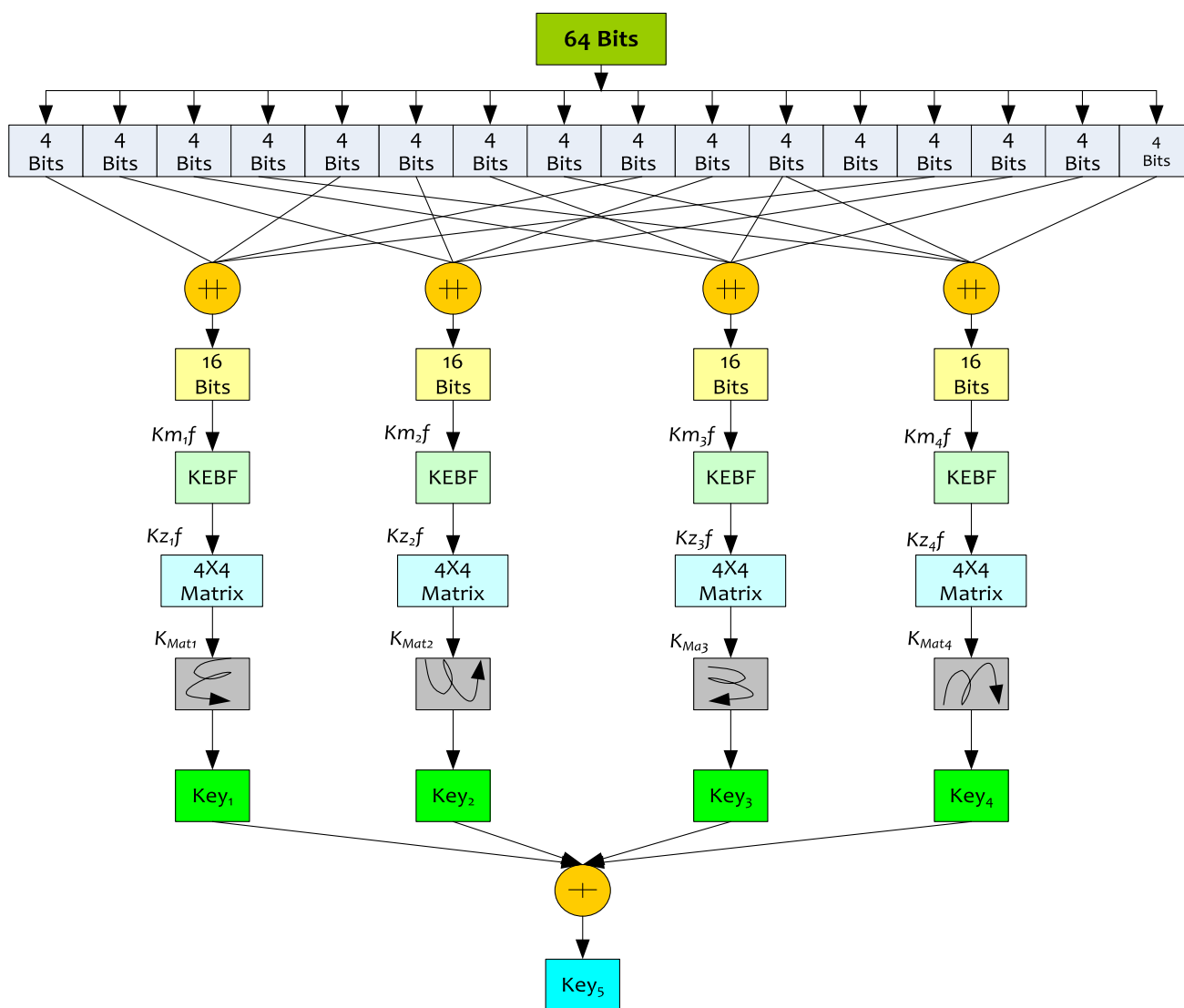


Fig. 1 KEBF assisted key expansion mechanism

Table 1 Notations

Notation	Function
\oplus	XOR
\odot	XNOR
$++$, $ $	Concatenation

generation and therefore key-generation is the most essential component of the key-generation and expansion step. To accommodate it, we applied Feistel architecture-based encryption, which has been performed in multiple rounds (here, five), where each round requires distinct key (i.e., five distinct keys). To achieve it, we developed a

function called “key-expansion block function (KEBF)”. Noticeably, KEBF intended to strengthen attack-resilience towards any search-based attack which is common in online environment, by maintaining sufficiently large key size k_t that made it impossible for the intruder to perform 2^{k_t-1} encryption/decryption to gain key information for data retrieval. We designed our security model as a 64-bit block cipher that means, it demands 64-bit key to perform encryption of the 64-bit input data. In our proposed model, we applied 64-bit’s cipher key k_c which has been further used as the input of the KEBF block that executes mathematical function to generate confusion and diffusion and eventually retrieves five distinct keys. Thus, it obtained five distinct keys for each round of encryption, which are subsequently applied for encryption and decryption process. Thus, unlike classical cryptosystems where single key is used for encryption, our proposed model presents more

robustness and attack-resilience due to five-distinct key-based encryption.

A snippet of the KEBF model and allied key-expansion mechanism is illustrated in Fig. 1. As depicted in Fig. 1, KEBF block applies a function “F” (say, KEBF Function) which has been developed as per the suggestions made for block-cipher generation in [71]. Factually, Khazad cipher as discussed in [71] doesn’t represent the Feistel cipher and hence employs broad-trial-mechanism (BTM), where it (i.e., BTM) executes multiple linear and non-linear transformations. Though, this process assures the definite relationship and inter-dependency amongst the output cipher bits and the input bits in a predefined complex approach [72]. As depicted in Fig. 1, the 64-bit input data is at first split into 16 distinct chunks of 4-bits each. The subsequent four distinct chunks of 4-bits are concatenated, thus constituting 16-bit of data for which Feistel network obtains the keys (Fig. 1). As illustrated in Fig. 1, once executing KEBF over the 16 bits of the concatenated input, it generates a matrix of 4-bits each. The overall process of KEBF encompasses the following steps:

4.2 Step-1

Take the 64-bit input cipher k_c from the user and split it into four distinct segments of 4-bits.

4.3 Step-2

As depicted in Fig. 1, initiate the KEBF Function over each split component (i.e., 16-bit data). Noticeably, with 4-bits distinct segments, we obtained 16-bits data for each block on which KEBF was applied. Obtaining the 16-bits data after processing KEBF, execute the initial substitution of the blocks or segments of k_c using (1), similarly we obtained 16-bits for each KEBF Function.

$$Km_{i \in \{1,2,3,4\}f} = \parallel_{(j=1)}^4 Kn_{4(j-1)+i} \tag{1}$$

In (1), the variable $i = 1$ to 4 for first 4 round keys.

4.4 Step-3

Once obtaining the values for $Km_{i \in \{1,2,3,4\}f}$, it has been further processed to give rise to Ka_{if} for each 16-bit blocks. Mathematically, Kz_{if} is obtained using (2).

$$Kz_{if} = f(Km_{if}) \tag{2}$$

4.5 Step-4

We designed KEBF Function as a strategic combination of dual functions PF and QF, as illustrated in Fig. 2. The functional schematic as illustrated in Fig. 2 states a linear (i.e., PF) and non-linear (i.e., QF) functions, respectively. The transformational mechanisms for both PF and QF are

Fig. 2 KEBF function

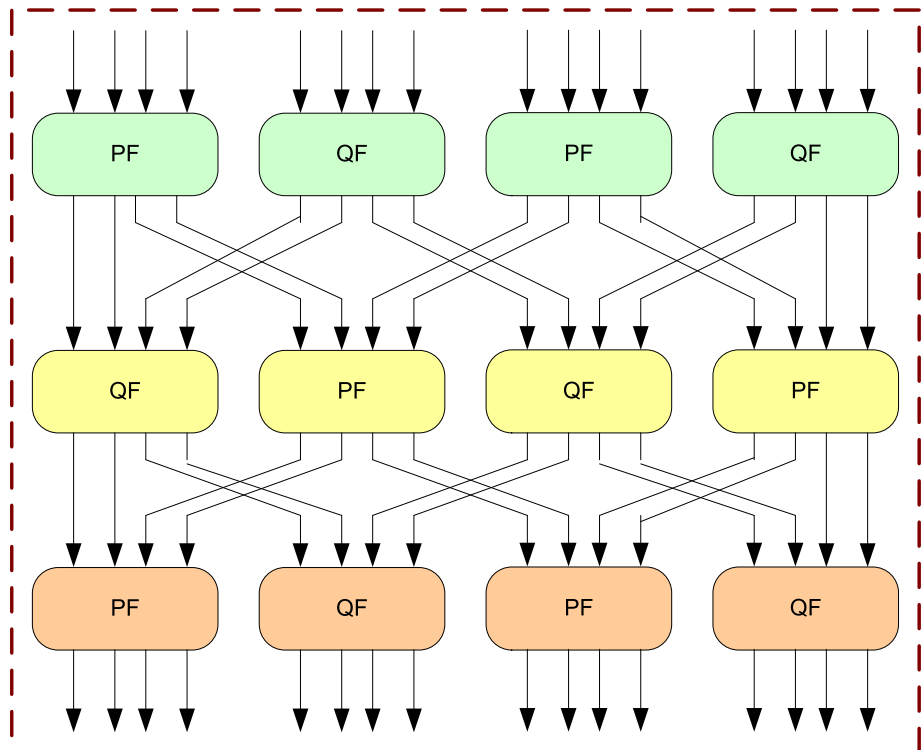


Table 2 PF function

$k_{n,i \in \{1,2,3,4\}}$	0	1	2	3	4	5	6	7	8	9	A	B	C	D	E	F
$p(k_{n,i \in \{1,2,3,4\}})$	3	F	E	0	5	4	B	C	D	A	9	6	7	8	2	1

Table 3 QF function

$k_{n,i \in \{1,2,3,4\}}$	0	1	2	3	4	5	6	7	8	9	A	B	C	D	E	F
$p(k_{n,i \in \{1,2,3,4\}})$	9	E	5	6	A	2	3	C	F	0	4	D	7	B	1	8

given in Tables 2 and 3, respectively. Thus, obtaining values of PF and QF functional blocks as illustrated in Fig. 2, KEBF has been applied the same way as shown in Fig. 1 to perform encryption.

Once obtaining the KEBF Function for each 16-bit block, the output (of KEBF Function) was re-sampled in 4×4 matrix. Mathematically,

$$K_{Mat1} = \begin{bmatrix} Kz1f_1 & Kz1f_2 & Kz1f_3 & Kz1f_4 \\ Kz1f_5 & Kz1f_6 & Kz1f_7 & Kz1f_8 \\ Kz1f_9 & Kz1f_{10} & Kz1f_{11} & Kz1f_{12} \\ Kz1f_{13} & Kz1f_{14} & Kz1f_{15} & Kz1f_{16} \end{bmatrix} \tag{3}$$

$$K_{Mat2} = \begin{bmatrix} Kz2f_1 & Kz2f_2 & Kz2f_3 & Kz2f_4 \\ Kz2f_5 & Kz2f_6 & Kz2f_7 & Kz2f_8 \\ Kz2f_9 & Kz2f_{10} & Kz2f_{11} & Kz2f_{12} \\ Kz2f_{13} & Kz2f_{14} & Kz2f_{15} & Kz2f_{16} \end{bmatrix} \tag{4}$$

$$K_{Mat3} = \begin{bmatrix} Kz3f_1 & Kz3f_2 & Kz3f_3 & Kz3f_4 \\ Kz3f_5 & Kz3f_6 & Kz3f_7 & Kz3f_8 \\ Kz3f_9 & Kz3f_{10} & Kz3f_{11} & Kz3f_{12} \\ Kz3f_{13} & Kz3f_{14} & Kz3f_{15} & Kz3f_{16} \end{bmatrix} \tag{5}$$

$$K_{Mat4} = \begin{bmatrix} Kz4f_1 & Kz4f_2 & Kz4f_3 & Kz4f_4 \\ Kz4f_5 & Kz4f_6 & Kz4f_7 & Kz4f_8 \\ Kz4f_9 & Kz4f_{10} & Kz4f_{11} & Kz4f_{12} \\ Kz4f_{13} & Kz4f_{14} & Kz4f_{15} & Kz4f_{16} \end{bmatrix} \tag{6}$$

4.6 Step-5

Once obtaining the key matrix, to further retrieve the keys for each 16-bit block (i.e., $K_{Mat1}, K_{Mat2}, K_{Mat3}$ and K_{Mat4}), it has been converted into four distinct arrays of 16 bits. Here we call these arrays as ‘‘per-round-key (PRK)’. The four distinct keys and allied attribute arrangement is depicted in Eq. (7) to Eq. (10). Noticeably, in below equations the operator # signifies the concatenation.

$$Key_1 = a_4 \# a_3 \# a_2 \# a_1 \# a_5 \# a_6 \# a_7 \# a_8 \# a_{12} \# a_{11} \# a_{10} \# a_9 \# a_{13} \# a_{14} \# a_{15} \# a_{16} \tag{7}$$

$$Key_2 = b_1 \# b_5 \# b_9 \# b_{13} \# b_{14} \# b_{10} \# b_6 \# b_2 \# b_3 \# b_7 \# b_{11} \# b_{15} \# b_{16} \# b_{12} \# b_8 \# b_4 \tag{8}$$

$$Key_3 = c_1 \# c_2 \# c_{32} \# c_4 \# c_8 \# c_7 \# c_6 \# c_5 \# c_9 \# c_{10} \# c_{11} \# c_{12} \# c_{16} \# c_{15} \# c_{14} \# c_{13} \tag{9}$$

$$Key_4 = d_{13} \# d_9 \# d_{52} \# d_1 \# d_2 \# d_6 \# d_{10} \# d_{14} \# d_{15} \# d_{11} \# d_7 \# d_3 \# d_4 \# d_8 \# d_{12} \# d_{16} \tag{10}$$

Now, estimating the key values, we have performed XOR logical operation amongst the four distinct keys (each for one round) as obtained above (7–10) to get a Fused-Key (11).

$$Key_5 = \bigoplus_{i=1}^4 Ki \tag{11}$$

4.7 Data encryption

Once retrieving the keys per round, data encryption was performed. For confusion and diffusion over encryption process, we applied different logical functions such as shifting (left–right), entity-swapping and substitution. The overall encryption process is illustrated in Fig. 3. As illustrated in Fig. 3, for the first round of operation the 64 bit plain text (Pt) is split into four chunks containing 16 bits distinctly, (i.e., $Px_{0-15}, Px_{16-31}, Px_{32-47}$ and Px_{48-63}). Progressing over bits operation in each round, the proposed model performs swapping to reduce the data originality by means of bit’s order-alteration. It increased confusion in cipher text. Meanwhile, it performs bitwise XNOR logical operation in between the corresponding round key Key_i and Px_{0-15} . This process is repeated between K_i and Px_{48-63} to generate Ro_{11} and Ro_{14} , respectively. Once obtaining the output from XNOR logical operator it is fed to the KEBF block (Fig. 3), and generates two distinct outputs Ef_{11} and Ef_{r1} . Noticeably, KEBF applied for encryption is same as used for KEBF (say, key expansion function), with

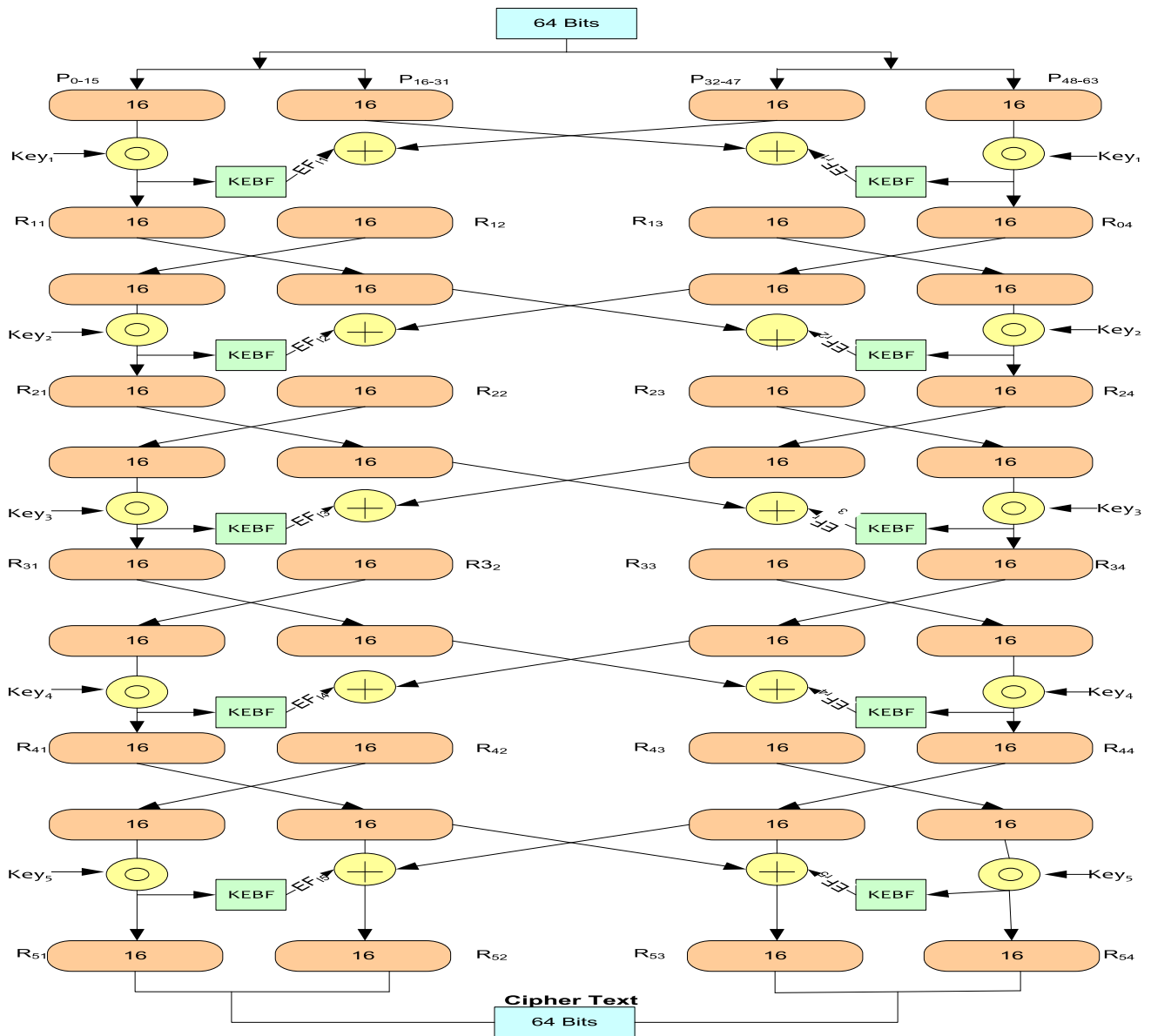


Fig. 3 Feistel network assisted data encryption

processes like swapping and substitution. Now, with the obtained Ef_{11} & Px_{32-47} , we performed bitwise XOR to obtain Ro_{12} , while the same in between Ef_{r1} and Px_{16-31} provided Ro_{13} (Fig. 3).

$$Ro_{i,j} = \begin{cases} Px_{ij} \odot K_i; & j = 1 \text{ and } 4 \\ Px_{i,j+1} \oplus Ef_{1i}; & j = 2 \\ Px_{i,j-1} \oplus Ef_{ri}; & j = 3 \end{cases} \quad (12)$$

Thus, after processing above methods, a transformation process was executed in such manner that for each subsequent round Ro_{11} turns out to be Px_{16-31} , while Ro_{12} becomes Px_{0-15} , Ro_{13} as Px_{48-63} , and Ro_{13} as Px_{32-47} . This process is continued for all remaining rounds as per (12), and thus the eventual result of final round are

concatenated to form the final cipher text (CT) to be used for further communication (13).

$$CT = R_{51} \# R_{52} \# R_{53} \# R_{54} \quad (13)$$

The detailed discussion of the simulation results and its inferences is given in the sub-sequent section.

Noticeably, with Feistel structure our proposed (block cipher) model exhibits decryption in the same way as encryption, though the structural sequence reverses the earlier (i.e., encryption). It reduces overall computation significantly making it lightweight and more cost-efficient.

5 Results and discussion

Considering the significance of a robust and lightweight security model for multimedia data security over cloud, in this research we focused on exploiting the efficacy of the advanced crypto-concepts such as Substitution and Permutation based diffusion to enable robust image encryption-decryption for attack-resiliency. To further strengthen the robustness under uncertain cloud environment we applied diffusion concept based on the well-known Feistel structure that performed Substitution Permutation based data encryption. To maintain lower computational overhead, our proposed model applied merely five rounds with 64-bit encryption. We applied Feistel structure to perform Substitution Permutation over multiple rounds so as to perform high level confusion and diffusion. As already stated, unlike classical RSA 256 bit or AES-256 models, we applied merely 64-bit block cipher and equally key-size which retained high computational efficiency with augmented security. The proposed crypto-model was developed using MATLAB 2019b tool, which was tested with both generic multimedia data as well as biomedical datasets such as diabetic retinopathy, glaucoma, MRI data etc. The performance of the proposed security model was examined qualitatively as well as quantitatively or empirically by simulating over benchmark datasets. The overall proposed model was simulated over Microsoft Operating System (OS) Windows 2010, with processor Intel – i3, with 8 GB RAM. Though, the computation time (Table 8) may be higher with better or more advanced processors like Intel i5 or i8. The detailed discussion of the performance assessment is given in the subsequent sections.

5.1 Quantitative assessment

To assess efficacy of the proposed multimedia data security model, we at first examined it for statistical performance parameters such as cipher generation, entropy, correlation and histogram results. To perform this assessment, we tested performance with different input images pertaining to normal life as well as biomedical significances such as fundus images, Magnetic Resonance Imaging (MRI) etc. As normal (daily) life images the standard images like Lena, Baboon, Panda, which are the well-known benchmark data for image analysis were tested. Noticeably, before executing our proposed crypto-model at first input images were converted into Gray from standard RGB data. Though, certain sophisticated pre-processing could have enabled better input environment; however since the focus of this research was to design security model, no pre-processing such as resizing, intensity equalization etc. was performed. As statistical performance assessment, we

obtained key features like key sensitivity, image entropy, correlation, image histogram etc. Before discussing the simulation results, a snippet of the above stated statistical parameters is given as follows

To assess performance of the proposed multimedia data security model, we have considered images of the different types, encompassing general images as well as medical images as these two different types of inputs have distinct demands. In other words, the normal life data such as object data, person's images etc. can have certain (limited or definite) image quality trade off after communicating over the cloud platform. On contrary, image data demands seamless and quality-centric communication as even a minute difference in image spatio-temporal feature might decisively impact assessment and eventual decision. Such miss-location or min-information might force professionals to make wrong telemedicine decision. Considering these facts, in this paper we considered different types of inputs encompassing benchmark images like Lena, Baboon, Panda, Cameraman, three different fundus images retrieved from DRISTI-GS datasets and Medical Resonance Imaging (MRI) data available online. The input images were at first processed for pre-processing where those were converted from RGB to Gray form, and were resized to 256×256 dimension. Noticeably, the considered images were in *.PNG and *.JPG formation; though the proposed algorithm could process any form of input image data. Once exhibiting pre-processing, the images were processed for respective encryption and decryption hypothesizing communication to be made over uncertain cloud framework or platform. Thus, with the simulated results we obtained performance outcome in terms of entropy, correlation, NPCR and UACI along with the corresponding histogram outputs. Before discussing the simulation results, a snippet of the different statistical as well as visual assessment parameters used in this research is given as follow.

5.1.1 Entropy

As multimedia security process undergoes cipher generation which can significantly increase the disturbances across the image input. This as a result can cause increase in image entropy which not only degrades (image) quality but also broadens horizon for intruders to attack specific data. On the other hand, encryption imposes additional information to the multimedia data so as to make it complex for the intruder to distinguish the encrypted data and the original multimedia information. In such cases, maintaining the optimal entropy with the data under transmission is must. With this motive, in this paper we estimated entropy for each encrypted data to retain quality-centric multimedia data security (14).

$$ENT(I) = - \sum_{i=1}^{2^8} P(I_i) \log_b P(I_i) \quad (14)$$

In (14), $ENT(I)$ states the entropy of an image, where I signify the intensity, and $P(I_i)$ signifies the probability of the intensity value I_i .

5.1.2 Correlation

Correlation being a statistical parameter signifies the dependencies, inter-relationship or correlation between two distinct values. Typically, a data element or point possessing significant dependency signifies significant correlation. Towards multimedia security it is important to remove dependency of the cipher information from the original image. With such minimal dependency, no significant information can be extracted, which strengthens the data security feature. In this paper, we obtained the correlation coefficient γ in between the original multimedia data and encrypted data using (15). For an optimal condition γ must be maintained either equal or near zero. Correlation coefficient of one signifies the worst cipher condition.

$$\gamma_{x,y} = \frac{cov(x,y)}{\sqrt{D(x)}\sqrt{D(y)}} \quad (15)$$

In (15), $cov(x,y)$ states the covariance value, while $D(x)$ and $D(y)$ states the variances for the variable x and y , correspondingly. In general, the distribution of the variance of any single dimension arbitrary variable is obtained using (16).

$$D(x) = \frac{1}{N} \sum_{i=1}^N (x_i - E(x))^2 \quad (16)$$

In (16), $D(x)$ states the variance value for random variable x . To estimate covariance between two distinct arbitrary values x and y , we apply (17).

$$cov(x,y) = \frac{1}{N} \sum_{i=1}^N (x_i - E(x))(y_i - E(y)) \quad (17)$$

In (17), $E(x)$ and $E(y)$ states the expected values for x and y random values. Expectation values can be obtained as per (18).

$$E(x) = \frac{1}{N} \sum_{i=1}^N x_i \quad (18)$$

In (18), N signifies the total number of pixels in the image, which is usually estimated as $N = Row \times Column$, and x states the N -dimensional vector. x_i refers the i th intensity value of the original multimedia data or image.

5.1.3 Image histogram analysis

Histogram variation analysis enables examining visual effect of the cipher so as to encrypt an image and assess the randomness it causes in the original image after encryption. We applied image histogram analysis model to visualize the introduced randomness within the original image. Here, we intend to maintain minimum or negligible histogram difference after encryption to retain better security and visual perception based attack probability.

5.1.4 Number of changing pixel rates (NPCR) and the unified average channel intensity (UACI)

NPCR and UACI are the randomness test measures often applied to assess differential attack resilience by an image encryption technique. Higher NPCR signifies more resilience towards differential attacks. The details of these randomness tests can be found in [73].

Table 4 presents the simulated results for the different input images and respective visual outcomes in the form of image histograms. Table 4 depicts the original inputs, histogram of the original inputs, encrypted image and its (encrypted) histogram results. As depicted (Table 4), we considered a total of nine images with different natures (normal, MRI and Fundus (for diabetic or Glaucomatic detection)). As depicted in the results (Table 4), after encryption the histogram of the cipher data is quite different making it imperceptible for an attacker to gain cipher access.

Table 5 presents the entropy level of the original images as well as corresponding encrypted image. As observed through the results (Table 5), the entropy level increases for encrypted images which helps introducing confusion to avoid easy detection of the original data. Noticeably, there are the different approaches advocating maintaining either low negligible entropy (such as steganography based approaches) or high entropy which is often considered in cryptography methods. The results affirm suitable entropy condition to avoid any detection by attacker over uncertain cloud conditions. In our proposed model, we considered 8 bits gray scale image which can have the highest entropy of 8 bits. Observing Table 5, it can be found that the highest entropy obtained over test cases is 7.99 (for encrypted images), which is fulfilling the above stated entropy condition for a quality-centric and secure multimedia data communication.

The correlation analysis of the proposed multimedia security model is given in Table 6. As already stated that for any encryption model achieving higher correlation difference can enable high-imperceptibility and hence high attack-resilience. As depicted through the results (Table 6), the proposed model shows significantly large correlation

Table 4 Histogram analysis


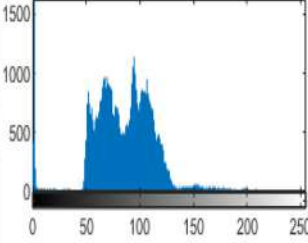
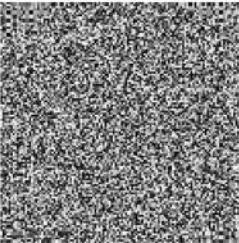
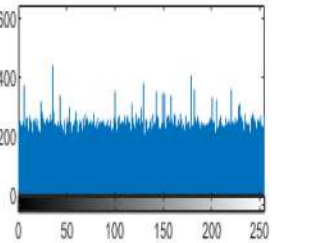
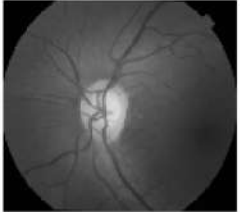
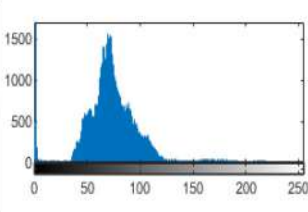
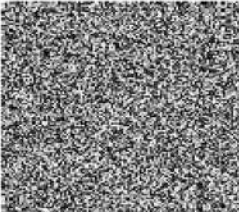
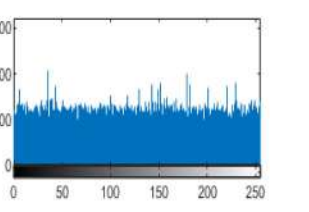
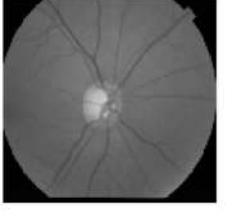
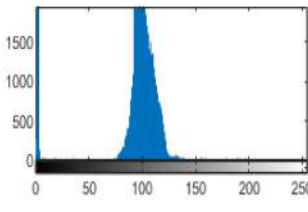

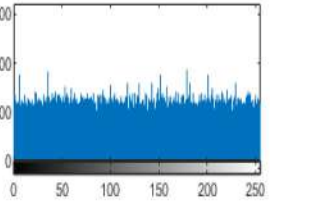
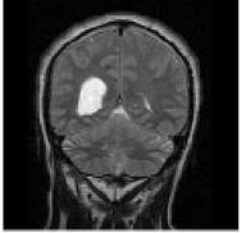
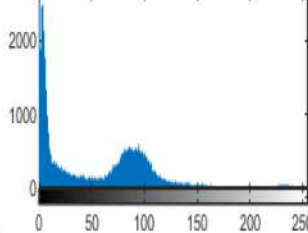
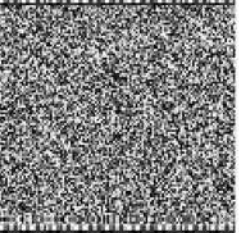
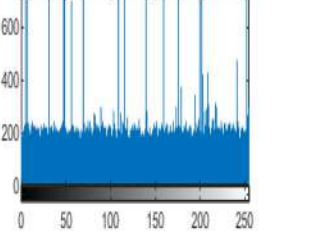
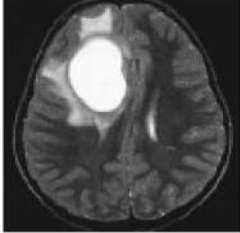
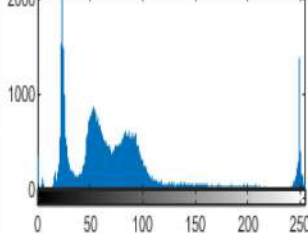
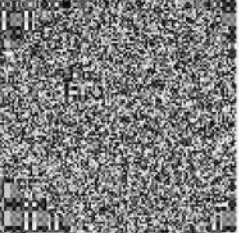
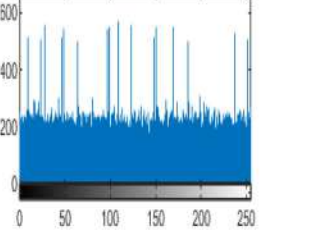
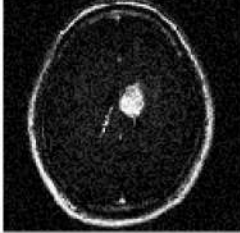
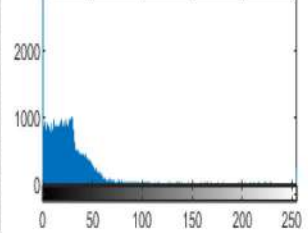
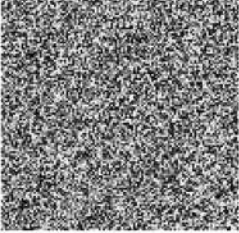
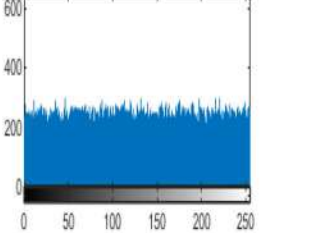
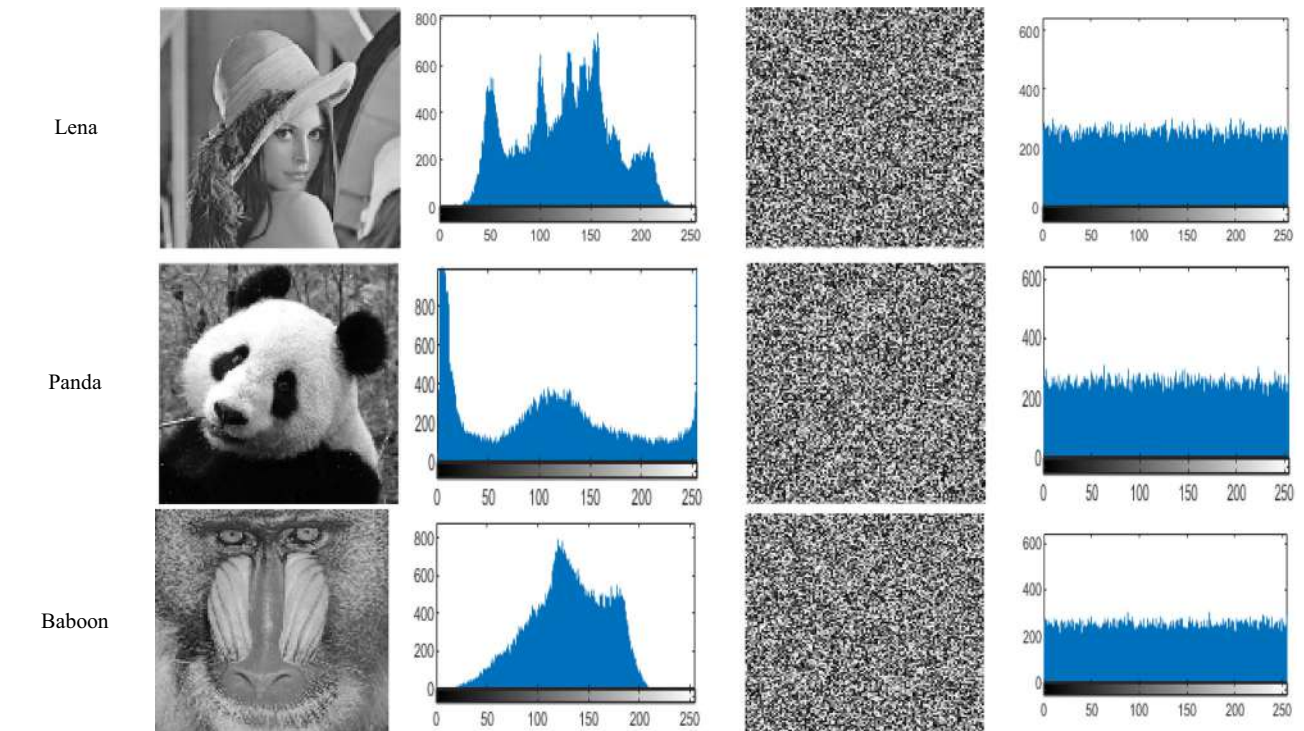
Dataset	Original Image (8 Bits gray scale image with 256×256 size)	Image Histogram	Encrypted Image	Encrypted Data Histogram
Fundus1				
Fundus2				
Fundus3				
MR11				
MR12				
MR13				

Table 4 continued



difference, signifying its robustness towards high attack resilience.

In addition to the above discussed visual and statistical characterization we have examined the efficacy of our proposed multimedia (data) security model in terms of the Number of Changing Pixel Rates (NPCR) and the Unified Average Channel Intensity (UACI) in Table 7. Typically, high values of NPCR and UACI signify higher randomness and hence high resilience against any differential attack probability [73]. The randomness test results with higher values of NPCR back up the attack resiliency nature of the proposed system. Similarly, UACI too confirms satisfactory performance. The detailed discussion of NPCR and UACI conditions for image randomness during encryption can be found in [73]. Thus, the above discussed robustness confirms the suitability of the proposed security model for any real-time multimedia communication, including our intended cloud communication purposes.

The encryption time is depicted in Table 8. Noticeably; the proposed model can be executed over more advanced processors such as Intel-i5 and i8 to achieve better time efficiency.

5.2 Qualitative assessment

In the previous section, the performance of the proposed security system was examined in terms of different statistical as well as visual parameters. The simulation results affirmed that the proposed model accomplishes optimal performance while retaining high security with low visual perception and entropy, confirming the suitability of the proposed security system for a cloud computing environment. Now, realizing the need to characterize efficacy in terms of attack-resiliency, we performed a qualitative assessment, where the proposed model has been examined for its robustness towards any breach-probability caused due to linear and differential cryptanalysis (Ex. RS analysis), Interpolation attacks, Weak key combination, square attacks and related key attack conditions.

Typically, the prime objective of a cipher in a security system is to ensure attack-resiliency and protection of the plaintext. In a classical cloud environment, an attacker often intercepts the cipher-text being transmitted through or over multimedia data and intends to extract or recover the text, though the target data or information can be in other forms as well such as image bits or multimedia-specific text presentation. Functionally, a cipher can be stated to be breached in case the attacker gets access or becomes able to retrieve the secret key. The situation when an attacker

Table 5 Image entropy analysis

Dataset	Original image entropy	Encrypted image entropy
Fundus1	6.3510	7.9898
Fundus2	6.2515	7.9913
Fundus3	5.4312	7.9936
MRI1	6.0468	7.1053
MRI2	6.3670	7.9514
MRI3	6.1031	7.8990
Lena	7.3904	7.6730
Panda	7.4938	7.9968
Baboon	7.1020	7.8993

Table 6 Correlation analysis

Dataset	Original image correlation	Correlation post-encryption
Fundus1	0.9920	0.0076
Fundus2	0.9918	0.0072
Fundus3	0.9883	0.0036
MRI1	0.9763	0.0336
MRI2	0.9929	0.0100
MRI3	0.8628	0.0031
Lena	0.9743	0.0041
Panda	0.9811	0.0003
Baboon	0.8198	0.0039

Table 7 NPCR and UACI randomness test

Dataset	NPCR (%)	UACI (%)
Fundus1	99.60	25.77
Fundus2	99.63	28.32
Fundus3	99.63	23.81
MRI1	99.59	36.61
MRI2	99.43	28.60
MRI3	99.63	41.06
Lena	99.52	14.87
Panda	99.62	13.31
Baboon	99.62	22.62

becomes capable enough to decrypt the cipher-text without estimating the secret key, the cipher is hypothesized to be breached partially. Considering cloud communication environment, we hypothesize that the attacker possesses unobstructed access of the data under transmission across the channel. Additionally, the attacker can also have key

Table 8 Execution time (system configuration Intel dual core)

Dataset	Time (ms)
Fundus1	87.97
Fundus2	72.60
Fundus3	70.63
MRI1	89.45
MRI2	71.06
MRI3	77.64
Lena	89.40
Panda	88.48
Baboon	82.26

information; however to assess the security of a cipher, it is significant to consider computational efficacy of the attacker. Unlike classical crypto-models, our proposed model inherits the strength of both Uniform Substitution and Permutation model as well as Feistel structure (with multiple rounds) it strengthens attack resilience. The robustness of the proposed model can be characterized in terms of its efficacy to avoid the following attack conditions.

5.2.1 Differential and linear (regular and singular) cryptanalysis

As already discussed in the previous section the KEBF function is developed based on the suggestions provided in [73], which itself justifies its robustness to avoid any kind of Differential and Linear (Regular and Singular) Cryptanalysis, our proposed security model can be considered to be robust enough to avoid any aforesaid attack probability. Moreover, as depicted in above discussion the correlation in between the original image data and the cipher data is significantly large even if the linear approximation is performed for two rounds. Since, we performed five distinct rounds of computation; it strengthened the proposed model to exhibit high correlation and hence more attack resilience. Additionally, since the (each) round transformation is maintained uniform which enables treating each bit similar and hence facilitates resilience to the differential attack. The results obtained in terms of NPCR and UACI, as discussed above reveals that the proposed security model can have sufficient resilience to avoid any kind of differential attacks problems in cloud environment. To be noted, correlation test, NPCR and UACI assessment are especially designed approach for differential attack analysis. The comparative performance assessment of the proposed security system as well as other existing approaches is given in Section C (Inter-Model Performance Assessment).

5.2.2 Weak key combination

In cloud computing environment users make a common mistake by keeping poor or weak key combination that helps attacker to get easy access to the ciphers. On contrary, the cipher information where the non-linear operations usually rely on the key value maps the block cipher in such manner that it causes detectable weakness. On the other hand, looking into the proposed security model where it avoids using the same (actual) key in the cipher (due to multiple round key manipulation and/or exchange by XORing the actual key followed by KEBF for five rounds). It makes proposed system robust enough to avoid any kind of weak-key attack probability. On the other hand, in the proposed KEBF function non-linearity is fixed significantly and thus there becomes no limitation on the key-selection.

5.2.3 Related keys combination trial attack

This is the matter of fact that the attack can be made with the help of certain partially known or unknown keys as well. The related keys primarily depend on either slow diffusion or possessing symmetry in key expansion block, as discussed in the previous section. In our proposed security model, we crafted the key expansion mechanism in such manner that it retains fast computation and non-linear diffusion, especially for the cipher key difference in comparison to the round keys that makes significant confusion to assess related key for data attack.

5.2.4 Square-attack

To assess efficacy of a security model, different attack modules are applied to investigate attack-resiliency by the proposed approach. Some of the key approaches applied in cloud-sensitive security models are the RS-Analysis and Square Attack. Considering Square Attack condition, it is capable enough to retrieve one byte of the last key combination and intends to retrieve or recover rest of the keys by repeating the attack iteratively. Let, such repetition be eight times, then also to achieve above stated information, the attacker needs to identify 28 keys precisely by 28 plaintexts which is equivalent to 216- S-box lookups. This becomes highly complicate and thus our proposed model avoids such attack probability.

5.2.5 Interpolation attack

In general, such kinds of attacks primarily rely on the generic architecture of the cipher components which could generate certain rational expression with relatively low complexity. However, as already discussed the S-box expression of the proposed security system with diffusion

characteristics strengthen it to avoid such limitations and thus makes it impracticable enough to avoid attack.

5.3 Inter-model performance assessment

Though, the proposed multimedia data security model encompasses novelties at the different level of computation, to assess its relative performance we considered some researches functional on the same motive “lightweight-encryption”. To achieve it, we referred a work done by Noura et al. [58], who applied dynamic structure based lightweight encryption system, titled “A new efficient lightweight and secure image cipher scheme”. As dynamic structure solution, authors applied forward and backward chaining block (FBC) that in conjunction with a permutation block enabled image encryption. In their proposed model, authors enabled change of the key for each input, which were applied subsequently to generate cipher layer. Noticeably, their proposed cipher layer comprised a binary diffusion matrix, substitution box and permutation box, in sequence. Authors [57, 58] stated that their proposed model with binary diffusion matrix, substitution and permutation table could achieve better performance (with two-rounds). Considering a common test case of “Lena.jpg” image data, which has been considered in our proposed model as well, we examined peak signal to noise ratio (PSNR) performance for the proposed security model as well as the existing [57] one in Table 9. Mathematically, we estimated PSNR using function.

$$PSNR = 10 \log_{10} \frac{M \times N \times 255^2}{\sum_{i,j} y_{ij} - x_{ij}^2}$$

In (19), the variable M and N states the image dimensions, while x and y are the before and after encryption positions. To assess performance, we considered maximum (Max) PSNR to assess relative performance.

Observing the result, it can easily be found that our proposed multimedia security model retains higher PSNR than the both existing methods [57, 58]. Similar to [58, 59], authors [61] developed a dynamic approach for a lightweight and secure cipher for medical images. Authors at first identified sensitive region as well as non-sensitive regions over the target image based on average of the sub-matrix in reference to a predefined threshold level.

Table 9 PSNR assessment

Data	PNSR		
Lena.jpg	[57] 9.2604	[58] 8.6054	Proposed 9.8610

Towards encryption of the image, authors applied dynamic structure-based concept. In fact, most of the key contributions of this work was same as [58]; though authors assess performance over different medical images. In their simulation, authors could achieve NPCR between the original and the cipher image as 50.1029, while UACI for the same sample was obtained as 99.6460. Entropy performance was found to be within the range of 7 to 7.3. Observing these results, our proposed system seems to be superior with lower entropy and differential attack resilience. Similar to the work in [57, 58], authors developed a dynamic structure-based encryption model for fingerprint security [59]. In this method, authors [59] where applied shifting concept for image encryption. Since, the exiting work [59] and our proposed model applied different data, direct comparison can't be done; however as relative performance analysis it can be found that the entropy of our proposed security model (Minimum observed entropy = 7.1053) is lower than the existing method ([59], 7.6448). In [60] as well authors claimed their approach as "light-weight" where chaos and Deoxyribo Nucleic Acid (DNA) computing (it states a dynamic structure model) for image encryption. Authors [60] considered benchmark Lena.jpg image for system test, where they obtained performance outcome in terms of NPCR, UACI and entropy (characterizing differential attack assessment).

Observing above results (Table 10) it can easily be found that the proposed image encryption model outperforms existing approaches by maintaining lower entropy with satisfactory higher correlation performance to avoid differential attack condition over cloud platforms. The NPCR and UACI results affirms the robustness of the proposed multimedia data (image) security model towards (differential) attack-resilience. Thus, observing overall performance and corresponding inferences, it can be affirmed that the proposed multimedia encryption model is more efficient than the other existing approaches. It enables our proposed security model to be applied in real-world cloud computing environment.

The overall research inference and conclusion is given in the subsequent section.

Table 10 Comparative assessment

Data	Method	Entropy	Correlation	NPCR	UACI
Lena.jpg	[60]	7.9992	0.0011	99.7570	0.3912
	Proposed	7.6730	0.0041	99.5200	0.1487
Baboon.jpg	[60]	7.9993	0.0015	98.0961	0.7702
	Proposed	7.8993	0.0039	99.6200	0.2262

6 Conclusion

Considering the significance of a secure multimedia communication environment over cloud environment, which has gained widespread attention globally, this research focused on designing a lightweight and robust "multimedia data security system". Unlike classical researches where to enhance security level authors have either increased key size or have exploited hybrid cryptosystems. Unfortunately, such approaches impose significantly high computational overheads and complexity. On contrary, cloud computing demands lightweight and computationally efficient security solution, especially for multimedia data transmission. Considering it as motive, in this research paper a robust multimedia data security model was developed by exploiting efficacy of the block cipher approach using substitution and permutation network (SPN) and Feistel structure. Similar to the block-cipher approaches such as AES, Grasshopper, SAFER, SHARK and Square attack methods etc., our proposed model employs SPN network in which the use of multiple-round or iterative substitution and transposition enabled Shannon's confusion and diffusion conditions. It enabled changing the cipher text in certain pseudo-random paradigm. To achieve it, this method applied Feistel architecture, which performs both encryption as well as decryption in similar manner. Thus, the use of Feistel architecture and SPN network provided a hybrid security system which applied 64-bit key processing with most robust attack-resiliency for multimedia data communication over cloud. The qualitative and quantitative assessment of the proposed security model affirms its suitability towards secure multimedia data communication over cloud computing environment while assuring low computational overheads and complexity. The proposed model also ensures different attack resiliency and hence is robust enough to be used under uncertain cloud environment.

References

1. Sajjad, M., Muhammad, K., Baik, S. W., et al. (2017). Mobile-cloud assisted framework for selective encryption of medical images with steganography for resource-constrained devices. *Multimed Tools Appl*, 76, 3519–3536. <https://doi.org/10.1007/s11042-016-3811-6>
2. Darwish, A., Hassanien, A. E., Elhoseny, M., et al. (2019). The impact of the hybrid platform of internet of things and cloud computing on healthcare systems: opportunities, challenges, and open problems. *J Ambient Intell Human Comput*, 10, 4151–4166. <https://doi.org/10.1007/s12652-017-0659-1>
3. Anwar, A. S., Ghany, K. K. A., & El Mahdy, H. (2015). Improving the security of images transmission. *Int. J. Bio-Med. Inform. e-Health*, 3(4), 7–13.

4. Bairagi, A. K., Khondoker, R., & Islam, R. (2016). An efficient steganographic approach for protecting communication in the Internet of Things (IoT) critical infrastructures. *Information Security Journal: A Global Perspective*, 25(4–6), 197–212. <https://doi.org/10.1080/19393555.2016.1206640>
5. Paschou, M., Sakkopoulos, E., Sourla, E., & Tsakalidis, A. (2013). Health Internet of Things: Metrics and methods for efficient data transfer. *Simulation Modelling Practice and Theory*, 34, 186–199. <https://doi.org/10.1016/j.simpat.2012.08.002>
6. Parah S.A., Sheikh J.A., Ahad F., Bhat G.M. (2018) High Capacity and Secure Electronic Patient Record (EPR) Embedding in Color Images for IoT Driven Healthcare Systems. In: Dey N., Hassanien A., Bhatt C., Ashour A., Satapathy S. (eds) Internet of Things and Big Data Analytics Toward Next-Generation Intelligence. Studies in Big Data, vol 30. Springer, Cham. https://doi.org/https://doi.org/10.1007/978-3-319-60435-0_17
7. Li, L., Hossain, M. S., El-Latif, A. A. A., et al. (2019). Distortion less secret image sharing scheme for Internet of Things system. *Cluster Comput*, 22, 2293–2307. <https://doi.org/10.1007/s10586-017-1345-y>
8. Gupta, R. K., & Singh, P. (2013). “A new way to design and implementation of hybrid crypto system for security of the information in public network”, *International Journal of Emergency. Technology Advanced Engineering*, 3(8), 108–115.
9. Muhammad Sajjad, Mansoor Nasir, Khan Muhammad, Siraj Khan, Zahoor Jan, Arun Kumar Sangaiah, Mohamed Elhoseny, Sung Wook Baik, Raspberry Pi assisted face recognition framework for enhanced law-enforcement services in smart cities, *Future Generation Computer Systems*, Volume 108, 2020, Pages 995–1007, ISSN 0167–739X, <https://doi.org/https://doi.org/10.1016/j.future.2017.11.013>.
10. Laskar, S. (2012). High Capacity data hiding using LSB Steganography and Encryption. *International Journal of Database Management Systems.*, 4, 57–68. <https://doi.org/10.5121/ijdms.2012.4605>
11. B. Xue, X. Li and Z. Guo, “A New SDCS-based Content-adaptive Steganography Using Iterative Noise-Level Estimation,” 2015 International Conference on Intelligent Information Hiding and Multimedia Signal Processing (IIH-MSP), Adelaide, SA, 2015, pp. 68–71, doi: <https://doi.org/10.1109/IIH-MSP.2015.80>.
12. Vipula Madhukar Wajgade, “Enhancing Data Security Using Video Steganography,” *International Journal of Emerging Technology and Advanced Engineering* Volume 3, Issue 4, April 2013.
13. Lokesh Kumar, “Novel Security Scheme for Image Steganography using Cryptography technique”, *International Journal of Advanced Research in Computer Science and Software Engineering*, Volume 2, Issue 4, April 2012 ISSN: 2277 128X.
14. Marwa E. Saleh, Abdelmgeid A. Aly and Fatma A. Omara, “Data Security Using Cryptography and Steganography Techniques” *International Journal of Advanced Computer Science and Applications (IJACSA)*, 7(6), 2016. <http://dx.doi.org/https://doi.org/10.14569/IJACSA.2016.070651>
15. M. E. Saleh, A. A. Aly, and F. A. Omara, “Enhancing Pixel Value Difference (PVD) Image Steganography by Using Mobile Phone Keypad (MPK) Coding,” *International Journal of Computer Science and Security (IJCSS)*, Volume (9), Issue (2), pp. 397 - 397, 2015
16. A. Duluta, S. Mocanu, R. Pietraru, D. Merezeanu and D. Saru, “Secure Communication Method Based on Encryption and Steganography,” 2017 21st International Conference on Control Systems and Computer Science (CSCS), Bucharest, 2017, pp. 453–458, doi: <https://doi.org/10.1109/CSCS.2017.70>.
17. Dhvani Panchal, “An Approach Providing Two Phase Security of Images Using Encryption and Steganography in Image Processing”, 2015 IJEDR, Volume 3, Issue 4, ISSN: 2321–9939.
18. Y. Leung and R. Y. Hou, “Unequal security protection for secure multimedia communication,” 2015 IEEE 4th Global Conference on Consumer Electronics (GCCE), Osaka, 2015, pp. 570–571, doi: <https://doi.org/10.1109/GCCE.2015.7398667>.
19. Mukhedkar, M., Powar, P., Gaikwad, P., & “Secure non real time image encryption algorithm development using cryptography & steganography”, . (2015). Annual IEEE India Conference (INDICON). *New Delhi, 2015*, 1–6. <https://doi.org/10.1109/INDICON.2015.7443808>
20. Li, J., Guo, X., Yu, Y., Tu, Q., Men, A., & “A robust and low-complexity video fingerprint for multimedia security”, . (2014). International Symposium on Wireless Personal Multimedia Communications (WPMC). *Sydney, NSW, 2014*, 97–102. <https://doi.org/10.1109/WPMC.2014.7014798>
21. D. E. M. Ahmed and O. O. Khalifa, “Robust and Secure Image Steganography Based on Elliptic Curve Cryptography,” 2014 International Conference on Computer and Communication Engineering, Kuala Lumpur, 2014, pp. 288–291, doi: <https://doi.org/10.1109/ICCCE.2014.88>.
22. Hajduk, V., Broda, M., Kovac, O., Levicky, D., & “Image steganography with using QR code and cryptography.” (2016). 26th International Conference Radioelektronika (RADIO-ELEKTRONIKA). *Kosice, 2016*, 350–353. <https://doi.org/10.1109/RADIOELEK.2016.7477370>
23. M. S. Alam, “Secure M-commerce data using post quantum cryptography,” 2017 IEEE International Conference on Power, Control, Signals and Instrumentation Engineering (ICPCSI), Chennai, 2017, pp. 649–654, doi: <https://doi.org/10.1109/ICPCSI.2017.8391793>.
24. N. Kumar and S. Agrawal, “An efficient and effective lossless symmetric key cryptography algorithm for an image,” 2014 International Conference on Advances in Engineering & Technology Research (ICAETR - 2014), Unnao, 2014, pp. 1–5, doi: <https://doi.org/10.1109/ICAETR.2014.7012788>.
25. D. Sharma and D. Sharma, “Steganography of the keys into an encrypted speech signal using Matlab,” 2016 3rd International Conference on Computing for Sustainable Global Development (INDIACom), New Delhi, 2016, pp. 721–724.
26. Z. Wang, J. Liu, W. Wan, J. Sun, J. Bo and Y. Liu, “Security Monitoring by Watermarking and Hashing for Multimedia Service on Internet Platform,” 2014 Tenth International Conference on Intelligent Information Hiding and Multimedia Signal Processing, Kitakyushu, 2014, pp. 630–633, doi: <https://doi.org/10.1109/IIH-MSP.2014.163>.
27. A. A. Zaher, “A cryptography algorithm for transmitting multimedia data using quadruple-state CSK,” 2015 International Conference on Computer, Communications, and Control Technology (I4CT), Kuching, 2015, pp. 87–92, doi: <https://doi.org/10.1109/I4CT.2015.7219543>.
28. M. B. Hossain, M. T. Rahman, A. B. M. S. Rahman and S. Islam, “A new approach of image encryption using 3D chaotic map to enhance security of multimedia component,” 2014 International Conference on Informatics, Electronics & Vision (ICIEV), Dhaka, 2014, pp. 1–6, doi: <https://doi.org/10.1109/ICIEV.2014.6850856>.
29. P. Saxena, D. Shahane, S. Rai and R. Boghey, “Enhancing image security using data compression and spread spectrum watermarking technique,” 2017 7th International Conference on Communication Systems and Network Technologies (CSNT), Nagpur, 2017, pp. 215–219, doi: <https://doi.org/10.1109/CSNT.2017.8418540>.
30. S. Gupta and R. Jain, “An innovative method of Text Steganography,” 2015 Third International Conference on Image Information Processing (ICIIP), Wanknaghat, 2015, pp. 60–64, doi: <https://doi.org/10.1109/ICIIP.2015.7414741>.

31. Ashwini, Bhadane et al. "A Hybrid Approach for Enhancing Data Security by Combining Encryption and Steganography." (2014).
32. J. Joshi, K. Nair, M. Warde, V. Rawalgaonkar and J. Kulkarni, "Secure semi-blind steganography using chaotic transforms," 2016 3rd International Conference on Computing for Sustainable Global Development (INDIACom), New Delhi, 2016, pp. 2669–2673.
33. N. Rashmi and K. Jyothi, "An improved method for reversible data hiding steganography combined with cryptography," 2018 2nd International Conference on Inventive Systems and Control (ICISC), Coimbatore, 2018, pp. 81–84, doi: <https://doi.org/10.1109/ICISC.2018.8398946>.
34. R. S. Phadte and R. Dhanaraj, "Enhanced blend of image steganography and cryptography," 2017 International Conference on Computing Methodologies and Communication (ICCMC), Erode, 2017, pp. 230–235, doi: <https://doi.org/10.1109/ICCMC.2017.8282682>.
35. Saraireh, S. (2013). A Secure Data Communication System Using Cryptogaphy And Steganography. *International journal of Computer Networks & Communications.*, 5, 125–137. <https://doi.org/10.5121/ijcnc.2013.5310>
36. G.Sateesh, E.Sai Lakshmi, M.Ramanamma, K.Jairam, A.Yeswanth "Assured Data Communication Using Cryptography and Steganography" *International Journal of Latest Technology in Engineering, Management & Applied Science-IJLTEMAS* vol.5 issue 3, pp.102–106 2016.
37. Shamim Ahmed Laskar, "Secure Data Transmission Using Steganography and Encryption Technique", *International Journal on Cryptography and Information Security (IJCIS)*, Vol.2, No.3, September 2012.
38. S. D. Torvi, K. B. ShivaKumar and R. Das, "An unique data security using text steganography," 2016 3rd International Conference on Computing for Sustainable Global Development (INDIACom), New Delhi, 2016, pp. 3834–3838.
39. S. Pleshkova and D. Kinanev, "Method of design public key infrastructure for secure audio information transmission in multimedia systems," 2017 15th International Conference on Electrical Machines, Drives and Power Systems (ELMA), Sofia, 2017, pp. 195–198, doi: <https://doi.org/10.1109/ELMA.2017.7955430>.
40. T. P. Pai, M. E. Raghu and K. C. Ravishankar, "Video Encryption for Secure Multimedia Transmission - A Layered Approach," 2014 3rd International Conference on Eco-friendly Computing and Communication Systems, Mangalore, 2014, pp. 127–132, doi: <https://doi.org/10.1109/Eco-friendly.2014.101>.
41. H. Cui, X. Yuan and C. Wang, "Harnessing Encrypted Data in Cloud for Secure and Efficient Mobile Image Sharing", in *IEEE Transactions on Mobile Computing*, vol. 16, no. 5, pp. 1315–1329, 1 May 2017, doi: <https://doi.org/10.1109/TMC.2016.2595573>.
42. Usman, M., Jan, M. A., He, X., & Chen, J. (2019). P2DCA: A Privacy-Preserving-Based Data Collection and Analysis Framework for IoMT Applications. *IEEE Journal on Selected Areas in Communications*, 37(6), 1222–1230. <https://doi.org/10.1109/JSAC.2019.2904349>
43. Zheng, Y., Yuan, X., Wang, X., Jiang, J., Wang, C., & Gui, X. (2017). Toward Encrypted Cloud Media Center With Secure Deduplication. *IEEE Transactions on Multimedia*, 19(2), 251–265. <https://doi.org/10.1109/TMM.2016.2612760>
44. Abdul, W., Ali, Z., Ghouzali, S., Alfawaz, B., Muhammad, G., & Hossain, M. S. (2017). Biometric Security Through Visual Encryption for Fog Edge Computing. *IEEE Access*, 5, 5531–5538. <https://doi.org/10.1109/ACCESS.2017.2693438>
45. Li, X., Yuan, J., Ma, H., & Yao, W. (2018). Fast and Parallel Trust Computing Scheme Based on Big Data Analysis for Collaboration Cloud Service. *IEEE Transactions on Information Forensics and Security*, 13(8), 1917–1931. <https://doi.org/10.1109/TIFS.2018.2806925>
46. Li, Q., Tian, Y., Zhang, Y., Shen, L., & Guo, J. (2019). Efficient Privacy-Preserving Access Control of Mobile Multimedia Data in Cloud Computing. *IEEE Access*, 7, 131534–131542. <https://doi.org/10.1109/ACCESS.2019.2939299>
47. H. A. Al Hamid, S. M. M. Rahman, M. S. Hossain, A. Almogren and A. Alamri, "A Security Model for Preserving the Privacy of Medical Big Data in a Healthcare Cloud Using a Fog Computing Facility With Pairing-Based Cryptography," in *IEEE Access*, vol. 5, pp. 22313–22328, 2017,doi: <https://doi.org/10.1109/ACCESS.2017.2757844>.
48. Khedr, A., & Gulak, G. (2018). SecureMed: Secure Medical Computation Using GPU-Accelerated Homomorphic Encryption Scheme. *IEEE Journal of Biomedical and Health Informatics*, 22(2), 597–606. <https://doi.org/10.1109/JBHI.2017.2657458>
49. Zhu, L., Song, H., Zhang, X., Yan, M., Zhang, L., & Yan, T. (2019). A Novel Image Encryption Scheme Based on Nonuniform Sampling in Block Compressive Sensing. *IEEE Access*, 7, 22161–22174. <https://doi.org/10.1109/ACCESS.2019.2897721>
50. Zhang, X., & Wang, X. (2018). Digital Image Encryption Algorithm Based on Elliptic Curve Public Cryptosystem. *IEEE Access*, 6, 70025–70034. <https://doi.org/10.1109/ACCESS.2018.2879844>
51. Tawalbeh, L., Mowafi, M., & Aljoby, W. (2013). Use of elliptic curve cryptography for multimedia encryption. *IET Information Security*, 7(2), 67–74. <https://doi.org/10.1049/iet-ifs.2012.0147>
52. M. Guan, X. Yang and W. Hu, "Chaotic image encryption algorithm using frequency-domain DNA encoding," in *IET Image Processing*, vol. 13, no. 9, pp. 1535–1539, 18 7 2019, doi: <https://doi.org/10.1049/iet-ipr.2019.0051>.
53. He, J., Huang, S., Tang, S., & Huang, J. (2018). JPEG Image Encryption With Improved Format Compatibility and File Size Preservation. *IEEE Transactions on Multimedia*, 20(10), 2645–2658. <https://doi.org/10.1109/TMM.2018.2817065>
54. R. Hamza, K. Muhammad, A. N. and G. RamiRez-GonzaLez, "Hash Based Encryption for Keyframes of Diagnostic Hysterescopy," in *IEEE Access*, vol. 6, pp. 60160–60170, 2018, doi: <https://doi.org/10.1109/ACCESS.2017.2762405>.
55. Z. Xia, Y. Zhu, X. Sun, Z. Qin and K. Ren, "Towards Privacy-Preserving Content-Based Image Retrieval in Cloud Computing," in *IEEE Transactions on Cloud Computing*, vol. 6, no. 1, pp. 276–286, 1 Jan.-March 2018, doi: <https://doi.org/10.1109/TCC.2015.2491933>.
56. Xu, Y., Zhao, X., & Gong, J. (2019). A Large-Scale Secure Image Retrieval Method in Cloud Environment. *IEEE Access*, 7, 160082–160090. <https://doi.org/10.1109/ACCESS.2019.2951175>
57. Zeinab Fawaz, Hassan Noura, Ahmed Mostefaoui, An efficient and secure cipher scheme for images confidentiality preservation, *Signal Processing: Image Communication*, Volume 42, 2016, Pages 90–108, ISSN 0923–5965, <https://doi.org/https://doi.org/10.1016/j.image.2016.01.009>.
58. Noura, H., Sleem, L., Noura, M., et al. (2018). A new efficient lightweight and secure image cipher scheme. *Multimed Tools Appl*, 77, 15457–15484. <https://doi.org/10.1007/s11042-017-5124-9>
59. Visalakshi, B., & Meyappan, T. (2017). Image Encryption and Decryption using Shifting Technique. *International Journal of Engineering Science and Computing*, 7(6), 12668–12671.
60. Bhaskar Mondal, Tarni Mandal, A light weight secure image encryption scheme based on chaos & DNA computing, *Journal of King Saud University - Computer and Information Sciences*, Volume 29, Issue 4, 2017, Pages 499–504, ISSN 1319–1578, <https://doi.org/https://doi.org/10.1016/j.jksuci.2016.02.003>.
61. Noura, M., Noura, H., Chehab, A., et al. (2018). A dynamic approach for a lightweight and secure cipher for medical images.

- Multimed Tools Appl*, 77, 31397–31426. <https://doi.org/10.1007/s11042-018-6051-0>
62. S. Belguith, A. Jemai, R. Attia, Enhancing data security in cloud computing using a lightweight cryptographic algorithm, in: ICAS 2015 : The Eleventh International Conference on Automatic and Autonomous Systems, IARIA, 2015, pp. 98–103.
 63. Daniel, E., & Vasanthi, N. A. (2019). LDAP: a lightweight deduplication and auditing protocol for secure data storage in cloud environment. *Cluster Comput*, 22, 1247–1258. <https://doi.org/10.1007/s10586-017-1382-6>
 64. P. Rad, M. Muppidi, S. S. Agaian and M. Jamshidi, “Secure image processing inside cloud file sharing environment using lightweight containers,” 2015 IEEE International Conference on Imaging Systems and Techniques (IST), Macau, 2015, pp. 1–6, doi: <https://doi.org/10.1109/IST.2015.7294578>.
 65. Xiong, J., Zhang, Y., Li, X., et al. (2018). RSE-PoW: a Role Symmetric Encryption PoW Scheme with Authorized Deduplication for Multimedia Data. *Mobile Netw Appl*, 23, 650–663. <https://doi.org/10.1007/s11036-017-0975-x>
 66. Gupta, B. B., Yamaguchi, S., & Agrawal, D. P. (2018). Advances in Security and Privacy of Multimedia Big Data in Mobile and Cloud Computing. *Multimed Tools Appl*, 77, 9203–9208. <https://doi.org/10.1007/s11042-017-5301-x>
 67. Alassaf, N., Gutub, A., Parah, S. A., et al. (2019). Enhancing speed of SIMON: A light-weight-cryptographic algorithm for IoT applications. *Multimed Tools Appl*, 78, 32633–32657. <https://doi.org/10.1007/s11042-018-6801-z>
 68. Shifa A, Asghar MN, Noor S, Gohar N, Fleury M. Lightweight Cipher for H.264 Videos in the Internet of Multimedia Things with Encryption Space Ratio Diagnostics. *Sensors*. 2019; 19(5):1228. <https://doi.org/https://doi.org/10.3390/s19051228>
 69. Liang, C., Ning Ye, R., & Malekian and Ruchuan Wang, “The hybrid encryption algorithm of lightweight data in cloud storage”, . (2016). 2nd International Symposium on Agent, Multi-Agent Systems and Robotics (ISAMSR). *Bangi, Malaysia, 2016*, 160–166. <https://doi.org/10.1109/ISAMSR.2016.7810021>
 70. Noura, H., Chehab, A., Sleem, L., et al. (2018). One round cipher algorithm for multimedia IoT devices. *Multimed Tools Appl*, 77, 18383–18413. <https://doi.org/10.1007/s11042-018-5660-y>
 71. P. Barreto and V. Rijmen, “The khazad legacy-level block cipher,” Primitive submitted to NESSIE, vol. 97, 2000.
 72. J. Daemen, “Cipher and hash function design strategies based on linear and differential cryptanalysis,” Ph.D. dissertation, Doctoral Dissertation, March 1995, KU Leuven, 1995.
 73. Y. Wu, J. Noonan and S. Agaian, “NPCR and UACI Randomness Tests for Image Encryption,” *Cyber Journals: Multidisciplinary, Journals in Science and Technology, Journal of Selected Areas in Telecommunications (JSAT)*, 2011, pp. 31–38.
 74. May Zaw, Z., & Phyto, S. W. (2015). Security Enhancement System Based on the Integration of Cryptography and Steganography. *International Journal of Computer (IJC)*, 19(1), 26–39.
 75. L. Yu, Z. Wang and W. Wang, “The Application of Hybrid Encryption Algorithm in Software Security,” 2012 Fourth International Conference on Computational Intelligence and

Communication Networks, Mathura, 2012, pp. 762–765, doi: <https://doi.org/10.1109/CICN.2012.195>.

Publisher's Note Springer Nature remains neutral with regard to jurisdictional claims in published maps and institutional affiliations.



Denis Rayappan has obtained Bachelor of Science (B.Sc.) from Loyola College (Autonomous), Madras University, Chennai, TN, India and Master of Computer Applications (MCA) from Sacred Heart College (Autonomous), Tirupattur in the year 2006 and 2009 respectively. Presently, he is a Assistant Professor at PG Department of Computer Science, Sacred Heart College (Autonomous) and also pursuing his Ph.D. in Computer Sci-

ence at Periyar University, Salem, TN, India. He has over 10 years of teaching experience and published research papers in peer reviewed Journals and conferences, one Indian Patent, and authored two books (Java Programming – for Core and Advanced Users, ISBN: 9789386235329 | Year: 2018 & Constructive Java Programming ISBN: 9789389211771 | Year: 2020–2021) by Universities Press (India) Pvt. Ltd, Hyderabad. His research interests include Data Security and Privacy, Cryptography Algorithms, Big Data Analytics, Data Mining and Bio-inspired algorithms.



Madhubala Pandiyan obtained Ph.D. in Computer Science from Mother Teresa Women's University, kodaikanal, TN, India in the year 2017. She is currently a Assistant Professor at Research Department of Computer Science, Don Bosco College of Arts and Science, Dharmapuri, TN, India since 2007. Also she is the University nominee for Board of Studies of BCA department at Sacred Heart College (Autonomous), Thiruvalluvar University, Tiru-

pattur, TN, India. She has published more than 13 research papers in peer reviewed international journals and conferences. Her research interests include Cloud Computing, Wireless Sensor Networking, Data security, advanced data mining and Artificial Intelligence. She has 19 years of teaching experience and 8 years of Research Experience. Currently she is guiding five Ph.D. students.



INTERNATIONAL JOURNAL OF CREATIVE RESEARCH THOUGHTS (IJCRT)

An International Open Access, Peer-reviewed, Refereed Journal

Auto-Detecting Perpetual Outliers Using Efficient Modified Fuzzy Clustering Approach

S.Rajalakshmi
Research Scholar

Department of Computer Science
Government Arts College for Women-Krishnagiri

P.Madhubala

Research Supervisor
Department of Computer Science
Don Bosco College – Dharmapuri

Abstract:

To create some outstanding new ideas of innovation during Pandemic, this paper reveals an augmented study of modified robust fuzzy clustering approach to detect the unusual outliers. Outlier Detection, an unsupervised learning used to detect complex dataset to identify perpetual outliers using membership function to tolerate the uncertainty. The first stage aims to estimate auto-detection of noise reduction, incorrect data points and so on as perpetual outliers. The second stage aims to determine the characterization of utilized input parameters of unending outliers using FCM (Fuzzy C-means Clustering) method to find FOF(Fuzzy Objective Function). This method enhances accuracy, efficacy over similarity measure and performance efficiency that assessed over some UCI repository datasets. Experimental results and statistical evaluation shows effectiveness of detecting perpetual outliers.

Keywords: Outliers, fuzzy, clustering, Fitness, Perpetual, FOF, Characterization

1. Introduction:

During Pandemic, the situation is worst and uncertain to predict the future events. Outlier detection is also an important and complex task due to its uncertainty intolerance. Outlier known as anomaly identifies the extreme points from the dataset [1]. Fuzzy clustering is the suitable method for handling the uncertainty. Due to technology development, rare events happen due to technology advancement. Data is pre-processed to reduce the noise and focused on predictions to reveal highly desirable task. No of clusters is determined for the iterations. Distance is evaluated using Euclidean measure. Fuzzy objective function is measured based on the threshold value. The Cluster validation is determined by the optimal no of clusters. All the input parameters are characterized using a threshold value. It is evaluated by no of intensive clusters in 'inliers' and in 'outliers'. The degree of membership belongs from 0 to 1. Accuracy is very close to cluster input parameters of detected prototypes. During Characterization, a random learning of false data point and dominating capability of influence structure is fixed.

2. Literature Survey

Outliers which may treated as error results in underestimation of uncertainty tolerance. Outlier analysis is studied from charu.C.Aggarwal[1][3][7]. The various types of anomaly detection and characteristics is studied from chandola, Banerjee and Kumar[2]. Clustering techniques are identified by aggarwal,chandan and reddy[3]. Outliers identity is studied from Hawkins[4][9]. How to detect the outliers in real time application using fuzzy clustering is studied from Rajalakshmi and Madhubala[5].R programming by Yanchang Zhao[9].Fuzzy set is studied from Bezdek[11] and klir yaun[10].

The Prediction model is used to calculate residuals of estimating various waves of fuzzy outliers. From the study, the non-adherence of protocol *stemmed* up by the characterization of extreme datapoints. The number of clusters indicate efficient generalization over learning of fuzzy objective function by less computational effort. It uses membership value, cardinality value, and cluster validation indices.

A modified approach using feature based indexing for the labeled patterns with high membership function is considered for generalization [7]. A generalized fuzzy index method and novel constraint function of membership is understood by the study [8]. A detailed study of estimating ERR and EDR for z-score is demonstrated in [14]. How the *psych* and *z-curve* package is evaluated in R-script to study the outlier fitness as well from [17][18][19].

3. About the software packages used:

R tool (r 4.0.2 version) is used to analyse the outliers using fuzzy clustering. “*psych*” package is installed for factor analyzing the Perpetual outlier fitness. William Revelle[17][18], clearly estimates ERR((Expected Replicability Rate), EDR(Expected Discovery Rate) and ODR(Observed Discovery Rate) using the packages *psych* and *z-curve*. Confirmatory factor analysis is estimated by using fuzzy clustering. *iclust()*, item cluster analysis used to partition space of the fitness rather than space of the variable. It explains an implementation of z-curves and method for estimating replicability rates (ERR) and expected discovery rates(EDR) on finding fitness, metrics etc

Algorithm

Phase I:

- Step 1: Initialize no of clusters ‘k’
- Step2: Compute fuzzy membership matrix ‘U’
- Step3: calculate fuzzy centers ‘Vj’ until j is minimum
- Step4: Estimate the centroid of each cluster center ‘c’
- Step5: Update the minimum distance to each cluster using Euclidean distance
- Step6:Auto-detect the centers to identify farthest neighbor
- Step7:If the object has no neighbor, define it is outlier

Algorithm

Phase II:

- Step 1:Initial the fuzzy variables
- Step2:Calculate the sum of all the objects which has similarities
- Step3:Fix a random point between two similar clusters (say for eg. Between 0.5 and 0.7, 0.6 as random intensity values)
- Step 3a: Compare the random object with threshold value.
- Step 3b: If it is equal to threshold, move to next neighbour cluster
- Step 3c: Repeat step 3a until the value is below threshold
- Step4:At the end, extreme points from the old cluster to is used to detect the perpetual outlier of new cluster
- Step5: Depending on threshold value, outlier is identified.
- Step6:The objective function is obtained from new cluster is called FOF (Fuzzy objective function)

4. Experimental Results

RStudio 4.0.2 is used for estimating statistical analysis. Packages used are “*psych*” and “*zcurve*”, where *zcurve* developed by Frantisek Bartos on 27,September -2020 to detect the accuracy of outliers[17][18][19]. By installing *zcurve* package, we used density method to find the increase number of iterations and decrease number of criterion for the dataset *stock_data*. Estimation of ERR(Expected Replicability Rate) and EDR(Expected Discovery Rate) is shown below.

Table 1: Estimation of z-curve 2.0 density algorithm

Estimation of z-curve 2.0 density algorithm		
Dataset	ERR	EDR
iris	NA	NA
Stock_data	0.6135274	0.5064392
Advertising	NA	NA

Using *zcurve* package, we used density method for the version 1 to increase the number of iterations for the dataset *stock_data*. Estimation of ERR(Expected Replicability Rate) and EDR(Expected Discovery Rate) is shown below.

Table 2: Estimation of z-curve to increase the number of iterations

Estimation of z-curve to increase the number of iterations		
Dataset	ERR	EDR
iris	NA	NA
Stock_data	0.6479701	0.5046194
Advertising	NA	NA

Using *zcurve* package, we furnished the details regarding total number of starting fits and the means of mixture components. Estimation of ERR(Expected Replicability Rate) and EDR(Expected Discovery Rate) is shown below.

Table 3: Estimation of z-curve to increase the number of starting fits and change in means of mixture component

Estimation of z-curve to increase the number of starting fits and change in means of mixture components		
Dataset	ERR	EDR
iris	NA	NA
Stock_data	0.5880518	0.4578420
Advertising	NA	NA

In the fourth table, we comprised the z-curve fitness to simulate z-statistics. The estimation of ERR(Expected Replicability Rate), EDR(Expected Discovery Rate) and ODR(Observed Discovery Rate) is shown below.

Table 4: Estimation of z-curve to simulate z-statistics and z-fitness for *stock_data* dataset

Estimation of z-curve to simulate z-statistics and z-fitness for <i>stock_data</i> dataset			
z-score	Estimation Range (0.64 – 5.51)	Percentage	CI-(Confidence Interval)
ERR	0.82	95%	0.73,0.89
EDR	0.55	95%	0.24,0.89
ODR	0.85	95%	0.80,0.89

In the fifth table, we calculated the power components of z-score for the value of alpha from 0 to 1.(0.05 to 0.999)

Table 5: Estimation of z-curve power components

Estimation of z-curve power components							
Power to z-score	I	II	III	IV	V	VI	VII
Range (0-1)	0.05	0.20	0.40	0.60	0.80	0.974	0.999
Reult	0.000197359	1.11451417	1.706298343	2.213272223	2.801581787	3.903097682	5.050194967

Table 6: Estimating the model to detect outliers using EM and confidence interval

Model 1: EM via EM					
z-score	Estimation of EM	l.CI	u.CI	Iterations	Outliers detected
ERR	0.620	0.501	0.746	45 +118	Q= -60.61
EDR	0.391	0.082	0.693		CI[-70.48, -47.79]

Table 7: Estimating the model to detect outliers using KD2 and confidence interval

Model 1: KD2 via EM			
z-score	Estimation of KD2	Iterations	RMSE
ERR	0.614	47	0.11
EDR	0.506		

```

Estimates:
  ERR      EDR
0.6479701 0.5046194
> ctrl<-list(fit_reps=50,mu=c(0,1.5,3,4.5,6))
> zcurve(OSC.z,method="EM",control=ctrl)
Call:
zcurve(z = OSC.z, method = "EM", control = ctrl)

Estimates:
  ERR      EDR
0.5880518 0.4578420
> z<-abs(rnorm(300,3))
> m.EM<zcurve(z,method="EM",bootstrap=100)
Error: object 'm.EM' not found
> m.EM<zcurve(z,method="EM",bootstrap=100)
> plot<-m.EM
> plot(m.EM,annotation=TRUE,CI=TRUE)
> plot(m.EM,annotation=TRUE,CI=TRUE,x_text=0)
> plot(m.EM,annotation=TRUE,CI=FALSE,x_text=0)
> POWER_TO_Z<C(0.05,0.20,0.40,0.60,0.80,0.974,0.999),ALPHA=.05)
Error in POWER_TO_Z<C(0.05,0.2,0.4,0.6,0.8,0.974,0.999),ALPHA = 0.05) :
could not find function "POWER_TO_Z"
> power_to_z<c(0.05,0.20,0.40,0.60,0.80,0.974,0.999),alpha=.05)
[1] 0.000197359 1.114571417 1.706298343 2.213272223 2.801581787 3.903097682
[7] 5.050194967
> OSC.z
 [1] 2.409175 3.245251 2.164192 3.191229 2.702059 3.137051 8.402858
 [8] 3.718460 4.293275 3.512496 1.973777 7.066053 4.383039 3.536266
[15] 3.392537 2.194877 3.059374 4.637228 3.982280 2.169338 1.946709
[22] 2.268213 4.180570 3.459550 3.731395 1.836848 3.100000 10.000000
[29] 2.967738 2.183487 2.408916 2.365618 2.257129 1.968592 3.909901
[36] 2.273435 10.000000 2.307984 2.290368 2.967738 2.014091 10.000000
[43] 10.000000 3.290527 2.432379 2.014091 2.575829 10.000000 2.307984
[50] 2.967738 2.967738 1.792831 3.290527 1.959964 2.297408 2.053749
[57] 10.000000 2.542699 2.403655 10.000000 3.410733 2.975294 3.849639
[64] 10.000000 2.273435 2.106589 3.694892 2.195944 2.307984 4.178900
[71] 1.951480 2.967738 2.226212 2.290368 2.967738 2.780638 2.612054
[78] 10.000000 2.652070 10.000000 2.725494 2.652070 3.042724 2.652070
[85] 2.970656 2.257129 2.386708 3.403461 2.120072 2.688852

```

Figure 1: No of clusters after removal of noise in stock__data dataset

```

Rterm (64-bit)
could not find function "POWER.TO.Z"
> power.to.z(c(0.05,0.20,0.40,0.60,0.80,0.974,0.999),alpha=.05)
[1] 0.000197359 1.114571417 1.706298343 2.213272223 2.801581787 3.903097682
[7] 5.050194967
> OSC.z
[1] 2.409175 3.245251 2.164192 3.191229 2.702059 3.137051 0.402858
[8] 3.718460 4.293275 3.512496 1.973777 7.066053 4.383039 3.536266
[15] 3.392537 2.194877 3.059374 4.637228 3.982280 2.169338 1.946709
[22] 2.268213 4.180570 3.459550 3.731395 1.836848 3.100000 10.000000
[29] 2.967738 2.183487 2.408916 2.365618 2.257129 1.968592 3.909901
[36] 2.273435 10.000000 2.307984 2.290368 2.967738 2.014091 10.000000
[43] 10.000000 3.290527 2.432379 2.014091 2.575829 10.000000 2.307984
[50] 2.967738 2.967738 1.792831 3.290527 1.959964 2.297408 2.053749
[57] 10.000000 2.542699 2.403655 10.000000 3.410733 2.975294 3.849639
[64] 10.000000 2.273435 2.106589 3.694892 2.195944 2.307984 4.178900
[71] 1.951480 2.967738 2.226212 2.290368 2.967738 2.780638 2.612054
[78] 10.000000 2.652070 10.000000 2.725494 2.652070 3.042724 2.652070
[85] 2.970656 2.257129 2.386708 3.403461 2.120072 2.688852
> m.EM<-zcurve(z,method="EM",bootstrap=FALSE)
Error in m.EM <= zcurve(z, method = "EM", bootstrap = FALSE) :
  comparison of these types is not implemented
In addition: Warning message:
In m.EM <= zcurve(z, method = "EM", bootstrap = FALSE) :
  longer object length is not a multiple of shorter object length
> m.EM<-zcurve(z,method="EM",bootstrap=FALSE)
> m.EM<-zcurve(OSC.z,method="EM",bootstrap=FALSE)
> m.EM<-zcurve(OSC.z,method="EM",bootstrap=100)
> m.D<-zcurve(OSC.z,method="density",bootstrap=FALSE)
> summary(m.EM)
Call:
zcurve(z = OSC.z, method = "EM", bootstrap = 100)

model: EM via EM

      Estimate  l.CI  u.CI
ERR      0.620 0.501 0.746
EDR      0.391 0.082 0.693

Model converged in 45 + 118 iterations
Q = -60.61, 95% CII=-70.48, -47.791
>

```

Figure 2: The Estimation of Using Expectation Method (EM) via Expectation Method (EM), for lower Confidential interval (l.CI) and upper Confidential interval (u.CI) for replicable iteration is as follows.

```

Rterm (64-bit)
[50] 2.967738 2.967738 1.792831 3.290527 1.959964 2.297408 2.053749
[57] 10.000000 2.542699 2.403655 10.000000 3.410733 2.975294 3.849639
[64] 10.000000 2.273435 2.106589 3.694892 2.195944 2.307984 4.178900
[71] 1.951480 2.967738 2.226212 2.290368 2.967738 2.780638 2.612054
[78] 10.000000 2.652070 10.000000 2.725494 2.652070 3.042724 2.652070
[85] 2.970656 2.257129 2.386708 3.403461 2.120072 2.688852
> m.EM<-zcurve(z,method="EM",bootstrap=FALSE)
Error in m.EM <= zcurve(z, method = "EM", bootstrap = FALSE) :
  comparison of these types is not implemented
In addition: Warning message:
In m.EM <= zcurve(z, method = "EM", bootstrap = FALSE) :
  longer object length is not a multiple of shorter object length
> m.EM<-zcurve(z,method="EM",bootstrap=FALSE)
> m.EM<-zcurve(OSC.z,method="EM",bootstrap=FALSE)
> m.EM<-zcurve(OSC.z,method="EM",bootstrap=100)
> m.D<-zcurve(OSC.z,method="density",bootstrap=FALSE)
> summary(m.EM)
Call:
zcurve(z = OSC.z, method = "EM", bootstrap = 100)

model: EM via EM

      Estimate  l.CI  u.CI
ERR      0.620 0.501 0.746
EDR      0.391 0.082 0.693

Model converged in 45 + 118 iterations
Q = -60.61, 95% CII=-70.48, -47.791
> summary(m.D)
Call:
zcurve(z = OSC.z, method = "density", bootstrap = FALSE)

model: KD2 via density

      Estimate
ERR      0.614
EDR      0.506

Model converged in 47 iterations
RMSE = 0.11
>

```

Figure 3: The Estimation of KD2 via Expectation Method (EM), for replicable iteration

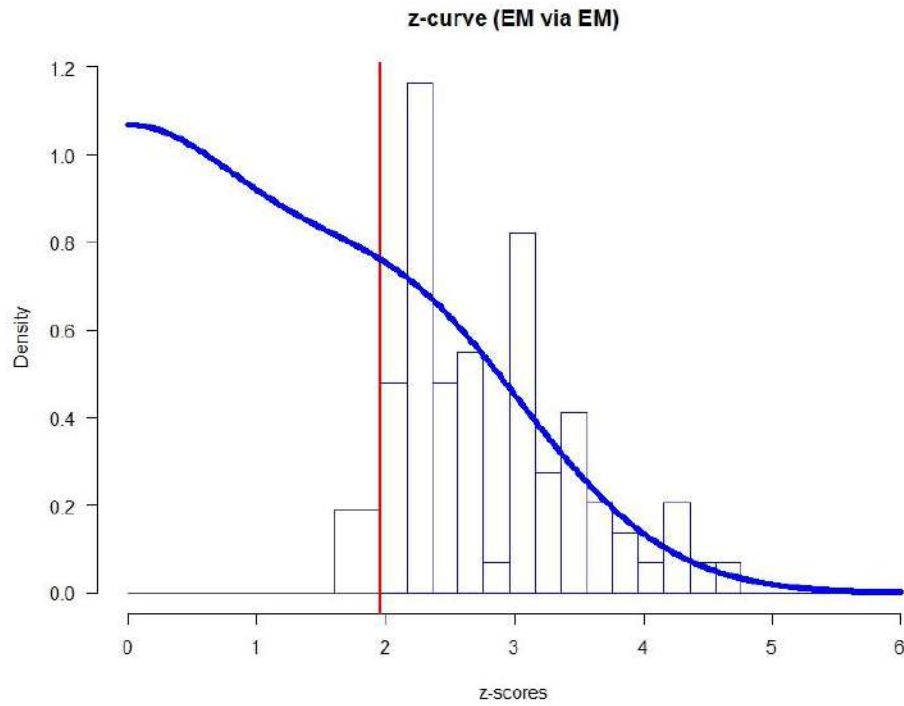


Figure 4: z-curve(EM Via EM)

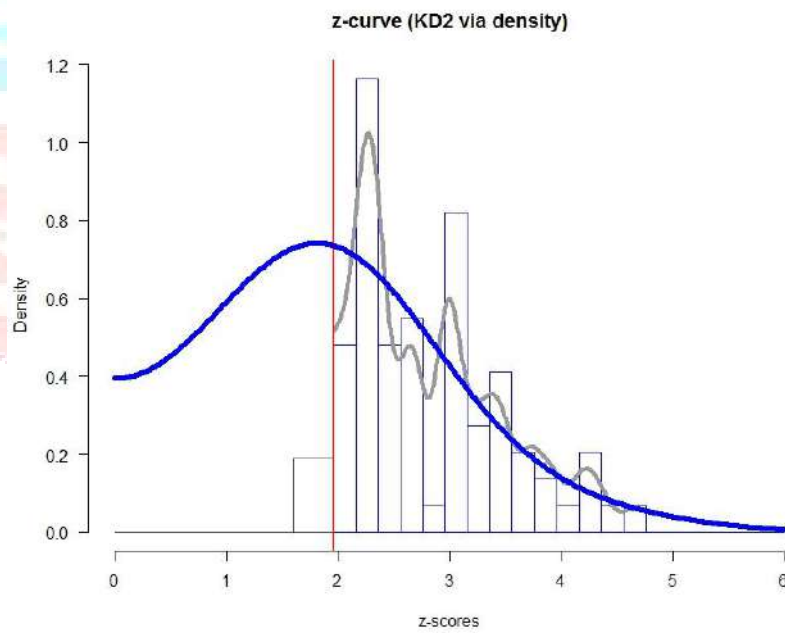


Figure 5: z-curve(KD2 Via DENSITY)

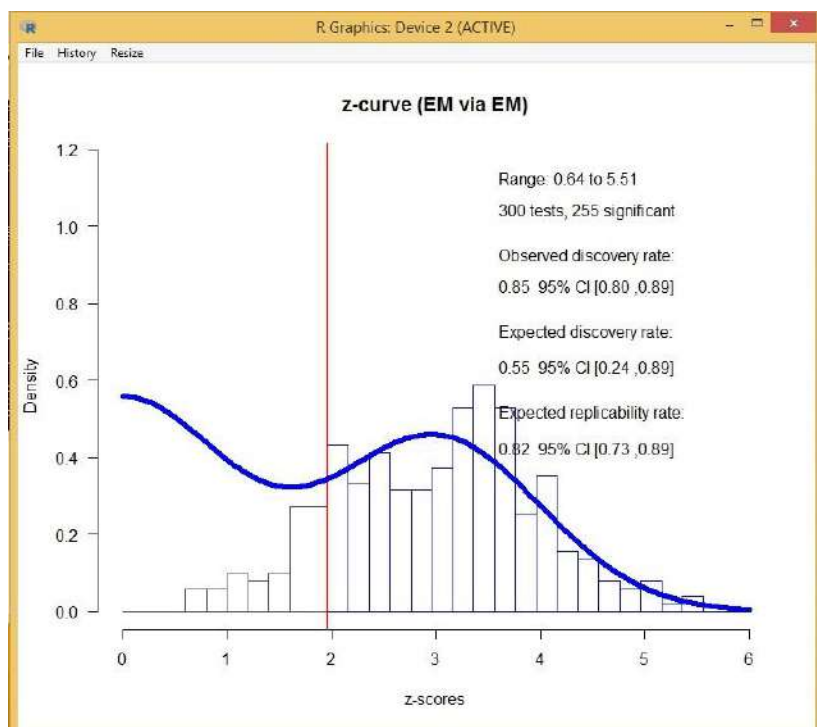


Figure 6: Using Expectation Method (EM),

From the figure (1) - (5) z-curve is estimated for many iterations of stock_dat the model converged at the rate of 0.09215481 with (25+66) iterations and (24+22) iterations with 92% detection of outliers.

FOF ~ ERR and EDR

5. Conclusion

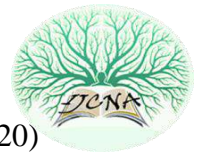
Towards the contemporary world of pandemic, researchers are making very close and accuracy to the machine understandable efforts rather than human. Using utilization factor, the number of observation comes under the study is more efficient for the outcome of the outliers. Estimating is based on replicability rates of statistical testing such as t-test, F-test, chi-square test, Z-test, ERR and EDR. It simulates the robustness of outliers that undergoes uncertainty as significant to the margin. FOF(Fuzzy Objective Function) determines the utilization factor by fitting random points of clusters and detecting the perpetual outliers (disabilities) to fade the replicability fitness over the outlierst to normalize. The test results shows a complete consent to measure the values of outliers using fuzzy clustering approach.

References

- [1].Charu C.Aggarwal, "Outlier Analysis", Springer,2013.
- [2].V.Chandola, A.Banerjee and V.Kumar, "Anomaly Detection: A survey", ACM
- [3].Charu c.Aggarwal, Chandan, K.Reddy, "Data clustering", CRC Press ,2014.
- [4]. Hawkins,"Identification of outliers",1980.
- [5]. S.Rajalakshmi,P.Madhubala," Outlier Detection: A research and Modified method using Fuzzy Clustering",IJITEE,ISSN:2278-3075,vol9,Issue 3s,Jan(2020).
- [6].F.Hoppner,F.Klawonn,R.Kruse,"Fuzzy cluster Analysis:Methods for classification, Data Analysis and Image.
- [7].Charu C.Aggarwal,Manish Gupta,Jing Gao,"Outlier Detection for Temporal Data: A Survey",IEEE, Jan-2014.
- [8].Irad Ben Gal,"Outlier Detection",Data Mining and Knowledge discovery Handbook,kluwer Academic Publishers,2005.
- [9].Yanchang zhao,"R and Data Mining: Examples and Case studies",May 29,2012.
- [10].Klir Yuan,"Fuzzy set and fuzzy logic-Theory and Applications"- BOOK
- [11]. J D Harris, J C Bezdek, "Fuzzy Partition and relation - An axiomatic basis for clustering", Fuzzy sets and systems, Elsevier, 1978.

- [12]. Francesco Marcelloni, Feature selection based on a modified fuzzy c-means algorithm with supervision, vol 151, pages 201-226, May 2003.
- [13].Lin Zhu et.al, Generalized fuzzy c-means clustering algorithm with improved fuzzy partitions, IEEE, June 2009.
- [14].Bartoš, F., & Schimmack, U. (2020, January 10). Z-Curve.2.0: Estimating Replication Rates and Discovery Rates. <https://doi.org/10.31234/osf.io/urgtn>
- [15].Bartoš, F., & Schimmack, U. (2020, January 10). Z-Curve. : An R package for fitting Z-Curves”, R package version 1.0.6.
- [16]. William Revelle, Department of Psychology Northwestern University, How To: Install R and the psych package, September 8, 2020
- [17]. William Revelle, Department of Psychology Northwestern University, An introduction to the psych package: Part I: data entry and data description, September 4, 2020
- [18]. William Revelle, Department of Psychology Northwestern University, An introduction to the psych package: Part II Scale construction and psychometrics, August 12, 2020
- [19]. Package‘zcurve’ September 27, 2020.





Evolutionary Computing Assisted Visually-Imperceptible Hybrid Cryptography and Steganography Model for Secure Data Communication over Cloud Environment

Denis R

Department of Computer Science, Periyar University, Salem, Tamil Nadu, India
denisatshc@gmail.com

Madhubala P

PG & Research Department of Computer Science, Don Bosco College, Dharmapuri, Tamil Nadu, India
madhubalasivaji@gmail.com

Published online: 25 December 2020

Abstract – The exponential growth of communication technologies and related application environments has broadened the cloud computing ecosystem horizon to meet major communication needs. However, in-parallel upsurge in online attacks, security breaches or allied intrusion events has alarmed industries to ensure optimal data security. Unlike text data transmission, image, or other multimedia communication over the cloud requires computational efficiency, imperceptibility, etc. to meet attack-resilient transmission. Amongst the major available security systems, the combination of cryptosystems and steganography has been identified as an augmented security model for data transmission. However, it demands enhancement in both stages to meet cloud-specific communication efficiency. Considering it as motivation, in this paper an efficient Visually Imperceptible Hybrid Crypto-Steganography (VIHCS) model is developed using Hybrid Cryptosystems followed by Adaptive Genetic Algorithm assisted Least Significant Bit (LSB) embedding process. We developed a novel Hybrid Cryptosystem by strategically applying Advanced Encryption Standard (AES) and Rivest–Shamir–Adleman (RSA) algorithms to secure secret data to be embedded in a cover image. In addition, the use of the Adaptive Genetic Algorithm based Optimal Pixel Adjustment (AGA-OPAP) strengthened the Least Significant Bit embedding while retaining the best possible image quality and visual imperceptibility. The proposed model achieved higher security, high embedding capacity as well as image quality, which is vital for cloud communication. To perform LSB embedding we applied 2D-Discrete Wavelet Transform (2D-DWT-2L) method with 8×8 dimensional block-wise embedding. It helps to achieve better embedding efficiency in conjunction with the AGA-OPAP model. Simulation results and respective visio-statistical assessment revealed that the proposed VIHCS model can accomplish better performance and reliable secure data communication over the cloud environment. Thus, the VIHCS model achieves maximum possible

imperceptibility and hence can avoid attacks- such as steganalysis based attack or RS-attacks.

Index Terms – Secure Data Transmission, Cloud Environment, Hybrid Cryptography-Steganography Model, Evolutionary Computing, Encryption and Decryption, Adaptive Genetic Algorithm (AGA), Least Significant Bit (LSB).

1. INTRODUCTION

The exponential growth of software and advanced hardware systems has expanded the scope to fully integrated services and solutions that meet diverse socio-industrial demands. Data communication and allied forces of the exchange of knowledge have gained broad popularity around the world among the largest emerging applications. On the other hand, high speed development in internet technology and related applications has resulted in different innovations such as cloud computing, Internet-of-Things (IoT), etc. However, ensuring secure communication across these application environments has always been a challenge for industries [1-8]. Various uses, including social networking sites, medical services industry, e-commerce, scientific societies, the financial sector, other industrial needs, such as monitoring and security systems, etc have been met daily by vast numbers of communication systems enabling the Internet.

Social networking and entertainment, tracking footages [3, 4, 5], user data and an IoT communications support environment [2], [4], [6-12] all have to be secured from unauthorized access to their data by protection measures and policies. Undeniably, corporate software has also seen a substantial increase in vast volumes of data generation and collaboration through the industry, government departments, banks, and other organizations. In practice, such data are used for certain targeted analysis or observation to make a suitable decision.

RESEARCH ARTICLE

Cloud computing has been created through the amalgamation of the various data sources and the combination of a large volume of data. Cloud computing refers to “free access to shared, configurable computing resources and applications that can be used for a price through telecommunications (such as the Internet) on request”. There are three main forms of cloud computing generally known as:

- IaaS – Infrastructure as a Service
- PaaS – Platform as a Service
- SaaS – Software as a Service.

XaaS is a term that refers to the provision of anything as a service. It recognizes the vast number of goods, software, and technology currently offered by suppliers to consumers as a service across a network, not locally or on-site in a sector. Few examples for XaaS include Storage as a Service, Database as a Service, Security as a Service, Malware as a Service, Distributed Denial of Services, Disaster Recovery as a Service, Communications as a Service and the Network as a Service, and so on.

One of the key features of cloud computing is that it provides a range of stakeholders with access to data, real-time computing, and cloud-based decisions, regardless of origin or geographical barriers. However, information exchange from one node or user to another or across the cloud platform is highly vulnerable until a robust security measure is not provided. One of the predominant concerns in cloud computing is the protection or seamless exchange of private data, particularly multimedia (video, audio, image) [1 - 4].

In addition to secure communication, enabling computational efficacy is also a must, as it (i.e., cloud computing) demands time-efficient and reliable computation to meet the application's real-time requirements. It signifies the assurance of security, scalability, and manageability in the cloud computing environment for up-surge computational and allied communication demands. Facilitating security of the data has become inevitable for cloud environments like social media, the healthcare sector, etc [3][4][6][9-11]. There are major threats to the complex design of cloud implementations with vision and control loss. The continuous change in the security perimeter due to the elastic boundary of cloud use also calls for a more complex security approach.

During data communication, once a miscreant gets data access or retrieves the data or allied content, it can easily be modified or misused for a certain targeted or intended goal. To avoid such incidents, various attempts have been made to incorporate protection systems; however, substantial efforts are being made either by integrating security models for data access or security of infrastructure or by introducing such on-data security features [12]. In other words, researchers have created protective models in which the user has to be

authenticated or the data itself is protected before accessing the data (access-control) to prevent the unauthorized access or intruder from revealing sensitive data.

Several attempts have been made over the past few years to strengthen data protection in the cloud computing world. However, ensuring both levels of security and computational efficiency has remained an open research area for academia-industries. Amongst the major data security models, steganography and cryptosystems have played a decisive role; however, in practice, these methods as a standalone solution have been found limited due to parallel increase in attacking models. This paved way to design Hybrid Cryptography-Steganography which has gained widespread attention [9-12], where the dual-level of security enables or provides better data security. However, as an application-specific scenario, retaining secure and attack resilient data transmission demands enhanced steganography as well as cryptosystem to accomplish the above stated eventual goal. Realizing the data communication over cloud infrastructure which is becoming vulnerable these days due to increased attacking efforts, in this paper the focus is made on enhancing both steganography as well as cryptosystems.

To achieve it, at first, a Hybrid Cryptosystem is designed using RSA and AES cryptography algorithms. In the proposed model these cryptography algorithms are applied in a strategic manner that ensures an enhancement in security level. The hybrid cryptosystem proposed is used to encrypt the secret text data which is embedded into the cover image. Once performing secret text encryption, an Evolutionary Computing (EC) assisted LSB embedding model is applied that helps to embed secret text (i.e., cipher data) into the cover image optimally without increasing or affecting PSNR or visual characteristics such as entropy, histogram patterns, etc. Because the inclusion of secret text might impact pixel arrangement and resulting entropy, PSNR, histogram patterns, and other statistical features such as regular and singular coefficients of image blocks, the AGA algorithm was applied to perform Optimal Pixel Adjustment Process (OPAP) during LSB embedding. The use of AGA-OPAP based LSB embedding has achieved an optimum Peak Signal to Noise Ratio (PSNR) with negligible histogram pattern variance and RS parameters, rendering the overall process quality-centric and Visio-imperceptible. Such novelties can help the proposed model avoid attacks like Steganalysis or RS attacks which are well known for their ability to exploit statistical variations in image data to detect secret or hidden information. The overall proposed model is developed using the MATLAB tool 2018a. The proposed security method achieves enhanced or augmented security for data communication over the cloud environment.

The remaining parts of the manuscript are as follows: Section 2 addresses related work, followed by section 3 research

RESEARCH ARTICLE

objectives and section 4 problem formulation. Section 5 discusses the proposed system model, while the findings obtained and their respective inferences are discussed in Section 6. Section 7 ends with the conclusion.

2. RELATED WORK

This research intends to propose a secure data communication model for a cloud computing environment for which amalgamating enhanced steganography and cryptosystem can be of utmost significance. With this motive, in this section, a few key literatures on these techniques are discussed with their respective strengths as well as limitations.

Xue et al [13] suggested adaptive steganography based on "Sum and Difference Covering Set" (SDCS) information, where the noisiest pixels are initially detected according to an iterative noise-level estimation model. The secret hidden data is then entrenched using the SDCS algorithm into these noisy pixels. However, this approach could not employ any additional layer of security to strengthen overall efficacy.

Vipula et al [14] merged crypto-algorithm AES with steganography to conceal secret text data in multimedia files. But the main issues of signal strength and imperceptibility, which are necessary for modern-day applications are not addressed.

Saleh et al [15] recommended the modified AES algorithm to encrypt a secret message, which was then processed for hiding in the cover image [16]. However, Duluta et al.[17] recently found that some traditional models for encryption have a range of limitations that can restrict their cloud computing environment suitability. Authors focused only on image type of data; though it needs further verification for computational efficacy and performance trade-off under different test conditions.

Pancha et al [18] applied a cryptosystem with steganography for safe data communication. First, the authors used encryption, in combination with the chirikov mapping, to turn the input image into a cipher image. Then authors used steganography to hide the encrypted image from the cover image during the sequential process. However, it did not discuss the enforced cases of entropy and histogram distortion.

Leung et al.[19] proposed uneven security protection by using multiple encryption technologies to secure various media pieces of different importance. Their model focuses primarily on augmenting only the cryptosystem and therefore needs further enhancement of signal retention in steganography.

Towards video fingerprinting, Li et al [20] applied the theory of recognition and clustering of the field of interest. However such approaches cannot be the optimal solution to meet the

current high-speed real-time communication requirements, especially over cloud infrastructure.

Ahmed et al [21] presented a model based on a user interface in which the sender could pick the appropriate cover and secret message that was processed using Elliptic Curve Cryptography based encryption trailed with LSB embedding. The processed data were transmitted to the same target through different channels. However, efforts can be made to improve their model for lightweight encryption and attack resilient embedding.

To achieve a better solution and high non-perceptibility, Hajduk et al [22] proposed a technique of image steganography where the text message was encrypted and inserted in the cover image using the Quick Response Code (QR). Besides that, the suitability for multimedia data communication in a cloud environment has not been addressed.

Mukhedkar et al [23] has applied various cryptosystems to encrypt secret data before embedding it in the cover image for efficient and reliable multimedia transmission. The main emphasis was on cryptosystem enhancement and other aspects of real-time multimedia transmission were not discussed.

Unlike traditional cryptosystems, Alam et al [24] used McElice's cryptosystem to encrypt or decrypt data to improve data protection across wireless networks. Their method could not be used for cloud communication with massive databases containing multimedia content. Depicting limitations of classical cryptosystems, Kumar et al [25] proposed a public key cryptographic algorithm for safe 3D color data communication.

Gupta et al [26] suggested the use of Discrete Wavelet Transform, given the fact that better multimedia data processing techniques such as wavelet analysis will help in increase the imperceptibility of hidden data over uncertain channels. DWT was applied to split the input image into four sub-bands, followed by hiding data within the splits. The image was compressed before transmission after hiding the secret text information. The authors [26][27] implemented a new hidden data communication method using RSA and AES in conjunction with steganography. However for cloud-based environments where QoS/QoE is of critical importance, splitting data into several chunks and embedding data, further decompression and/or decryption of original data elements may be too cumbersome and voluminous in computation.

Anwar et al [28] suggested a combination of algorithms to improve the protection of medical images during transmission in uncertain channels. Liao et al [29] developed a medical JPEG image steganographic scheme aimed at maintaining inter-block DCT coefficient dependences. Both the

RESEARCH ARTICLE

approaches exhibit good results in image quality but the security of the data still needs enhancement.

Using blended chaotic maps and Haar Integer Wavelet Transform (HIWT), Balakrishnan et al [30] suggested a transform domain hybrid image cryptosystem. It can be improved by efficient key generation, substitution-permutation, uncertainty, and diffusion processes.

Based on deoxyribonucleic acid and several chaotic maps, a hybrid encryption algorithm was projected to encrypt DICOM color images by Divya et al [31]. It requires a better concept of embedding with minimal noise probability and lightweight cloud computing encryption.

To ensure optimal communication over volatile networks, Mansour et al [32] suggested the Discrete Ripplet Transformation technique for embedding messages in medical cover images. This model focuses on embedding and can be further improved to be attack-resilient with hybrid cryptosystems and effective wavelets.

Usman et al [33] employed Swapped Huffman tree encoding to provide multiple encryptions for medical data. It still has computational overheads, however, and is likely to be attacked by advanced steganalysis/attacks.

To secure medical data, Hashim et al [34] suggested a new steganography mechanism based on the Bit Invert Method (BIS) using three random control parameters. It can be further improved by implementing the required embedding principle to prevent all types of attacks.

Nithya et al [35] have developed an integrated security system using DNA coding and image encryption methods to provide enhanced security. This strategy has shown good results but does not solve data redundancy.

Harnal et al [36] proposed an end-to-end cryptography (E2EE) hybrid cryptography algorithm to maintain integrity and confidentiality in a multimedia cloud computing environment. This mechanism was easy and deals with limited database sizes.

Using a nuclear spin generator, Stoyanov et al [37] implemented a medical image stego hiding approach and examined the findings based on histogram analysis and peak signal-to-noise ratio. However, there is significant potential to enhance the authentication mechanism for the cloud computing environment.

A robust, quasi-quantum walk-based image steganography mechanism has been developed by Baseem et al [38] to support secure transmission on the cloud-based E-healthcare platform. The scheme has achieved good visual quality, resistance to data loss attacks, high embedding capability, and robust protection. It can be improved by applying an effective

bio-inspired optimization technique to attain even better performance.

Madhusudhan et al [39] have implemented a secure multimedia transmission algorithm based on binary bits and a map of Arnold. The idea of hiding data can be implemented to improve security.

Emy et al [40] proposed a viable method for transmitting color images using a compression-encryption model with a dynamic key generator and robust symmetric key distribution. Pandey et al [41] developed a bit mask-oriented genetic algorithm based on a resilient data transmission mechanism. Encrypted data was embedded in medical images through Discrete Wavelet Transformation at 1 and 2 levels (DWT). Protection can be further improved with a hybrid cryptosystem so that there is no possibility of any cryptanalysis/attacks.

This is a matter of fact that a range of research has been done to perform data embedding in images/medical image using steganography techniques, but most of the methodologies use wavelet transformation techniques and focus on either PSNR enhancement or capability enhancement embedding. The requirements such as Region of Interest preservation, maximum imperceptibility, small or negligible histogram variations, resistance to statistical attacks, higher PSNR, low entropy, MAE, Correlation analysis etc. were in need to be enhanced for better performance.

Literature also reveals that in the field of image encryption and cryptography techniques, only few have used metaheuristic algorithms. In some recent studies, evolutionary algorithms have been successfully applied to overcome the issue of safe data communication. It is vital to build a computationally equipped algorithm based on the discussion thus far, that not only provides security while data transmission but also addresses broad search regions.

The work carried out to date provides security and privacy, but mostly suffers from some barriers, such as managing wide search spaces, avoiding duplication, etc. Therefore by developing a fusion of cryptography theory and steganography with adaptive genetic algorithm-based RS attack, we propose an effective algorithm to resolve these limitations by resilient embedding-based secure data transmission over the cloud environment.

3. RESEARCH OBJECTIVES

- To propose a Hybrid Crypto-Steganography Model for effective secure data communication over the cloud environment.
- To implement a Hybrid Cryptosystem to secure text data to be embedded in the cover image.

RESEARCH ARTICLE

- To apply the Genetic Algorithm (GA) principle to the Optimal Pixel Adjustment Process to preserve maximum possible data embedding capability, maximum imperceptibility, and higher PSNR for reliable cloud-based data communication.
- To test the simulation analysis and the performance of the proposed model against the existing approaches.
- To prove the Adaptive Genetic Algorithm based OPAP assisted LSB embedding with Hybrid Cryptosystem accomplish an optimal solution for secure data communication over the cloud environment.

4. PROBLEM FORMULATION

As already stated, the exponential rise in Cloud assisted IoTs also called Cloud-IoT has also alarmed scientific society to develop QoS centric (image) transmission systems. Unlike conventional research so far where the emphasis is merely on increasing efficiency and timely delivery, there is an unavoidable need to build a more effective and robust safe transmission system. Several attempts have been made, such as cryptosystems, steganography, etc., considering the inevitable significance of secure communication, particularly for the Cloud-IoT environment. Taking Cryptosystem as a potential solution, two types of symmetric and asymmetric crypto algorithms are still subject to major limitations, such as computation overheads, time, and the probability of security breaches that have occurred globally in recent years. Strategies such as Brute-Force attacks, MySql attacks, and many other well-known methods of attack often carry data security under suspicious circumstances.

Considering the contemporary application environment, where users use internet technologies, cloud infrastructures, or wireless communication media to transmit data from one peer to another, the risk of attack becomes more severe. In the last few years, the cases of unauthorized multimedia content access, image manipulation, personal multimedia file access, and publication, etc. have increased significantly. Towards multimedia data, especially image data security two techniques named steganography and cryptography have gained widespread attention. However, the steganography concept has broader significance towards multimedia data security over the cloud environment.

Steganography uses the principle of signal destruction by increasing entropy to the cover image or the division and transmission of content across various channels to the receiver. This mechanism allows data protection and reliability even after the intruder or miscreants have access to the data through the use of modern attacker modules or intrusion efforts. Considering the classical methods of steganography, it can be found that such methods cannot guarantee optimum efficiency due to increased entropy in the

original image which makes data communication suspicious. On the other hand, splitting image data into multiple parts and transmitting it to the receiver through different channels to avoid unauthorized attacker access to data can impose huge computational costs, delays, resource exhaustion, etc., which cannot be used for a present cloud environment.

Considering the contemporary shortcomings of both cryptosystems, such as classical RSA, Elliptic Curve Cryptography (ECC), AES, etc. and steganography, using these methods together can be of critical importance. Such hybrid security models can provide a dual level of security where steganography can assist in hiding significant details in cover data, while cryptography can ensure that the intruder could not access the data hidden without authorizing credentials. Exploring in-depth, it can be found that introducing Hybrid Crypto-Steganography (HCS) concept can help to achieve a more efficient outcome, however at the increased computational overheads. This is because in major conventional approaches, to increase security prospects authors have applied a high bit size cryptosystem; however, it functions at the cost of increased computational complexities at both transmitter as well as receiver side. It reduces the efficacy of the HCS systems. On contrary, embedding data inside a cover image to ensure its security depends on the method or efficacy of the steganography, as with a less effective approach embedding higher data might expose data to get noticed by an intruder. Moreover, embedding excessive or inappropriate data to the cover image might reduce or degrade data quality at the receiver and hence can affect overall communication efficiency. In such cases, enabling optimal trade-off between computational efficiency as well as data quality is vital for HCS.

Considering it as motivation, in this research paper, the focus is made on developing a robust and computationally efficient HCS model for a cloud computing environment. Undeniably, HCS systems encompass both cryptography and steganography as computing models; however, the classical cryptosystems such as RSA, ECC, AES, etc are computationally costly, especially when the level of security has to be achieved higher. In other words, a 64 bit RSA or AES would have relatively lower coefficients for data encryption [4-5][42-43]; on contrary increasing bit size often results in amplified computational overheads. However, on the other side, the efficacy of ECC cryptosystem's too decisively depends on the selection of curve points or the allied parameter selection, which turns out to be a computationally complex task. On contrary, cloud computing and allied data transmission require a time and computation efficient environment.

In this research we have designed a Hybrid Cryptosystem model by strategically implementing AES and RSA cryptography algorithms to secure secret data to be embedded

RESEARCH ARTICLE

with a cover image. In the HCS system, the second and most critical function is steganography too requires efficient data decomposition, data embedding, and further data reconstruction. In major conventional researches authors have merely focused on either achieving higher PSNR or embedding capacity; however, maintaining an optimal balance between these two has always been a trivial task. On the other hand, data communication over cloud infrastructure requires optimal data quality, higher transmission rate as well as more time-efficient computation. However, there is numerous cloud-based application environment where maintaining an optimal quality of the multimedia data is a must. In major conventional efforts where authors have tried to embed more data in the cover have undergone an increased level of entropy and resulting degradation in data quality. Such approaches can't be suitable for applications such as telemedicine, critical multimedia image transmission, etc. The inclusion of entropy and its visual reveal might help intruders attacking that specific data under communication. In such cases maintaining optimal data embedding with low entropy and maximum possible data quality can be vital.

To achieve it, enhancement in data (say, image) decomposition, strategically optimized data embedding, and highly efficient pixel adjustment followed by data reconstruction is a must. Exploring in-depth, it can be found that optimizing pixel adjustment when embedding data within the cover image can be of great significance to enhance both embedding capacity as well as PSNR. Considering it as a motive, in this research an Evolutionary Computing concept-based OPAP model is developed that intends to achieve

optimal LSB embedding with optimal adaptive pixel adjustment. Specifically, in this paper Multi-Objective Optimization (MOO) centric GA algorithm has been developed which intends to optimize both PSNR as well as regular and singular coefficients of each image block simultaneously (to ensure quality as well as visual imperceptibility).

The proposed AGA-OPAP model dynamically adjusts pixels of the cover images to retain optimal PSNR, low entropy with maximum possible data embedding capacity. Noticeably, in the steganography model, DWT is often used to facilitate image decomposition with 8x8 window size and performs 8 bit LSB embedding, which has been further optimized using AGA-OPAP. Thus, the proposed model achieves more secure, high-capacity, and attack-resilient steganography to perform data communication over cloud infrastructure. Thus, the proposed HCS backed AGA-OPAP based LSB embedding model and resulting Visio-Imperceptible-HCS (VIHCS) model can achieve an optimally secure and computationally efficient data communication paradigm for cloud environment. The proposed VIHCS model can effectively alleviate the possibilities of low pass filtering, Regular and Singular (steganalysis) RS attack, Brute-Force etc. type of attack scenarios.

5. PROPOSED SYSTEM MODEL

This section discusses the proposed VIHCS model and allied implementation. The Figure 1 depicts the process flow of the proposed model.

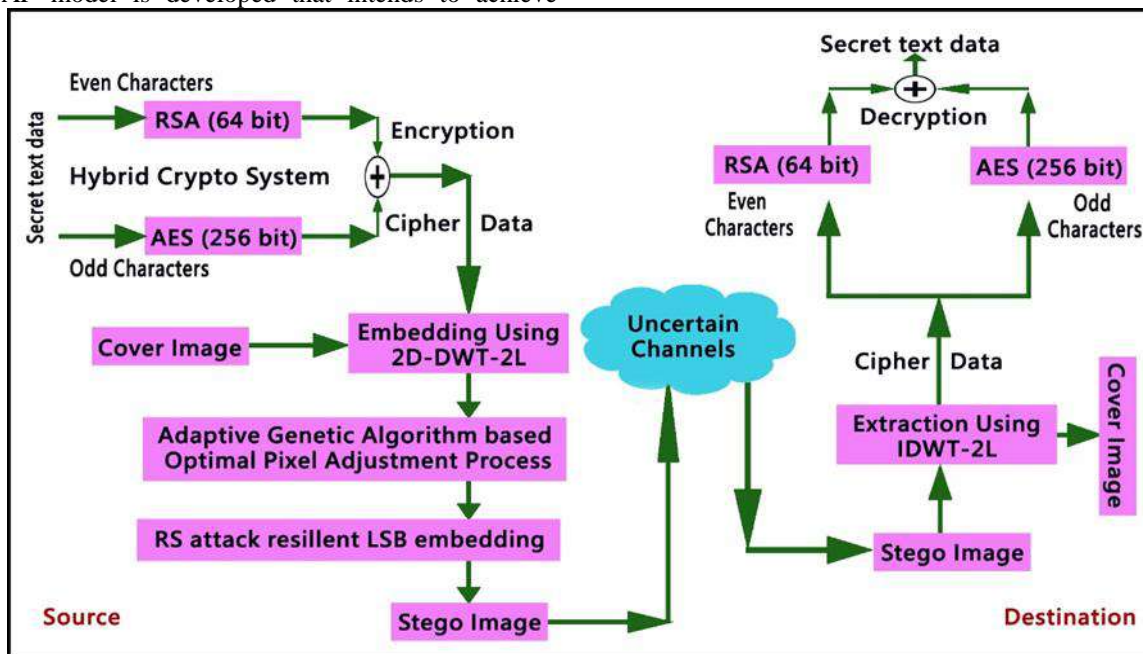


Figure 1 The Proposed VIHCS Model for Secure Data Communication

RESEARCH ARTICLE

5.1. Data Encryption

There are numerous cloud-assisted application environments in which different data, including image and text, are transmitted under uncertain channel conditions. Some of the common applications are telemedicine in the healthcare sector, social media, etc. Such applications can even have composite data as the amalgamation of text as well as an image (for example, in telemedicine both patients scanning medical reports as well as allied diagnosis details in text). In such cases, ensuring respective seamless transmission is of utmost significance. Towards this motive, the proposed model can be a viable solution. However, ensuring multilevel security can have augmented strength to alleviate any breach of security or unauthorized data access. Taking into account it as an objective, a novel hybrid cryptosystem is first developed in this research. Here, the prime motive behind this is to increase the level of security by applying two different cryptosystems together, which as a result can avoid any easy attack on the data. Consequently, it can achieve a higher level of security. It embodies strategic implementation of both RSA and AES, which has been used to encrypt input text data which is at first converted into ciphertext to be embedded within the cover image.

The cryptographic model $\mathbb{C} = \{F\eta, F\eta^{-1}, C, S, T\}$ encompasses encryption and decryption processes. During the encryption process, at first, the text data (it can be the diagnosis details of a patient which is expected to be transmitted along with the medical imaging reports) is split into two distinct parts, T_{odd} and T_{Even} . Splitting the text data doesn't signify dividing content into two fractional parts, rather once converting the entire text into binary form, the overall bit sequence is processed in such a way that the odd-sequence value is assigned to T_{odd} , while bits at even place or sequence is allocated to the T_{Even} component. Thus, it converts overall input text data into two data-chunk or components T_{odd} and T_{Even} . We applied AES cryptosystem to encrypt T_{odd} , while RSA was used for T_{Even} encryption method same as [42]; however, we employed 256-bit AES, while the existing approach [42] considered 128-bit AES for encryption. Considering computational efficiency demands, we considered 64-bit RSA, while AES was applied as 256 bit. Though, RSA with low bit-size has often been criticized to have inferior robustness; however, such a hypothesis can be applied merely with RSA as a standalone encryption algorithm. Its implementation with AES-256 can help to achieve a dual goal. First, the amalgamation of AES-RSA as a cryptographic algorithm can avoid easy attack probability (which can be possible with standalone encryption), and second, the consideration of low-bit size can avoid unwanted computation that eventually will make it robust to serve real-world applications. Additionally, AES-256 is almost six times faster and more efficient than classical triple-DES. Therefore,

the inclusion of AES as a cryptographic method seems viable towards a robust encryption environment.

On the other hand, the combination of RSA with low-bit size can help to make overall encryption more robust to avoid any attack. In other words, the strategic amalgamation of AES-256 and RSA-64 can confuse the attacker(s) to get real and exact information of the data being processed or communicated. In our proposed encryption model, AES-256 has 14 rounds of computation, while 64-bit RSA was applied as a single round itself, as it doesn't employ round-computation for confusion creation (to avoid side-channel attack). Though, with our proposed concept, AES-256 can be executed with lower rounds as well; however, will recommend more than 10 rounds to avoid detrimental consequences. Noticeably, AES applies an encryption key or the round key s to encrypt the text data component T_{odd} , while RSA being public-key cryptography applies a secret public key m to encrypt the data T_{Even} . We used a private key x to perform decryption of the RSA encrypted data at the receiver. On the contrary, we performed a standard decryption method for AES encrypted data. To be noted, AES decryption is the reverse of encryption, which is performed by executing inverse round transformations to retrieve original text data (from the encrypted data). Here, the inverse round transformation method applies four key functions, AddRoundKey, InvMixColumns, InvShiftRows, and InvSubBytes, sequentially. Due to the lack of space, the details of these key functions are not given in this manuscript. Thus, the overall process is mathematically modeled as follows:

$$C = \{E_{AES}, E_{RSA}, T_{odd}, T_{Even}, \hat{T}_{odd}, \hat{T}_{Even}, s, m, x\} \quad (1)$$

$$\hat{T}_{odd} = \{E_{AES}(T_{odd}, s)\} \quad (2)$$

$$\hat{T}_{Even} = \{E_{RSA}(T_{Even}, m)\} \quad (3)$$

Input: Secret Text Input Data (S_{Text})

Output: Cipher Text, Key s

Initiate the process

Step-1 Split the input text S_{Text} into two components S_{Text_odd} and S_{Text_Even}

Step-2 Generate AES keys (see, [42])

Step-3 Encrypt S_{Text_odd} using AES-256 bit key size

$$Enc_{S_{Text_odd}} = AES - 256 (S_{Text_odd}, s)$$

Step-4 Generate RSA keys (Public key m and private key x)

Step-5 Encrypt S_{Text_Even} using 64 bit-RSA

$$Enc_{S_{Text_Even}} = RSA - 64(S_{Text_Even}, m)$$

RESEARCH ARTICLE

Step-6 Construct combined Encrypted cipher data $Cipher_{F_Total}$ by using both $Enc_{S_{Text_odd}}$ and $Enc_{S_{Text_Even}}$ in their indices

Step-7 $Enc_{Key} = AES(x, s)$ # x -round key, # s -secret key

Step-8 Create final cipher data $Cipher_{Tx}$

$$Cipher_{Tx} = Concatenate(Cipher_{F_Total}, Enc_{Key})$$

Step-9 Return $Cipher_{Tx}$ and s

End

Algorithm 1 Secret Data Encryption

Secret data encryption is shown in Algorithm 1. Once the text data has been encrypted it has been processed for Adaptive Genetic Algorithm based Optimal Pixel Adjustment Process assisted Least Significant Bit embedding. The detailed discussion of the proposed AGA-OPAP based LSB embedding model is given as follows:

5.2. AGA-OPAP Assisted LSB Embedding for VIHCS

5.2.1. DWT Analysis and LSB Embedding

To embed the critical information within the cover image to be transmitted over cloud infrastructure, at first it is important to decompose the input cover image and embed the cipher data optimally while ensuring minimum entropy, histogram variations, or PSNR reductions. To achieve this, we applied DWT because of its robustness and efficacy towards time as well as spatial domain analysis. In our proposed method, we applied a DWT with HAAR mother wavelet. We applied 2D-DWT-2L which was formulated as a sequential transformation process with the help of low pass and high pass filters towards the row of the image (blocks). To be noted, in the proposed 2D-DWT-2L concept, we considered level-2 coefficients to perform embedding, the key reason is it can provide a significant local feature set for text-embedding without impacting image quality significantly. Moreover, it can provide a more depth (feature) space for embedding, which as a cumulative solution with the proposed encryption can help to strengthen attack-resiliency and confusion.

Performing embedding with a single layer can cause higher visibility or perceptibility, and can also impact image quality post-embedding. On the other hand, embedding with a higher level coefficient can be more effective; however at the cost of increased computation, which can't be suitable for contemporary real-time application demands. Therefore, in this paper, we performed embedding with a 2-level DWT coefficient only. In this process, the results are decomposed towards the columns of the image. A snippet of this process is depicted through Figure 2 & Figure 3. The above-mentioned illustration (Figure 2 & Figure 3) depicts the elemental decomposition of the $C_j(N \times M)$, image of size $N \times M$ in the

four distinct decomposed sub-bands (images), which are stated as high-high (HH), a high-low (HL), a low-high (LH), and a low-low (LL) frequency bands. Our proposed VIHCS model is designed to support visually imperceptible steganography to ensure maximum possible visual-imperceptibility that not only ensures seamless communication but also assists quality-data transmission, which is a must for cloud communication.

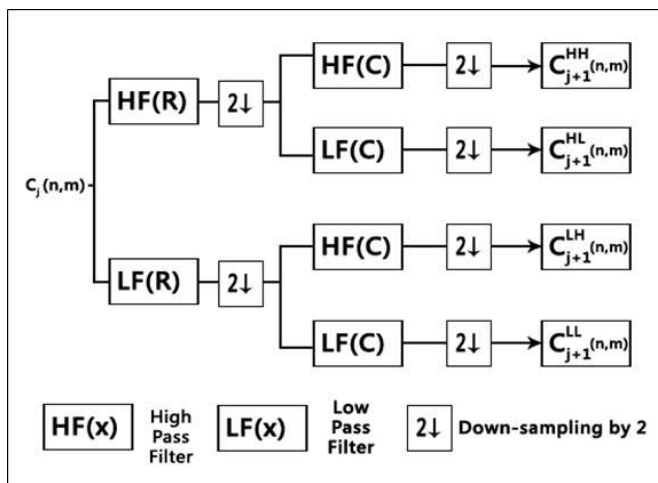


Figure 2 2D-DWT-2L Decomposition Process

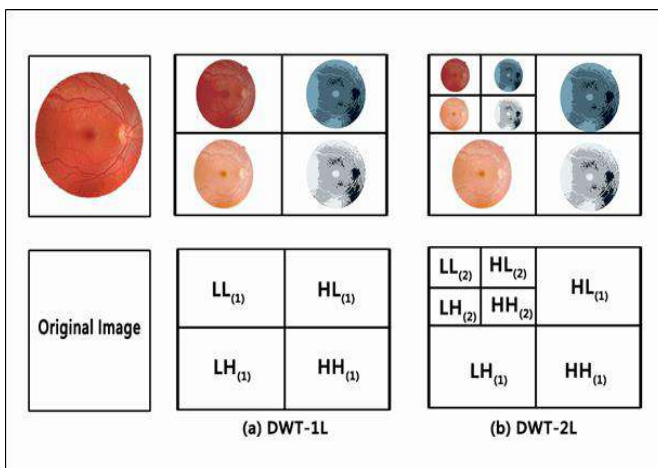


Figure 3 (a) DWT-1L (b) DWT-2L

To achieve it, we have designed VIHCS with $\hat{S} = \{F\eta, F\eta^{-1}, C, S, T\}$. It comprises of three distinct methods including LSB embedding; AGA-OPAP assisted embedding optimization, and extraction processes. In the LSB embedding process, we consider a cover image C , the secret data T (which is already processed as cipher data ($Cipher_{Tx}$)) is embedded using LSB embedding to produce stego image S .

Unlike classical efforts where authors have to embed text or cipher data arbitrarily or LSB without any optimization measure, in our proposed system, we have implemented an

RESEARCH ARTICLE

EC assisted (say, heuristic model-based) pixel adjustment process. Our proposed system intends to ensure optimal pixel adjustment to retain maximum possible imperceptibility, quality preserve, and seamless transmission even under cloud attack conditions such as RS-Analysis or Steganalysis. In our proposed method, at first input image also called cover-image is processed using HAAR-DWT and the entire image is split into multiple blocks or 8×8 blocks. Considering literature and allied inferences towards the LSB embedding process, we have applied this approach to embed ciphertext in each block. Before discussing the process of AGA-OPAP assisted LSB embedding, a snippet of embedding mechanism is given as follows:

To perform embedding, at first cipher text is transformed into an ASCII format, which is then split into S_{Text_odd} and S_{Text_Even} . In this method, the odd values (i.e., S_{Text_odd}) are concealed in vertical coefficients as stated by LH2. Similarly, the even values are concealed in diagonal coefficients specified by high-level coefficients HH2.

The algorithm applied to perform embedding is given Algorithm 2.

Input: Cover Image
 Output: Stego-Image

Step-1 Initiate the process
 Step-2 Transform the secret message (say, diagnosis details for telemedicine) in ASCII code S_{Text_ASCII}
 Step-3 Scan cover image for each row
 Step-4 Estimate the 2D wavelet coefficients for the first level using HAAR filter ($LL1$), ($HL1$), ($LH1$), and ($HH1$).
 Step-5 Estimate the 2D wavelet coefficients for the second level using HAAR wavelet filter ($LL2$), ($HL2$), ($LH2$), and ($HH2$).
 Step-6 Initiate a Loop
 Hide S_{Text_ASCII} using LSB embedding concept.
 Initiate AGA-OPAP for adaptive pixel optimization and RS-Attack resilient LSB embedding.
 EndLoop
 Return Stego-Image
 End

Algorithm 2 2D-DWT-2L Analysis and LSB Embedding

Unlike major conventional Hybrid Cryptography and Steganography models where authors have either focused on increasing embedding capacity or the basic histogram sensitive quality preserve, our proposed VIHCS model

intends to retain maximum image data quality as well as security against recently acknowledged online attacks such as RS-Analysis or steganalysis. To achieve it, we have developed a novel and robust EC-assisted LSB embedding concept, where AGA intends to fit S_{Text_ASCII} in such a manner that it doesn't introduce any significant entropy or visual trait signifying the presence of secret data.

5.2.2. AGA-OPAP Assisted LSB Embedding and Optimization

In the last few years, numerous attacker modules have been developed to target, detect, and attack data over uncertain communication channels, such as a cloud network. Amongst the major attacks, RS-Analysis also called Steganalysis has surfaced as the dominant attacker model which intends to retrieve stego-information from the multimedia data communication. Before discussing our proposed AGA-OPAP based LSB embedding model, a snippet of the RS Analysis or Steganalysis model is given as follows.

In this research, AGA has been applied to enhance image quality, embedding capacity as well as statistical factors such as regular and singular coefficient values in each block. This approach can ensure maximum possible embedding while retaining optimal data quality and visual imperceptibility. Consequently, it can help to avoid those attacks which use either visual changes or statistical changes to detect hidden information or secret information within the cover image during transmission. Considering RS-Analysis, also called steganalysis attack condition which employs statistical features to detect the presence of hidden information in multimedia data under transmission; in our proposed VIHCS model we have considered RS parameters and PSNR sensitive LSB embedding to ensure optimal data security. The detailed discussion of the proposed embedding model is given as follows:

5.2.2.1. RS Analysis (Steganalysis)

In RS analysis or steganalysis approach, there are three distinct kinds of block flipping; Positive flipping (F_1), Negative flipping (F_{-1}) and Null flipping (F_0). Noticeably, F_1 signifies the transformation association in between the $2i$ and $2i + 1$ pixels (say, 0-1, 2-3, ..., 254-255), which is equivalent to the LSB coefficient. Similarly, the transformation association in between $2i$ and $2i - 1$ pixels (say, -1, -1-0, 1-2, ... 255-256) signifies the negative flipping F_{-1} . Thus, the association between positive and negative flipping follows (4).

$$F_{-1} = F_1(x + 1) - 1 \tag{4}$$

Similarly, the null flipping, which stated the identity permutation follows the following condition (5).

$$F_0(x) = x \tag{5}$$

RESEARCH ARTICLE

These parameters (i.e., F_1, F_{-1} and F_0) are often called the flipping functions. Employing these flipping functions on each pixel of the input image data block or image block, we obtain the flipped group ($F(G)$). Mathematically,

Here, we define a parameter called flipping mask M . Mathematically, $M = M(1), M(2), \dots, M(n)$, where $M(i)$ states for 1, 0 and -1.

$$F(G) = (F_{M(1)}(x_1), F_{M(2)}(x_2), \dots, F_{M(n)}(x_n)) \quad (6)$$

The group G would remain consistent only when $f(F(G)) > f(G)$. Similarly, G is singular when $f(F(G)) < f(G)$. To perform the RS analysis, the following mechanism is taken into consideration. In this process, at first, the input multimedia data (here, image) is split into multiple non-overlapping sections or blocks where each block is rearranged to constitute a vector G . where $G = (x_1, x_2, \dots, x_n)$ is ordered in certain random (say, Zigzag) manner. Here, the correlation amongst the pixel is obtained using a discrimination function, defined in (7).

$$f(x_1, x_2, \dots, x_n) = \sum_{i=1}^{x_n-1} |x_i - x_{i+1}| \quad (7)$$

In (7), the variable x states the value of the pixel, while the total number of pixels is given by n . Here, the resulting value of f signifies the spatial correlation between the neighboring pixels. Noticeably, the small value of f states the strong correlation between the adjacent pixels. Once obtaining the complete value of $f(G)$, the non-negative flipping is applied (i.e., $M(1), M(2), \dots, M(n)$) either 0 or 1. On contrary, for non-positive flipping, we apply 0 or -1 for each block of the input image. Now, processing flipping over each block, we estimate $f(F(G))$ for each block and thus the relative count of regular or consistent blocks after positive flipping is obtained as R_m . Similarly, the relative number of singular blocks is obtained as S_m . Similarly, for negative flipping, the regular and singular blocks are obtained as R_{-m} and S_{-m} . Because in the natural images, the total number of above-stated blocks after performing flipping follow the following associations.

$$R_m \approx R_{-m}, S_m \approx S_{-m} \text{ and } R_m > S_m, R_{-m} > S_{-m} \quad (8)$$

Typically, the difference between R_m and R_{-m} increases as per the size of the embedding message. Similarly, the difference values of S_m and S_{-m} too increase with an increase in embedding text. Such facts help attackers on a cloud platform or environment to detect the presence of hidden information that can result in a significant loss of data privacy. Considering it as motivation, in this research the focus is made on developing a robust embedding model where the above-stated parameters (i.e., the difference between the values of R_m and R_{-m} and S_m and S_{-m}) could be

reduced while ensuring higher embedding capacity. This as a solution can accomplish an attack-resilient secure cloud communication model. To achieve it, in this paper, an AGA algorithm has been developed that intends to adjust pixels optimally $R_m \approx S_m, R_{-m} \approx S_{-m}$. A detailed discussion of the proposed AGA-based OPAP is given in the subsequent section.

5.2.2.2. AGA based OPAP

As already stated in the above section, to avoid any stego-information retrieval or data attack, we focus on achieving the condition given in (8) by performing OPAP. Here, we perform pixel adjustment to achieve a standard or natural condition defined as $R_m \approx S_m, R_{-m} \approx S_{-m}$. Since the variations in the bits in the higher place might violate or reduce the multimedia (here, image) data quality of the stego-image, merely the 2nd and 3rd LSBs are modified.

For illustration, let B as given in (9), be the original value of the input image (block). Now, in case of the strategic modification is made merely in LSB place (only 2nd LSB plane), the variation or the changes in between the original image block and the modified image block can be considered as a matrix called Adjustment Matrix (AM), given as A_1 and A_2 . Thus, the modified image blocks are $B'_1 = B + A_1$ and $B'_2 = B + A_2$. For illustration, let B be the original image block while $f(B) = 99$, while $f_{-}(B) = 120$, where f_{-} states the non-positive flipping. Now for the modified image block B'_1 , $f_{-}(B'_1) = 90$, only when F is non-positive flipping. Similarly, for B'_2 , $f_{-}(B'_2) = 150$.

$$B = \begin{bmatrix} 107 & 109 & 107 & 105 & 104 & 102 & 102 & 104 \\ 107 & 106 & 105 & 104 & 105 & 103 & 105 & 102 \\ 107 & 105 & 107 & 105 & 102 & 103 & 104 & 103 \\ 107 & 107 & 105 & 106 & 104 & 103 & 103 & 104 \\ 107 & 109 & 107 & 104 & 104 & 102 & 103 & 102 \\ 104 & 107 & 106 & 103 & 103 & 104 & 102 & 100 \\ 110 & 109 & 109 & 105 & 105 & 105 & 105 & 102 \\ 109 & 109 & 109 & 106 & 104 & 105 & 105 & 104 \end{bmatrix}$$

$$A_1 = \begin{bmatrix} 0 & 2 & 0 & 2 & 0 & 2 & 0 & 0 \\ 0 & 2 & 0 & 2 & 0 & 2 & 0 & 0 \\ 2 & 2 & 0 & 2 & 2 & 2 & 2 & 2 \\ 0 & 0 & 2 & 2 & 0 & 0 & 2 & 2 \\ 0 & 2 & 0 & 0 & 0 & 2 & 0 & 2 \\ 2 & 2 & 0 & 0 & 2 & 0 & 2 & 0 \\ 0 & 2 & 2 & 2 & 2 & 2 & 2 & 2 \\ 2 & 0 & 2 & 2 & 0 & 0 & 0 & 0 \end{bmatrix} \quad (10)$$

$$A_2 = \begin{bmatrix} 2 & 2 & 0 & 0 & 0 & 0 & 2 & 2 \\ 0 & 2 & 0 & 2 & 2 & 0 & 0 & 0 \\ 2 & 0 & 2 & 0 & 2 & 2 & 2 & 2 \\ 0 & 0 & 2 & 2 & 2 & 0 & 2 & 0 \\ 2 & 0 & 0 & 0 & 2 & 0 & 0 & 0 \\ 2 & 0 & 0 & 2 & 2 & 2 & 2 & 2 \\ 2 & 0 & 0 & 2 & 0 & 2 & 0 & 2 \\ 2 & 2 & 0 & 2 & 2 & 0 & 0 & 2 \end{bmatrix} \quad (11)$$

RESEARCH ARTICLE

Summarily, the kind of block (i.e., regular or singular) can be modified by changing or making a suitable adjustment. In such cases, adjusting the pixels optimally, the RS-Analysis attack of steganalysis attack can be avoided in a cloud environment. To achieve it, in this paper we have applied an Adaptive Genetic Algorithm (AGA) which obtains the Optimal Adjustment Matrix (OAM) to ensure minimum disparity amongst the values of regular and singular image blocks. A snippet of the AGA-based OPAP method and resulting OAM estimation is discussed in the subsequent section.

GA is a nature-based EC model, which employs Darwin's principle of survival to obtain the optimal or sub-optimal solution after a defined number of generations. Functionally, it applies the concept of human evolution to obtain an optimal solution by transforming an optimization of search problem into the phenomenon of chromosome evolution. Processing the evolution concept, once it achieves an optimal or the best solution after iterating a predefined number of generations (or, stopping criteria), the optimal solution obtained is presented as the final solution of that problem. Functionally, GA employs the processes named Population Generation, Crossover, and Mutation. In practice, the adaptive values influence the copy operation and an individual with a significantly high fitness value is considered for the next generation. Noticeably, the fitness value of a candidate solution signifies its maximum likelihood of becoming or getting selected for breeding in the next generation. To reduce computational overheads caused due to increase search space, a mutation process is applied that drops the individual with minimum fitness value, and such individuals are not carried forward for crossover in the next generation. Once embedding the secret data within the cover image using LSB embedding, we execute AGA-OPAP. A snippet of the applied AGA-OPAP is given as follows:

In our proposed LSB embedding method, at first, the stego-image is split into 8×8 blocks, where each block is categorized and labeled by applying the following mechanisms.

Step-1: Let the image block be B, then for B implement the non-positive flipping F_- as well as non-negative flipping F_+ .

Step-2: Generate the flipping mask M_+ and M_- , randomly and obtain the results B'_+ and B'_- .

Step-3: With the obtained value of B'_+ and B'_- , estimate the values of $f(B'_+)$, $f(B'_-)$ and $f(B)$.

Step-4: Process steps 1, 2 and 3 iteratively for 1000 generations and defines four distinct variables to classify the blocks by comparing $f(B'_+)$, $f(B'_-)$ and $f(B)$.

P_{+R} , it states the number of occurrences when the block remains regular under the non-negative flipping,

P_{+S} , it states the number of occurrences when the block remains singular under the non-negative flipping,

P_{-R} , states the number of occurrences when the block remains regular under the non-positive flipping.

P_{-S} , states the number of occurrences when the block remains singular under the non-positive flipping.

Step-5 Perform P_{+R} to P_{+S} and P_{-R} to P_{-S} and perform labeling of the image blocks as per following conditions:

$$R +, \text{ if } \frac{P_{+R}}{P_{+S}} > 1.8$$

$$S +, \text{ if } \frac{P_{+S}}{P_{+R}} > 1.8$$

$$R -, \text{ if } \frac{P_{-R}}{P_{-S}} > 1.8$$

$$S -, \text{ if } \frac{P_{-S}}{P_{-R}} > 1.8$$

Step-6 Classify blocks into four distinct groups, $R + R -$, $R + S -$, $S + R -$, $S + S -$. Ignore the blocks not a part of the above-stated types.

Step-7 Perform a comparison of the original input image, the magnitude of $R + R -$ and $S + R -$ blocks, which often shows an increase in stego-images.

Such an increase in the above-stated parameter can be detected using RS Analysis, which can further be used as the intrusion tool to attack that specific multimedia data to get unauthorized access of the stego-image as well as hidden information. Considering above stated fact and motive to alleviate the distinguishable or perceptible disparity between the values of $R + R -$ and $S + R -$ blocks, in this research we have applied the AGA algorithm which intends to decrease the value of $R -$ blocks. The implementation of AGA-based OPAP executes three key functions, Initialization (population initialization), crossover, and mutation. The procedures involved in AGA-OPAP optimization and allied pixel adjustment is detailed as follows:

5.2.3. Population Initialization

From the initial pixel or the first pixel, chose 3 adjoining pixels in each image block as the initial chromosome (Figure 4).

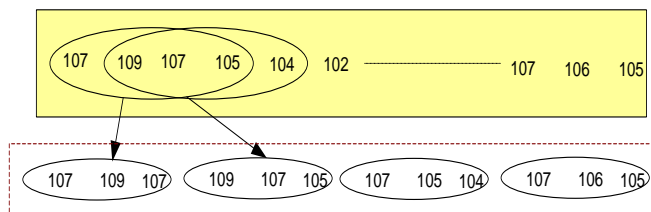


Figure 4 Selection of the Chromosomes

RESEARCH ARTICLE

5.2.4. Reproduction and Mutation

Perform flipping of the second least bits in the chromosomes arbitrarily and generate the (second generation) chromosomes C_i .

5.2.5. Selection

Estimate the fitness value of each chromosome and select the best chromosome using (12).

$$Fitness = \alpha(e_1 + e_2) + PSNR \quad (12)$$

In (12), the variable e_1 states the likelihood of $f(F_-(C_i)) < f(C_i)$. Similarly, e_2 signifies the likelihood of $f(F_+(C_i)) > f(C_i)$. The variable PSNR signifies the Peak Signal to Noise Ratio of the participating chromosome, while α presents a weight parameter that has been obtained empirically. Mathematically, PSNR has been obtained using (13).

$$PSNR = 10 \log_{10} \frac{M \times N \times 255^2}{\sum_{i,j} (y_{i,j} - x_{i,j})^2} \quad (13)$$

In (13), M and N signify image dimension while x and y state the image intensity before and after embedding. Here, α states a weight parameter that controls the visual quality of the input multimedia data and the secrecy of the secret text. For a specific value of α , higher the values of e_1 and e_2 , we hypothesize VIHCS to achieve higher data security. Hence, in the proposed model, optimizing (specifically maximizing) the value of (13) (say, fitness value) has been considered as the fitness function. In our proposed method, we ensure maintaining e_1 and e_2 higher than a threshold, which is experimentally decided. We have applied the threshold as 0.5.

5.2.6. Estimate

P_{-R} and P_{-S} of the neighboring image block and check whether $P_{-S} > P_{-R}$. If so, the block is considered as successfully adjusted.

5.2.7. Crossover

In the crossover process, shift the chromosome by one pixel and reinitiate step-2. Once performing crossover twice, stop the cycle.

This overall process is called OPAP that makes HCS more resilient to any attacks such as RS Analysis or steganalysis, which can achieve optimal security over the cloud platform. Now, once all image blocks are successfully adjusted, estimate the value of R_m , R_{-m} , S_m and S_{-m} of the image and in case the disparity of R_m and R_{-m} (and, S_m and S_{-m}) is more than 5%, perform adjustment of the next or the subsequent image blocks. In the VIHCS model, each block is labeled before initiating OPAP and thus, we reduce computational overheads significantly. Furthermore, the use of AGA reduces the exhaustive search operation and hence

achieves computational-efficiency which makes it suitable for secure multimedia data transmission over cloud infrastructure.

5.3. Data Extraction

Once embedding the data inside the cover image and obtaining the stego image it is transmitted over cloud communication channels. Receiving the data at the receiver end, we have obtained secret data as well as the original cover image by performing extraction using the 2D-DWT-2L method. In this method, at first Inverse DWT (IDWT) algorithm is applied over the received stego-image. An algorithmic-snippet of the extraction process is given Algorithm 3.

Input: Stego Image

Output: Secret message, Cover image.

Initiate the process

Step-1 Scan the stego image row-by-row

Step-2 Estimate the 2D wavelet coefficients for the 1-level of HAAR wavelet filter

Step-3 Estimate the 2D wavelet coefficients for the 2-level of HAAR wavelet filter

Step-4 Prepare message ""

Step-5 Initiate a loop

Perform extraction of the text embedded in vertical coefficients and assign odd values = $LH2(x, y)$

Perform extraction of the text embedded in horizontal coefficients and assign even values = $HH2(x, y)$

Step-6 End loop

Step-7 Reconstruct message $msg = append(odd, even)$

Step-8 Perform IDWT for the constructed approximation which generates the original multimedia data or cover image

Step-9 Return text message as retrieved secret message and cover image.

End

Algorithm 3 Data Extraction

Once extracting the text data, we have synthesized the cover image from the reconstructed approximation by applying the IDWT technique for 2nd level followed by 1st level. Figure 5 elucidates the DWT synthesis process.

Now, considering the need to decrypt the secret text data from the cover image, similar to the encryption phase, Hybrid Cryptosystem applies AES and RSA algorithms to decrypt the secret data at the receiver. Receiving the stego image at the receiver unit, we decrypt the text using private key x to obtain

RESEARCH ARTICLE

the original secret message transmitted. The decryption algorithm used to retrieve the original secret data is given Algorithm 4.

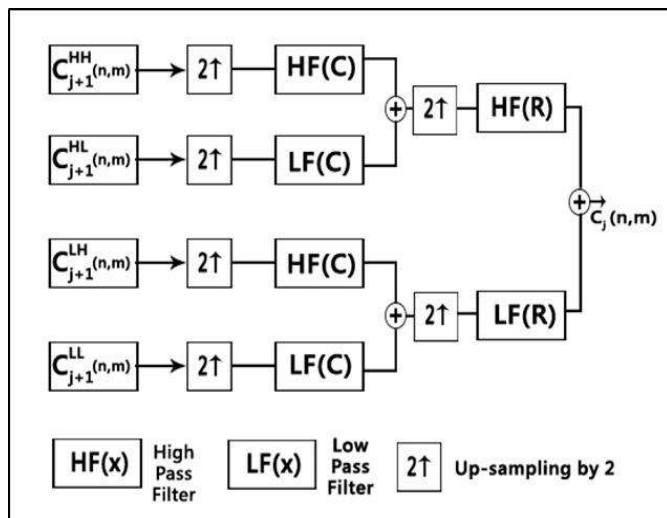


Figure 5 Extracting Encrypted Text from Images Showing the Procedure of Synthesis of DWT-2L

Input: Ciphertext received Cipher T_x , key

Output: Secret message.

Initiate the process

Step-1 Split the received cipher text into two components; HashedText and HashedKey

Step-2 $Enc_msg = decompress(HashedText)$

Step-3 $Enc_{Key} = decompress(HashedKey)$

Step-4 $x = decrypt_AES-256(Enc_{Key}, s)$

Step-5 $Enc_S_{Text_odd} = split(Cipher_{F_{Total}}, S_{Text_odd})$

Step-6 $Enc_S_{Text_Even} = split(Cipher_{F_{Total}}, S_{Text_Even})$

Step-7 $S_{Text_odd} = decrypt_AES - 256(Enc_S_{Text_odd}, s)$

Step-8 $S_{Text_Even} = decrypt_RSA(Enc_S_{Text_Even}, x)$

Define plain text message

Step-9 Initiate loop for all characters

If odd

Insert odd characters into odd indices within plain text message

else

Insert even characters into even indices within plain text message.

End loop

Step-10 Retrieve original secret text and image transmitted.

End

Algorithm 4 Data Decryption

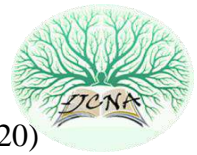
Thus, implementing the above-stated approach, we have obtained a computationally efficient VIHCS model which has been strengthened by employing cryptosystem enhancement as well as attack resilience (for example steganalysis or RS-Attack). The proposed system can be employed for secure data transmission over the cloud environment while ensuring optimal performance. A detailed discussion of the simulation results and their inferences is given in the subsequent section.

6. RESULTS AND DISCUSSIONS

Considering the exponential rise in data communication in the cloud environment, this research focused on amalgamating strengths of the different security models such as cryptography and steganography, which is well known for multimedia data security. Realizing the communication demands and allied user interfaces, we modeled the overall system as transmitter and receiver, where the first (i.e., transmitter) intended to transmit the secret data embedded within the multimedia cover image. Noticeably, the transmitter terminal performs encryption, AGA-OPAP assisted LSB embedding, compression, and transmission. On contrary, the receiver performs extraction and decryption that eventually retrieves original secret data and cover image transmitted by the transmitter or user. The overall proposed model is developed using MATLAB 2018a tool, which has been simulated with the computer specifications of 2.27 GHz Intel (R) Core (TM), 3rd generation processor (I3 CPU), 8 GB RAM, and Windows-7 operating system. To assess the performance of the proposed VIHCS model, we used multiple images as the cover image and secret message of varied sizes.

The Hybrid Cryptography and Steganography (HCS) model can be effective or more efficient when it fulfills the following as shown in Table 1.


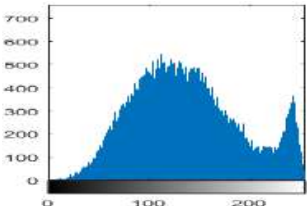
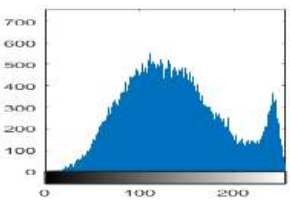

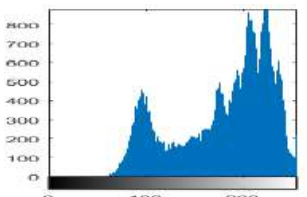
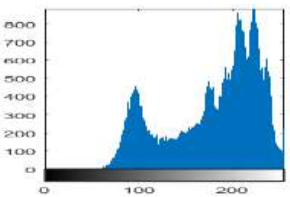
S.No.	Parameter	Definition
1.	PSNR	To preserve the quality of the multimedia data even after embedding secret text data, PSNR should be higher. The significant reduction in PSNR value can depict the presence of certain hidden information which can trigger attacker models to target and attack the data under the transmission.



RESEARCH ARTICLE

2.	Entropy	It signifies the disturbance in the original image. To ensure minimum perceptibility, the HCS model requires maintaining minimum entropy after message embedding. The minimum value of entropy can avoid getting attention from attacker modules.
3.	Embedding Capacity	It signifies the extent to which the secret text data can be embedded per unit of the cover image. An HCS model can be superlative or better if it ensures or maintains higher embedding capacity without introducing significant entropy and PSNR reduction (in addition to the regular and singular coefficient changes in RS analysis).
4.	Changes in Regular coefficients ($R_m - R_{-m}$)	It signifies the variation or the difference between the regular coefficient before and after embedding. Higher differences are the indicator for hidden information which invites attackers such as RS attackers or Steganalysis attacking modules to target data under the transmission. Lower the differences, higher the imperceptibility and resulting data security.
5.	Changes in Singular coefficients ($S_m - S_{-m}$)	It signifies the variation or the difference between the singular coefficient before and after embedding. Higher differences are the indicator for hidden information which invites attackers such as RS attackers or Steganalysis attacking modules to target data under the transmission. Lower the differences, higher the imperceptibility and resulting data security.
6.	Histogram Variations	It signifies the difference between the histogram patterns of the cover image as well as the stego image, before and after the embedding. Lower or negligible variations in the histogram graph show near-optimal embedding, which supports imperceptibility and hence attack resilience.

Table 1 Performance Criteria

S.No.	Dataset	Histogram of the cover image	
		Before	Post Embedding and OPAP
1. [44]			
2. [44]			

RESEARCH ARTICLE

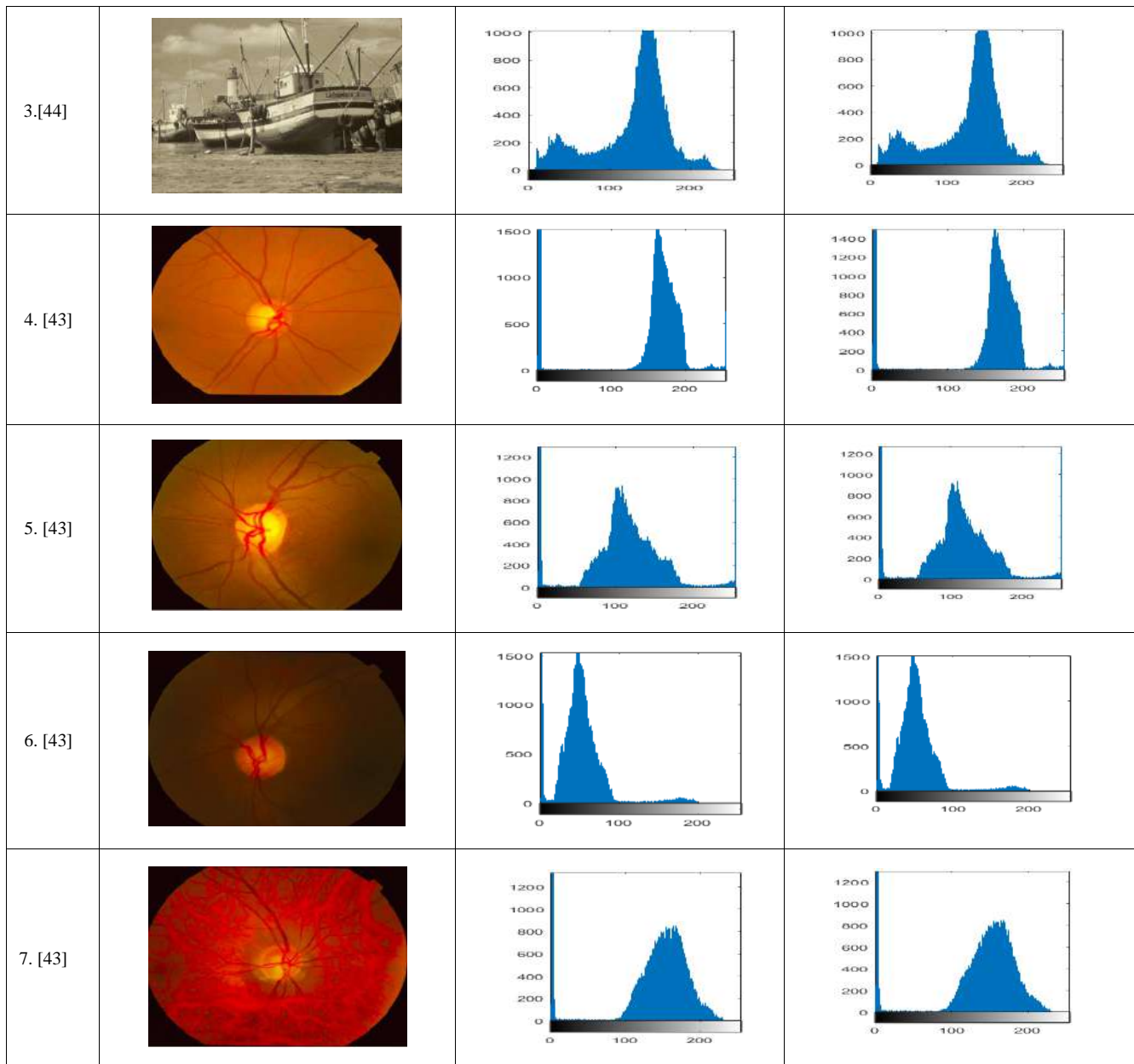


Figure 6 Histogram Pattern Analysis

Unlike major conventional researches, where authors have either focused on MSE, PSNR, or embedding capacity enhancement, in this research, we emphasize on accomplishing cumulative performance as mentioned in the above table. This as a result can accomplish optimal performance by the proposed VIHCS model to ensure an optimally secure communication environment for multimedia data over cloud platforms. As stated in Table 1, minimizing histogram pattern variations before and after message embedding in the cover image can help reducing visual perception or resulting tracking by attackers. Histogram

variations take place due to increased entropy within the cover image due to text embedding, and therefore to retain visual imperceptibility reducing entropy through optimal pixel adjustment is vital. To achieve it, we introduced AGA-OPAP based LSB embedding that resulted in minimum histogram variations (Figure 6).

As depicted in Figure 6, our proposed VIHCS model exhibits negligible or near-zero variation in histogram after message embedding. Observing the results (Figure 6), it can be inferred that the proposed VIHCS model achieves optimal histogram pattern and retain its normalcy even after

RESEARCH ARTICLE

embedding, which supports the visual imperceptibility aspect for secure communication.

To assess the efficacy of the proposed VIHCS model, in this work we considered normal benchmark images such as Lena, Baboon, Boat [43] [44] as well as the medical images (DRISHTI-GS dataset). Here, the prime objective was to assess whether the proposed method can be effective or suitable for the healthcare application environment. Since in healthcare images retaining image-quality and the inherent feature is of utmost significance, we have applied very critical healthcare data for "Diabetic Retinopathy", where even a single nerve can have significant information regarding the presence of diabetes.

Introduction of additional text (secret) data could cause entropy and hence quality degradation. However, VIHCS intended to optimize such entropy and ensure that stego-image (image after embedding) retains maximum possible image quality and originality. As depicted in Figure 6, image number 1, 2, and 3 are taken randomly from benchmark image dataset (Baboon, Lena and Boat dataset [44], respectively in *.jpg format), while images (4, 5, 6 and 7) are taken from DRISHTI-GS [43] dataset which is in *.png format. The second column presents the histogram pattern or the original image "before embedding", while the histogram pattern after OPAP assisted LSB embedding is given in the 3rd column. Observing the results, it can be found that the proposed method achieves optimal performance in terms of visual imperceptibility. It can avoid numerous attack scenarios online in the cloud environment.

To simulate the proposed model for performance verification, random text information such as a snippet of common test sentences such as "My Own Address", "My Personal Biography" with different sizes (in notepad, *.txt) was applied. Due to space constraints and inferior significance of text (embedding data) details, we have not mentioned it in this manuscript. Dataset images (Fig. 6) are the cover images considered for the simulation and performance assessment.

In addition to the visual assessment through histogram analysis, we examined the performance in terms of the well-known statistical parameters such as PSNR (in dB) analysis, Regular and Singular coefficient variations in each block of the image due to LSB embedding, etc. Figure 7 presents the PSNR performance of the proposed VIHCS model for 250 bytes in the text (secret data) embedding. Observing the result in Figure 7, where the PSNR has been obtained for the text embedding size of 250 bytes, it can be found that after embedding the text or secret data, the PSNR decreases; however, the contribution goes to the proposed AGA-OPAP assisted LSB embedding method, which improves the message embedding and even optimizes the PSNR. Interestingly, observing PSNR performance it can be found that the proposed VIHCS model either achieves near original

PSNR or even improves the image quality which results in improved PSNR value (post-embedding and OPAP optimization). The mathematical model for PSNR estimation was applied as given in (13) for the image processed after 2D-DWT-2L and post AGA-OPAP optimization.

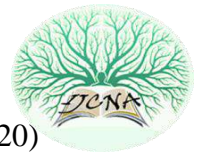
The results obtained (Table 2) reveals that the proposed AGA-OPAP assisted LSB embedding method is of utmost significance towards retaining and optimizing image quality for quality-centric communication over a cloud environment.

As the image security process undergoes cipher generation which can significantly increase the disturbances across the image input. This, as a result, can cause an increase in image entropy which not only degrades (image) quality but also broadens the horizon for intruders to attack specific data. On the other hand, encryption imposes additional information to the multimedia data to make it complex for the intruder to distinguish the encrypted data and the original image information. In such cases, maintaining the optimal entropy with the data under transmission is a must. With this motive, in this paper, we estimated entropy for each encrypted data to retain quality-centric image security (14).

$$ENT(I) = - \sum_{i=1}^{2^8} P(I_i) \log_b P(I_i) \quad (14)$$

In (14), $ENT(I)$ states the entropy of an image, where I signifies the intensity, and $P(I_i)$ signifies the probability of the intensity value I_i .

Analyzing the above results (Figure 8), it can be observed clearly that the spike in entropy is insignificant and thus keeps the image quality unchanged. It affirms the suitability of the encrypted images for critical applications such as healthcare (telemedicine) or critical data communication purposes. Similarly, we have examined the embedding capacity of the proposed model, which signifies the extent or the percentile to which a unit image can embed the text data (i.e., while ensuring no reduction in PSNR and correlation, and maintaining low entropy). Figure 9 presents the embedding capacity performance of the proposed model. Observing Figure 9, it can be easily found that the proposed method achieves a significantly large enhancement in the embedding capacity post-optimization. This can be because of the robustness of the proposed OPAP concept, which ensures optimal embedding while retaining entropy low and PSNR high, which are the key objectives of the employed AGA heuristic model. Thus, the results obtained signify the suitability of the proposed model for large-scale size encryption and secure communication purposes. This is the matter of fact that the addition or more secret information (text data) in the image might impose high entropy that eventually could lead to a reduction in image quality (i.e., PSNR).



RESEARCH ARTICLE

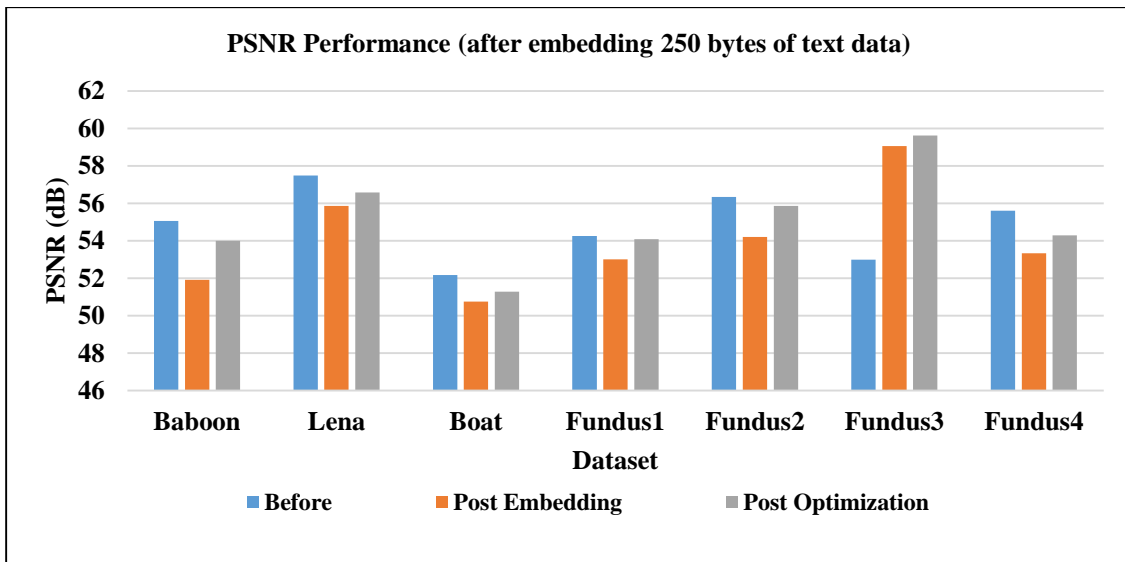
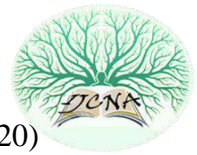


Figure 7 PSNR Performance (After Embedding 250 Bytes of Text Data)

Dataset	Data Size (bytes)	PSNR (dB)		
		Before	Post Embedding	Post Optimization
Baboon	250	55.0600	51.9200	54.0053
	500	58.8630	56.2003	57.8942
	1000	56.7491	55.8990	56.1804
Lena	250	57.4873	55.8762	56.5852
	500	53.1041	52.0072	52.9183
	1000	55.4901	54.0700	55.1003
Boat	250	52.1850	50.7611	51.2970
	500	56.8931	55.4180	55.9814
	1000	56.2443	55.0134	55.9993
Fundus1	250	54.2667	53.0110	54.1010
	500	52.2442	51.6320	52.1248
	1000	58.0012	57.4021	57.8732
Fundus2	250	56.3450	54.2101	55.8701
	500	59.1251	57.3427	58.6391
	1000	58.8422	56.1120	58.1297
Fundus3	250	53.0070	59.0629	59.6255
	500	56.0367	53.6730	54.9834
	1000	54.5259	52.1147	53.5895
Fundus4	250	55.6216	53.3414	54.3060
	500	58.8736	56.5290	57.9201
	1000	57.9910	56.3019	57.1003

Table 2 PSNR Performance over Different Sizes of the Secret Text Data



RESEARCH ARTICLE

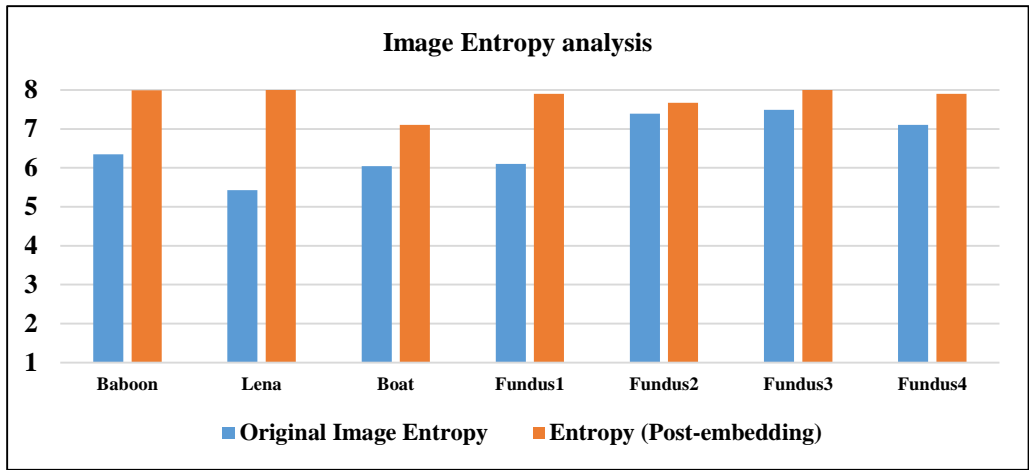


Figure 8 Image Entropy Analysis

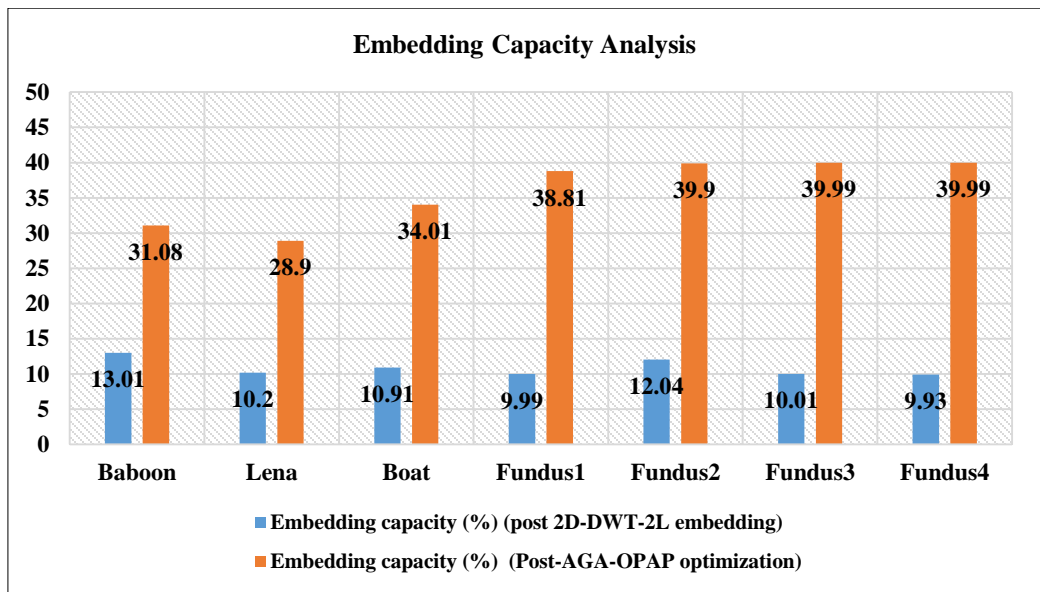


Figure 9 Embedding Capacity Analysis

In such a case, it is significant to assess whether the inclusion of the proposed AGA-OPAP assisted LSB embedding helps retaining maximum possible image quality even after large secret data embedding. With this motive, in this paper, we assessed the performance for the different sizes of the secret text data to be embedded in the cover image. Observing the results (Table 2) it can easily be found that though with an increase in secret data size (to be embedded into the cover image), the PSNR decreases; however the use of our proposed AGA-OPAP based LSB embedding method reduces entropy and retains better PSNR. It affirms that the proposed method can achieve optimal PSNR irrespective of the data size. The results affirmed that the inclusion of AGA-OPAP can be vital to ensure higher data embedding inside the cover image

without imposing any significant quality degradation or visual traits, which might invite intruders to attack over uncertain cloud communication channels or allied networks.

In addition to the PSNR assessment, in this research, we have considered the probability of statistical-assessment-based attack-proneness. In the majority of the existing HCS models, authors have either focused on enhancing embedding capacity or histogram pattern improvement. However, there are the attack models such as RS-Attack or Steganalysis attack which might explore into the multimedia data under the transmission to attack the specific data-carrying certain significant information or secret information. To alleviate such issues, we examined the variations in regular and singular coefficients per block of the image. As stated in Table 1, higher

RESEARCH ARTICLE

differences in the regular and singular coefficients can reveal the attackers about the presence of secret data within the multimedia data, and therefore maintaining lower differences can be advantageous.

Observing Table 3, it can be found that the proposed method achieves relatively lower differences in regular coefficient value ($R_m - R_{-m}$) and singular difference value ($S_m - S_{-m}$). It reveals that the proposed method can achieve a high level of

visual imperceptibility that as a result can help to achieve secure data communication over a cloud channel. To assess the time efficiency of the proposed model for encryption, we applied MATLAB functions $*(tic - toc)$. We obtained overall execution time for the different datasets (Refer Table 2 for the different datasets and corresponding sequence). The execution time consumed over the different datasets is given in Table 4.

Dataset	RS Parameters					
	Regular Coefficient Difference ($R_m - R_{-m}$)			Singular Coefficient Difference ($S_m - S_{-m}$)		
	Before	Post Embedding	Post Optimization	Before	Post Embedding	Post Optimization
Baboon	0.0064	0.0055	0.0058	0.0030	0.0016	0.0088
Lena	0.0036	0.0026	0.0033	0.0007	0.0113	0.0009
Boat	0.0040	0.0055	0.0066	0.0067	0.0016	0.0055
Fundus1	0.0092	0.0075	0.0077	0.0090	0.0077	0.0060
Fundus2	0.0030	0.0026	0.0035	0.0044	0.0113	0.0005
Fundus3	0.0040	0.0078	0.0020	0.0002	0.0074	0.0063
Fundus4	0.0084	0.0028	0.0062	0.0035	0.0113	0.0042

Table 3 RS Analysis (Secret Data Size 250 Bytes)

Dataset	Data Size (bytes)	Execution Time (ms)	
		Encryption	Decryption
Baboon	250	87.97	39.01
	500	72.60	33.01
	1000	70.63	32.97
Lena	250	89.45	41.00
	500	71.06	41.80
	1000	77.64	43.80
Boat	250	89.40	44.91
	500	88.48	43.31
	1000	82.26	43.73
Fundus1	250	71.31	39.92
	500	70.00	37.79
	1000	64.33	37.79
Fundus2	250	69.83	33.31
	500	69.91	33.67
	1000	69.91	33.55
Fundus3	250	71.01	38.89
	500	71.01	38.41
	1000	71.20	39.00
Fundus4	250	68.88	32.87
	500	71.60	39.18
	1000	76.00	41.47

Table 4 Execution Time over Different Sizes of the Secret Text Data

Observing the above-stated results, it can easily be found that the proposed system consumes low execution time, including both encryption as well as decryption, which exhibit its robustness towards time-efficient computation. We evaluated the efficacy of the proposed model in terms of the number of pixel changes (NPCR) and the unified average channel intensity (UACI). The high value of NPCR and UACI

typically means higher randomness and therefore high tolerance to any kind of differential attack [45].

Results of the randomness test with a higher NCPR value confirm the purpose of the proposed method's attack resistance. UACI also affirms our proposed data security model's good result. The above-mentioned reliability thus ensures the efficacy of the proposed security model for any data transmission in real-time, including the purposes of our intended cloud communication.

Dataset	NPCR (%)	UACI (%)
Baboon	99.60	25.77
Lena	99.83	28.32
Boat	99.83	23.81
Fundus1	99.59	36.61
Fundus2	99.43	28.60
Fundus3	99.63	41.06
Fundus4	99.52	14.87

Table 5 NPCR and UACI Randomness Test

Recalling the overall design where the key goal of employing hybrid cryptosystems with AGA-OPAP was to avoid any attack conditions such as Man-In-The-Middle attack (MITM), steganalysis, or linear and differential based attack approaches since our proposed model avoids providing any scope of visual perceptibility and maintains low entropy, high PSNR, it would be able to resilient any attack conditions. Additionally, as the implementation of AGA-OPAP was done to avoid any statistical attack probability such as steganalysis or RS-attack approaches, it can withstand any attack condition to ensure

RESEARCH ARTICLE

secure communication. To assess the quality of the decrypted image at the receiver side, we obtained the mean absolute error (MAE) value using (15).

$$MAE = \frac{1}{n} \sum_{i=1}^n (|Y'_i - Y_i|) \tag{15}$$

Where Y'_i refers the calculated output, while Y_i states for the expected value. The results obtained for sample inputs (with 250 bytes of text input) are given in Table 6. The results (Table 6) signifies the robustness in terms of a very negligible error profile, which undoubtedly affirms its superior image quality (post-decryption).

Dataset	MAE (%)
Baboon	0.1968
Lena	0.0996
Boat	0.3001

Fundus1	0.3109
Fundus2	0.4111
Fundus3	0.1557
Fundus4	0.1904

Table 6 MAE Performance with Different Input Samples (250 Bytes of the Text Secret Data)

The performance of the proposed model is assessed against state-of-the-art approaches where these algorithms have been developed to secure data in medical images. For comparison we have chosen Fundus image after embedding 250 bytes of secret text data. Comparative results are shown in Figure 10, which shows that the proposed algorithm clearly shows better results. The proposed VIHCS for data security showed better performance than the existing algorithms.

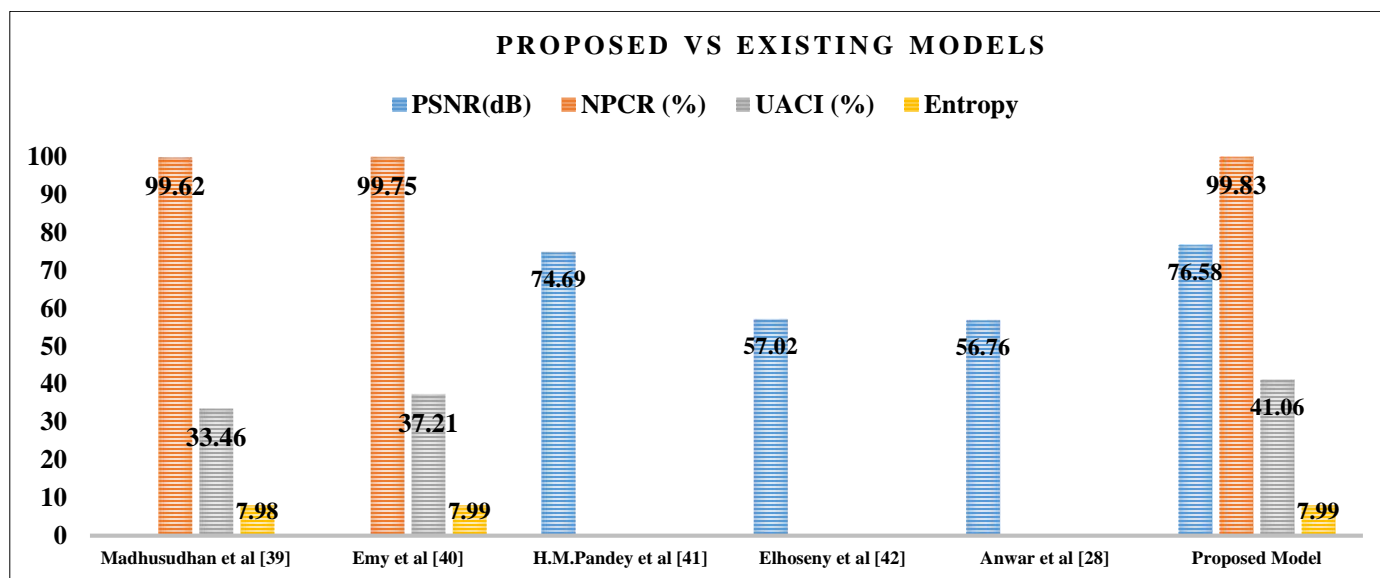
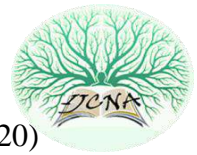


Figure 10 Comparison of Results

Thus, taking into consideration the proposed VIHCS model and its simulation-based performance, it can be inferred that the proposed system achieves optimal efficiency, which makes it suitable for secure data communication over the cloud environment. Observing the overall results, it can be found that the use of the HCS model with Hybrid Cryptosystems (AES and RSA together) and AGA-OPAP based embedding optimization can yield optimal VIHCS for secure multimedia communication over the cloud platform. Similarly, results indicate that the use of 64-RSA and 256-AES as strategically combined hybrid solution can be better towards VIHCS, though in this study we have not performed individual performance assessment for RSA and AES (distinctly).

Results obtained (Table 1 - Table 6) & (Figure 6 - 10) confirms that the use of AGA-OPAP has strengthened the VIHCS model to achieve optimal pixel adjustment which has eventually yielded PSNR enhancement, minimum histogram changes, or entropy. Besides, it has helped (due to PSNR and RS sensitive optimization) achieving optimal values for Regular and Singular coefficient values for each block. The simulation results reveal that the use of AGA-OPAP based LSB embedding has achieved maximum possible visual imperceptibility as well as data (image) quality which affirms the suitability of the proposed model for the cloud environment.



RESEARCH ARTICLE

Considering overall structure, implementation mechanism and key goals, where the prime focus was made on achieving:

1. High PSNR and Low entropy (to preserve quality, see Figure 6, Table 2 and Figure 8)
2. Low-delay (to support time-efficient communication, see Table 4)
3. High embedding capacity (to enable resource-efficient secure communication, see Figure 9)
4. High visual quality and imperceptibility (to confuse or avoid any MITM attacks based on image quality and certain statistical calculations such as steganalysis, RS-attack, correlation information, etc for better attack-resiliency, see Figure 6).
5. High image quality (higher NCPR and UACI, see Table 5) and low MAE (see, Table 6).
6. The efficiency of the proposed model is examined alongside the existing algorithm where the results have been stated in Figure 10. The result reveals that the proposed algorithm achieved improved results related to the existing algorithms.

Observing the overall results and corresponding inferences, it can be inferred that a better or suitable programming paradigm for our proposed VIHCS model can enable an optimal security solution for the different cloud purposes, including Electronic Healthcare Records (EHR), Tele-medicine, critical image and allied annotation information hiding for future (security) purposes. Contemporarily, a large number of cloud applications provide data security, and undeniably our proposed VIHCS model can be of great significance to support them, either as a standalone security solution or as a plug-in or Application Program Interface (API). The overall research conclusion is given in the subsequent sections.

7. CONCLUSION

Considering the exponential rise of data communication over the cloud environment, which is often considered as uncertain in this research the emphasis was made on developing a robust and efficient secure data transmission model. Unlike conventional approaches such as cryptosystems, this research intended to exploit the efficacy of both cryptosystems as well as steganography. However, realizing the fact that the majority of the classical approaches are prone to get attacked if used in conventional form, a hybrid cryptosystem was developed using RSA and AES cryptography algorithms. The use of these two algorithms and their strategic implementation towards secret data encryption and decryption strengthened the overall level of security and ensured that the secret information can't be retrieved easily. On the other hand, realizing the quality preserve aspect of steganography which

is often used in image data security, an Adaptive Genetic Algorithm assisted OPAP was developed that optimized the least significant bit embedding over image-blocks. The AGA-OPAP model considered PSNR as well as Regular and Singular Coefficient values per block of the image as objective functions to perform secret message embedding and allied pixel adjustment (optimization). It affirms proposed AGA-OPAP model itself is a novel and robust approach to achieve better image quality, visual imperceptibility, and higher embedding capacity even without losing original quality. These all features make the proposed system suitable for numerous data communication purposes including cloud communication, healthcare data communication, IoT communication purposes, etc. MATLAB based model development and its simulation with different image datasets as well as secret text of varied sizes revealed that the proposed VIHCS model can be attack resilient (statistical assessment based attack models) and quality-centric (high PSNR) which make it suitable for secure communication over cloud platforms. The proposed VIHCS model can be resilient to the state-of-art attacking models such as RS-Attack, Steganalysis, etc. Summarily, the proposed VIHCS model is suitable for secure data transmission over a cloud platform. Though, the use of HCS is a novel concept, in the future focus can be made on designing a single lightweight cryptosystem with equivalent or better security provision for multimedia data.

REFERENCES

- [1] R. K. Gupta and P. Singh, "A new way to design and implementation of hybrid crypto system for security of the information in public network," *Int. J. Emerg. Technol. Adv. Eng.*, vol. 3, no. 8, pp. 108-115, 2013.
- [2] Anupam Kumar Bairagi, Rahamatullah Khondoker & Rafiqul Islam (2016) An efficient steganographic approach for protecting communication in the Internet of Things (IoT) critical infrastructures, *Information Security Journal: A Global Perspective*, 25:4-6, 197-212, DOI: 10.1080/19393555.2016.1206640.
- [3] Sajjad, M., Muhammad, K., Baik, S.W. et al. Mobile-cloud assisted framework for selective encryption of medical images with steganography for resource-constrained devices. *Multimed Tools Appl* 76, 3519–3536 (2017). <https://doi.org/10.1007/s11042-016-3811-6>
- [4] Darwish, A., Hassani, A.E., Elhoseny, M. et al. The impact of the hybrid platform of internet of things and cloud computing on healthcare systems: opportunities, challenges, and open problems. *J Ambient Intell Human Comput* 10, 4151–4166 (2019). <https://doi.org/10.1007/s12652-017-0659-1>
- [5] Y. Xu, X. Zhao and J. Gong, "A Large-Scale Secure Image Retrieval Method in Cloud Environment," in *IEEE Access*, vol. 7, pp. 160082-160090, 2019, doi: 10.1109/ACCESS.2019.2951175
- [6] Mersini Paschou, Evangelos Sakkopoulos, Efrosini Sourla, Athanasios Tsakalidis, Health Internet of Things: Metrics and methods for efficient data transfer, *Simulation Modelling Practice and Theory*, Volume 34, 2013, Pages 186-199, <https://doi.org/10.1016/j.simpat.2012.08.002>
- [7] Muhammad Sajjad, Mansoor Nasir, Khan Muhammad, Siraj Khan, Zahoor Jan, Arun Kumar Sangaiah, Mohamed Elhoseny, Sung Wook Baik, Raspberry Pi assisted face recognition framework for enhanced law-enforcement services in smart cities, *Future Generation Computer Systems*, Volume 108, 2020, Pages 995-1007, ISSN 0167-739X, <https://doi.org/10.1016/j.future.2017.11.013>.

RESEARCH ARTICLE

- [8] Laskar, Shamim. (2012). High Capacity data hiding using LSB Steganography and Encryption. *International Journal of Database Management Systems*. 4, 57-68. 10.5121/ijdms.2012.4605.
- [9] May Zaw, Z., & Phyo, S. W. (2015). Security Enhancement System Based on the Integration of Cryptography and Steganography. *International Journal of Computer (IJC)*, 19(1), 26-39
- [10] L. Yu, Z. Wang and W. Wang, "The Application of Hybrid Encryption Algorithm in Software Security," 2012 Fourth International Conference on Computational Intelligence and Communication Networks, Mathura, 2012, pp. 762-765, doi: 10.1109/CICN.2012.195.
- [11] Parah S.A., Sheikh J.A., Ahad F., Bhat G.M. (2018) High Capacity and Secure Electronic Patient Record (EPR) Embedding in Color Images for IoT Driven Healthcare Systems. In: Dey N., Hassanien A., Bhatt C., Ashour A., Satapathy S. (eds) *Internet of Things and Big Data Analytics Toward Next-Generation Intelligence*. Studies in Big Data, vol 30. Springer, Cham. https://doi.org/10.1007/978-3-319-60435-0_17
- [12] Li, L., Hossain, M.S., El-Latif, A.A.A. et al. Distortion less secret image sharing scheme for Internet of Things system. *Cluster Comput* 22, 2293–2307 (2019). <https://doi.org/10.1007/s10586-017-1345-y>
- [13] B. Xue, X. Li and Z. Guo, "A New SDCS-based Content-adaptive Steganography Using Iterative Noise-Level Estimation," 2015 International Conference on Intelligent Information Hiding and Multimedia Signal Processing (IIH-MSP), Adelaide, SA, 2015, pp. 68-71, doi: 10.1109/IIH-MSP.2015.80.
- [14] Vipula Madhukar Wajgade, "Enhancing Data Security Using Video Steganography," *International Journal of Emerging Technology and Advanced Engineering*, Volume 3, Issue 4, April 2013.
- [15] Marwa E. Saleh, Abdelmegeid A. Aly and Fatma A. Omara, "Data Security Using Cryptography and Steganography Techniques" *International Journal of Advanced Computer Science and Applications (IJACSA)*, 7(6), 2016. <http://dx.doi.org/10.14569/IJACSA.2016.070651>
- [16] M. E. Saleh, A. A. Aly, and F. A. Omara, "Enhancing Pixel Value Difference (PVD) Image Steganography by Using Mobile Phone Keypad (MPK) Coding," *International Journal of Computer Science and Security (IJCSS)*, Volume (9), Issue (2), pp. 397 - 397, 2015
- [17] A. Duluta, S. Mocanu, R. Pietaru, D. Merezeanu and D. Saru, "Secure Communication Method Based on Encryption and Steganography," 2017 21st International Conference on Control Systems and Computer Science (CSCS), Bucharest, 2017, pp. 453-458, doi: 10.1109/CSCS.2017.70.
- [18] Dhvani Panchal, "An Approach Providing Two Phase Security of Images Using Encryption and Steganography in Image Processing", 2015 *IJEDR*, Volume 3, Issue 4, ISSN: 2321-9939.
- [19] Y. Leung and R. Y. Hou, "Unequal security protection for secure multimedia communication," 2015 IEEE 4th Global Conference on Consumer Electronics (GCCE), Osaka, 2015, pp. 570-571, doi: 10.1109/GCCE.2015.7398667.
- [20] J. Li, X. Guo, Y. Yu, Q. Tu and A. Men, "A robust and low-complexity video fingerprint for multimedia security," 2014 International Symposium on Wireless Personal Multimedia Communications (WPMC), Sydney, NSW, 2014, pp. 97-102, doi: 10.1109/WPMC.2014.7014798.
- [21] D. E. M. Ahmed and O. O. Khalifa, "Robust and Secure Image Steganography Based on Elliptic Curve Cryptography," 2014 International Conference on Computer and Communication Engineering, Kuala Lumpur, 2014, pp. 288-291, doi: 10.1109/ICCCE.2014.88.
- [22] V. Hajduk, M. Broda, O. Kovac and D. Levicky, "Image steganography with using QR code and cryptography," 2016 26th International Conference Radioelektronika (RADIOELEKTRONIKA), Kosice, 2016, pp. 350-353, doi: 10.1109/RADIOELEK.2016.7477370.
- [23] M. Mukhedkar, P. Powar and P. Gaikwad, "Secure non real time image encryption algorithm development using cryptography & steganography," 2015 Annual IEEE India Conference (INDICON), New Delhi, 2015, pp. 1-6, doi: 10.1109/INDICON.2015.7443808.
- [24] M. S. Alam, "Secure M-commerce data using post quantum cryptography," 2017 IEEE International Conference on Power, Control, Signals and Instrumentation Engineering (ICPCSI), Chennai, 2017, pp. 649-654, doi: 10.1109/ICPCSI.2017.8391793.
- [25] N. Kumar and S. Agrawal, "An efficient and effective lossless symmetric key cryptography algorithm for an image," 2014 International Conference on Advances in Engineering & Technology Research (ICAETR - 2014), Unnao, 2014, pp. 1-5, doi: 10.1109/ICAETR.2014.7012788.
- [26] S. F. Mare, M. Vladutiu and L. Prodan, "Secret data communication system using steganography, AES and RSA," 2011 IEEE 17th International Symposium for Design and Technology in Electronic Packaging (SIITME), Timisoara, 2011, pp. 339-344, doi: 10.1109/SIITME.2011.6102748.
- [27] P.V.Nithyabharathi, T.Kowsalya, V.Baskar, "To Enhance Multimedia Security in Cloud Computing Environment Using RSA and AES", *IJSETR*, Volume 3, Issue 2, February 2014.
- [28] Anwar, Asmaa & A.Ghany, Kareem & Elmahdy, Hesham. (2015). Improving the security of images transmission. *International Journal of Bio-Medical Informatics and e-Health*. 3. 7-13.
- [29] Xin Liao, Jiaojiao Yin, Sujing Guo, Xiong Li, Arun Kumar Sangaiah, Medical JPEG image steganography based on preserving inter-block dependencies, *Computers & Electrical Engineering*, Volume 67, 2018, Pages 320-329, ISSN 0045-7906. <https://doi.org/10.1016/j.compeleceng.2017.08.020>.
- [30] Balakrishnan Ramalingam , Amirtharajan Rengarajan , John Bosco Balaguru Rayappan , Hybrid Image Crypto System for Secure Image Communication- A VLSI Approach, *Microprocessors and Microsystems* (2017), doi:10.1016/j.micpro.2017.02.003
- [31] D. Ravichandran, P. Praveenkumar, J. B. B. Rayappan and R. Amirtharajan, "DNA Chaos Blend to Secure Medical Privacy," in *IEEE Transactions on NanoBioscience*, vol. 16, no. 8, pp. 850-858, Dec. 2017, doi: 10.1109/TNB.2017.2780881.
- [32] Mansour, R.F., Abdelrahim, E.M. An evolutionary computing enriched RS attack resilient medical image steganography model for telemedicine applications. *Multidim Syst Sign Process* 30, 791–814 (2019). <https://doi.org/10.1007/s11045-018-0575-3>
- [33] M. A. Usman and M. R. Usman, "Using image steganography for providing enhanced medical data security," 2018 15th IEEE Annual Consumer Communications & Networking Conference (CCNC), Las Vegas, NV, 2018, pp. 1-4, doi: 10.1109/CCNC.2018.8319263.
- [34] M. M. Hashim, M. S. Taha, A. H. M. Aman, A. H. A. Hashim, M. S. M. Rahim and S. Islam, "Securing Medical Data Transmission Systems Based on Integrating Algorithm of Encryption and Steganography," 2019 7th International Conference on Mechatronics Engineering (ICOM), Putrajaya, Malaysia, 2019, pp. 1-6, doi: 10.1109/ICOM47790.2019.8952061.
- [35] Chidambaram, N., Raj, P., Thenmozhi, K. *et al.* A cloud compatible DNA coded security solution for multimedia file sharing & storage. *Multimed Tools Appl* 78, 33837–33863 (2019). <https://doi.org/10.1007/s11042-019-08166-z>
- [36] Shilpi Harnal, R.K. Chauhan, "Hybrid Cryptography based E2EE for Integrity & Confidentiality in Multimedia Cloud Computing", *IJITEE*, Volume 10, Issue 8, August 2019.
- [37] Stoyanov B, Stoyanov B. BOOST: Medical Image Steganography Using Nuclear Spin Generator. *Entropy*. 2020; 22(5):501.
- [38] Abd-El-Atty B, Iliyasu AM, Alaskar H, Abd El-Latif AA. A Robust Quasi-Quantum Walks-based Steganography Protocol for Secure Transmission of Images on Cloud-based E-healthcare Platforms. *Sensors*. 2020; 20(11):3108
- [39] Madhusudhan, K.N., Sakthivel, P. A secure medical image transmission algorithm based on binary bits and Arnold map. *J Ambient Intell Human Comput* (2020). (online first) <https://doi.org/10.1007/s12652-020-02028-5>
- [40] Emy Setyaningsih, Retantyo Wardoyo, Anny Kartika Sari, Securing color image transmission using compression-encryption model with dynamic key generator and efficient symmetric key distribution, *Digital Communications and Networks*, 2020, (online first) ISSN 2352-8648, <https://doi.org/10.1016/j.dcan.2020.02.001>.

RESEARCH ARTICLE

- [41] Hari Mohan Pandey, Secure medical data transmission using a fusion of bit mask oriented genetic algorithm, encryption and steganography, *Future Generation Computer Systems*, Volume 111, 2020, Pages 213-225, ISSN 0167-739X, <https://doi.org/10.1016/j.future.2020.04.034>.
- [42] M. Elhoseny, G. Ramírez-González, O. M. Abu-Elnasr, S. A. Shawkat, N. Arunkumar and A. Farouk, "Secure Medical Data Transmission Model for IoT-Based Healthcare Systems," in *IEEE Access*, vol. 6, pp. 20596-20608, 2018.
- [43] A Comprehensive Retinal Image Dataset for the Assessment of Glaucoma from the Optic Nerve Head Analysis. Sivaswamy J, S. R. Krishnadas, Arunava Chakravarty, Gopal Dutt Joshi, Ujjwal and Tabish Abbas Syed, *JSM Biomedical Imaging Data Papers*, 2(1):1004, 2015.
- [44] Input images available URL, "<https://homepages.cae.wisc.edu/~ece533/images/>".
- [45] Y. Wu, J. P. Noonan, S. Agaian, "NPCR and UACI Randomness Tests for Image Encryption", *Cyber Journals: Multidisciplinary Journals in Science and Technology, Journal of Selected Areas in Telecommunications (JSAT)*, April Edition, 2011, pp.31-38, 2011.
- [46] Rayappan, D., Pandiyan, M. Lightweight Feistel structure based hybrid-crypto model for multimedia data security over uncertain cloud environment. *Wireless Netw* (2020). <https://doi.org/10.1007/s11276-020-02486-x>.

Authors



Denis R has obtained a Bachelor of Science (B.Sc.) from Loyola College (Autonomous), Madras University, Chennai, TN, India, and Master of Computer Applications (MCA) from Sacred Heart College (Autonomous), Tirupattur in the year 2006 and 2009 respectively. Presently, he is pursuing a Ph.D. in Computer Science at Periyar University, Salem, TN, India. He has published research papers in peer-reviewed journals and conferences, one Indian Patent, and authored two books (Java Programming – for Core and Advanced Users, ISBN: 9789386235329 | Year: 2018 & Constructive Java Programming ISBN: 9789389211771 | Year: 2020-2021) by Universities Press (India) Pvt. Ltd, Hyderabad. His research interests include Data Security and Privacy, Cryptography Algorithms, Big Data Analytics, Data Mining, and Bio-inspired algorithms.



Madhubala P obtained a Ph.D. in Computer Science from Mother Teresa Women's University, Kodaikanal, TN, India in the year 2017. She is currently a Assistant Professor at the Research Department of Computer Science, Don Bosco College of Arts and Science, Dharmapuri, TN, India since 2007. Also, she is the University nominee for the Board of Studies of the BCA department at Sacred Heart College (Autonomous), Thiruvalluvar University, Tirupattur, TN, India. She has published more than 13 research papers in peer-reviewed international journals and conferences. Her research interests include Cloud Computing, Wireless Sensor Networking, Data security, advanced data mining, and Artificial Intelligence. She has 19 years of teaching experience and 8 years of Research Experience. Currently, she is guiding four Ph.D. students.



Hybrid data encryption model integrating multi-objective adaptive genetic algorithm for secure medical data communication over cloud-based healthcare systems

R. Denis¹ · P. Madhubala²

Received: 18 February 2020 / Revised: 4 February 2021 / Accepted: 10 February 2021

Published online: 13 March 2021

© The Author(s), under exclusive licence to Springer Science+Business Media, LLC, part of Springer Nature 2021

Abstract

The exponential rise in the development of cloud computing environments in the healthcare field, the protection and confidentiality of the medical records become a primary concern for healthcare services applications. Today, health data stored in the cloud is highly confidential information concealed to avoid unauthorized access to protect the patient's information. As cloud-based medical data transmission becomes more common, it receives growing attention from researchers and academics. Despite the potential for misuse, medical data transmitted through unreliable networks can be manipulated or compromised. The current cryptosystems alone are not sufficient to deal with these issues, and hence this paper introduces a new hybridization of data encryption model to shelter the diagnosis data in medical images. The proposed model is developed by combining either 2D Discrete Wavelet Transform 1 Level (2D-DWT-1 L) or 2D Discrete Wavelet Transform 2 Level (2D-DWT-2 L) steganography with the proposed hybrid encryption scheme. The hybrid encryption scheme is built by strategically applying Advanced Encryption Standard (AES) and Rivest–Shamir–Adleman (RSA) algorithms to secure diagnosis data to be embedded with the RGB channels of medical cover image. One of the key novelties is the use of an Adaptive Genetic Algorithm for Optimal Pixel Adjustment Process (AGA-OPAP) that enriches data hiding ability as well as imperceptibility features. To evaluate the efficiency of the proposed model, numerical tests are performed. The results show that the proposed algorithm is capable of safely transmitting medical data. Comparison of results is carried out concerning the datasets with the state-of-the-art algorithm. In terms of various statistical measures, the results showed the superiority of the proposed algorithm, such as peak signal to noise ratio (PSNR), correlation, structural content (SC), structure similarity (SSIM), entropy, histogram, NPCR, UACI and embedding capacity. The proposed model can also prevent attacks, such as steganalysis or RS attacks.

✉ R. Denis
denisatshc@gmail.com

Keywords Encryption · Decryption · Data hiding · Cloud environment · Health information exchange · Adaptive genetic algorithm · Steganalysis

1 Introduction

The high-paced technological revolution and subsequent computing strategies have led to a broad horizon providing a range of applications of which medical image communication is predominant. Biomedical image transmission became one of the imminent needs in the current health care system to ensure reliable, seamless and secured data transmission across uncertain channels. The Internet of Things (IoT) and cloud healthcare models have helped to launch a vast amount of healthcare data that is being distributed across the network. It is vital to ensure the confidentiality and security of the patient's diagnosis from an IoT and cloud ecosystem [21].

The arrival of new developments has increased the amount of multimedia information exchanged between individuals, which has sparked concern for preserving personal information privacy and security [44]. Besides, mammoth data storage growth has led to the invention of new storage technologies such as cloud [55], fog [65], edge [52], etc., which have played a pivotal role in each organization's IT infrastructure. However, irrespective of communication and storage systems, information security is still a concern. Confidentiality, authentication, integrity and non-repudiation play a fair role among the protection components in shaping the security algorithms used to secure the transmission of multimedia artefacts such as text, images, audio, video, etc. The incredible amount of internet-enabled communication systems has produced enormous data in real-time to meet various application requirements, such as social networking sites, the healthcare sector, e-commerce, scientific communities, financial sectors and other industrial requirements surveillance and security systems, etc. Social media and entertainment, surveillance footages, user multimedia data, and IoT services require security measures and policies to protect their data from unauthorized access. Undeniably, enterprise software has undergone tremendous growth in many sectors and government departments, producing and communicating vast data volumes (including multimedia data). In reality, these data are used to make appropriate decisions and recommendations. The combination of multiple data sources and associated voluminous aggregation of data has given rise to the cloud computing paradigm.

One of the main advantages of cloud computing is that it allows data access by multiple stakeholders, real-time computation and decision-making using cloud resources regardless of location or geographical boundaries. However, until a robust protection measure is not provided, data exchange from one node or user to another or across the cloud platform is highly vulnerable. Security or seamless information sharing of private data, particularly multimedia data (video, audio, image) [21, 44, 55, 65], is critical concerns in the cloud computing world. In addition to secure communication, enabling computational efficiency is also critical, as it demands time-efficient and reliable computation to meet the application's real-time needs. This means ensuring the security, scalability and manageability of up-surging computational and allied communication requirements in the cloud computing world. Facilitating the privacy of digital information has now become unavoidable for the cloud setting, such as social media, healthcare, etc. [2, 24, 39, 40, 48, 55, 65, 66].

Medical data, including individual reports, clinical results, etc., are exchanged between hospitals information to decrease tests' redundancy. The exchange of medical information accelerates the care of patients. The sharing of medical data is, thus, the demand of the current era. One of the key concerns is that medical officers use the internet (cloud) to share medical data, which is fast but at the same time, secure such information. Different attempts have been made to protect medical data

transmission by implementing various protocols such as HTTPs, but the secure transmission of medical data is still an open issue. When a miscreant gets access to data or retrieves the data or related information during communication networks, it can be easily altered or misused for any targeted or intended goals. Numerous attempts have been made to prevent such occurrences in implementing security systems; however, significant efforts are either creating data access security models or infrastructure security or applying several data security features [31]. Researchers have developed security mechanisms for which the user needs to be authenticated before accessing the data (access-control), or the data itself is protected so as not to expose secret information inside the data to the unauthorized user intruder. In recent years, various attempts have been made to strengthen data protection in the cloud. However, ensuring that both security and computing performance has remained an open issue for academics and industry.

Encryption of data is the most common cryptographic technique. Here, the data is used to be inserted or concealed within the image so that the attacker will not retrieve the data while the approved person will be provided with a key called the encryption/decryption key to retrieve the data. In this case, it is not easy to find a practical encryption/decryption key mainly due to the combination of numbers used to produce exponential key ranges as the key length increases linearly. Therefore, it is considered as an NP-hard problem. Also, locating a particular key is a search problem. The identity key length of the encryption/decryption key increases exponentially, so simple search methods such as linear and binary searching would not be possible. Metaheuristic algorithms have been introduced to deal with this sort of situation. Metaheuristic algorithms are algorithms for search and optimization. These techniques have been successfully used to solve complex problems of optimization [53, 67].

Among the powerful multimedia data privacy techniques, steganography and cryptosystems have played a decisive role in practice, but these methods are limited due to the growing prevalence of parallel attacks. There has been widespread attention to the Hybrid Cryptography and Steganography (HCS) model design, where the dual-level of security makes or offers better data security. However, as an application-specific scenario, preserving safe and attack resilient multimedia (medical data) transmission requires enhanced steganography and the cryptosystem to achieve the above specified eventual target.

This paper focuses on improving steganography and cryptosystems by realizing multimedia (medical data) communication over cloud infrastructure that is becoming vulnerable these days due to increased attack efforts. The Advanced Encryption Standard (AES) and the Rivest-Shamir-Adleman (RSA) algorithm are the two principal algorithms used in this work for data encryption [41]. AES is a symmetric cipher where the same key is used on both sides [59]. It is generated by a fixed message block size of 128 bits of plain text and keys of length 128, 192, or 256 bits. When sending longer messages, it must be split up into 128-bit chunks. Longer keys make the cipher more challenging to crack, but they also impose a longer encrypt and decrypt method. On the other hand, RSA is a public key algorithm commonly used in the business and private communication sectors [6]. It has the benefit of a variable key size ranging from (2–2048) bits.

The primary research in hiding data began with steganography, which refers to the science and art of hiding information inside an image. The advantage of steganography is that it can be used without the transmission being detected to send classified messages. The DWT has immense spatial localization, frequency distribution, and multi-resolution features consistent with the theory of forms in the human visual system. This paper implements both 1-level and 2-level of DWT steganography techniques that work on the frequency domain. It segmented the image into parts by high and low iteration. Edge information is stored in the high iteration portion, while the low iteration part is often split into high and low iteration parts.

Steganography aims to prevent anyone from knowing secret information and remove the suspicion of hidden information. The message is a secret text to be sent and camouflaged in the carrier to remain harder to detect. There are two main aspects of any steganography method, which are embedding capacity and imperceptibility. However, these two properties are confusing because it is challenging to increase capability while preserving a steganography system's imperceptibility. Besides, for the use of data transfer communication protocols, few concealing information methods can be unconventional, but its future is promising.

Once performing secret data encryption, an enhanced Adaptive Genetic Algorithm assisted LSB embedding model is developed that helps to embed secret text (i.e., cipher data) into the cover image optimally without increasing or affecting PSNR or visual characteristics such as entropy, histogram patterns etc. Because the inclusion of secret text might impact pixel arrangement and resulting entropy, PSNR, histogram patterns and other statistical features such as regular and singular coefficients of image blocks, AGA algorithm was applied to perform Optimal Pixel Adjustment (OPAP) during LSB embedding. The proposed method is evaluated under statistical attack assessment, and it has demonstrated high PSNR, low entropy, negligible perceptibility, and histogram deviations. Such novelties can help the proposed model avoid attacks like Steganalysis attack or RS attacks which are well known for exploiting statistical variations in multimedia data to detect secret or hidden information. The overall model is built with MATLAB2018a tool. The proposed security achieves enhanced or augmented security for medical data communication over the cloud environment.

The remaining parts of the manuscript presented are given as follows. The related works are provided in Section 2, preceded in Section 3 by the proposed model. Section 4 examines the results obtained and their respective inferences. In Section 5, the conclusion of the overall research is given.

2 Related works

This section presents some of the main works on multimedia and medical data privacy using steganography and various related technologies. In recent years, the importance of healthcare services has been realized globally and has emerged as one of the dominant research domains across academia industries. However, the preservation of optimum medical data privacy is a must to ensure smooth and flawless processes. Steganography, being one of the most efficient medical data security approaches, applied image transformation schemes to incorporate essential data into the cover image (i.e., medical image). In reality, the efficiency of reversible steganography techniques depends solely on image transformation effectiveness, data embedding and pixel adaptation to allow maximum imperceptibility.

Razzaq et al. [46] proposed a fusion of encryption, steganography and watermarking for digital image security. Authors [46] developed three key components: (a) the original image was encrypted using the sizeable secret key by rotating pixel bits the right using XOR operator; (b) for steganography, the encrypted image was altered through the least significant bits (LSBs) of the cover image and stego images were obtained; and (c) stego images were watermarked in time and frequency domain to ensure ownership. This approach showed promising results, but it does not deal with data redundancy (repeated transmission of the same data).

Bairagi et al. [9] suggested three coloured image steganography method where the 1st and 3rd method used red, green and blue channels to provide security. On the other side, green and blue colours were used in the 2nd method to implement protection during data transmission.

Anwar et al. [7] implemented a model to safeguard any images, specifically clinical images. It seeks to balance digitalized clinical data integrity, ensuring the accessibility of desired information and information integrity to ensure that people's authorities can use the data. The AES encryption model is used initially in the primary region. In this process, the ear print has been integrated, from which seven values are filtered from the ear picture as a function vector. The developed model improved the protection of clinical images by transmitting online images that have to be provided with more security to prevent access by third parties.

Jain et al. [20] provided a safe transfer of the patient's medical information inside the medical cover image using a decision tree to conceal details. Breadth-first searching (BFS) was implemented at the sender end, in steganography, for mapping hidden cipher blocks to carrier images for data insertion. The RSA decryption algorithm was applied at the received end to extract the patient's confidential medical information. A single approved recipient could therefore understand the plain text. This technique yielded excellent results, but was not ideal for large and exponentially increasing search spaces.

Authors [30] suggested a stable method for colour image steganography using grey-level modification and multi-level encryption (MLE). The secret key and secret data were encrypted using the MLE algorithm before mapping it to the cover images' grey level. A transposing function was then added to the cover image before the data was hidden.

Zaw and Phyo et al. [32] used both cryptographic and steganographic topographies to add security features. The Blowfish encryption algorithm was used to enforce encryption. The superiority of the blowfish encryption algorithm over single encryption was represented experimentally. This method was straightforward and dealt with databases on a small scale.

Sreekutty and Baiju et al. [57] suggested a verification system for medical data integrity to introduce medical image transformation security. It works in two stages: (a) protection; and (b) verification. The message is embedded within the image using the 2-stage Haar DWT frequency in the HH band during the protection process. On the other hand, the extraction algorithm was used in the verification stage to extract the secret message and check the message's integrity.

Bashir et al. [10] described a new image encryption technique based on integrating shifted image blocks and basic AES, where the shifted algorithm technique is used to divide the image into blocks. In each block, a set of pixels will be available, and the blocks are used to perform a "swapping" technique so that the content of the data will not be the same as the original image. After being shuffled, the image will be processed using the AES algorithm for encryption. By running numerous simulations and displaying histograms, the test demonstrated the proposed algorithm's effectiveness. The algorithm worked well but was not able to manage the exponential growth in the search space.

Khalil et al. [22] suggested a method for studying image degradation from manipulating frequency components in medical images. The plaintext was encrypted using RSA-based ciphers (i.e. RC4) before being inserted. The Discrete Fourier Transform (DFT) was applied to convert the cover image into the frequency domain by decomposing it into its sinusoidal (sine and cosine) fundamental components in different frequencies. The results show that the image's quality is significantly diminished when the data to be embedded close to the low-frequency bands, and the effect decreases in the upper-frequency bands.

Li, L. et al. [26] suggested a secret image sharing scheme for embedding secret image shares consistent with the IoT-Cloud system. The proposed system consists of two modules; a module for generating shadow images to generate secret shares based on Shamir's polynomial,

and the main formulation module for incorporating secret image shares into the cover image based on a 24-ary notational system.

Sajjad, M. et al. [47] introduced an assisted domain-specific mobile-cloud system to outsource medical stego-images for selective encryption to the cloud. The visual saliency detection model was used to detect the region of interest (ROI) from the transmitted image. The directed-edge steganography method was used to embed the detected ROI into the cover image and create the stego image sent to the cloud for selective encryption.

Vipula et al. [62] combined steganography with the AES crypto-algorithm to conceal confidential data inside the multimedia cover files. Saleh et al. [49] used the modified AES algorithm to encrypt the hidden message that was then processed into the cover image for hiding. However, recently, Duluta et al. [12] have found that such classical encryption-based models have numerous limitations that can restrict their suitability for the era of cloud computing.

Panchal et al. [37] applied steganographic cryptosystems for efficient data communication. Authors initially performed encryption by applying the encryption key combined with Chirikov mapping for image encryption, which transformed the input image into a cipher image. Authors applied steganography in the subsequent process in order to mask the cipher image inside the cover image.

Leung et al. [25] recommended unequal security encoding by implementing several encryption methods to encrypt various media sections of different significance. Ahmed et al. [4] developed a model based on a user interface in which the sender could pick the appropriate cover and secret message that was processed using ECC-based encryption, followed by LSB embedding. The data was processed through various methods to arrive at the same goal. To achieve better performance, Hajduk et al. [17] suggested image steganography where the hidden message was encrypted and inserted within the cover image data using QR codes (Quick Response Codes).

Mukhedkar et al. [34] also applied various ciphers such as DES, 3DES, AES, and blowfish encryption algorithms to encrypt the hidden data before embedding into a cover image for efficient and stable multimedia transmission. Unlike traditional cryptosystems, McEliece's cryptosystem was used by Alam et al. [5] to encrypt or decrypt data to improve data protection across wireless networks. Depicting limitations of the classical cryptosystems, Kumar et al. [23] formulated an asymmetric key cryptography algorithm for secure colour 3D data communication. Because the better multimedia data analysis technique such as wavelet analysis can enhance the confidential data's imperceptibility over an uncertain channel, Gupta et al. [16] recommended using Discrete Wavelet Transform (DWT). Authors applied DWT to split input image into four sub-bands, followed by data hiding within the splits. After hiding the text information, the image was compressed before transmission. The authors [30, 35] implemented a new hidden communication method for data that used RSA and AES combined with steganography.

Liao et al. [27] introduced a steganographic medical JPEG image scheme based on stabilizing inter-block DCT coefficient dependencies. Balakrishnan et al. [43] proposed a unique image crypto method in the transform domain using blended chaotic maps and Haar Integer Wavelet Transform (HIWT). A hybrid encryption algorithm was projected based on deoxyribonucleic acid and several chaotic maps to encrypt DICOM colour images by Divya et al. [45].

Mansour et al. [29] suggested the Discrete Ripplet Transformation technique for data embedding in medical cover images to ensure seamless communication over an unsecured network. Usman et al. [60] applied Swapped Huffman tree encoding to provide multiple

encryptions of medical data. Hashim et al. [18] proposed a new Bit Invert System (BIS) based steganography scheme using three random control parameters to secure medical data. Nithya et al. [11] developed an integrated security framework using DNA coding methods and image encryption to provide enhanced security. Harnal et al. [54] have proposed a dynamic cryptography algorithm based on end-to-end cryptography (E2EE) to maintain integrity and confidentiality in the environment of multimedia cloud computing.

Stoyanov et al. [58], using a nuclear spin generator method, proposed a medical image stego hiding technique and discussed the results based on histogram analysis and peak signal-to-noise ratio. A robust, quasi-quantum walk-based image steganography mechanism has been introduced by Baseem et al. [1] to support secure transmission on the cloud-based E-healthcare platform. Madhusudhan et al. [28] created a stable multimedia transmission mechanism involving binary bits and the Arnold map.

Emy et al. [50] invented a stable colour image transmission system using the compression-encryption model and dynamic key generator, and a highly efficient symmetric key distribution. Pandey et al. [38] have developed a secure medical data transfer framework based on a bit mask driven genetic algorithm.

Rajesh Kumar et al. [42] suggested a hidden image communication scheme that uses visual cryptography and tetrolological tiling patterns. The original image is first broken up into 4×4 sub-blocks. The alternative rows and columns of sub-blocks are grouped into tetrolet and non-tetrolet blocks. The proposed scheme encodes the original image's tetrolet blocks into meaningful secret shares using the tetrominoes patterns. The non-tetrolet blocks are entirely replaced by zero. Finally, a new shadow image is obtained at regular intervals with different tetrolet patterns. A dynamic virtual cluster cloud encryption using the hybrid steganographic image authentication algorithm was suggested by Venkataraman et al. [61]. With the hybrid blowfish and genetic operator, this model performs expeditiously and ensures greater security. The proposed model of Puspha et al. [8] was presented by combining the 2D DWT method with the hybridization of Blowfish and Two fish encryption algorithms.

In image encryption and cryptography theory, literature shows that only a few have used metaheuristic algorithms. Bio-inspired algorithms and evolutionary algorithms have been successfully implemented in recent research to solve secure multimedia (medical) data transmission. Considering these factors, a Discrete Wavelet Transform, LSB embedding, Adaptive GA-based OPAP, AES and RSA-based hybrid encryption has been built in this research (dual-level biomedical image security). The discussion of the proposed model of steganography is given in the following sections.

3 Proposed model

This paper proposes a security model for healthcare to safeguard the transfer of medical data in cloud environments. Four continuous processes make up the proposed model:

- (1) The secret data is encrypted using a proposed hybrid encryption scheme, combining AES and RSA algorithms.
- (2) The encrypted data is being concealed in a cover image in the RGB channels using either 2D-DWT-1 L or 2D-DWT-2 L and AGA based Optimal Pixel Adjustment Process produces a stego-image.

- (3) Extraction of embedded data
- (4) To recover the original data, the data extracted is decrypted.

3.1 Secret data encryption

There are numerous cloud-assisted application environments in which different data, including multimedia and text, are transmitted under uncertain channel conditions. Some of the typical applications are telemedicine in the healthcare sector, social media, etc. Such applications can even have composite data as the amalgamation of text and image (for example, telemedicine both patients scanning medical reports and allied diagnosis details in text). In such cases, ensuring respective seamless transmission is of utmost significance. Towards this motive, the proposed model can be a viable solution. However, ensuring multi-level security can have augmented strength to alleviate any breach of security or unauthorized data access. Considering it as an impetus, a hybrid encryption model is designed at first. Here, the prime motive behind this is to increase the level of security by applying two different cryptosystems together, which, as a result, can avoid any easy attack on the data.

Consequently, it can achieve a higher level of security. In the proposed model, we have exploited the efficacy of two well-known cryptosystems RSA and AES to design the hybrid encryption scheme. The proposed cryptographic model embodies the strategic implementation of both RSA and AES, which has been used to encrypt input text data that is first converted into ciphertext embedded within the medical image.

The cryptographic model $\mathcal{C} = \{F, F^{-1}, C, S, T\}$ encompasses encryption and decryption processes. During the encryption process, at first, the secret text data (it can be the diagnosis details of a patient which is expected to be transmitted along with the medical imaging reports) is split into two distinct parts, T_{odd} and T_{Even} . Splitting the text data does not signify dividing content in two fractional parts, instead once converting entire text into binary form, the overall bit sequence is processed in such way that the odd-sequence value is assigned to T_{odd} , while bits at even place or sequence is allocated to the T_{Even} component. Thus, it converts overall input text data into two data-chunk or components T_{odd} and T_{Even} . We applied AES cryptosystem to encrypt T_{odd} and while RSA was used for T_{Even} encryption. Considering computational efficiency demands, we considered 64-bit RSA, while AES was applied as 256-bit. RSA with low bit-size has often been criticized for having inferior robustness; however, such a hypothesis can be applied merely with RSA as a standalone encryption algorithm. Its implementation with AES-256 can help to achieve a dual goal. First, the amalgamation of AES-RSA as a cryptographic algorithm can avoid easy attack probability (which can be possible with standalone encryption). Second, the consideration of low-bit size can avoid unwanted computation that eventually will make it robust to serve real-time applications. Additionally, AES-256 is six times faster and more efficient than classical triple-DES. Therefore, the inclusion of AES as a cryptographic method seems viable towards an influential encryption environment. On the other hand, the combination of RSA with low-bit size can help to make overall encryption more robust to avoid any attack. In other words, the strategic amalgamation of AES-256 and RSA-64 can confuse the attacker(s) to get real and exact information of the data being processed or communicated.

In the proposed encryption model, AES-256 has 14 rounds of computation, while 64-bit RSA was applied as single round itself, as it does not employ round-computation for confusion creation (to avoid side-channel attack). Noticeably, AES applies an encryption key or the round key s to encrypt the text data component T_{odd} , while RSA being public-key

cryptography applies a secret public key m to encrypt the data T_{Even} . We used a private key x to perform decryption of the RSA encrypted data at the receiver. On the contrary, we performed standard decryption method for AES encrypted data. To be noted, AES decryption is the reverse of encryption, which is performed by executing inverse round transformations to retrieve original text data (from the encrypted data). Here, inverse round transformation method applies four essential functions, $AddRoundKey$, $InvMixColumns$, $InvShiftRows$ and $InvSubBytes$, sequentially. Thus, the overall process is mathematically modelled as follows:

$$C = \{E_{AES}, E_{RSA}, T_{odd}, T_{Even}, \hat{T}_{odd}, \hat{T}_{Even}, s, m, x\} \tag{1}$$

$$\hat{T}_{odd} = \{E_{AES}(T_{odd}, s)\} \tag{2}$$

$$\hat{T}_{Even} = \{E_{RSA}(T_{Even}, m)\} \tag{3}$$

Hybrid Encryption Algorithm for Secret Data Encryption is given as follows:

Input: Secret Text Input Data (S_{Text})

Output: Cipher Text, Keys

Initiate the process

Step-1 Split the input text S_{Text} into two components S_{Text_odd} and S_{Text_Even}

Step-2 Generate AES keys[57]

Step-3 Encrypt S_{Text_odd} using AES-256 bit key size

$$Enc_{S_{Text_odd}} = AES - 256(S_{Text_odd}, s)$$

Step-4 Generate RSA keys (Public key m and private key x)

Step-5 Encrypt S_{Text_Even} using 64 bit-RSA

$$Enc_{S_{Text_Even}} = RSA - 64(S_{Text_Even}, m)$$

Step-6 Accumulate the encrypted cipher data $Cipher_{F_Total}$ by using both $Enc_{S_{Text_odd}}$ and $Enc_{S_{Text_Even}}$

Step-7 $Enc_{Key} = AES(x, s)$ # x -round key, # s -secret key

Step-8 Generate $Cipher_{Tx} = Concatenate(Cipher_{F_Total}, Enc_{Key})$

Step-9 Return $Cipher_{Tx}$ and s

End

Once the text data has been encrypted, it has been processed for AGA-OPAP assisted LSB embedding.

3.2 Embedding procedure and AGA based OPAP

To embed the critical information within the medical image to be transmitted over cloud infrastructure, it is essential to decompose the input cover image and embed the cipher data optimally, while ensuring minimum entropy, histogram variations, or PSNR reductions. In this process, DWT with HAAR mother wavelet is applied. The model starts by separating each

colour channel's intensity (Red, Green and Blue). In each colour channel, the process of decomposition is then carried out. The method is split into two elements, namely compression and embedding. This approach will ensure the security of the image data and enable rapid encryption and decryption processes. It can also decrease the potency of attacks from frequency analysis, make it longer for brute force attacks, and minimize the plaintext redundancy so that cryptanalytic attacks can be thwarted. The 2D-DWT-2 L is formulated as a sequential transformation process with a low pass and high pass filters towards the image's row (blocks). The key reason for considering 2D-DWT-2 L coefficients is that it can significantly provide a significant local feature set for text-embedding without impacting image quality.

Moreover, it can provide a more depth (feature) space for embedding. A cumulative solution with the proposed encryption can help strengthen attack-resiliency and confusion. Performing embedding with a single layer can cause higher-visibility perceptibility and impact image quality post-embedding. On the other hand, embedding with higher-level coefficient can be more effective at the cost of increased computation, which cannot be suitable for contemporary real-time application demands.

For optimal use of high and low pass filters, a pragmatic transformation is necessary. In Fig.1, the process followed in steganography using DWT is shown. We can see that Fig. 1 highlights the method of the elemental decomposition of the image in $C_j(n \times m)$ dimensions which will be applied to the RGB colour channels. Further, the image of each colour channels is divided into four groups of frequency bands, which are stated as high-high (HH), a high-low (HL), a low-high (LH), and a low-low (LL) frequency bands as shown in Fig. 2. The proposed model is designed to support visually imperceptible steganography to ensure maximum possible visual-imperceptibility that ensures seamless communication and assists quality-data transmission, which is a must for cloud communication.

To achieve it, the proposed model implements the steganographic scheme $\hat{S} = \{ \{ F\eta, F\eta^{-1}, C, S, T \} \}$ comprises of Least Significant Bit (LSB) embedding, AGA-OPAP assisted embedding optimization and extraction processes. The embedding process takes a cover (medical) image C and a secret text message $Cipher_{Tx} T$ as input and generates a

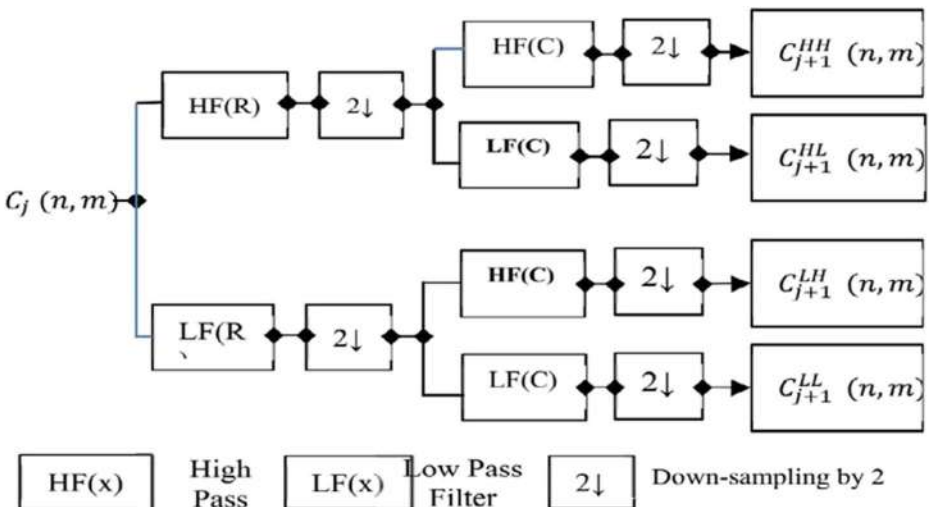


Fig. 1 2D-DWT-2 L decomposition process

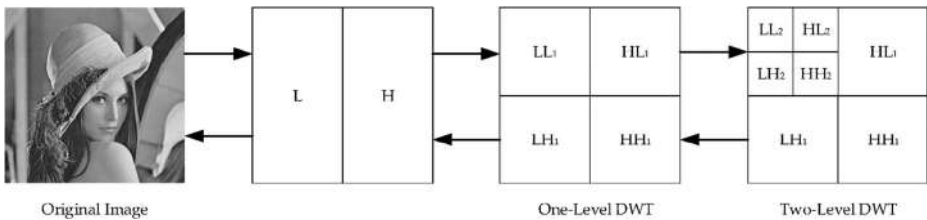


Fig. 2 DWT-1 L decomposition & DWT-2 L decomposition

stego-image S . While the extraction process inversely extracts the embedded message. Unlike classical efforts, where authors have to embed text or cipher data arbitrarily or LSB without any optimization measure, an AGA-based optimal pixel adjustment process is implemented in the proposed system. It ensures to retain maximum possible imperceptibility, quality preserve and seamless transmission even under cloud attack conditions such as RS-Analysis or Steganalysis. At first, the input medical image is processed using HAAR-DWT and split into multiple 8×8 blocks. Considering works of literature and allied inferences towards LSB embedding process, this approach intends to embed ciphertext in each block.

To perform embedding, at first ciphertext is transformed into an ASCII format, which is then split into S_{Text_odd} and S_{Text_Even} . The odd values S_{Text_odd} are concealed in vertical coefficients, as stated by LH2 in each of the RGB channel [50]. The even values are concealed in diagonal coefficients specified by high-level coefficients HH2 in each RGB channel [50]. The algorithm applied to perform embedding is given as follows:

<p>Input: Cover Image</p> <p>Output: Stego-Image</p>
--

Step-1 Start the process

Step-2 Convert the secret message (say, diagnosis details) in ASCII code S_{Text_ASCII}

Step-3 Scan the image for row by row to each of red, green, and blue channels

Step-4 Assess the 2D wavelet coefficients for the 1L using HAAR filter $(LL1)$, $(HL1)$, $(LH1)$, and $(HH1)$ for the RGB channels

Step-5 Assess the 2D wavelet coefficients for the 2L level using HAAR wavelet filter $(LL2)$, $(HL2)$, $(LH2)$, and $(HH2)$ for the RGB channels

Step-6 Begin a Loop

Embed S_{Text_ASCII} using LSB embedding concept.

Process AGA-OPAP for adaptive pixel optimization and RS-Attack resilient LSB embedding.

end loop

Return Stego-Image

End

To retain maximum medical image quality as well as security against online attacks such as RS-Analysis or steganalysis an AGA intends to fit S_{Text_ASCII} in such manner that it does not lead to any substantial entropy or visual trait portentous presence of confidential data.

In the last few years, numerous attacker modules have been developed to target, detect and attack data over uncertain communication channels, such as cloud network. Amongst the significant attacks, RS-Analysis also called steganalysis has surfaced as the dominant attacker model intended to retrieve stego-information from the multimedia data communication. Before discussing the proposed AGA-OPAP based LSB embedding model, a snippet of RS Analysis or Steganalysis model is given as follows:

AGA has been applied to enhance image quality, embedding capacity, and statistical factors such as regular and singular coefficient values in each block. This approach can ensure maximum possible embedding while retaining optimal data quality and visual imperceptibility. Consequently, it can help avoid those attacks that use visual changes or statistical changes to detect hidden information or secret information within cover image during transmission. Considering RS-Analysis, also called steganalysis attack condition which employs statistical features to detect hidden information in multimedia data under transmission; the proposed model takes account of RS parameters and PSNR sensitive LSB embedding to ensure optimal data security. The detailed discussion of the proposed embedding model is given as follows:

A. RS analysis (Steganalysis) There are three distinct kinds of block flipping; Positive flipping (F_1), Negative flipping (F_{-1}) and Null flipping (F_0). F_1 signifies the transformation association between the $2i$ and $2i + 1$ pixels (say, 0–1, 2–3, ..., 254–255), equivalent to the LSB coefficient. Similarly, the transformation association in between $2i$ and $2i - 1$ pixels (say, -1, -1-0, 1–2...255–256) signifies the negative flipping F_{-1} . Thus, the association between positive and the negative flipping follows (4).

$$F_{-1} = F_1(x + 1) - 1 \quad (4)$$

The null flipping, which stated the identity permutation follows the following condition (5).

$$F_0(x) = x \quad (5)$$

$$F(G) = (F_{M(1)}(x_1), F_{M(2)}(x_2), \dots, F_{M(n)}(x_n)) \quad (6)$$

These parameters (i.e., F_1 , F_{-1} and F_0) are often called as the flipping functions. Employing these flipping functions on each pixel of the input image block the flipped group ($F(G)$) is obtained. Mathematically,

Here, we define a parameter called flipping mask M . Where $M = M(1), M(2), \dots, M(n)$, and $M(i)$ states for 1, 0 and -1.

The group G would remain constant only when $f(F(G)) > f(G)$. Similarly, G is singular when $f(F(G)) < f(G)$. To perform the RS analysis, the following mechanism is taken into consideration. At first, the input image is split into multiple non-overlapping sections or blocks where each block is re-arranged to constitute a vector G , where $G = (x_1, x_2, \dots, x_n)$ is ordered in specific random (say, Zigzag) manner. The correlation amongst the pixel is obtained using a discrimination function, defined in (7).

$$f(x_1, x_2, \dots, x_n) = \sum_{i=1}^{n-1} |x_i - x_{i+1}| \quad (7)$$

In (7), the variable x states the pixel's value, while the total number of pixels is given by n . Here, the resulting value of f signifies the spatial correlation between the neighbouring pixels.

The small value of f states the strong correlation between the adjacent pixels. Once obtaining the complete value of $f(G)$, the non-negative flipping is applied (i.e., $M(1), M(2), \dots, M(n)$) either 0 or 1. On the contrary, for non-positive flipping, we apply 0 or -1 for each input image block. Now, processing flipping over each block, estimate $f(F(G))$ for each block and thus the relative count of regular or consistent blocks after positive flipping is obtained as R_m . Similarly, the relative number of singular blocks is obtained as S_m . Similarly, for negative flipping, the regular and singular blocks are obtained as R_{-m} and S_{-m} . The total number of above-stated blocks in the raw images after performing flipping follows the following associations.

$$R_m \approx R_{-m}, S_m \approx S_{-m} \text{ and } R_m > S_m, R_{-m} > S_{-m} \tag{8}$$

The difference between R_m and R_{-m} increases as per the size of embedding message. Similarly, the difference values of S_m and S_{-m} too increases with increase in embedding text. Such facts help attackers on a cloud platform or environment detect hidden information that can significantly lose data privacy. Considering it as motivation, the focus is made on developing an embedding model where the above-stated parameters (i.e., the difference between the values of R_m and R_{-m} and S_m and S_{-m}) could be reduced while ensuring higher embedding capacity. This, as a solution, can accomplish attack-resilient secure cloud communication model. To achieve it, an AGA algorithm has been developed that intends to adjust pixels optimally $R_m \approx S_m, R_{-m} \approx S_{-m}$. The detailed discussion of the proposed AGA based OPAP is given in the subsequent section.

B. AGA based OPAP To avoid any stego-information retrieval or data attack, the focus is on achieving the condition given in (8) by performing OPAP. Here, we perform pixel adjustment to achieve a standard or natural condition defined as $R_m \approx S_m, R_{-m} \approx S_{-m}$. Since the variations in the bits in the higher place might violate or reduce the image quality of the stego-image, merely the 2nd and 3rd LSBs are modified. For illustration, let B as given in (9), be the original value of the input image (block). Now, in case of the strategic modification is made merely in LSB place (only 2nd LSB plane), the variation or the changes in between the original image block and the modified image block can be considered as a matrix called Adjustment Matrix (AM), given as A_1 and A_2 . Thus, the modified image blocks are $B'_1 = B + A_1$ and $B'_2 = B + A_2$. For illustration, let B be the original image block while $f(B) = 99$, while $f_-(B) = 120$, where f_- states the non-positive flipping. Now for the modified image block $B'_1, f_-(B'_1) = 90$, only when F is non-positive flipping. Similarly, for $B'_2, f_-(B'_2) = 150$.

$$B = \begin{bmatrix} 107 & 109 & 107 & 105 & 104 & 102 & 102 & 104 \\ 107 & 106 & 105 & 104 & 105 & 103 & 105 & 102 \\ 107 & 105 & 107 & 105 & 102 & 103 & 104 & 103 \\ 107 & 107 & 105 & 106 & 104 & 103 & 103 & 104 \\ 107 & 109 & 107 & 104 & 104 & 102 & 103 & 102 \\ 104 & 107 & 106 & 103 & 103 & 104 & 102 & 100 \\ 110 & 109 & 109 & 105 & 105 & 105 & 105 & 102 \\ 109 & 109 & 109 & 106 & 104 & 105 & 105 & 104 \end{bmatrix} \tag{9}$$

$$A_1 = \begin{bmatrix} 0 & 2 & 0 & 2 & 0 & 2 & 0 & 0 \\ 0 & 2 & 0 & 2 & 0 & 2 & 0 & 0 \\ 2 & 2 & 0 & 2 & 2 & 2 & 2 & 2 \\ 0 & 0 & 2 & 2 & 0 & 0 & 2 & 2 \\ 0 & 2 & 0 & 0 & 0 & 2 & 0 & 2 \\ 2 & 2 & 0 & 0 & 2 & 0 & 2 & 0 \\ 0 & 2 & 2 & 2 & 2 & 2 & 2 & 2 \\ 2 & 0 & 2 & 2 & 0 & 0 & 0 & 0 \end{bmatrix} \quad (10)$$

$$A_2 = \begin{bmatrix} 2 & 2 & 0 & 0 & 0 & 0 & 2 & 2 \\ 0 & 2 & 0 & 2 & 2 & 0 & 0 & 0 \\ 2 & 0 & 2 & 0 & 2 & 2 & 2 & 2 \\ 0 & 0 & 2 & 2 & 2 & 0 & 2 & 0 \\ 2 & 0 & 0 & 0 & 2 & 0 & 0 & 0 \\ 2 & 0 & 0 & 2 & 2 & 2 & 2 & 2 \\ 2 & 0 & 0 & 2 & 0 & 2 & 0 & 2 \\ 2 & 2 & 0 & 2 & 2 & 0 & 0 & 2 \end{bmatrix} \quad (11)$$

Summarily, the kind of block (i.e., regular or singular) can be modified by changing or making a suitable adjustment. In such cases, adjusting the pixels optimally, RS-Analysis attack of steganalysis attack can be avoided on the cloud environment. An Adaptive Genetic Algorithm (AGA) is applied to achieve it, which obtains the Optimal Adjustment Matrix (OAM) to ensure minimum disparity amongst the values of regular and singular image blocks. A snippet of the AGA based OPAP method and resulting OAM estimation is discussed in the subsequent section.

GA is a nature-based EC model, which employs Darwin's principle of survival to obtain the optimal or sub-optimal solution after a defined number of generations. Functionally, it applies the concept of human evolution to obtain an optimal solution by transforming an optimization of search problem into the phenomenon of chromosome evolution. Processing the evolution concept, once it achieves an optimal or the best solution after iterating a predefined number of generations (or, stopping criteria), the optimal solution obtained is presented as the final solution of that problem. Functionally, GA employs the processes named Population Generation, Crossover and Mutation. In practice, the adaptive values influence the copy operation, and an individual with significantly high fitness value is considered for the next generation. A candidate solution's fitness value signifies its maximum likelihood of becoming selected for breeding in the next generation. To reduce computational overheads caused due to increase search space, the mutation process is applied that drops the individual with minimum fitness value, and such individuals are not carried forward for crossover in the next generation. Once embedding the secret data within the cover image using LSB embedding, we execute AGA-OPAP. A snippet of the applied AGA-OPAP is given as follows:

In the proposed LSB embedding method, the stego-image is split into 8×8 blocks, where each block is categorized and labelled by applying the following mechanisms.

- Step-1: Let the image block be B , then for B implement the non-positive flipping F_- as well as non-negative flipping F_+ .
- Step-2: Generate the flipping mask M_+ and M_- , randomly and obtain the results B'_+ and B'_- .
- Step-3: With the obtained value of B'_+ and B'_- , estimate the values of $f(B'_+)$, $f(B'_-)$ and $f(B)$.
- Step-4: Process the steps 1, 2 and 3 iteratively for 1000 number of generations and define four distinct variables to classify the blocks by comparing $f(B'_+)$, $f(B'_-)$ and $f(B)$.
- P_{+R} , it states the number of occurrences when the block remains regular under the non-negative flipping,
- P_{+S} , it states the number of occurrences when the block remains singular under the non-negative flipping,
- P_{-R} , it states the number of occurrences when the block remains regular under the non-positive flipping.
- P_{-S} , it states the number of occurrences when the block remains singular under the non-positive flipping.
- Step-5: Perform P_{+R} to P_{+S} and P_{-R} to P_{-S} and perform labelling of the image blocks as per the following conditions:

$R+$, if $\frac{P_{+R}}{P_{+S}} > 1.8$.

$S+$, if $\frac{P_{+S}}{P_{+R}} > 1.8$

$R-$, if $\frac{P_{-R}}{P_{-S}} > 1.8$

$S-$, if $\frac{P_{-S}}{P_{-R}} > 1.8$

- Step-6: Classify blocks into four distinct groups, $R + R-$, $R + S-$, $S + R-$, $S + S-$. Ignore the blocks, not a part of above-stated types.
- Step-7: Perform the comparison of the original input image, the magnitude of $R + R-$ and $S + R-$ blocks, which often shows increased in stego-images.

Such increase in the above-stated parameter can be detected using RS Analysis, which can be used as the intrusion tool to attack that specific multimedia data to get unauthorized access of the stego-image and hidden information. Considering the above-stated fact and motive to alleviate the distinguishable or perceptible disparity between the values of $+-$ and $+-$ blocks, this research applies the AGA algorithms to decrease the value of $R-$ blocks. The implementation of AGA-based OPAP comprises three essential functions: initialization (population initialization), crossover, and mutation. The procedures involved in AGA-OPAP optimization and allied pixel adjustment is detailed as follows:

4 Population initialization

The initial pixel, or the first pixel, chose three adjacent pixels in each image block as the initial chromosome (Fig. 3).

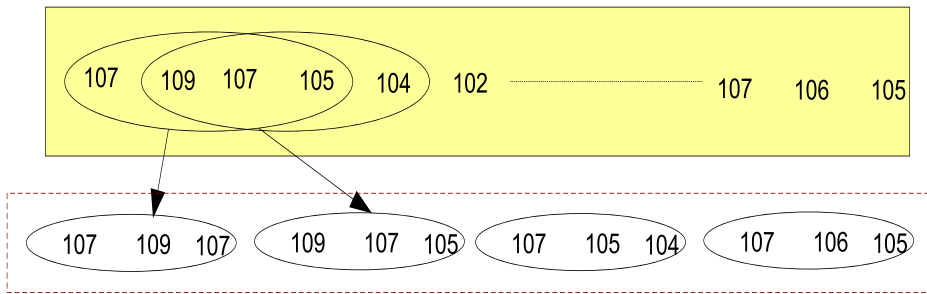


Fig. 3 Selection of the chromosomes

5 Reproduction and mutation

Perform flipping of the second least bits in the chromosomes arbitrarily and generate the (second generation) chromosomes C_i .

6 Selection

Estimate the fitness value of each chromosome and select the best chromosome using (12).

$$Fitness = \alpha(e_1 + e_2) + PSNR \quad (12)$$

In (12), the variable e_1 states the likelihood of $f(F_-(C_i)) < f(C_i)$. Similarly, e_2 signifies the likelihood of $f(F_+(C_i)) > f(C_i)$. The variable PSNR signifies the Peak Signal to Noise Ratio of the participating chromosome, while α presents a weight parameter which has been obtained empirically. Mathematically, PSNR has been obtained using (13).

$$PSNR = 10 \log_{10} \frac{M \times N \times 255^2}{\sum_{i,j} (y_{i,j} - x_{i,j})^2} \quad (13)$$

In (13), M and N signify image dimension while x and y state the image intensity before and after embedding. Here, α states a weight parameter which controls the visual quality of the input multimedia data and secrecy of the secret text. For a specific value of α , higher the values of e_1 and e_2 , we hypothesize to achieve higher data security. Hence, in the proposed model, optimizing (specifically maximizing) the value of (13) (say, fitness value) has been considered as the fitness function. In our proposed method, we ensure maintaining e_1 and e_2 higher than a threshold, which is experimentally decided. We have applied the threshold as 0.8.

1. **Estimate** P_{-R} and P_{-S} of the neighbouring image block and check whether $P_{-S} > P_{-R}$. If so, the block is considered as successfully adjusted.

2. **Crossover** In the crossover process, shift the chromosome by one pixel and reinitiate step-2. Once performing crossover twice, stop the cycle.

This overall process is called OPAP, making hybrid cryptography and steganography more resilient to attacks such as RS Analysis or steganalysis, achieving optimal security over the cloud platform. Now, once all image blocks are successfully adjusted, estimate the value of R_m , R_{-m} , S_m and S_{-m} of the image and in case the disparity of R_m and R_{-m} (and, S_m and S_{-m}) is more than 5%, perform adjustment of the next or the sub-sequent image blocks. In the proposed model, each block is labelled before initiating OPAP, and thus, we reduce computational overheads significantly. Furthermore, AGA's use reduces the exhaustive search operation and achieves computational efficiency, making it suitable for secure medical data transmission over cloud infrastructure.

6.1 Secret data extraction

Once embedding the data inside the cover image and obtaining the stego image, it is transmitted over cloud communication channels. Receiving the data at the receiver end, we have obtained confidential data and original cover image by performing extraction using the 2D-DWT-2 L method.

Figure 4 illustrates the procedure of extracting encrypted text from the images. This process will begin after the successful completion of the decomposition of images using DWT-2 L. The extraction algorithm is described below

Input: Stego Image

Output: Secret message, Cover image.

Initiate the process

Step-1 Scan the stego image row-by-row for the red, blue and green channels

Step-2 Assess the 2D wavelet coefficients for the 1-level of HAAR wavelet filter for the RGB channels

Step-3 Assess the 2D wavelet coefficients for the 2-level of HAAR wavelet filter for the RGB channels

Step-4 Formulate message “ ”

Step-5 Start a loop

Perform extraction of the text embedded in vertical coefficients and assign odd values = $LH2(x, y)$ in the RGB channels

Perform extraction of the text embedded in horizontal coefficients and assign even values = $HH2(x, y)$ in the RGB channels

Step-6 Close loop

Step-7 Restructure message $msg = append(odd, even)$

Step-8 Perform IDWT to generate the original cover image

Step-9 Return text message as retrieved secret message and cover image.

End

Once extracting the text data from the images, it is reconstructed employing IDWT technique for 2nd level followed by 1st level. Figure 4 elucidates the DWT synthesis process.

Considering the need to decrypt the secret text data from the cover image, similar to the encryption phase, the hybrid scheme applies AES and RSA algorithms to decrypt the receiver's confidential data. Receiving the stego image at the receiver unit, we decrypt the

text using a private key to obtain the original secret message transmitted. The decryption algorithm used to retrieve the original secret data is given as follows:

Input: Ciphertext received $Cipher_{Tx}$, key

Output: Secret message.

Initiate the process

Step-1 Split the received ciphertext into two components; $HashedText$ and $HashedKey$

Step-2 $Enc_{msg} = decompress(HashedText)$

Step-3 $Enc_{Key} = decompress(HashedKey)$

Step-4 $x = decrypt_AES-256(Enc_{Key}, s)$

Step-5 $Enc_{S_{Text_odd}} = split(Cipher_{F_{Total}}, S_{Text_odd})$

Step-6 $Enc_{S_{Text_Even}} = split(Cipher_{F_{Total}}, S_{Text_Even})$

Step-7 $S_{Text_odd} = decrypt_AES - 256(Enc_{S_{Text_odd}}, s)$

Step-8 $S_{Text_Even} = decrypt_RSA(Enc_{S_{Text_Even}}, x)$

Define plain text message

Step-9 Initiate loop for all characters

If odd

Insert odd characters into odd indices within the plain text message

else

Insert even characters into even indices within the plain text message.

End loop

Step-10 Return original secret text and image transmitted.

End

By implementing the above-stated approach, a robust and computationally efficient model strengthened by employing hybrid encryption enhancement and attack resilient (for example, steganalysis or RS-Attack), Visually Imperceptible model is developed. The proposed system can secure medical data transmission over different environments while ensuring optimal performance. The detailed discussion of the simulation results and its inferences is given in the subsequent section.

7 Results and discussion

Considering the exponential increase in cloud-based secure medical data communication, this research focused on developing a hybrid encryption strategy combining cryptography and steganography that provide data privacy. The overall proposed model is developed using MATLAB 2018a tool, which has been simulated with the computer specifications of 2.27 GHz Intel (R) Core (TM), 3rd generation processor (I3 CPU), 8 GB RAM and

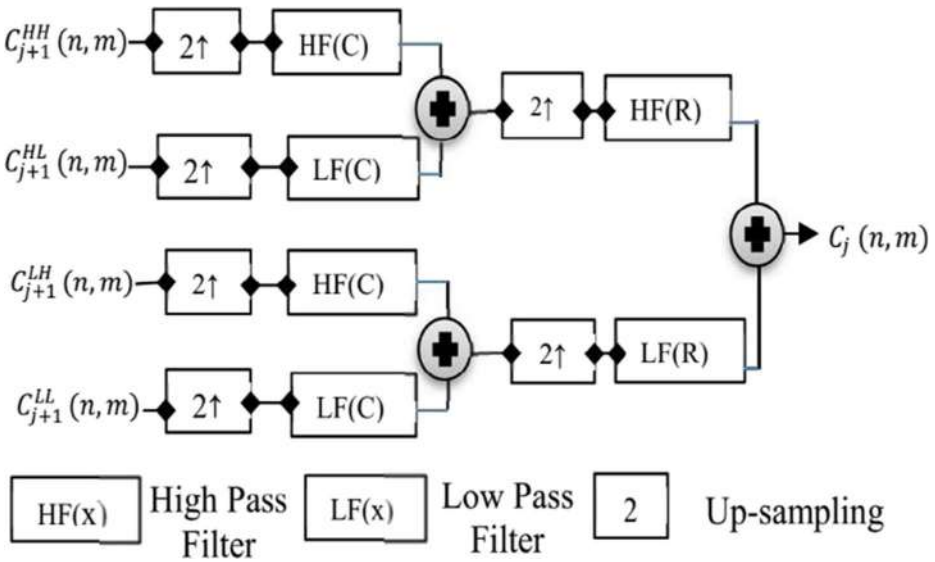


Fig. 4 Extracting encrypted text from images showing the procedure of synthesis of DWT-2 L.

Windows-7 operating system. Multiple images as the cover image and secret message of varied sizes are employed to assess the proposed model’s performance.

The Hybrid encryption and Steganography model can be useful or more efficient when it fulfils the following:

7.1 Histogram analysis

As stated in Table 1, minimizing histogram pattern variations before and after message embedding in the cover image can reduce visual perception or result tracking by attackers. Histogram variations occur due to increased entropy within the cover image due to text embedding, and therefore to retain visual imperceptibility reducing entropy through optimal pixel adjustment is vital. To achieve it, an AGA-OPAP based LSB embedding resulted in minimum histogram variations (Table 2). As depicted in Table 2, the proposed model exhibits negligible or near-zero variation in histogram after message embedding, supporting the visual imperceptibility aspect for secure communication.

To assess the efficacy of the proposed model, in this work we considered standard benchmark images such as Baboon, Lena, Baboon, Sailboat, Peppers, Female [19] [33] (*.jpg) as well as the medical images [56] (DRISHTI-GS dataset in *.png). Here, the prime objective was to assess whether the proposed method can be adequate or suitable for the healthcare application environment. Since in healthcare images retaining image-quality and the inherent feature is of utmost significance, we have applied critical healthcare data of “Diabetic Retinopathy”, where even a single nerve can have important diabetes information. Introduction of additional text (secret) data could cause entropy and hence quality degradation. However, the proposed model intended to optimize such entropy and ensure that stego-image (image after embedding) retains maximum possible image quality and originality. Observing the results, it can be found that the proposed method achieves optimal performance in terms of visual imperceptibility. It can avoid numerous attack scenarios online in the cloud

Table 1 Performance criteria

S.No.	Parameter	Definition
1.	PSNR	To preserve the image quality even after embedding secret text data, PSNR should be higher. The significant reduction in PSNR value can depict certain hidden information that can trigger attacker models to target and attack the transmission data.
2.	Entropy	It signifies the disturbance in the original image. To ensure minimum perceptibility, the model requires maintaining minimum entropy after message embedding. The minimum value of entropy can avoid getting attention from attacker modules.
3.	Embedding Capacity	It signifies how the secret text data can be embedded per unit of the cover image. The model can be superlative or better if it ensures or maintains higher embedding capacity without introducing significant entropy and PSNR reduction (in addition to the regular and singular coefficient changes in RS analysis).
4.	Changes in Regular coefficients ($R_m - R_m$)	It signifies the variation or the difference between the regular coefficient before and after embedding. Higher differences are the indicator for hidden information which invites attackers such as RS attacker or steganalysis attacking modules to target data under the transmission. Lower the differences, higher the imperceptibility and resulting data security.
5.	Changes in Singular coefficients ($S_m - S_m$)	It signifies the variation or the difference between the singular coefficient before and after embedding. Higher differences are the indicator for hidden information which invites attackers such as RS attacker or steganalysis attacking modules to target data under the transmission. Lower the differences, higher the imperceptibility and resulting data security.
7.	Histogram Variations	It signifies the different histogram patterns of the cover image and stego image, before and after the embedding. Lower or negligible histogram graph variations show near-optimal embedding, which supports imperceptibility and hence attack resilience.

environment. To simulate the proposed model for performance verification, random text information such as a snippet of common test sentences such as “My Own Address”, “My Personal Biography” with different sizes (in notepad, *.txt) was applied. Due to space constraints and inferior significance of text (embedding data) details, we have not mentioned it in this manuscript. Dataset images (Table 2) are the cover images considered for the simulation and performance assessment.

7.2 PSNR assessment

It is calculated to measure the quality of images created by Peak Signal to Noise Ratio (PSNR) compression. If it produces a high PSNR value, the compression technique is considered significant, which means that the error is deficient and the reconstructed error is minimal. The image seems to be very similar to the original image. When the PSNR value is between 30 and 50 dB, lossy image quality is considered acceptable. The quality of the image is considered

Table 2 Histogram Pattern Analysis


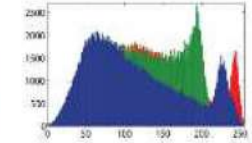
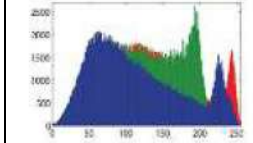

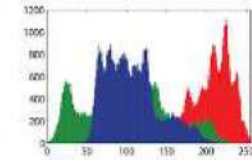
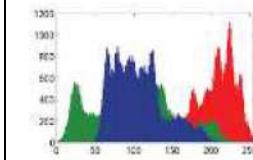

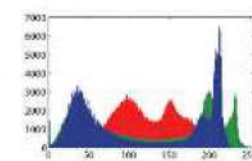
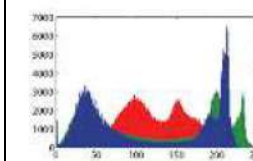

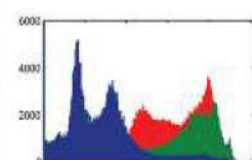
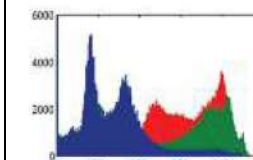

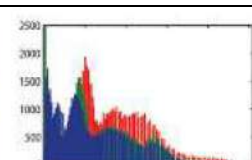
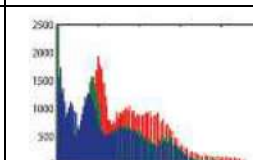

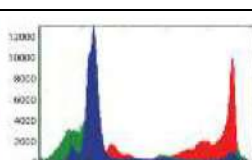
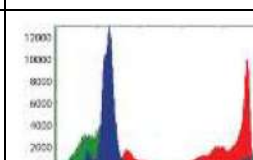

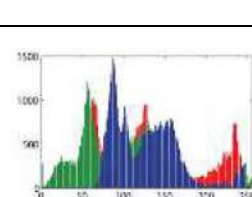
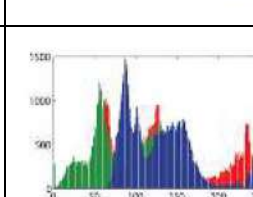
Name	Dataset	Histogram of the cover image	
		Before	Post Embedding and OPAP
Baboon			
Lena			
Sailboat			
Peppers			
Retina1			
Retina2			
Female			

Table 3 PSNR Performance (for 250 bytes of text data)

Dataset	PSNR (dB)		
	Before	Post Embedding	Post Optimization
Baboon	35.0600	31.9200	34.0053
Lena	37.4873	35.8762	36.5852
Sailboat	33.1850	30.7611	31.2970
Peppers	37.2667	33.0110	34.1010
Retina1	43.3450	41.2101	42.8701
Retina2	46.8071	44.0629	45.6255
Female	35.6216	33.3414	34.3060

ideal if the PSNR value is above 40 dB. The compression technique is highly not appropriate if the PSNR value is below 20 dB.

Table 3 presents the PSNR performance of the proposed model for 250 bytes in text (secret data) embedding. Observing the result in Table 3, where the PSNR has been obtained for the text embedding size of 250 bits, it can be found that after embedding the text or secret data, the PSNR decreases; however, the contribution goes to the proposed AGA-OPAP assisted LSB embedding method, which improves the message embedding and even optimizes the PSNR. Interestingly, observing PSNR performance, the proposed model either achieves near original PSNR or even improves the image quality, which results in improved PSNR value (post-embedding and OPAP optimization). The mathematical model for PSNR estimation was applied in (13) for the image processed after 2D-DWT-2 L and post-AGA-OPAP optimization. The results obtained (Table 4) reveals that the proposed AGA-OPAP assisted LSB

Table 4 PSNR performance over different sizes of the secret text data

Dataset	Data Size (bytes)	PSNR (dB)		
		Before	Post Embedding	Post Optimization
Baboon	250	35.0600	31.9200	34.0053
	500	38.8630	36.2003	37.8942
	1000	36.7491	35.8990	36.1804
Lena	250	37.4873	35.8762	36.5852
	500	33.1041	32.0072	32.9183
	1000	35.4901	34.0700	35.1003
Sailboat	250	33.1850	30.7611	31.2970
	500	36.8931	35.4180	35.9814
	1000	36.2443	35.0134	35.9993
Peppers	250	37.2667	33.0110	34.1010
	500	32.2442	31.6320	32.1248
	1000	38.0012	37.4021	37.8732
Retina1	250	43.3450	41.2101	42.8701
	500	49.1251	47.3427	48.6391
	1000	48.8422	46.1120	48.1297
Retina2	250	46.8071	44.0629	45.6255
	500	46.0367	43.6730	44.9834
	1000	44.5259	42.1147	43.5895
Female	250	35.6216	33.3414	34.3060
	500	38.8736	36.5290	37.9201
	1000	37.9910	36.3019	37.1003

embedding method is of utmost significance towards retaining and optimizing image quality for quality-centric communication over the cloud environment.

7.3 Entropy analysis

As an image security operation, the cipher generation is performed, which will increase the image input disturbances. Consequently, this can lead to a surge in image entropy that degrades the quality of the image and broadens the horizon for intruders to target specific data. On the other hand, to make it difficult for the attacker to differentiate the encrypted data and the original image information, encryption imposes additional information on the image. In such instances, it is vital for preserving the optimum entropy of the data being transmitted. With this strategy, the encrypted image data's entropy is quantified with Eq. (14).

$$ENT(I) = - \sum_{i=1}^{2^8} P(I_i) \log_b P(I_i) \quad (14)$$

In (14), $ENT(I)$ states the entropy of an image, where I signify the intensity and $P(I_i)$ signifies the probability of the intensity value I_i .

Observing the above results (Table 5), it can easily be visualized that the increase in entropy is significantly low and therefore retains the image quality. It affirms the encrypted images' suitability for critical applications such as healthcare (telemedicine) or critical data communication purposes.

7.4 Embedding capacity analysis

The embedding capacity signifies the extent or the percentile to which a unit image can embed the text data (i.e., ensuring no reduction in PSNR and correlation, and maintaining low entropy). Table 6 presents the embedding capacity performance by the proposed model.

Observing Table 6, it can be easily found that the proposed method accomplishes significantly large enhancement in the embedding capacity post-optimization. This can be because of the proposed OPAP concept's robustness, which ensures optimal embedding while retaining entropy low and PSNR high, the employed AGA heuristic model's key objectives. Thus, the results obtained signify the proposed model's suitability for sizeable scale-sized encryption and secure communication purposes. The addition of more secret information (text data) in the image might impose high entropy that eventually could reduce image quality (i.e., PSNR). In such a case, it is significant to assess whether the inclusion of the proposed AGA-

Table 5 Image entropy analysis

Dataset	Initial Image Entropy	Entropy (Post-embedding)
Baboon	6.3510	7.9898
Lena	5.4312	7.9958
Sailboat	6.0468	7.9053
Peppers	6.1031	7.8998
Retina1	7.3904	7.6730
Retina2	7.4938	7.9968
Female	7.1020	7.9993

Table 6 Embedding capacity analysis

Dataset	Embedding capacity (%) (post 2D-DWT-2 L embedding)	Embedding capacity (%) (Post-AGA-OPAP optimization)
Baboon	13.01	46.90
Lena	10.20	47.81
Sailboat	10.91	35.01
Peppers	17.99	48.84
Retina1	12.04	57.90
Retina2	10.01	59.99
Female	19.93	56.91

OPAP assisted LSB embedding helps retaining maximum possible image quality even after extensive secret data embedding. In this paper, we assessed the performance for the different sizes of the secret text data embedded in the cover image with this motive. Observing the results (Table 4), it can easily be found that though with an increase in secret data size (to be embedded into image), the PSNR decreases; however, our proposed AGA-OPAP based LSB embedding method reduces entropy and retains better PSNR. It affirms that the proposed method can achieve optimal PSNR irrespective of the data size. The results affirmed that the inclusion of AGA-OPAP could be vital to ensure higher data embedding inside the medical image without imposing any significant quality degradation or visual traits, which might invite intruders to attack over uncertain cloud communication channels allied network.

7.5 Regular and singular coefficient analysis

The attack models such as RS-Attack or Steganalysis attack might explore the medical data under the transmission to attack the specific data-carrying certain significant information or secret information. The variations in regular and singular coefficients per block of the image are examined to alleviate such issues. As stated in Table 1, higher differences in the regular and singular coefficients can reveal the attackers about the presence of private data within the multimedia data, and therefore maintaining lower difference can be advantageous.

Observing Table 7, it can be found that the proposed method achieves relatively lower differences in regular coefficient value ($R_m - R_m$) and the singular difference value ($S_m - S_m$).

Table 7 RS analysis (secret data size 250 bytes)

Dataset	RS Parameters					
	Regular Coefficient Difference ($R_m - R_m$)			Singular Coefficient Difference ($S_m - S_m$)		
	Before	Post Embedding	Post Optimization	Before	Post Embedding	Post Optimization
Baboon	0.0063	0.0054	0.0057	0.0029	0.0015	0.0087
Lena	0.0035	0.0025	0.0031	0.0006	0.0112	0.0008
Sailboat	0.0039	0.0054	0.0065	0.0066	0.0015	0.0054
Peppers	0.0091	0.0074	0.0076	0.0089	0.0076	0.0059
Retina1	0.0029	0.0025	0.0034	0.0043	0.0112	0.0004
Retina2	0.0039	0.0077	0.0019	0.0002	0.0073	0.0062
Female	0.0081	0.0026	0.0056	0.0031	0.0108	0.0038

It reveals that the proposed method can achieve a high level of visual imperceptibility to secure medical data communication over a cloud channel.

7.6 Encryption and decryption speed analysis

To assess the time efficiency of the proposed model for encryption is calculated using MATLAB functions $*(tic - toc)$. The execution time consumed over the different dataset is given in Table 8.

Observing the above-stated results, it can easily be found that the proposed system consumes low execution time, including both encryption as well as decryption, which exhibit its robustness towards time-efficient computation.

7.7 NCPR and UACI test

In addition to the visual and statistical characterization discussed above, we have analyzed our proposed security model's effectiveness in Number of Changing Pixel Rate (NCPR) and the Unified Average Channel Intensity (UACI). High NPCR and UACI value usually imply higher randomness and therefore, high tolerance against any differential attack probability [63]. The randomness test results with a higher NCPR value confirm the proposed system's attack resiliency's essence. Similarly, via our proposed medical data security model, UACI also confirms satisfactory results. The thorough discussion of NCPR and UACI conditions during encryption for image randomness can be found in [63].

Recalling the overall design where the fundamental goal of employing hybrid encryption with AGA-OPAP was to avoid any attack conditions such as Man-In-The-Middle attack (MITM), steganalysis or linear and differential based attack approaches since the proposed model avoids providing any scope of visual perceptibility and maintains low entropy, high PSNR, it would be able to be resilient any attack conditions. Tables 9 display NPCR and UACI values for the images.

7.8 Mean absolute error analysis

To determine the receiver side's image quality, we used Mean Absolute Error (MAE) to evaluate accuracy (15).

Table 8 Execution time over of the secret text data (250 bytes)

Dataset	Data Size (bytes)	Execution Time (seconds)	
		Encryption	Decryption
Baboon	250	12.97	14.01
Lena	250	12.45	14.00
Sailboat	250	12.40	14.91
Peppers	250	11.31	14.92
Retina1	250	12.83	14.31
Retina2	250	12.01	14.89
Female	250	12.88	14.87

Table 9 NPCR and UACI randomness test

Dataset	NPCR (%)	UACI (%)
Baboon	99.6057	28.7671
Lena	99.7345	36.5632
Sailboat	99.7576	33.8148
Peppers	99.7942	36.6581
Retina1	99.7464	36.6070
Retina2	99.7398	36.5610
Female	99.7672	33.3847

$$MAE = \frac{1}{n} \sum_{i=1}^n (|Y'_i - Y_i|) \quad (15)$$

where Y'_i refers to the calculated output, while Y_i states for the expected value. The results obtained for inputs (with 250 bytes of text input) are given in Table 10. The results (Table 10) signifies the robustness in terms of very negligible error profile, which undoubtedly affirms its superior image quality (post-decryption).

7.9 Bit error rate (BER), structural similarity (SSIM), structural content (SC) and

Correlation analysis

a) Bit Error Rate (BER):

BER calculates the error rate of the transformed bits. This variance can be attributed to the attenuation noise or other disturbances. Eq. 16 is used to test BER.

$$BER = \frac{E}{\#Bits} \quad (16)$$

Where E indicates errors.

b) Structural Similarity (SSIM):

The structural similarity of images is calculated using SSIM. Here, we used the SSIM value to evaluate the similarity of the cover and steganographic images. Eq. (17) is used to construct the SSIM estimation.

Table 10 MAE performance with different input (250 bytes of the text secret data)

Dataset	MAE (%)
Baboon	0.1842
Lena	0.0963
Sailboat	0.3103
Peppers	0.3206
Retina1	0.4087
Retina2	0.1559
Female	0.1794

$$SSIM = \frac{2 \times \mu(\rho_1) \cdot \mu(\rho_2) + C_1}{\mu(\rho_1)^2 + \mu(\rho_2)^2 + C_1} \times \frac{2 \times C(\rho) + C_2}{\sigma_1(\rho)^2 + \sigma_2(\rho)^2 + C_2} \tag{17}$$

Where μ and σ are mean and standard deviation, respectively.

c) **Structural Content (SC):**

The resemblance between the cover and the steganographic image is assessed using SC. Eq. (18) to calculate the SC value.

$$SC = \frac{\sum_{i=1}^{|N|} \sum_{j=1}^{|M|} (C_{ij})^2}{\sum_{i=1}^{|N|} \sum_{j=1}^{|M|} (O_{ij})^2} \tag{18}$$

Where C and O represent cover and original images.

d) **Correlation:**

The similarity and disparity between the magnitude and the data phase are determined by correlation. Equation (19) is used to determine the correlation.

$$Corr = \frac{X \cdot \sum O \cdot S - \sum O \sum S}{\sqrt{X(\sum O^2) - (\sum O)^2} \sqrt{X(\sum S^2) - (\sum S)^2}} \tag{19}$$

X denotes the pairs in the data, the original image is O, and the steganographic image is S.

Table 11 BER, SSIM, SC and correlation of images

Dataset	Text Size(byte)	BER	SSIM	SC	Correlation
Baboon	250	0	1	1	1
	500	0	1	1	1
	1000	0	1	1	1
Lena	250	0	1	1	1
	500	0	1	1	1
	1000	0	1	1	1
Sailboat	250	0	1	1	1
	500	0	1	1	1
	1000	0	1	1	1
Peppers	250	0	1	1	1
	500	0	1	1	1
	1000	0	1	1	1
Retina1	250	0	1	1	1
	500	0	1	1	1
	1000	0	1	1	1
Retina2	250	0	1	1	1
	500	0	1	1	1
	1000	0	1	1	1
Female	250	0	1	1	1
	500	0	1	1	1
	1000	0	1	1	1

Table 12 Histogram of original image and post embedding of dark quality


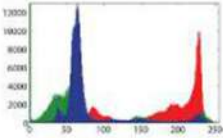
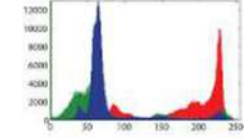

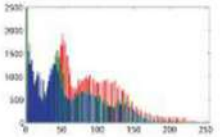
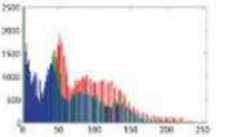
Name	Image	Original image Histogram	Histogram of post embedding and optimization
Retina[58]			
Zelda [52]			

Table 11 displays the BER, SSIM, SC and Correlation values of the images. These findings have shown that the proposed model has the potential to transmit secure medical data.

7.10 Dark and bright tone classification of images

The plain image, a histogram of the plain image and an encrypted image (post embedding and optimization) from an image of dark quality are shown in Table 12. The results show that the histogram retains similar visual quality for both the plain and cipher image.

The plain image, a histogram of the plain image, and an encrypted image (post embedding and optimization) from a bright image are presented in Table 13. The results show that the histogram retains similar visual quality for both the plain and cipher image.

Table 13 Histogram of original image and post embedding of bright quality


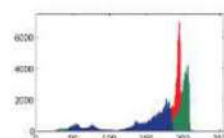
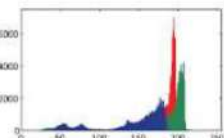

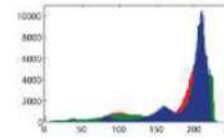
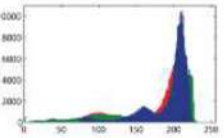
Name	Image	Original image Histogram	Histogram of post embedding and optimization
Jelli_Beans[52]			
Airplane[61]			

Table 14 Correlation coefficients based on the classification of image data quality (256 × 256)

Characteristic	Name	Red Channel			Green Channel			Blue Channel		
		Vertical	Horizontal	Diagonal	Vertical	Horizontal	Diagonal	Vertical	Horizontal	Diagonal
Dark	Retina2	-0.0048	-0.0005	0.0007	-0.0016	0.0024	0.0012	-0.0032	-0.0058	0.0032
Bright	Jelli_Beans	0.0002	-0.0133	0.0002	0.0046	0.0022	-0.0021	0.0008	0.0068	-0.0006
High Contrast	Lena	-0.0021	0.0025	-0.0011	-0.0058	0.0027	-0.0024	0.0053	0.0075	-0.0037

Table 15 Correlation coefficients based on the classification of image data quality (512 × 512)

Characteristic	Name	Red Channel			Green Channel			Blue Channel		
		Vertical	Horizontal	Diagonal	Vertical	Horizontal	Diagonal	Vertical	Horizontal	Diagonal
Dark	Zelda	-0.0014	0.0031	0.0013	0.0038	-0.0066	0.0079	-0.0031	0.0028	0.0053
Bright	Airplane	0.0002	-0.0133	0.0002	0.0046	0.0022	-0.0021	0.0008	0.0068	-0.0006
High Contrast	Female	-0.0059	0.0031	-0.0083	0.0061	-0.0011	0.0052	-0.0039	-0.0107	0.0070

Table 16 Result based on PSNR (dB)

Image	[7]	[30]	[11]	[38]	[61]	[8]	[14]	[33]	[13]	Proposed
Retina	56.76	57.02	46.06	74.69	45	58.96	57.02	56.34	60.8	74.92

7.11 Correlation analysis between adjacent pixels

To calculate the intensity of the linear relationship between two random variables, correlation is used. In a random image, the correlation value between neighbouring pixels is zero. Image encryption aims to render the association of neighbouring pixels close to zero in the encrypted image. The colour-encrypted image pixel correlation coefficient is determined between two horizontally adjacent pixels, two vertically adjacent pixels, and two diagonally adjacent pixels on each colour channel. The correlation coefficient values for the horizontal, vertical and diagonal components in the red, green and blue image channels are shown in Table 14 and Table 15.

7.12 Comparative assessment

The proposed model's accuracy is verified against state-of-the-art techniques where these algorithms [7, 8, 11, 13, 14, 30, 33, 38, 61] have been built to secure the healthcare data. The comparison of PSNR values with existing models is shown in Table 16. The proposed model for the security of medical data exhibited a better PSNR.

The comparison of the entropy values of the established model with existing models is provided in Table 17. The entropy value of the model designed is marginally better than the developed methods of Nithya et al. [11] focused on securing images in cloud storage environments with an integrated security framework using the DNA coding and image encryption methods to provide heightened security, Emy et al. [50] proposed an approach for improving the security of the colour image data by distributing the symmetric keys, Gupta et al. [15] employed Compressed Hybrid Cryptosystem that constitutes compression, encryption and secure session key exchange along with the transmission of image and Zhang et al. [68] proposed a new image compression and encryption scheme based on the nearest-neighbouring coupled-map lattices (NCML) and Non-uniform Discrete Cosine Transform (NDCT).

Table 18 portrays the comparison of Embedding Capacity Analysis (%) of the proposed model against existing models, where the results are better than the state-of-the-art approaches of Mansour et al. [29] and Ou et al. [36] where an efficient adaptive embedding and optimization of colour images is proposed.

Table 19 displays the proposed method's overall processing time for encoding and decoding information on the sender and recipient's end, respectively. The results demonstrate

Table 17 Results based on Entropy Values

Image	[11]	[50]	[15]	[68]	Proposed
Lena	7.9030	7.9955	7.9839	–	7.9958
Baboon	7.9020	7.9989	–	7.9952	7.9898

Table 18 Comparison based on embedding capacity

Image	[29]	[36]	Proposed
Lena	47.70	46.67	47.81
Baboon	36.17	38.42	46.90
Peppers	45.79	46.21	48.81

Table 19 Comparison based on encryption and decryption speed

Image	Time (Second)	[11]	[50]	[61]	Proposed
Baboon	Encryption	–	12.53	–	12.97
	Decryption	–	14.93	–	14.01
Lena	Encryption	22.53	12.21	86.012	12.45
	Decryption	20.56	14.69	86.547	14.00
Sailboat	Encryption	–	12.51	–	12.40
	Decryption	–	14.82	–	14.91
Peppers	Encryption	22.58	12.39	–	11.31
	Decryption	20.42	14.78	–	14.92

that the proposed method can better perform the state-of-the-art methods [11, 50, 61] for colour images.

The comparative NPCR and UACI values from the model built with the three previous research models are shown in Tables 20. All image data tested from the developed cryptographic method for NPCR and UACI values are higher than the previous studies of [50], seyedzadeh et al. [51], Niyat et al. [64] and Ahmad et al. [3] incorporates color image encryption algorithm based on chaotic system and cellular automata. It can be inferred based on the test results that the improved cryptosystem model is safer against differential attacks.

Table 21 shows the correlation coefficients between the proposed model and other cryptosystem models in each colour channel. The correlation value is closer to zero for the proposed model than for the model by Ref. [68] where a new algorithm for image compression and encryption based on spatiotemporal cross chaotic system is proposed.

Thus, considering the proposed model and its simulation-based performance, it can be inferred that the proposed system achieves optimal efficiency, which makes it suitable for secure medical data communication over the cloud environment. Observing the overall results, it can be found that the use of hybrid encryption (AES and RSA together) and AGA-OPAP

Tables 20 Result analysis of NPCR and UACI values

Image	Values	[50]	[51]	[64]	[3]	Proposed
Baboon	NPCR	99.7457	99.6823	99.6378	99.5830	99.6057
	UACI	38.2023	33.5031	33.4673	33.6110	28.7671
Lena	NPCR	99.7470	99.6827	99.6525	99.6450	99.7345
	UACI	36.7368	33.4898	33.4331	33.5610	36.5632
Sailboat	NPCR	99.7500	99.6847	–	99.5580	99.7576
	UACI	38.5050	33.5115	–	33.4830	33.8148
Peppers	NPCR	99.7509	99.6818	99.6254	99.6140	99.7942
	UACI	34.7577	33.5308	33.4566	33.5870	36.6581

Table 21 Comparison based on Correlation of RGB Channels

Ref.	Image	Red Channel			Green Channel			Blue Channel		
		Vertical	Horizontal	Diagonal	Vertical	Horizontal	Diagonal	Vertical	Horizontal	Diagonal
[68]	Lena	0.0259	0.0213	0.0562	0.0256	0.0143	0.0724	0.0259	0.0166	0.0602
Proposed	Lena	-0.0021	0.0025	-0.0011	-0.0058	0.0027	-0.0024	0.0053	0.0075	-0.0037

based embedding optimization can yield an optimal solution for secure medical data communication over the cloud platform. Similarly, results indicate that RSA-64 and AES-256 as a strategically combined solution can be better towards the proposed model, though in this study we have not performed individual performance assessment for RSA and AES (distinctly). Results obtained (Tables 2, 3, 4, 5, 6, 7, 8, 9, 10, 11, 12, 13, 14, 15, 16, 17, 18, 19, 20, 21) confirm that the use of AGA-OPAP has strengthened the proposed model to achieve optimal pixel adjustment, which eventually yielded PSNR enhancement, minimum histogram changes or entropy. It has also helped (due to PSNR and RS sensitive optimization) achieving optimal Regular and Singular coefficient values of each block. The simulation results reveal that the use of AGA-OPAP based LSB embedding has achieved maximum possible visual imperceptibility and data (image) quality which affirm suitability of the proposed model for the cloud environment.

Observing the overall results and corresponding inferences, it can be inferred that proposed model can enable an optimal security solution for the different cloud purposes, including Electronic Healthcare Records (EHR), Tele-medicine, critical image and allied annotation information hiding for future (security) purposes. Contemporarily, a large number of cloud applications provide data security, and undeniably our proposed model can be of great significance to support them, either as a standalone security solution or as a plug-in or Application Program Interface (API). The overall research conclusion is given in the subsequent sections.

8 Conclusion

Considering the exponential rise of medical data communication over the cloud environment, which is often considered uncertain, in this research, the emphasis was made on developing a robust and efficient secure data transmission model. The proposed model utilizes cryptographic and steganography features to introduce security and quality-centric data transmission. The use of hybrid encryption (AES and RSA) and their strategic implementation towards secret data encryption and decryption strengthened the overall security level and ensured that the secret information could not be retrieved easily. On the other hand, realizing the quality preserve aspect of steganography which is often used in medical data security, an Adaptive Genetic Algorithm based OPAP was developed that optimized least significant bit embedding over image-blocks. The AGA-OPAP model considered PSNR and Regular and Singular Coefficient values per block of the image as objective functions to perform secret message embedding and allied pixel adjustment (optimization). This approach leads to better image quality, visual imperceptibility and higher embedding capacity even without losing original quality. These all features make the proposed system suitable for numerous communication purposes including cloud communication, healthcare data communication, IoT communication purposes etc. MATLAB based model development and its simulation with different datasets as well as secret text of varied sizes revealed that the proposed model could be attack resilient (statistical assessment based attack models) and quality-centric (high PSNR) which make it suitable for secure medical data transmission over cloud platforms.

Acknowledgements The authors like to express their great appreciation to Mr. M. Santhoshkumar for his valuable and constructive suggestions during this research work's planning and development. His willingness to give his time so generously has been very much appreciated. The authors also would like to thank the anonymous reviewers for their insightful suggestions and careful reading of the manuscript.

References

1. Abd-El-Atty B, Iliyasa AM, Alaskar H, Abd El-Latif AA (2020) A robust quasi-quantum walks-based steganography protocol for secure transmission of images on cloud-based E-healthcare platforms. *Sensors*. 20(11):3108
2. Ahmad S, Thanikaiselvan V, Amitharajan R (2017) Data security through data hiding in images: a review. *J Artif Intell* 10:1–21
3. Ahmad M, Doja M, Sufyan Beg M (2018) Security analysis and enhancements of an image cryptosystem based on hyperchaotic system, *J. King Saud Univ Comput Inf Sci*:1–9
4. Ahmed DEM, Khalifa OO Robust and Secure Image Steganography Based on Elliptic Curve Cryptography, vol 2014. 2014 International conference on computer and communication engineering, Kuala Lumpur, pp 288–291. <https://doi.org/10.1109/ICCCE.2014.88>
5. Alam MS (2017) Secure M-commerce data using post quantum cryptography. 2017 IEEE International Conference on Power, Control, Signals and Instrumentation Engineering (ICPCSI), Chennai, pp 649–654. <https://doi.org/10.1109/ICPCSI.2017.8391793>
6. Al-barazanchi I, Shawkat S, Hameed M, Al-badri K (2019) Modified RSA-based algorithm: a double secure approach. *Telkomnika Indonesian J Electric Eng* 17:2818–2825. <https://doi.org/10.12928/TELKOMNIKA.v17i6.13201>
7. Anwar A, A.Ghany K, Elmahdy H (2015) Improving the security of images transmission. *Int J Bio-Med Informat e-Health* 3:7–13
8. B. PUSHPA (2020) Hybrid Data Encryption Algorithm for Secure Medical Data Transmission in Cloud Environment,” 2020 Fourth international conference on computing methodologies and communication (ICCMC), Erode, India, pp. 329–334, DOI: <https://doi.org/10.1109/ICCMC48092.2020.ICCMC-00062>.
9. Anupam Kumar Bairagi, Rahmatullah Khondoker, and Rafiqul Islam. 2016. An efficient steganographic approach for protecting communication in the Internet of Things IoT critical infrastructures. *Inf. Sec. J.: A Global Perspective* 25, 4–6 (2016), 197–212. DOI: <https://doi.org/10.1080/19393555.2016.1206640>
10. Bashir Abugharsa A, Basari AS, Almangush H (2012) A New Image Encryption Approach using the Integration of a Shifting Technique and the AES Algorithm. *Int J Comput Appl* 42:36–45. <https://doi.org/10.5120/5723-7785>
11. Chidambaram N, Raj P, Thenmozhi K, Rajagopalan S, Amirtharajan R (2019) A cloud compatible DNA coded security solution for multimedia file sharing & storage. *Multimed Tools Appl* 78:33837–33863. <https://doi.org/10.1007/s11042-019-08166-z>
12. Duluta A, Mocanu S, Pietraru R, Merezeanu D, Saru D (2017) Secure Communication Method Based on Encryption and Steganography. 2017 21st international conference on control systems and computer science (CSCS), Bucharest, pp 453–458. <https://doi.org/10.1109/CSCS.2017.70>
13. El-Emam NN, Al-Diabat M (2015) A novel algorithm for colour image steganography using a new intelligent technique based on three phases. *Appl Soft Comput* 37:830–846
14. Elhoseny M, Ramirez-González G, Abu-Elnasr OM, Shawkat SA, Arunkumar N, Farouk A (2018) Secure medical data transmission model for IoT-based healthcare systems. *IEEE Access* 6:20596–20608
15. Gupta K, Silakari S (2012) Novel approach for fast compressed hybrid color image cryptosystem. *Adv Eng Softw* 49:29–42
16. Gupta RK, Singh P (2013) A new way to design and implementation of hybrid crypto system for security of the information in public network. *Int J Emerg Technol Adv Eng* 3(8):108–115
17. Hajduk V, Broda M, Kovac O, Levicky D (2016) Image steganography with using QR code and cryptography. 2016 26th International Conference Radioelektronika (RADIOELEKTRONIKA), Kosice, pp 350–353. <https://doi.org/10.1109/RADIOELEK.2016.7477370>
18. Hashim MM, Taha MS, Aman AHM, Hashim AHA, Rahim MSM, Islam S Securing Medical Data Transmission Systems Based on Integrating Algorithm of Encryption and Steganography, vol 2019. 2019 7th international conference on mechatronics engineering (ICOM), Putrajaya, pp 1–6. <https://doi.org/10.1109/ICOM47790.2019.8952061>
19. Input images available URL (2021), “<https://homepages.cae.wisc.edu/~ece533/images/>”.
20. Jain M, Choudhary RC, Kumar A (2016) Secure medical image steganography with RSA cryptography using decision tree. 2016 2nd International Conference on Contemporary Computing and Informatics (IC3I), Noida, pp 291–295. <https://doi.org/10.1109/IC3I.2016.7917977>
21. Kadhim KT, Alsahlany AM, Wadi SM, Kadhun HT (2020) An overview of Patient’s health status monitoring system based on internet of things (IoT). *Wireless Pers Commun* 114:2235–2262. <https://doi.org/10.1007/s11277-020-07474-0>
22. Khalil MI (2017) Medical image steganography: study of medical image quality degradation when embedding data in the frequency domain. *Int J Comput Network Inform Secur* 9:22–28. <https://doi.org/10.5815/ijcnis.2017.02.03>

23. Kumar N, Agrawal S (2014) An efficient and effective lossless symmetric key cryptography algorithm for an image. 2014 International Conference on Advances in Engineering & Technology Research (ICAETR - 2014), Unnao, pp 1–5. <https://doi.org/10.1109/ICAETR.2014.7012788>
24. Laskar S (2012) High capacity data hiding using LSB steganography and encryption. *Int J Database Manag Syst* 4:57–68. <https://doi.org/10.5121/ijdms.2012.4605>
25. Leung Y, Hou RY (2015) Unequal security protection for secure multimedia communication. 2015 IEEE 4th Global Conference on Consumer Electronics (GCCE), Osaka, pp 570–571. <https://doi.org/10.1109/GCCE.2015.7398667>
26. Li L, Hossain MS, El-Latif AAA et al (2019) Distortion less secret image sharing scheme for internet of things system. *Cluster Comput* 22:2293–2307. <https://doi.org/10.1007/s10586-017-1345-y>
27. Liao X, Yin J, Guo S, Li X, Sangaiah AK (2018) Medical JPEG image steganography based on preserving inter-block dependencies. *Comput Electri Eng* 67:320–329, ISSN 0045-7906. <https://doi.org/10.1016/j.compeleceng.2017.08.020>
28. Madhusudhan KN, Sakthivel P (2020) A secure medical image transmission algorithm based on binary bits and Arnold map. *J Ambient Intell Human Comput*. <https://doi.org/10.1007/s12652-020-02028-5>
29. Mansour RF, Abdelrahim EM (2019) An evolutionary computing enriched RS attack resilient medical image steganography model for telemedicine applications. *Multidim Syst Sign Process* 30:791–814. <https://doi.org/10.1007/s11045-018-0575-3>
30. Mare SF, Vladutiu M, Prodan L (2011) Secret data communication system using steganography, AES and RSA. 2011 IEEE 17th International Symposium for Design and Technology in Electronic Packaging (SIITME), Timisoara, pp 339–344. <https://doi.org/10.1109/SIITME.2011.6102748>
31. Masood I, Wang Y, Daud A, Aljohani NR, Dawood H (2018) Towards Smart Healthcare: Patient Data Privacy and Security in Sensor-Cloud Infrastructure. *Wireless Commun Mobile Comput* 2018(2143897): 23. <https://doi.org/10.1155/2018/2143897>
32. May Zaw, Z., and S. W. Phyo. “Security Enhancement System Based on the Integration of Cryptography and Steganography”. *Int J Comput (IJC)*, Vol. 19, no. 1, Oct. 2015, pp. 26–39.
33. Muhammad K, Sajjad M, Mehmood I, Rho S, Baik SW (2018) Image steganography using uncorrelated color space and its application for security of visual contents in online social networks. *Future Gener Comput Syst* 86:951–960
34. Mukhedkar M, Powar P, Gaikwad P (2015) Secure non real time image encryption algorithm development using cryptography & steganography. 2015 Annual IEEE India Conference (INDICON), New Delhi, pp 1–6. <https://doi.org/10.1109/INDICON.2015.7443808>
35. Nithyabharathi PV, Kowsalya T, Baskar V (2014) To Enhance Multimedia Security in Cloud Computing Environment Using RSA and AES. *IJSETR* 3(2)
36. Ou B, Li X, Zhao Y, Ni R (2015) Efficient color image reversible data hiding based on channel dependent payload partition and adaptive embedding. *Signal Process* 108:642–657. <https://doi.org/10.1016/j.sigpro.2014.10.012>
37. Panchal D (2015) An Approach Providing Two Phase Security of Images Using Encryption and Steganography in Image Processing. *IJEDR* 3(4) ISSN: 2321-9939
38. Pandey HM (2020) Secure medical data transmission using a fusion of bit mask oriented genetic algorithm, encryption and steganography. *Future Gener Comput Syst* 111:213–225, ISSN 0167-739X. <https://doi.org/10.1016/j.future.2020.04.034>
39. Parah SA, Sheikh JA, Ahad F, Bhat GM (2018) High capacity and secure electronic patient record (EPR) embedding in color images for IoT driven healthcare systems. In: Dey N, Hassanien A, Bhatt C, Ashour A, Satapathy S (eds) *Internet of things and big data analytics toward next-generation intelligence*. Studies in big data, vol 30. Springer, Cham. https://doi.org/10.1007/978-3-319-60435-0_17
40. Paschou M, Sakkopoulos E, Sourla E, Tsakalidis A (2013) Health internet of things: metrics and methods for efficient data transfer. *Simulation Modelling Practice and Theory* 34:186–199, ISSN 1569-190X. <https://doi.org/10.1016/j.simpat.2012.08.002>
41. Patil P, Narayankar P, Narayan DG, Meena SM (2016) A Comprehensive Evaluation of Cryptographic Algorithms: DES, 3DES, AES, RSA and Blowfish. *Procedia Comput Sci* 78:617–624, ISSN 1877-0509. <https://doi.org/10.1016/j.procs.2016.02.108>
42. RajeshKumar N, Yuvaraj D, Manikandan G, Balakrishnan R, Karthikeyan B et al (2020) Secret image communication scheme based on visual cryptography and tetrolet tiling patterns. *Comput Mater Continua* 65(2):1283–1301
43. Ramalingam B, Rengarajan A, Rayappan JBB (2017) Hybrid Image Crypto System for Secure Image Communication- A VLSI Approach. *Microprocess Microsyst*. <https://doi.org/10.1016/j.micpro.2017.02.003>

44. Rathore S, Sharma PK, Loia V, Jeong Y-S, Park JH (2017) Social network security: Issues, challenges, threats, and solutions, *Information Sciences*, vol 421, pp 43–69, ISSN 0020-0255, <https://doi.org/10.1016/j.ins.2017.08.063>.
45. Ravichandran D, Praveenkumar P, Rayappan JBB, Amirtharajan R (2017) DNA Chaos blend to secure medical privacy. *IEEE Trans NanoBiosci* 16(8):850–858. <https://doi.org/10.1109/TNB.2017.2780881>
46. Razaq MA, Shaikh RA, Baig MA, Memon AA (2017) Digital image security: Fusion of encryption steganography and watermarking, *Int. J Adv Comput Sci Appl* 8(5):224–228
47. Sajjad M, Muhammad K, Baik SW, Rho S, Jan Z, Yeo SS, Mehmood I (2017) Mobile-cloud assisted framework for selective encryption of medical images with steganography for resource-constrained devices. *Multimed Tools Appl* 76:3519–3536. <https://doi.org/10.1007/s11042-016-3811-6>
48. Sajjad M, Nasir M, Muhammad K, Khan S, Jan Z, Sangaiah AK, Elhoseny M, Baik SW (2020) Raspberry Pi assisted face recognition framework for enhanced law-enforcement services in smart cities. *Future Gener Comput Syst* 108:995–1007, ISSN 0167-739X. <https://doi.org/10.1016/j.future.2017.11.013>
49. Saleh ME, Aly AA, Omara FA (2016) Data security using cryptography and steganography techniques. *Int J Adv Comput Sci Appl (IJACSA)* 7(6). <https://doi.org/10.14569/IJACSA.2016.070651>
50. Setyaningsih E, Wardoyo R, Sari AK (2020) Securing color image transmission using compression-encryption model with dynamic key generator and efficient symmetric key distribution. *Digital Commun Networks*, ISSN 2352-8648. <https://doi.org/10.1016/j.dcan.2020.02.001>
51. Seyedzadeh SM, Mirzakuchaki S (2012) A fast color image encryption algorithm based on coupled two-dimensional piecewise chaotic map. *Signal Process* 92(5):1202–1215
52. Shahzadi S, Iqbal M, Dagiuklas T, Qayyum ZU (2017) Multi-access edge computing: open issues, challenges and future perspectives. *J Cloud Comput* 6. <https://doi.org/10.1186/s13677-017-0097-9>
53. Shankar K, Lakshmanaprabu SK, Gupta D, Khanna A, de Albuquerque VHC (2020) Adaptive optimal multi key-based encryption for digital image security. *Concurrency Computat Pract Exper* 32:e5122. <https://doi.org/10.1002/cpe.5122>
54. Shilpi Hamal RK Chauhan (2019) Hybrid Cryptography based E2EE for Integrity & Confidentiality in Multimedia Cloud Computing. *IJITEE* 10(8)
55. Singh A, Chatterjee K (2017) Cloud security issues and challenges: a survey. *J Network Comput Appl* 79: 88–115, ISSN 1084-8045. <https://doi.org/10.1016/j.jnca.2016.11.027>
56. Sivaswamy J, Krishnadas SR, Joshi GD, Jain M, Ujjwaft Syed Tabish A (2015) Drishti-GS: Retinal image dataset for optic nerve head (ONH) segmentation. 2014 IEEE 11th International Symposium on Biomedical Imaging, ISBI 2014. pp. 53–56. <https://doi.org/10.1109/ISBI.2014.6867807>
57. Sreekutty MS, Baiju PS (2017, pp. 1-5) "security enhancement in image steganography for medical integrity verification system," 2017 international conference on circuit, Kollam, Power and Computing Technologies (ICCPCT). <https://doi.org/10.1109/ICCPCT.2017.8074197>
58. Stoyanov B, Stoyanov B (2020) BOOST: medical image steganography using nuclear spin generator. *Entropy*. 22(5):501
59. Su N, Zhang Y, Li M (2019) Research on Data Encryption Standard Based on AES Algorithm in Internet of Things Environment. 2019 IEEE 3rd information technology, networking, electronic and automation control conference (ITNEC), Chengdu, pp 2071–2075. <https://doi.org/10.1109/ITNEC.2019.8729488>
60. Usman MA, Usman MR (2018) Using image steganography for providing enhanced medical data security. 2018 15th IEEE Annual Consumer Communications & Networking Conference (CCNC), Las Vegas, pp 1–4. <https://doi.org/10.1109/CCNC.2018.8319263>
61. Venkatraman K, Geetha K (2019) Dynamic virtual cluster cloud security using hybrid steganographic image authentication algorithm. *Automatika* 60(3):314–321. <https://doi.org/10.1080/00051144.2019.1624409>
62. Wajgade VM (2013) Enhancing Data Security Using Video Steganography. *Int J Emerg Technol Adv Eng* 3(4)
63. Y. Wu, J. P. Noonan, S. Agaian, "NPCR and UACI randomness tests for image encryption", *Cyber J: Multidisc J Sci Technol, J Select Areas Telecommun (JSAT)*, April Edition, 2011, pp.31–38, 2011.
64. Yaghouti Niyat A, Moattar MH, Niazi Torshiz M (2017) Color image encryption based on hybrid hyperchaotic system and cellular automata. *Optic Laser Eng* 90:225–237
65. Rupeng Yang, Qiuliang Xu, Man Ho Au, Zuoxia Yu, Hao Wang, Lu Zhou, Position based cryptography with location privacy: a step for fog computing, *Future Gener Comput Syst*, volume 78, Part 2, 2018, Pages 799–806, ISSN 0167-739X. <https://doi.org/10.1016/j.future.2017.05.035>.
66. Yu L, Wang Z, Wang W (2012) The Application of Hybrid Encryption Algorithm in Software Security. 2012 Fourth international conference on computational intelligence and communication networks, Mathura, pp 762–765. <https://doi.org/10.1109/CICN.2012.195>

67. Yu J, Li H, Liu D (2020) Modified Immune Evolutionary Algorithm for Medical Data Clustering and Feature Extraction under Cloud Computing Environment. *J Healthcare Eng* 2020(1051394):11. <https://doi.org/10.1155/2020/1051394>
68. Zhang M, Tong X-J (2015) A new algorithm of image compression and encryption based on spatiotemporal cross chaotic system. *Multimed Tool Appl* 74(24):1125–11279

Publisher's note Springer Nature remains neutral with regard to jurisdictional claims in published maps and institutional affiliations.

Affiliations

R. Denis¹ • P. Madhubala²

P. Madhubala
madhubalasivaji@gmail.com

¹ Department of Computer Science, Periyar University, Salem, TN, India

² Department of Computer Science, Don Bosco College (Affiliated to Periyar University), Dharmapuri, TN, India

See discussions, stats, and author profiles for this publication at: <https://www.researchgate.net/publication/354021959>

PERSONALITY TRAIT AND ENVIRONMENTAL ATTITUDE

Article · August 2021

CITATIONS
0

READS
295

1 author:



Selvaraj Varaprasadham
Sacred Heart College

5 PUBLICATIONS 0 CITATIONS

SEE PROFILE

Some of the authors of this publication are also working on these related projects:



Psychology [View project](#)

PERSONALITY TRAIT AND ENVIRONMENTAL ATTITUDE

Robert Ramesh Babu. P, Research Scholar, Department of Social Work, Central University of Tamil Nadu, Thiruvavur, Tamilnadu;

Sigamani Panneer Professor and Head, Department of Social Work, School of Social Sciences and Humanities and Centre for Happiness, Central University of Tamil Nadu, Thiruvavur, Tamilnadu

Selvaraj. V, Research Scholar, University of Madras, Chennai, Tamilnadu

Shanmugam. D, Research Scholar, Presidency College, Chennai, Tamilnadu

James Bernard N.F, Research Scholar, Department of Management Studies, BIHER, Chennai, Tamilnadu

Joseph DesouzaKamalesh. F Research Scholar, Department of English, Vellore Institute of Technology (VIT), Vellore, Tamilnadu

Abstract

The relationship between the personality traits of college students and their environmental attitude is investigated. It involves a sample of 268 students of Arts and Science college students from the places of Tirupattur and Karaikal. The disproportionate stratified random sampling method is applied to collect the data by using the following tools. Taj environmental attitude scale developed by Hasseen Taj which has got six dimensions to understand the attitude of the respondents towards the environment. The HEXACO-PI-R scale developed by Kibeom Lee and Michael C. Ashton is used to assess the personality traits of the respondents. The Pearson's product moment correlation is used for analysing the data. The study had found out that there is significant gender difference among the dimensions of the personality traits such as honesty and emotionality with the $P < 0.05$ and $P < 0.01$ respectively. The result also posited that there was a significant relationship between environmental attitude and the personality traits of emotionality, health hygiene, environmental concern with $P < 0.05$. The results of the study indicate that the female have the higher level of honesty and emotionality traits of personality than male. The study also reveals that high level of emotional stability among students likely to improve the dimensions of positive hygiene and better environmental concern.

Keywords: Attitude, Environment, Emotionality, Environmental Concern, Personality

Keywords:

Environment, Attitude, Climate Change, Students, Pollution, Health and Hygiene, Wildlife

Introduction

In the cosmos, everyone is born as an individual but still, all are connected. Just because the oxygen is not seen doesn't mean it is not there. In the same way, this connection is manifested in the vicious cycle of nature. Statistical data of the UN report of 2001 proves the insurmountable increase in massive environmental abuse around the world. The report calculates that humans are using 30% more resources than the earth could reproduce each year (Economical and Social Council, 2002). This would lead to natural hazards causing serious threats to all aspects of life, both mental and physical wellbeing. One hand speeding the growth of population and on the other hand shrinking resources and environment degradation had created an urgent cry for pro-environmental behaviour to preserve the ecosystem for the future generation. There are enormous studies have been done on the relationship between environmental attitude and personality. There are considerable researches done to prove that Honesty, Agreeableness, Openness, Proactive personality and Pro-environmental attitude predict environmental behaviour (Pavalache-Ilie & Cazan, 2018). There are recent studies stated that females hold more pro-environmental attitudes and engage in more conservation behaviour, relative to males, is one of the most robust effects in the field of environmental psychology (Desrochers et al, 2019). Environmentalists time and again come out with huge cry to protect the mother earth. Only knowledge and awareness could bring spring into life from ignorance. It is knowledge from an environment or situation that develops skills, attitude and finally

a personality. Barr (2007) has found that situational variables, environmental attitudes, and psychological traits are important factors in environmental concern. The researcher considers the social demographical factors as one of the situational variables in that study. Tai-Yi and Tai-Kuei (2017) found that the impact of undergraduate students' environmental attitudes was moderated by personality traits such as agreeableness with $p < 0.05$ and conscientiousness with $p < 0.01$ level of significance.

The future of the nation is in the hands of today's young people. Around the world young people who are part of today's context are victimized under economically, culturally and psychologically. This scenario highly prevails in the economically emerging countries like India which finds it very hard to face the challenge to control environmental abuses. Indian youngsters are influenced by the drastic change of climatic and economical conditions. The impact of globalization has changed the attitude of people to the culture of use and throw, instead of pro-environmental culture (Larijani and Yeshodhara, 2008). This environmental deprivation or crisis has become a severe issue as it warns not only the harmony of people's existence but their health and lives as well. It is very obvious that environmental protection and preservation has been an urgent need of the hour. The awareness on this will not come unless serious scientific researchers are supported by the different organization and by the government sectors on various disciplines. This study on personality trait and environmental attitude on the college students will bring a new understanding of the present situation and awareness for the students.

Under this condition, the study envisages investigating the relationship of the five characteristics of personality traits such as honesty, emotionality, conscientiousness, extraversion, agreeableness and openness. Attitude is a predisposition of one's process of thought towards his/her behaviour. Therefore everyone has freedom of personal attitude which is influenced by various life conditions. On the other hand, personality trait is also developed according to the life developmental process which is affected by various conditions and situations. Therefore, this study finds out whether a person's personality trait affects environmental attitude. In other words, which type of personality trait could be more related to (predictive of) pro-environmental behaviour or anti-environmental behaviour?

Review of the Literature

Tai-Yi and Tai-Kuei (2017) had indicated in their study that the behaviour intention of the undergraduate students had predicted 38% towards environmental concern. Grosch and Rau (2017) found on a study called Gender Differences in Honesty: The Role of Social Value Orientation, that women were significantly more honest than men at the level of $p < 0.01$. This was found to be consistent with the study done by Feingold (1994) where he stated that females had higher extraversion, anxiety, trust, and, especially, tender-mindedness than males at the level of $p < 0.01$ significance. The review of literature of Lodewyk and Sullivan (2017) found consistent result in a study on Gender-Specific Associations between Personality Traits, Physical Activity, and Body Size Dissatisfaction. It stated that females had significantly higher honesty-humility, $F(1, 320) = 19.69$, $p < 0.01$, $\eta^2 = .06$; emotionality, $F(1, 320) = 123.81$, $p < 0.01$, $\eta^2 = .28$; and, conscientiousness $F(1, 320) = 10.87$, $p < 0.01$, $\eta^2 = .03$. Wuertz (2015) in a study on personality traits associated with environmental concern and found that for environmental concern, the only significant predictive trait was openness, $r(91) = 0.36$, $p < 0.01$. The personality trait of openness was correlated with general ecology. Markowitz et al. (2012); Brick and Lewis (2016), had made associations between traits and environmental actions which could be a step in explaining the role of traits as causal determinants of environmental behaviours. Milfont et al. (2010); Brick and Lewis (2016), conducted a study on attitudes and pro-environmental behaviour. They found out through regression analysis that attitudes could be considered as a powerful predictor of effective pro-environmental behaviour. An interesting comparative study was done by Dunlap (1994) on developed nations and so-called poor or developing countries with huge populations. The study indicated that residents of the wealthy nations were ready to take the deal of responsibility for environmental problems, on the other hand, those

people from poorer nations do not have the resources to invest huge money on research to study about saving environments. In the same way, when it studied the contributing factors for environmental problems within less developed nations, it was found that the consumption among industrialized nations and overpopulation was the contributing factor in the developing nations.

Objective and Hypotheses

The objective of the study is to find out the differences among gender, stream, personality traits and the environmental attitude and to find out the relationship between the personality traits and the environmental attitude among the college students. From the review of the literature, it is assumed that there would be a significant difference between gender, personality trait and environmental attitude. It was also hypothesised that there would be a difference between the streams regarding personality trait and environmental attitude. Finally, the dimensions of personality traits would be positively related to the dimensions of environmental concerns.

Method of Study

The study selected two colleges from the rural setting. The students' parents hailed from the farming background and working in various sectors like education, daily wages, business etc. Most of the students are from middle-class families. Samples from these demographical conditions would be helpful to the study and reduce biased results. The sample size for this study involves 268 students from two different Arts and Science colleges. The sample was collected based on disproportionate stratified random sampling. For data collection, two standardized scales were used. The first is the Taj environmental attitude scale developed by Haseen Taj. The scale has 6 dimensions and gives a better understanding of the attitude of the respondents towards the environment. The dimensions of the tool studies about the attitude towards population, health and hygiene, pollution and wildlife. The second one is the HEXACO-PI-R scale developed by Kibeom Lee & Michael C. Ashton, to identify the personality traits of the respondents. The data received from the respondents were randomized and obtained with the proper permission from the management. The candidates were assured of their anonymity and all research ethical conditions were explained. The names of the colleges will not be mentioned in the study and the findings of the study will be published with proper permission. The respondents weren't forced or taxed in any form to collect the data. The correlational research design was used in the study. The regression analysis was not carried out in the present case, because there were only two dimensions that significantly correlated, the rest were only inter collinearity. In the future, the study can be extended further to find out the predictive factors by including few more independent variables and many more colleges as the sample.

Research Findings

The study had used the SPSS to analyse the data. In table 1 and 2 *t*-tests were used to find out the difference between gender and stream. The Pearsons' Product Moment correlation was used to find out the relationship between the variables (Tables 3 and 4). From the statistical analysis of the data, only the significant values were culled out and listed as the results in the table. The rest is omitted for discussion.

Table – 1 Difference between mean scores of Personality Traits by Gender distribution

Traits	Gender	N	Mean	Std. Deviation	
Honesty	Male	143	31.7203	4.15781	.031*
	Female	125	32.7520	3.52561	
Emotionality	Male	143	30.8951	4.31622	.000**
	Female	125	33.3120	4.81164	

* $p < 0.05$

** $p < 0.01$

The research finding from the t-test analysis indicated that there was a significant difference among the dimensions of personality traits such as honesty and emotionality between male and female students. The college girls had a significantly higher level of honesty with $r=0.031$, which is $p<0.05$ level of significance. In the same way, the college girls scored a higher level of emotionality than boys with $r=0.000$ which is highly significant. In general, there was no significant gender difference among all the dimensions of personality traits. The study found that there was a clear difference between boys and girls with regard to the personality traits of emotionality and honesty. Girls exhibited more emotionality and honesty than the boys. For example, Dietz, Kalof, and Stern (2002) examined sex differences in value structures that have previously been associated with environmental concern and behaviour (altruism, traditionalism, self-interest, and openness to change). In the present study, it was identified that the female students who are more emotionally mature have a better environmental concern. Arnocky and Stroink (2011) found that emotional empathy mediated relationship between gender and environmental, which means girls had more emotional empathy.

Table – 2 Difference between mean scores of Environment attitude by the education institution distribution

Environmental Attitude	College	N	Mean	Std. Deviation	
	SHC	168	14.07	2.39	
Wild life	KC	100	15.11	2.13	0.00**

** $p<0.01$

The finding from Table-2 indicated that there was a significant difference among the dimensions of environmental attitude such as wild life between institutions. It explains that the students of SHC had scored low level of wild life than the students of KC with $r=0.00$ which is $p<0.01$ level of high significance. In general there was no difference among all the dimensions of environmental attitude between the institutions.

The Table-3 indicates the correlation analysis of dimensions among personality traits and dimensions of environmental attitude. The Pearson's Product Moment Analysis showed that significant inter-correlation among the dimensions. But it was omitted in this Table since it is not the purpose of the present study.

Table – 3 Relationship of Personality Traits with Environmental Attitude

Variable	N	Mean	Std. Deviation	
Emotionality		32.02	0.287	
Health Hygiene	168	12.89	0.119	0.127*
Environment concern		35.67	0.210	0.134*

* $p<0.05$

The result found that there was a significant positive relationship between the dimension of personality trait such as emotionality and the dimensions of environmental attitude such as health hygiene and environment concern. This denotes that when there is increase in the level of emotionality there would be an increase in the level of health hygiene, which is significant at the level of $r=0.127$ with $p<0.05$ level. In the same way, when there was an increase in the level of environmental concern there was a significant increase in the level of emotionality among the college students. It was noted from the result that there was a significant link between emotionality and environmental concern. Students who had better ways of expressing their emotions were more pro-environmental. Similarly, a research conducted by Pettus and Giles, (1987) indicated a positive relationship between favourable environmental attitudes and personality characteristics such as self-control and determination in working toward goals. In Table 3, it is found that students who had healthy hygiene behave with right attitudes towards protecting the environment from pollutions and to saving nature. It was also again substantiated by the results from the study conducted by Pettus

and Giles, (1987) that there is a positive relationship between attitudes toward Social and Governmental Actions for Environmental Quality (Environmental Attitude Scale), and personality characteristics related to being self-controlled, self-confident, hard-working, responsible, goal oriented, sincere and dependable.

Table – 4 Inter-Correlation Relationship of Dimensions of Personality Traits And Environmental Attitude

Variable	Extraversion	Conscientiousness	Emotionality
Extraversion	-	0.258**	0.215**
Conscientiousness	-		0.144*
Openness	0.253**	0.241**	-

*p=<0.05

**p=<0.01

It can be interpreted that students whose personality characteristics of extraversion and openness are more willing to accept or advocate societal actions and restrictions to preserve environmental quality. In the present study conducted on the college students reveals that they were more willing to sacrifice individual freedoms for the good of the environment and the good of society. In general, students are well motivated towards environmental awareness and they are mature enough to make right decisions. This is highlighted in the inter-correlation Table 4. Persons who had scored high on extraversion have more of conscientiousness and emotionality. In the same way persons with the personality trait of openness had characteristics such as conscientiousness and extraversion.

Conclusion

On the whole, the findings of the present study cannot be taken as the standard or ultimate solution until further research is done using some more related variables on a larger sample size. The findings of the study indicate that if proper environmental education and awareness programmes are conducted for the students it would certainly enhance their environmental attitudes and promote right use of nature. On the management level the policies on pro-environmental activities would make an effective impact on the student's life. Student initiatives can be encouraged and reinforced by way of awarding and appreciating them in the common forum and would promote better environmental consciousness or attitude.

Conflict of interest: None

Authors contribution: The authors worked together to formulate the concepts, collected data, analyzed and interpreted them. The final draft was prepared with several corrections and suggestions based comments.

Funding support: None

Acknowledgements: Grateful to all the college the Principals for allowing to meet the students for collecting the data successfully.

References

- Arnocky, S., & Stroink, M. L. (2011). Gender differences in environmental concern and cooperation: The mediating role of emotional empathy. *Current Research in Social Psychology*, 16(9), 1–14. <https://crisp.org.uiowa.edu/sites/crisp.org.uiowa.edu/files/2020-04/16.9.pdf>
- Barr, S. (2007). Factors influencing environmental attitudes and behaviours: A UK case study of household waste management. *Environment and Behaviour*, 39(4), 435-473. <https://doi.org/10.1177%2F0013916505283421>
- Balderjahn, I. (1988). Personality variables and environmental attitudes as predictors of ecologically responsible consumption patterns. *Journal of Business Research*, 17(1), 51-56. [https://doi.org/10.1016/0148-2963\(88\)90022-7](https://doi.org/10.1016/0148-2963(88)90022-7)

- Brick, C., & Lewis, G. J. (2016). Unearthing the “green” personality: Core traits predict environmentally friendly behavior. *Environment and Behavior*, 48(5), 635-658. <https://doi.org/10.1177%2F0013916514554695>
- Desrochers, J. E., Albert, G., Milfont, T. L., Kelly, B., & Arnocky, S. (2019). Does personality mediate the relationship between sex and environmentalism?. *Personality and Individual Differences*, 147, 204-213. <https://doi.org/10.1016/j.paid.2019.04.026>
- Dietz, T., Kalof, L., & Stern, P. C. (2002). Gender, values, and environmentalism. *Social Science Quarterly*, 83(1), 353–364. <https://doi.org/10.1111/1540-6237.00088>
- Dunlap, R. E., & Catton, W. R. (1994). Struggling with human exemptionalism: The rise, decline and revitalization of environmental sociology. *The American Sociologist*, 25(1), 5-30. <https://doi.org/10.1007/BF02691936>
- Feingold, A. (1994). Gender differences in personality: a metaanalysis. <https://psycnet.apa.org/doi/10.1037/0033-2909.116.3.429>
- Grosch, K., & Rau, H. A. (2017). Gender differences in honesty: The role of social value orientation. *Journal of Economic Psychology*, 62, 258-267. <https://doi.org/10.1016/j.joep.2017.07.008>
- Larijani, M., & Yeshodhara, K. (2008). An empirical study of environmental attitude among higher primary school teachers of India and Iran. *Journal of Human Ecology*, 24(3), 195-200. <https://doi.org/10.1080/09709274.2008.11906114>
- Lodewyk, K., & Sullivan, P. (2017). Gender-Specific Associations between Personality Traits, Physical Activity, and Body Size Dissatisfaction. *JTRM in Kinesiology*.ISSN: EISSN-0778-3906
- Markowitz, E. M., Goldberg, L. R., Ashton, M. C., & Lee, K. (2012). Profiling the “pro-environmental individual”: A personality perspective. *Journal of personality*, 80(1), 81-111. <https://doi.org/10.1111/j.1467-6494.2011.00721.x>
- Mercy, A. and Arjunan, N.K.: Environmental attitude and pro-environmental behaviour among secondary school children. EDUTRACKS,-A Monthly Scanner of Trends in Education, 4:32-34(2005)
- Milfont, T. L., Duckitt, J., & Wagner, C. (2010). A cross-cultural test of the value–attitude–behavior hierarchy. *Journal of Applied Social Psychology*, 40(11), 2791-2813. <https://doi.org/10.1111/j.1559-1816.2010.00681.x>
- Pavalache-Ilie, M., & Cazan, A. M. (2018). Personality correlates of pro-environmental attitudes. *International journal of environmental health research*, 28(1), 71-78. <https://doi.org/10.1080/09603123.2018.1429576>
- Pettus, A. M., & Giles, M. B. (1987). Personality characteristics and environmental attitudes. *Population and Environment*, 9(3), 127-137. <https://doi.org/10.1007/BF01259303>
- UN Economic and Social Council (ECOSOC), *UN Economic and Social Council Resolution 2002/12: Basic Principles on the Use of Restorative Justice Programmes in Criminal Matters*, 24 July 2002, E/RES/2002/12, available at: <https://www.refworld.org/docid/46c455820.html> [accessed 7 May 2020]
- Wuertz, Tara Rae, "Personality Traits Associated with Environmental Concern" (2015). *Walden Dissertations and Doctoral Studies*. 308. <https://scholarworks.waldenu.edu/dissertations/308>
- Yu, T. Y., & Yu, T. K. (2017). The moderating effects of students’ personality traits on pro-environmental behavioral intentions in response to climate change. *International journal of environmental research and public health*, 14(12), 1472. <https://doi.org/10.3390/ijerph14121472>

AN ANALYSIS OF GROWTH AND PERFORMANCE OF MSMEs in TamilNadu

***K. Saritha,**

Research Scholar,

Don Bosco College Dharmapuri

**** Dr. R. Venkatesh**

Assistant professor, Department of Commerce

Don Bosco College Dharmapuri

ABSTRACT

Micro, Small and Medium Enterprises (MSMEs) have played an crucial role in the economic development of a country. MSMEs are the chief support of the country and provide a large number of employees to the youths. It support to the growth of Indian economy with the wide network of 36 million units as of today and it providing employment to 80 million people. The MSME's sector has consistently registered higher growth rate compare to the overall industrial sector. In the present year MSMEs is growing in the state and it had promoted the entrepreneurship development and startup schemes in the state. The objectives of the present study are to evaluate the growth and performance of MSMEs. In recent years MSME sector has registered higher growth rate than the overall industrial sector. The present study in empirical in nature and it is based on secondary data. The data collected from DIC, Annual reports of MSMEs, journals and periodicals.

Key Words: Growth and Performance of MSMEs

INTRODUCTION

The Micro, Small and Medium Enterprises (MSMEs) have been accepted as the engine of economic growth and for promoting equitable development. The MSME also play an important role in the development of the economy with their effective, efficient, flexible and innovative entrepreneurial spirit. If we go through the following tables, we would able to know that the number of MSMEs as well as its contribution is increasing day by day. MSMEs are the nursery where small existing businesses have the potential to become world beaters tomorrow.

Review of Literature

Dr. K. Kumaravel (2017)¹, evaluated the development of entrepreneurs through small and medium enterprises. The study concluded that there are various opportunities available for the growth of MSME, but entrepreneurship is very good platform to promote and growth of this industry.

Anis Ali, Firoz Husain(2014)² This study focuses upon the growth pattern of the MSMEs, number of units, investment, production and employment. The main objectives of this paper to study the present status of MSMEs in India. They researcher found that the MSMEs are providing more employment per unit.

Seena P.P., Dr.Swarupa.R.,(2018)³, they conducted a study to analyse the region wise growth and performance of MSME in Kerala. The study revealed that southern region good in industrialization and has showed a stable performance. Number of unit, employment generation production and investment are lowest in northern region but the compound growth rate is highest.

Objectives of the Study

- To evaluate the overall growth and performance of MSMEs Sector in Tamilnadu.

Research Methodology

The study is based on secondary data, which is collected from various issues of Annual Reports on MSMEs and Handbook of Statistics on the Indian Economy published by Ministry of MSMEs and various research articles. The study considers the time period from 2004-05 to 2017-18. To examine the performance of MSMEs in Tamilnadu, the available data have been processed and presented in suitable tables.

¹ *Dr. K. Kumaravel (2017), " Growth and Performance of MSME Sector in India", International Journal of Management and Humanities, Vol.No. 4 Issue No.2.*

² *Anis Ali, Firoz Husain(2014), Msme's In India: Problems, Solutions And Prospectus In Present Scenario", International Journal of Engineering and Management Sciences, Vol.No.5(2),2014 P-No. 109-115.*

³ *Seena P.P., Dr.Swarupa.R.,(2018)³, Growth and performance of Small Scale Industries/Micro Small and Medium Enterprises in Kerala-Region Wise Analysis, International Journal of Management Studies, Vol-V Issue No 2(1), April 2018, p-no. 117 -122*

Statistical Tools used:

The information gathered was tabulated and analyzed by using average and correlation.

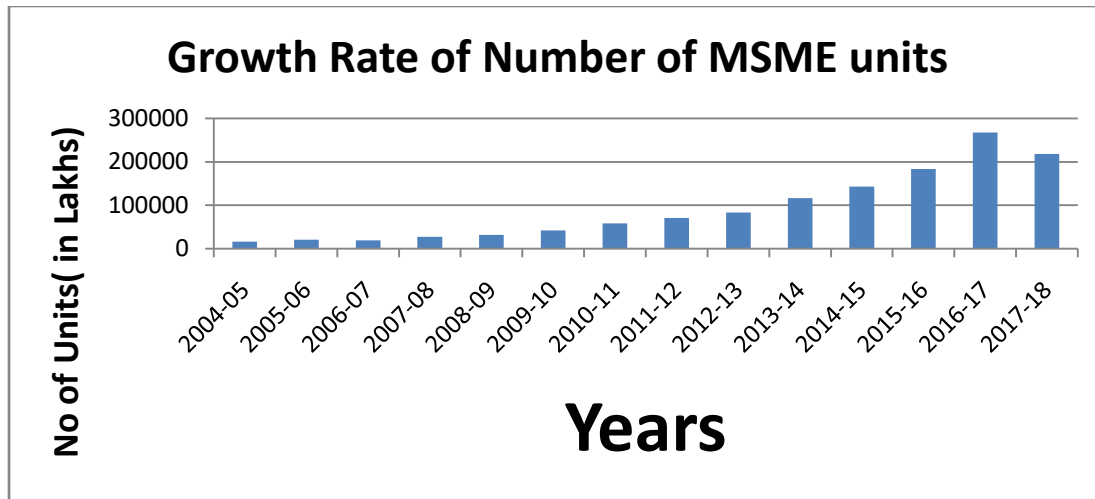
Table-1: Performance of MSMEs In TamilNadu

Year	No Of Units	Investment (Rs. Crore)	Production (Rs.in crore)	Employment (Rs. Lakhs)
2004-05	16253	1105.81	4556.97	60280
2005-06	20399	1705.20	4414.87	67800
2006-07	19201	714.41	2067.87	110026
2007-08	27209	2547.14	8739.95	242855
2008-09	32049	3557.89	13354.86	294255
2009-10	41799	3214.22	10880.01	151743
2010-11	57902	5872.37	12500.86	405233
2011-12	70758	7429.59	15496.00	502381
2012-13	83348	8751.57	17503.08	583436
2013-14	116393	18939.87	16832.25	494990
2014-15	143104	24349.65	59789.70	651180
2015-16	183792	40630.59	59332.19	1112002
2016-17	267310	36221.78	NA	1897619
2017-18	217981	25373.12	NA	1378544
Average	101894.3	12442.47	NA	546832.6

Sources: Annual Report2017-18, MSME in India.

The average growths of Micro, Small and Medium enterprises are 101897.3,12442.47 and 1378544 respectively with overall average growth rate of Unit, Investment, Production and Employment.

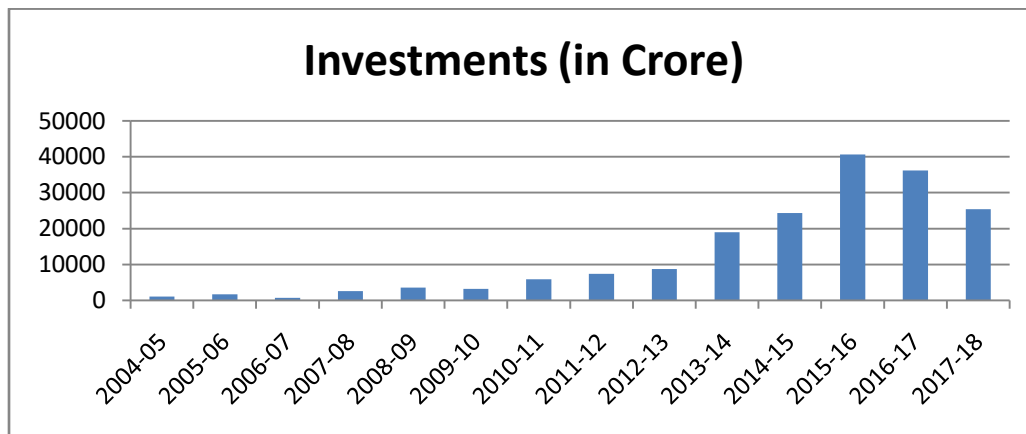
Figure-1: Growth Rate of Number of MSME units



Source : Annual Report MSME 2017-2018(Government of India)

According to Ministry of Micro, Small and Medium Enterprises, the number of MSME units are steadily increasing. The number of MSME units has increased from 16253 (lakhs) to 217981 (lakhs) from 2004-2005 to 2017-18period (see figure 1)

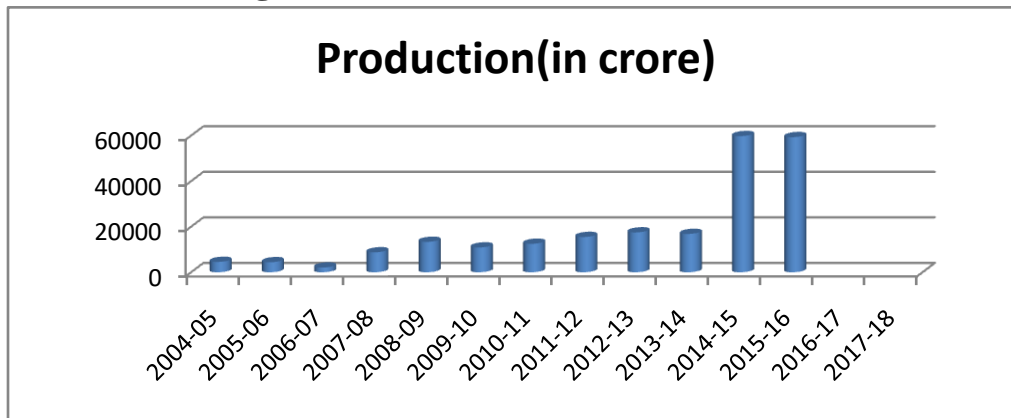
Figure-2: Growth Rate of Investment



Source : Annual Report MSME 2017-2018(Government of India)

The fixed investment (see figure 2) during the period of 2004-05 to 2017-2018 from Rs. 1105.81(crore) to Rs. 25373.12(crore).

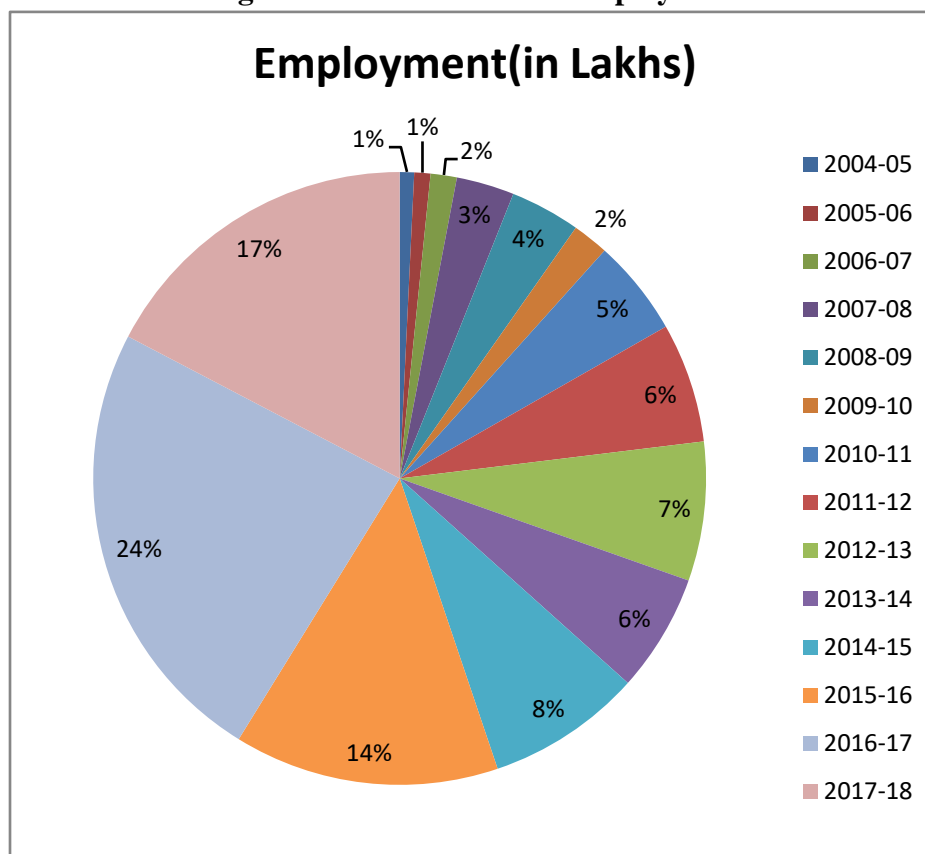
Figure-3: Growth Rate of Production



Source : Annual Report MSME 2017-2018(Government of India)

The total production in the MSMEs sector in the country as per the Final Report of the Fourth Census of MSMEs in 2004-2005 (Registered Sector) was 4556.97 crore persons and the same stands 59332.19 crore persons in the year 2015-2016 (see figure 3)

Figure-4: Growth Rate of Employment



Source : Annual Report MSME 2017-2018(Government of India)

The total employment in the MSMEs sector in the country as per the Final Report of the Fourth Census of MSMEs in 2004-2005 (Registered Sector) was 60280 crores persons and the same stands 1378544 crores persons in the year 2017-2018(see figure 4)

Table- 2:Results of Correlation for the growth of MSMEs in TamilNadu: Units, Investment, Production and Employment, 2004-2018

		Fixed Investment(Rs.in crore)	Production (in Crore)	Employment(in lakh)
Total No MSME(in lakh)	Pearson p-value	0.940** 0.000	0.912** 0.000	0.974** 0.000
Fixed Investment (Rs.in Crore)	Pearson p-value	1	0.917** 0.000	0.883** 0.000
Production (Rs. In Crore)	Pearson p-value		1	0.860** 0.000

** Correlation is significant at the 0.01 level(2-tailed)

The above results show that there exists the highest positive correlation between total MSMEs and fixed investment at 0.940 followed by total MSMEs and production at 0.912 and total MSMEs and employment at 0.974. Similarly, highest positive correlation at 0.917 is observed between fixed investment and production followed by fixed investment and employment at 0.883. The results also show that there is high positive correlation observed between production and employment at 0.860.

SUMMARY AND CONCLUSION

The summary of the study helped to conclude that the MSME sector plays a unique role in the socio-economic development of any country. A comparison of the growth rate of the MSME sector with that of the overall industrial sector in Tamilnadu indicated that MSMEs have registered a high growth rate which increased from 16253 to 217981 lakhs during the period 2004-2018.

Similarly highest positive correlation is observed in the case of fixed investment and production which stood at 0.917, employment stood at 0.883. It is also observed from the statistical analysis that a positive growth in production, investment and employment could be seen.

Reference:

www.msme.gov.in

www.rbi.org

Dr. K. Kumaravel (2017), “ Growth and Performance of MSME Sector in India”, International Journal of Management and Humanities, Vol.No. 4 Issue No.2.

Anis Ali, Firoz Husain(2014), Msme’s In India: Problems, Solutions And Prospectus In Present Scenario”, International Journal of Engineering and Management Sciences, Vol.No.5(2),2014 P-No. 109-115.

Seena P.P., Dr.Swarupa.R.,(2018)¹, Growth and performance of Small Scale Industries/Micro Small and Medium Enterprises in Kerala-Region Wise Analysis, International Journal of Management Studies, Vol-V Issue No 2(1), April 2018, p-no. 117 -122



Quantum dot sensitized solar cells using type-II CdSe-Cu₂Se core-shell QDs

N.J. Simi^a, S. Bharathi Bernadsha^b, Ajith Thomas^a, V.V. Ison^{a,*}

^aCentre for Nano Bio Polymer Science and Technology, Department of Physics, St. Thomas College, Palai, Kottayam-686574, Kerala, India

^bDepartment of Physics, Loyola College (Affiliated to the University of Madras), Chennai-600034, Tamilnadu, India

ARTICLE INFO

Keywords:

Type-II core-shell quantum dots
Quantum dot sensitized solar cells
Organometallic high temperature synthesis

ABSTRACT

Oleylamine capped CdSe-Cu₂Se type-II core-shell quantum dots were synthesised by organometallic high temperature route. The nanostructures were characterized using XRD, XPS, HRTEM, optical absorption and EDS and their suitability to serve as an effective sensitizer for TiO₂ deposited fluorine doped tin oxide coated glass slides was explored. Employing aqueous sulfide/polysulfide redox couple as the electrolyte, Cu₂S as the counter electrode, ZnS as the surface passivation layer and TiO₂ as the anode material, quantum dot sensitized solar cells were constructed. A power conversion efficiency of 4.3% was observed for the best performing device. Sintering of the photoanode, before embedding in the cell structure, resulted in an efficiency enhancement to 4.83%.

1. Introduction

In the era of third generation solar cells, quantum dot sensitized solar cells (QDSSC) received considerable interest in the past few decades due to their advantages like mechanical flexibility and cost-effectiveness in fabricating large-area solar cells (Chebroly and Kim, 2019). Apart from their material related merits, quantum dots (QDs) offer the possibility of surmounting the theoretical Shockley-Queisser efficiency limit of the conventional cell technology in solar photovoltaics (Ganesan et al., 2018). Colloidal QDs are promising light harvesters for the development of QDSSCs due to their distinct optical and electrochemical characteristics as well as their solution processability (Sharma et al., 2016; Kim et al., 2015; Wang et al., 2010). Among the colloidal explorations, type-II core-shell QDs are particularly important in photovoltaics because of their staggered band offset, capable of localizing the photo-generated the electron-wave function largely in one material and the hole-wave function in the other (Donega, 2011; Leontiadou et al., 2017). When employed in a cell, the charge separation capability of these systems is effective in facilitating electron injection from a QD sensitizer to any suitable wide band gap semiconductor (WBGSC) (Zhao et al., 2016).

The role of type-II core-shell QDs structures in enhancing the charge carrier density on photoanodes is evidenced through several investigations. Zhong group has designed a ZnTe-CdSe core-shell

QDs sensitized device, delivering a power conversion efficiency of 7.17% with an upshift of the CB edge and a wide absorption range (Jiao et al., 2015). A cell structure based on CuInS₂ has been reported to be delivering an efficiency of 5.38% after a type-II shelling with Mn-CdS, as compared to those working with bare structures, CuInS₂ (0.62%), CdS (1.45%) and Mn-CdS (2.11%) (Luo et al., 2013). Wang et al. has confirmed that device architectures utilizing CdTe-CdSe core-shell structures could exhibit higher electron injection rate than those working simple CdSe dots (Wang et al., 2013). Agren and co-workers could improve the efficiency of Cu₂GeS₃ based devices 5 times by forming Cu₂GeS₃/InP structures (Jamshidi Zavaraki et al., 2018).

In an earlier study, we have reported the synthesis of a novel oleylamine capped CdSe-Cu₂Se core-shell type-II structure using organometallic procedures. The present paper is based on the fabrication of photovoltaic devices utilizing these structures as a sensitizer by depositing them on TiO₂ adsorbed (ex-citu) fluorine doped tin oxide coated glass slides, forming the photoanode. The studies were further extended to investigating how far the sintering of the photoanode enhances the performance of the cell. A ZnS surface passivation layer was grown over the photoanode for suppressing the electron recombination. The ZnS passivation has been reported to be increasing the electron transportation from the QDs to WBGSCs, thrusting Fermi energy and improving the photovoltage (Kim et al., 2015; Pan and Zhong, 2016; Ruhle et al., 2010; Zhao et al., 2016).

* Corresponding author.

E-mail address: isonv@rediffmail.com (V.V. Ison).

2. Materials and methods

2.1. Materials

Copper (I) iodide (CuI, puratronic, 99.998%), titanium IV oxide (TiO₂ powder, anatase, 99.9%), titanium chloride (TiCl₄, 14% in dichloromethane), brass foil alloy (1 mm thick) were purchased from Alfa Aesar. Cadmium oxide (CdO, 99.99%), selenium powder (Se, 200 mesh, 99.99%), sulfur powder (S, 99.98%), oleylamine (OAm, 97%), 1-octadecene (ODE, 90%), trioctylphosphine (TOP, 90%), potassium chloride (KCl, 99%), sodium sulfide nonahydrate (Na₂S, 98%), zinc acetate dihydrate (99.8%) and fluorine doped tin oxide (FTO, 13 Ω/sq) coated glass were received from Sigma-Aldrich. All chemicals were used as such without further purification.

2.2. Characterization

The optical absorption spectra of the QDs sensitized photoanodes were recorded using a Shimadzu-3600 UV-Vis-NIR spectrophotometer. A Bruker AXS D8 Advance X-ray diffractometer (XRD) employing Cu K α radiation was used for structural studies. The morphological studies of the TiO₂ films and the QDs-sensitized TiO₂ films were performed by scanning electron microscopy (FESEM-Zeiss sigma 300) and high resolution transmission electron microscopy (HRTEM) (JEOL 200 kV JEM-2100 microscope). For HRTEM studies, the samples were prepared by scraping the TiO₂ films and the QDs-sensitized TiO₂ films and the particles were dispersed in ethanol, which were drop-casted on carbon coated copper grids. The elemental composition of the QDs-sensitized TiO₂ was studied using the energy dispersive X-ray spectroscopy (EDS) system attached to the HRTEM system and the X-ray photoelectron spectroscopy (Shimadzu Axis Ultra X-ray photoelectron spectrometer using Mg K α radiation). The cell parameters were determined using an HP 4155A programmable semiconductor parameter analyzer under AM1.5 simulated sunlight with a power density 100 mW cm⁻².

2.3. Synthesis of CdSe-Cu₂Se core-shell QDs

The synthesis of the core-shell structures has been discussed in detail in our previous study (Simi et al., 2019). In brief, 16.8 mg of CdO was taken in a round bottom (RB) flask along with 3 ml of OAm and 6 ml ODE. Under continuous stirring, the system temperature was raised to 120 °C and was held at that temperature for 1 h

under vacuum. The temperature was further raised to 310 °C under argon atmosphere and was kept for 30 min for stabilization. The reaction temperature was then lowered to 300 °C and an injection mixture containing TOPSe (23.7 mg of Se in 0.6 ml TOP) was introduced into it swiftly. For the growth of the Cu₂Se shell, CuI (13.4 mg) dissolved in 0.5 ml TOP and 1 ml ODE kept under continuous stirring, was injected into the RB flask 3 min after the TOPSe injection. The growth was arrested after 4 min and the core-shell structures obtained were purified by precipitation using methanol, followed by centrifugation three times and a further purification with acetone. The purified QDs were dispersed in hexane and filtered using a syringe filter (PTFE 13 mm, 0.2 μm non-sterile) for the sensitization process.

2.4. Fabrication of CdSe-Cu₂Se core-shell QDs-sensitized solar cells

The TiO₂ photoanodes were prepared by a modified version of the reported procedures (Wang et al., 2013)(Jara et al., 2014). Typically, FTO coated glass slides were cleaned ultrasonically in soap solution for 15 min, followed by a washing with deionized water 15 min and further with ethanol. The glass slides were dried first, on which the blocking and the active layers were deposited. The blocking layer was deposited by treating the FTO glass with 40 mM TiCl₄ aqueous solution for 30 min at 70 °C. It was then annealed for 30 min at 500 °C. To form the active layer, a paste of anatase TiO₂ was prepared (250 mg of ~25 nm TiO₂ powder mixed with 500 μl of deionized water and one drop of Triton X-100) and coated on top of the blocking layer using doctor blade technique. The samples were dried at 125 °C for

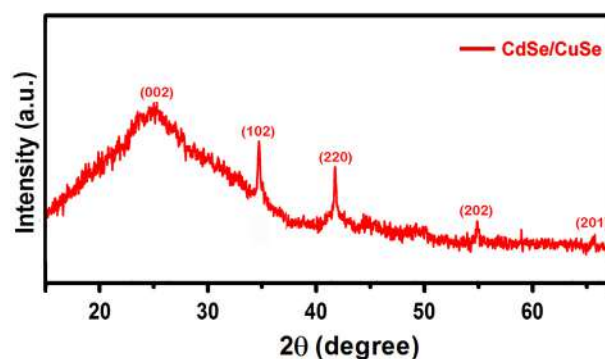


Fig. 2. XRD pattern of CdSe/Cu₂Se QDs.

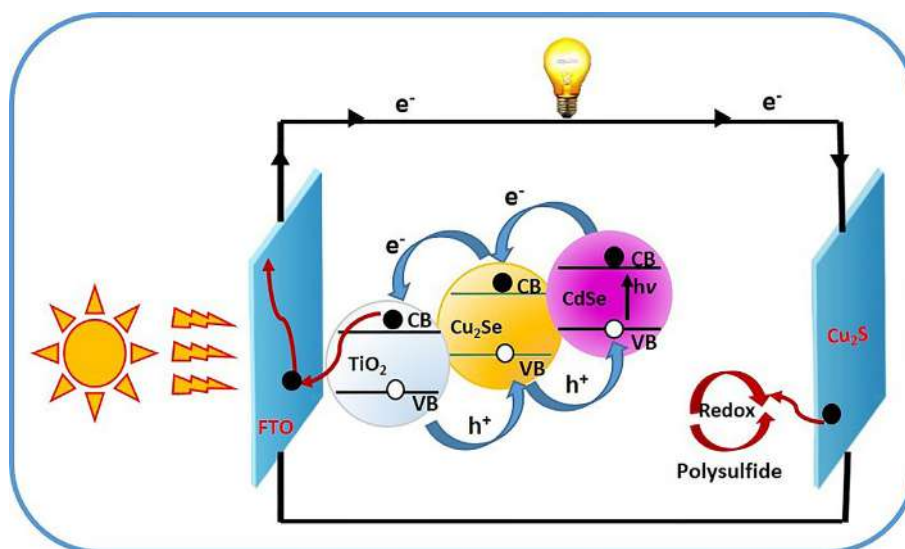


Fig. 1. Schematic of the construction and working of the QDSSCs.

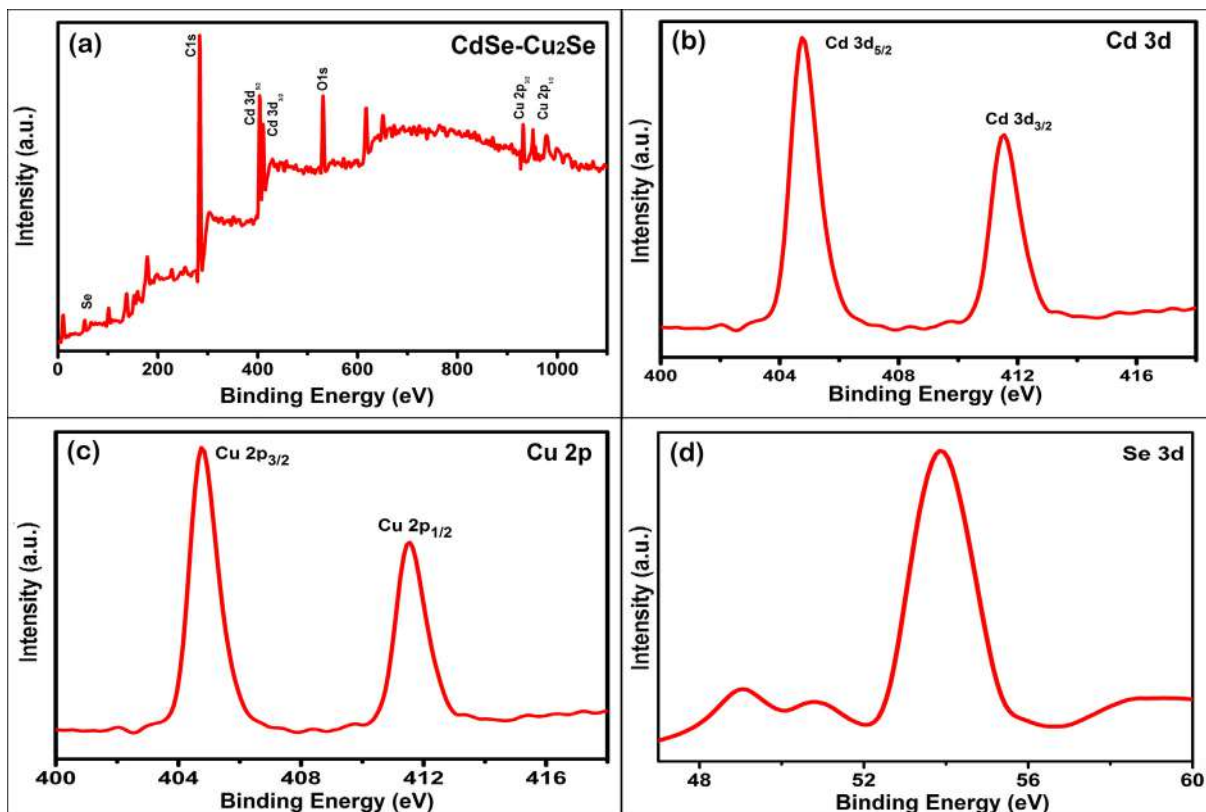


Fig. 3. High resolution XPS spectra of (a) the core-shell QDs over the entire scan range (b) Cd 3d (c) Cu 2p (d) Se 3d.

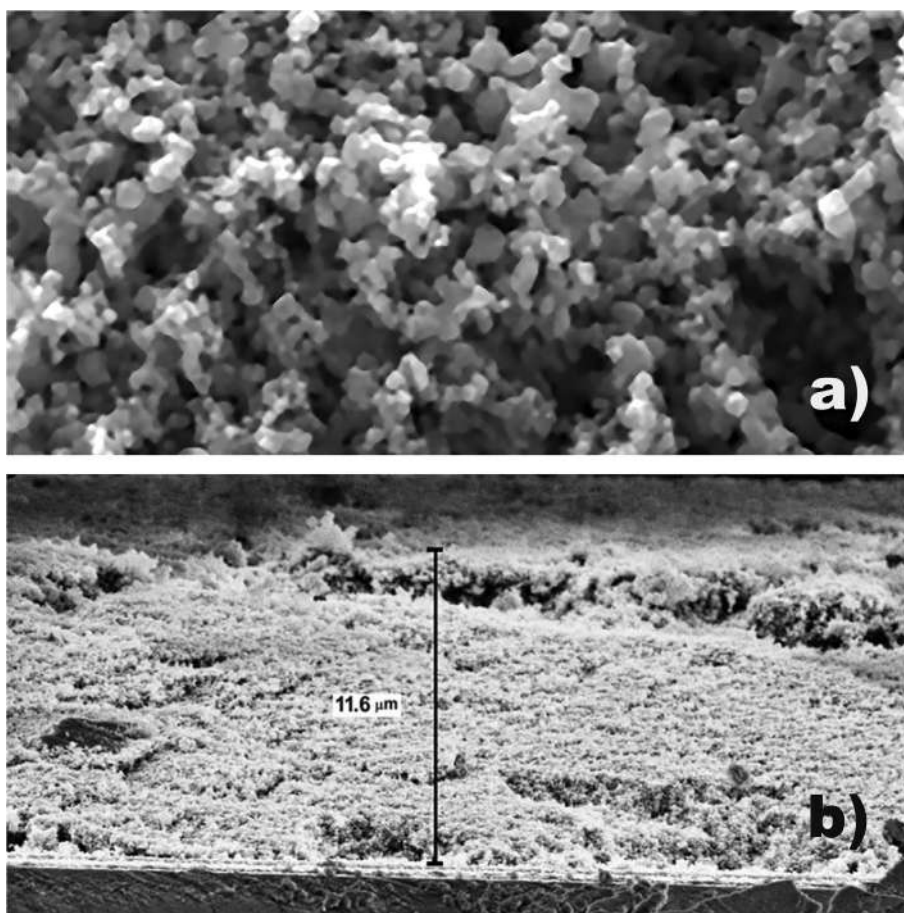


Fig. 4. (a) SEM image of a TiO₂ photoanode film surface and (b) Cross-sectional SEM image of a QDs sensitized TiO₂ film.

6 min and calcined at 500 °C for 45 min, followed by a post treatment process with TiCl_4 again. Sensitization of the photoanode with QDs was done ex-citu by dipping the electrode directly into the QD dispersion for 1 h (Sharma et al., 2016; Kim et al., 2015).

The ZnS layer was grown by SILAR method by dipping the QDs sensitized photoanodes in an aqueous solution of 0.1 M $\text{Zn(OAc)}_2 \cdot 2\text{H}_2\text{O}$ three times for 1 min each and then in 0.1 M $\text{Na}_2\text{S} \cdot 9\text{H}_2\text{O}$ for 1 min. After each immersion, the films were rinsed with deionized water and dried before subsequent dipping. The films were finally dried at 300 °C for 3 min. The Cu_2S counter electrodes were prepared using brass foil (Cu:Zn = 64:27). The brass foils were immersed in 35% HCl solution at 70 °C for 30 min and were then dried on a hot plate. The foils were dipped into polysulfide solution, comprising 1 M Na_2S , 1 M S and 0.1 M KCl in distilled water, for 10 min to vulcanize. The polysulfide solution was used as an electrolyte too.

The solar cells were constructed by assembling the QDs sensitized TiO_2 photoanode and the Cu_2S counter electrode into a sandwich configuration using parafilm as a spacer with a droplet of polysulfide electrolyte in between (Chang et al., 2013; Kamat, 2008; McDaniel et al., 2013 (Ye et al., 2017)). A schematic representing the construction and working of the QDSSC is shown in Fig. 1.

3. Results and discussion

The structural and optical characterizations of the core-shell structures are given in detail in our previous work (Simi et al., 2019). Fig. 2 represents the XRD pattern of the CdSe- Cu_2Se QDs sample. The broad peaks with 2θ values at 24.9°, 35.3°, 42.3°, 49.2°, 54.9° correspond to the reflections at (002), (102), (220), (202), (201) respectively. The average size of the nanoparticles was estimated from a prominent peak

at 35.3° giving the value 5.86 nm, which matches well with the size obtained from the HRTEM results. The chemical composition and the valence states of the elements were determined by XPS analysis (Fig. 3). The survey scan carried out shows the presence of C 1s, O 1s, Cd 3d, Cu 2p and Se core levels in the sample. The binding energies obtained were corrected by referring the C 1s peak to the energy 284.60 eV. Spin orbit coupling of Cd 3d spectrum (Fig. 3(b)) resulted in $3d_{5/2}$ and $3d_{3/2}$ peaks, positioned at 404.75 eV and 411.49 eV, respectively, with a spin orbit separation of 6.74 eV, which is in close agreement with that reported in the literature (Sung et al., 2007 (Hota et al., 2007)). The Cu 2p spectrum (Fig. 3(c)) splits into $2p_{3/2}$ and $2p_{1/2}$ with binding energies 931.65 eV and 951.54 eV, respectively, with a spin orbit separation of 19.89 eV. The absence of any characteristic peak of Cu^{2+} in the spectrum confirms its monovalency (Bo et al., 2014; Deka et al., 2010 (Chen et al., 2015)). Fig. 3(d) shows the spectra of Se with binding energy at 53.89 eV (Jamble et al., 2017).

The SEM image of TiO_2 photoanode surface is shown in Fig. 4(a), exhibiting uniform distribution of the particles over the FTO surface. The uniformity is also evident in the cross-sectional SEM image of the QDs sensitized photoanode shown in Fig. 4(b). The image also shows that the average thickness of the TiO_2 layer is about 11.6 μm

Fig. 5(b) shows the TEM image of QDs sensitized TiO_2 particles, exhibiting dense and effective covering of the TiO_2 particles. The sharpness of the TiO_2 surfaces has gone down in the QDs sensitized TiO_2 due to the adhesion of the QDs over the TiO_2 particles. The lattice planes of the QDs and TiO_2 are evident in the HRTEM image shown in Fig. 5(c). The EDS image provides elemental composition of the QDs sensitized TiO_2 with the ratio of the elements Ti, O, Cd, Se and Cu as 18.42:36.12: 3.56: 8.72: 33.09 (Fig. 6). The percentage of Cu is pretty large because the samples were drop casted on copper grids.

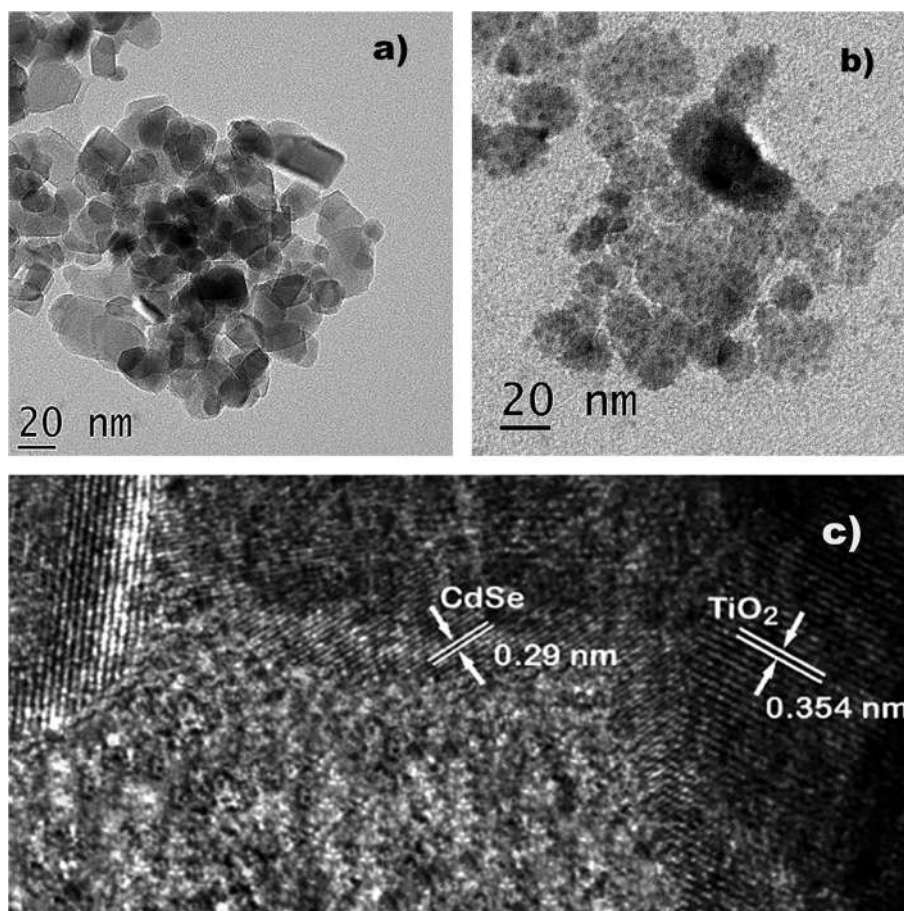


Fig. 5. (a) TEM image of TiO_2 particles (b) TiO_2 photoanode sensitized with QDs (c) HRTEM image of QDs sensitized TiO_2 .

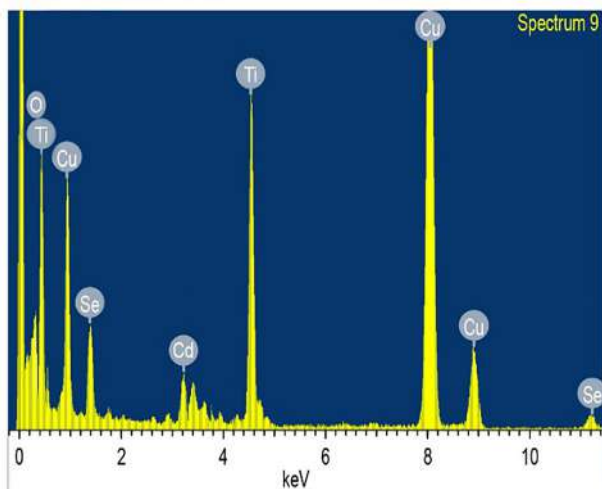


Fig. 6. EDS spectrum of QDs sensitized TiO₂.

Cell structures were fabricated with and without sintering of the QDs sensitized photoanode. The sintering was done at 300 °C for 3 min. J-V curves of the solar cells (illuminated at 100 mW cm⁻²) fabricated with and without sintering of the photoanode are shown in Fig. 7. The photoactive area in the two cases was estimated to be 0.28 cm². The cell parameters obtained were $J_{sc} = 16.05 \text{ mA cm}^{-2}$, $V_{oc} = 0.54 \text{ V}$, $FF = 0.49$ and $\eta = 4.3\%$ for the non-sintered case and for the sintered case, the cell parameters were improved to $J_{sc} = 17.29 \text{ mA cm}^{-2}$, $V_{oc} = 0.55 \text{ V}$, $FF = 0.51$ and $\eta = 4.83\%$.

We could observe a 9.2% improvement in the J_{sc} with a notable improvement of the power conversion efficiency upon sintering. It has been reported that the effect of sintering is highly contingent on time and temperature (Pan et al., 2012). Sintering mainly influences the electron-injection efficiency. Here, the current density of the devices has shown an increment due to an advancement in the connection between the wide band gap semiconductor and the QDs ((Pan et al., 2012) Fan et al., 2009a, 2010b, 2010c). The optical absorption spectra of two QDs sensitized photoanodes before and after sintering are shown in Fig. 8, indicating that absorption characteristics of the QDs remain the same even after the sintering process (Fan et al., 2010c; Hota et al., 2007). The inset shows the photographs of the photoanodes before and after the sintering process. Using the data obtained for the sintered photoanode, a Tafel polarization curve was drawn (Fig. 9), to illustrate the variation of the current density (logarithmic) versus potential. The curve shows that the cathodic and anodic slopes are unequal, indicating that the number of electrons

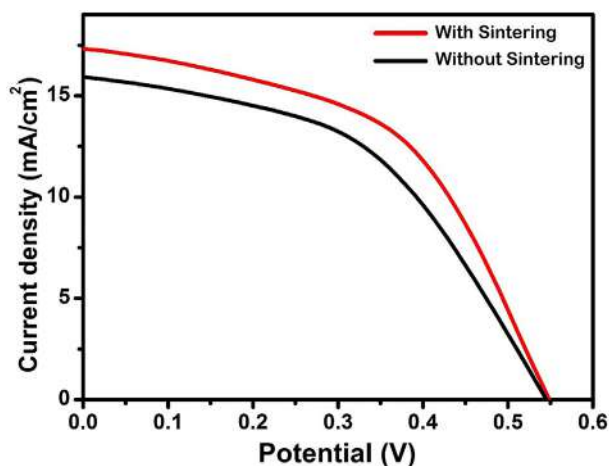


Fig. 7. J-V curves of the QDSSCs fabricated with and without sintering.

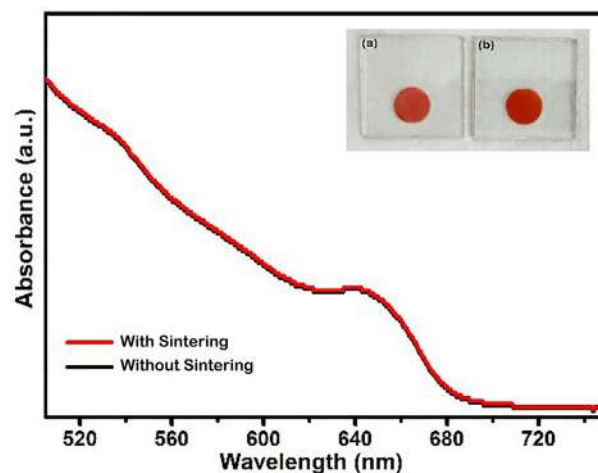


Fig. 8. Absorption spectra of the QDs sensitized photoanodes with and without sintering. (Inset shows the photoanodes (a) without sintering and (b) with sintering.)

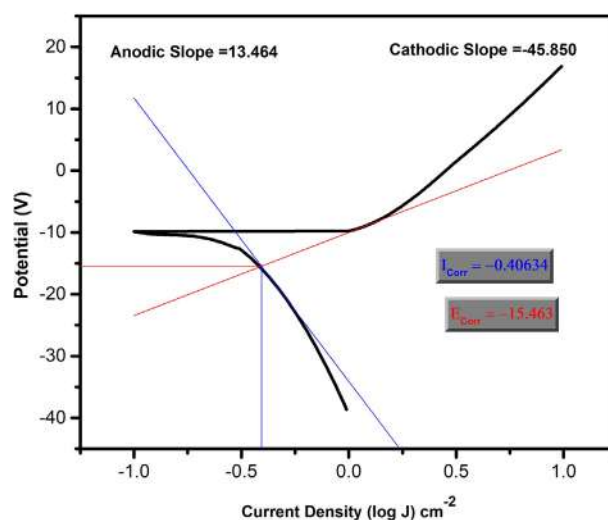


Fig. 9. Tafel plot of the sintered photoanode.

involved in both the reactions are not equal. The values obtained are 0.40634 amps as the corrosion current (I_{corr}) and 15.463 V as the corrosion potential (E_{corr}), showing that the several steps are involved in the reaction. Since the difference between the obtained values of anodic and cathodic Tafel slopes is a minimum, we suppose that the kinetics related to the electron transfer and the number and nature of electrons involved in the two reactions (anodic and cathodic) are partly similar.

4. Conclusions

Quantum dot sensitized solar cells employing type-II CdSe-Cu₂Se core-shell QDs were fabricated under ordinary laboratory conditions. The OAm capped QDs were adsorbed ex-citu on TiO₂ to form the photoanodes and Cu₂S was used for making the counter electrode. Aqueous sulfide/polysulfide redox couple was employed as the electrolyte and a layer of ZnS was used as the surface passivation layer. Cells were fabricated with and without sintering of the QDs sensitized photoanode and the devices were found to be exhibiting $J_{sc} = 17.29 \text{ mA cm}^{-2}$, $V_{oc} = 0.55$, $FF = 0.51$ and $\eta = 4.83\%$ after sintering. A 9.2% improvement of J_{sc} with a notable increase of the power conversion efficiency has been observed upon sintering of the photoanode.

Investigations are going on in utilizing the molecular linker assembly method of sensitization of the photoanode.

Declaration of Competing Interest

The authors declare that they have no known competing financial interests or personal relationships that could have appeared to influence the work reported in this paper.

Acknowledgements

The corresponding author V.V. Ison gratefully acknowledges SERB, DST, Govt. of India, for an earlier fast track project (Order No. SR/FTP/PS-108/2010). The authors thank Dr. Biju P.R., Associate Professor, School of Pure and Applied Physics, Mahatma Gandhi University, Kottayam for his support during the solar cell fabrications.

References

- Bo, F., Zhang, C., Wang, C., Xu, S., Wang, Z., Cui, Y., 2014. *J. Mater. Chem. A* 2, 14585–14592.
- Chang, C.C., Chen, J.K., Chen, C.P., Yang, C.H., Chang, J.Y., Appl, A.C.S., 2013. *Mater. Interfaces* 5, 11296–11306.
- Chebrolov, V.T., Kim, H.J., 2019. *J. Mater. Chem. C* 7, 4911–4933.
- Chen, X.Q., Li, Z., Bai, Y., Sun, Q., Wang, L.Z., Dou, S.X., 2015. *Chemistry–A Eur. J.* 21, 1055–1063.
- Deka, S., Genovese, A., Zhang, Y., Miszta, K., Bertoni, G., Krahne, R., Giannini, C., Manna, L., 2010. *J. Am. Chem. Soc.* 132, 8912–8914.
- Donega, C.M., 2011. *Chem. Soc. Rev.* 40, 1512–1546.
- Fan, S.Q., Kim, D., Kim, J.J., Jung, D.W., Kang, S.O., Ko, J., 2009a. *Electrochem. Commun.* 11, 1337–1339.
- Fan, S.Q., Fang, B., Kim, J.H., Kim, J.J., Yu, J.S., Ko, J., 2010c. *Appl. Phys. Lett.* 96, 063501.
- Fan, S.Q., Fang, B., Kim, J.H., Jeong, B., Kim, C., Yu, J.S., Ko, J., 2010b. *Langmuir* 26, 13644–13649.
- Ganesan, A.A., Houtepen, A.J., Crisp, R.W., 2018. *Appl. Sci.* 8, 1867.
- Hota, G., Idage, S.B., Khilar, K.C., 2007. *Colloids Surf., A* 293, 5–12.
- Jamble, S.N., Ghoderao, K.P., Kale, R.B., 2017. *Mater. Res. Express* 4, 115029.
- Jamshidi Zavaraki, A., Huang, J., Ji, Y., Jørgensen, H., 2018. *J. Renewable Sustainable Energy* 10, 043710.
- Jara, D.H., Yoon, S.J., Stamplecoskie, K.G., Kamat, P.V., 2014. *Chem. Mater.* 26, 7221–7228.
- Jiao, S., Shen, Q., Mora-Sero, I., Wang, J., Pan, Z., Zhao, K., Zhong, X., Bisquert, J., 2015. *ACS Nano* 9, 908–915.
- Kamat, P.V., 2008. *J. Phys. Chem. C* 112, 18737–18753.
- Kim, J.Y., Yang, J., Yu, J.H., Beak, W., Lee, C.H., Son, H.J., Hyeon, T., Ko, M.J., 2015. *ACS Nano* 9, 11286–11295.
- Leontiadou, M.A., Tyrrell, E.J., Smith, C.T., Espinobarro Velazquez, D., Page, R., Miloszewski, J., Walsh, T., Binks, D., Tomić, S., 2017. *Sol. Energy Mater. Sol. Cells* 159, 657–663.
- Luo, J., Wei, H., Huang, Q., Hu, X., Zhao, H., Yu, R., Li, D., Luo, Y., Meng, Q., 2013. *Chem. Commun.* 49, 3881–3883.
- McDaniel, H., Fuke, N., Pietryga, J.M., Klimov, V.I., 2013. *J. Phys. Chem. Lett.* 4, 355–361.
- Pan, Z., Zhong, X., 2016. *J. Mater. Chem. A* 4, 18976–18982.
- Pan, Z., Zhang, H., Cheng, K., Hou, Y., Hua, J., Zhong, X., 2012. *ACS Nano* 6, 3982–3991.
- Ruhle, S., Shalom, M., Zaban, A., 2010. *ChemPhysChem* 11, 2290–2304.
- Sharma, D., Jha, R., Kumar, S., 2016. *Sol. Energy Mater. Sol. Cells* 155, 294–322.
- Simi, N.J., Vinayakan, R., Ison, V.V., 2019. *RSC Adv.* 9, 15092–15098.
- M.S. Sung, Y.B. Lee, Y.J. Kim, Y.D. Kim, In *Solid State Phenomena*, 2007, Vol. 124, Trans Tech Publications, 1229–1232.
- Wang, J., Wang, Y., Cao, F., Guo, Y., Wan, L., 2010. *J. Am. Chem. Soc.* 132, 12218–12221.
- Wang, J., Mora-sero, I., Pan, Z., Zhao, K., Zhang, H., Feng, Y., Yang, G., Zhong, X., Bisquert, J., 2013. *J. Am. Chem. Soc.* 135, 15913–15922.
- Wang, Y.Q., Rui, Y.C., Zhang, Q.H., Li, Y.G., Wang, H.Z., 2013. *ACS Appl. Mater. Interfaces* 5, 11858–11864.
- Ye, M., Gao, X., Hong, X., Liu, Q., He, C., Liu, X., Lin, C., 2017. *Sustainable Energy Fuels* 1, 1217–1231.
- Zhao, K., Pan, Z., Zhong, X., 2016. *J. Phys. Chem. Lett.* 7, 406–417.



Comparative study of the morphological and optical properties of RE³⁺ (=Nd³⁺, Dy³⁺) doped TiO₂: A pursuit for suitable anode material for DSSCs



S. Bharathi Bernadsha*, V. Anto Feradrick Samson, J. Madhavan, M. Victor Antony Raj

Department of Physics, Loyola College, University of Madras, Chennai 34, India

ARTICLE INFO

Article history:

Received 12 December 2020
Received in revised form 4 January 2021
Accepted 9 January 2021
Available online 19 January 2021

Keywords:

Nano particles
Structural
Solar Energy Materials
XPS
Thin films

ABSTRACT

Nano scaled trivalent Rare-earth Elements (RE³⁺ = Nd³⁺ and Dy³⁺) doped TiO₂ anode materials were synthesized by hydrothermal method and characterized to analyze the morphological and optical properties. Having N719 as the dye and Platinum as counter electrode, the solar cells were fabricated to harness the solar energy. The reduction in bandgap and the enhanced efficiency of DSSCs in the TiO₂-dye-electrolyte system were analyzed. Nd³⁺ doped TiO₂ exhibits the desired results and superior efficiency than the pure and Dy³⁺ doped TiO₂. Thus comparing the materials' morphological and optical properties as well as the solar cell efficiency, Nd³⁺ doped TiO₂ proved to be an improved anode material for the fabrication of DSSCs.

© 2021 Elsevier B.V. All rights reserved.

1. Introduction

One of the greatest challenges poised to the human society is the production of unadulterated renewable energy [1]. This milieu of technology understands indubitably the indispensability of innocuous and renewable energy. For this vacillating future, harnessing the solar light for energy production through Photovoltaic (PV) applications can be a remedy [2]. Dye-sensitized solar cells (DSSCs), as renowned PV systems, exhibit many advantages over other solar cells [3]. TiO₂ is an acclaimed flagship material for the production of cost-effective and eco-friendly anode material [4]. A mixed oxide consisting of TiO₂ as the major phase and RE³⁺ as the dopant phase was prepared to generate a suitable anode material for the enhancement of the efficiency and fabrication of DSSCs. In this work, like Nd³⁺ and Dy³⁺, are doped with TiO₂ to improve the photoelectric conversion efficiency. The DSSCs were fabricated and the efficiencies of them were measured. However, study on the comparison of doping Nd³⁺ and Dy³⁺ with TiO₂ with 2 wt% is not prevalently available in literatures and thus this work will capture the attention of the researchers.

2. Preparation technique

Pure TiO₂ and Rare Earth Element doped TiO₂ were prepared by solution reaction-based tactic. Titanium(IV)isopropoxide (anatase, 99.9%) and acetic acid are taken in the molar ratio of 1:4. Under the magnetic stirring, distilled water (20 M) was added dropwise to obtain the desired solution. The obtained solution was kept in furnace for 100 °C using Teflon autoclave. The well ground product was calcined at 400 °C for 3 h using a heating rate of 5 °C/min to obtain TiO₂ nanoparticles. Similarly RE³⁺ doped TiO₂ samples were synthesized by introducing Neodymium (2 wt%) and Dysprosium (2 wt%) to the above during the stirring process. All chemical reagents used here were obtained from commercial sources with the highest purity hence used without further purification.

3. Preparation of DSSC

0.1 g of prepared materials (TiO₂, Nd³⁺ and Dy³⁺ doped) were mixed with Triton X 100 and ethanol were coated on separated FTO plates using spin coating technique. The coated FTO plates were left to dry at the room temperature. 5 mmol/N719 dye was allowed to spread evenly on the anode FTO glass for 12 h. Another FTO glass was taken and a few drops of H₂PtCl₆ were placed on and permitted to spread evenly and exposed to 350 °C for 25 min to obtain the platinum counter electrode. The two electrodes were sandwiched and through a hole made on the counter electrode

* Corresponding author.

E-mail address: bharathisasa@gmail.com (S. Bharathi Bernadsha).

the electrolyte solution (I^-/I_3^-) was injected to make the DSSC active. Current density–Voltage (J–V) measurements were taken in the presence of atmosphere at room temperature using a Keithley 2400 high current source power meter under white-light illumination from a 500 W Xenon lamp (AM1.5G).

4. Results and discussions

4.1. XRD

The XRD analysis of the crystalline phases provide strong diffraction peaks at $2\theta \approx 25.2^\circ, 37.9^\circ, 48.1^\circ, 54.1^\circ, 54.9^\circ, 62.7^\circ, 68.9^\circ, 70.1^\circ$ and 75.1° assigned to the reflections (101),(004),(200), (105),(211),(204),(116),(220), and (215), respectively, as in Fig. 1A. The Fig. 1A(b&c) show that the incorporation of RE^{3+} (Nd^{3+} and Dy^{3+}) do not distort the morphology of TiO_2 . Any other polymorph of titania also wasn't present. The broadening of diffraction peaks indicates smaller size of nanocrystals. The average size (t) of crystallites was calculated using Scherrer's equation. The size of the grains are 9.2 nm for pure and 7.74 nm for Nd^{3+} and 7.75 nm for Dy^{3+} doped TiO_2 calculated from the plane 101. The size decreases with nominal content of rare earth (RE) compared to its pure form as a repercussion of the presence of RE–O–Ti in the doped samples.

4.2. HR-TEM

HR-TEM images (Fig. 1B) expounds that the nanoparticles present are spherical. The small amount of doping (Nd^{3+} and Dy^{3+}) ions covers the TiO_2 surface to form uneven surface and result in considerable decrease in particle size of the analyte. The particle size calculated is in good agreement with XRD results. Anchoring of Nd^{3+} and Dy^{3+} ion with TiO_2 has produced an expected stimulus on the crystallite structure and morphology of TiO_2 analyte. The

fringes of doped anatase lattice are expanded and showed considerable waviness which were possibly attributed to electric stress, which might originate from the earth ions doping [6,7]. Thus the presence of Nd^{3+} and Dy^{3+} are doped into the lattice of TiO_2 .

4.3. Absorption spectra

Band gap estimation of the samples was examined by optical absorption properties. Fig. 2A show the absorption spectra of the TiO_2 and Nd^{3+} and Dy^{3+} doped TiO_2 respectively. The relationship of the absorption coefficient and the incident photon energy were given by Tauc equation. For finding optical bandgap (E_g), the $\alpha/2$ is extrapolated vs. photon energy for indirect transition mechanism [8]. The insets (Fig. 2B) provide the optical bandgap values of pure TiO_2 , Nd^{3+} doped TiO_2 and Dy^{3+} doped TiO_2 as 3.04, 2.92 and 2.96 eV, respectively.

The results show that the absorption activity of the samples Nd^{3+} and Dy^{3+} doped TiO_2 is wide spread in UV-A, UV-B and visible spectrum region. Thus both the samples are more active to absorb the light compared to undoped TiO_2 . Such an effective band gap dropping due to doping Nd^{3+} and Dy^{3+} may lead to Fermi level reducing, improving the photosensitivity of the samples.

4.4. XPS

Fig. 3(a-c) is the high resolution X-ray Photoelectron Spectroscopy (XPS) of the synthesized samples. Fig. 3a guarantees the presence of Ti, C, O, Dy and Nd, moreover, the impurities are not evident here. It also illustrates that the presence of Neodymium ($Nd3d_{5/2}$) in the surface is more limpid than Dysprosium ($Dy4d_{5/2}$). Fig. 3b assures the presence and location of $Ti2p_{3/2}$ and $Ti2p_{1/2}$ at 458.56 eV and 464.22 eV for Nd^{3+} and Dy^{3+} doped TiO_2 samples [5]. The findings are in conformity with the reference data[a] results that the tetravalent $Ti(Ti^{4+})$ atoms are consistent

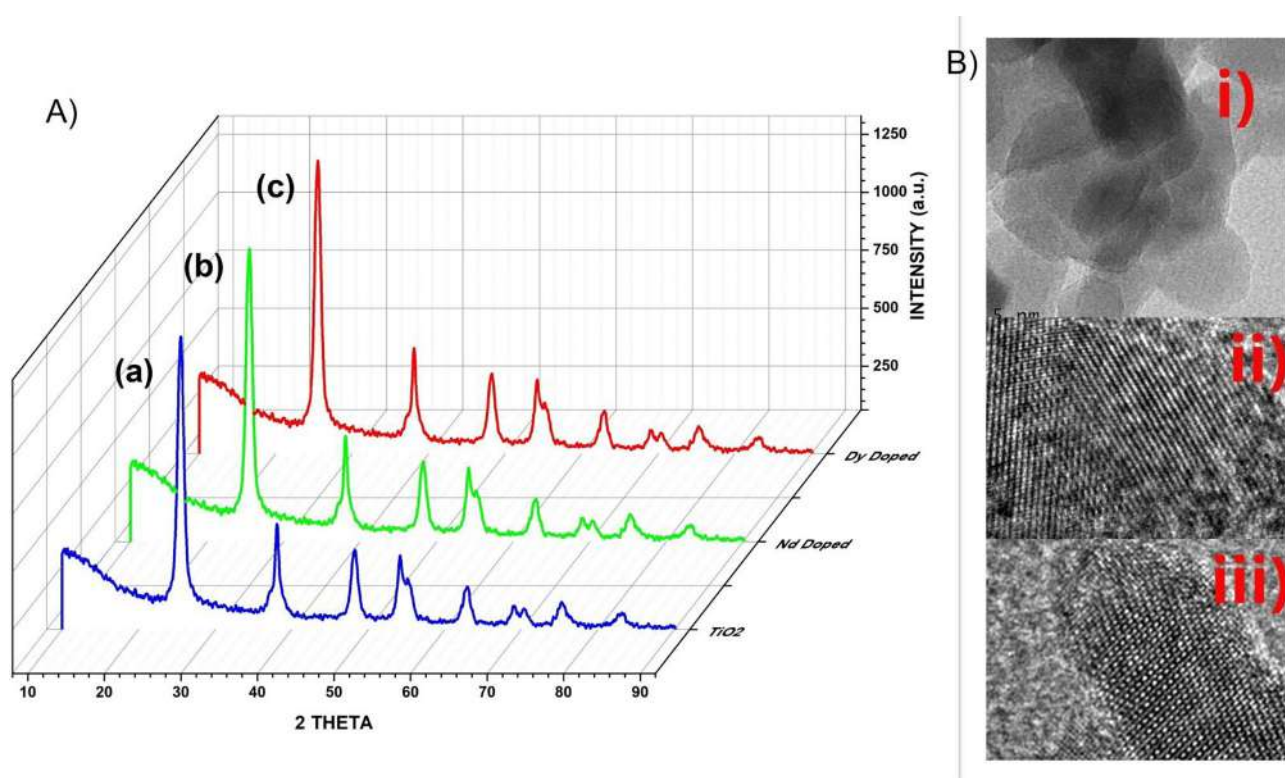


Fig. 1. (A) a) Pure TiO_2 b) Nd Doped c) Dy Doped (B) HRTEM images of i) Pure TiO_2 ii) Nd Doped iii) Dy Doped.

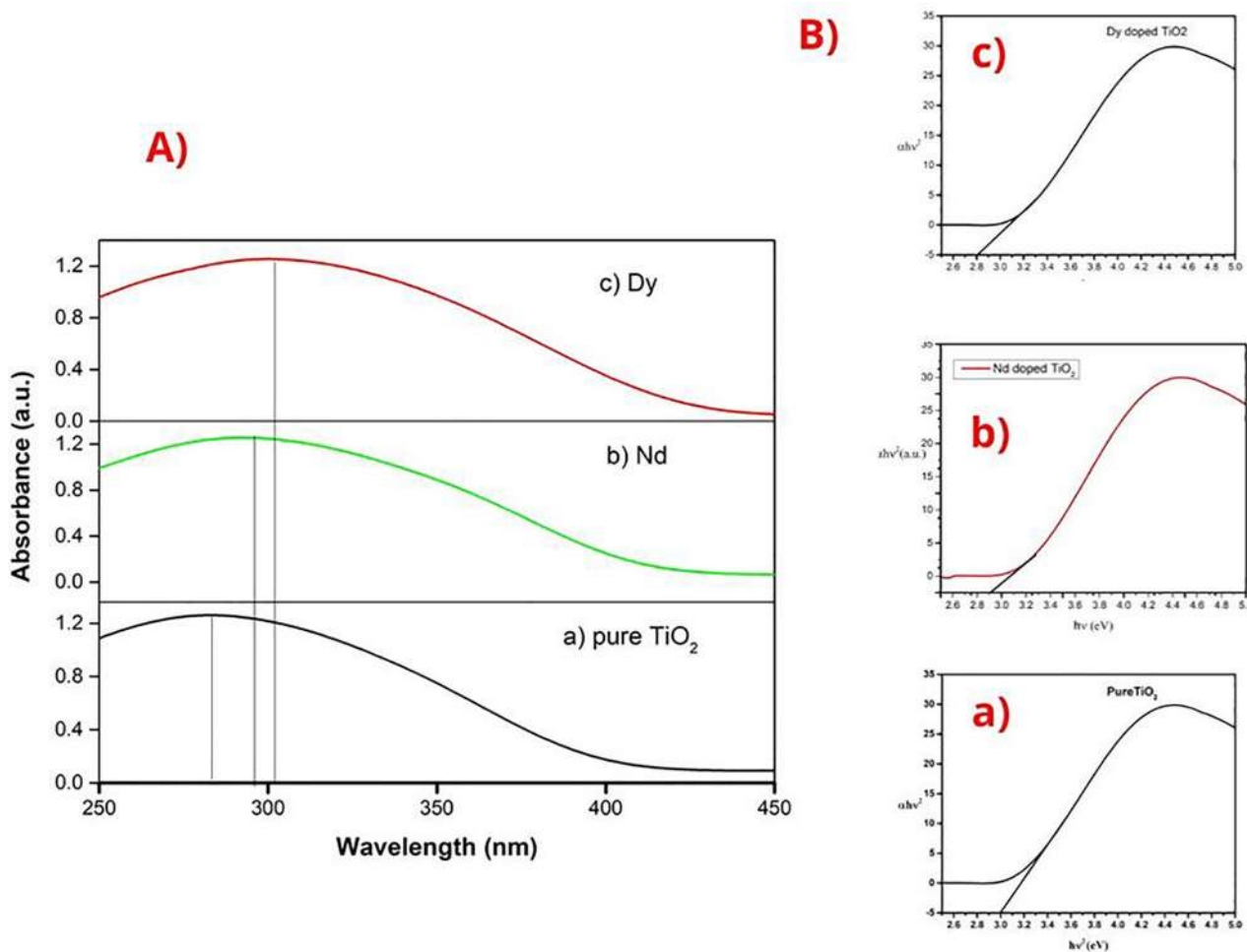


Fig. 2. (A) Absorption spectra of (a) PureTiO₂, (b) Nd Doped (c) Dy Doped.

in TiO₂ lattice. This also proves that Nd³⁺ doped material has higher binding energy shift than Dy³⁺ doped. For Doped Samples, peak values are slightly shifted as Nd³⁺ and Dy³⁺ ions replaced Ti⁴⁺ ions in the lattices. The O1s configuration peaks at 529.68 eV for Dy and 529.74 eV for Nd, observed in Fig. 3c are due to oxygen presence in crystal lattice, on the surface. The shifting of binding energy entails the accumulation and transmission of electrons. The presence of Nd³⁺ and Dy³⁺ ion (4f electrons) in the TiO₂ matrix induced the impurity energy level between the O2p orbital and Ti3d orbital, which narrowed the charge transfer band. Hence the XPS analysis is in good conformity in proving the surface morphology with XRD and HRTEM studies

4.5. I-V characteristics

The Current density-Voltage curves for Pure, Nd³⁺ and Dy³⁺ doped TiO₂ DSSCs are depicted as Fig. 4. The performances of these are provided in Table 1. After the doping the conversion efficiency is obtained in the order of Nd³⁺-TiO₂ > Dy³⁺-TiO₂ > pureTiO₂, due to the changes in the surface. These results show the lower charge recombination sites and enhanced efficiency. The enhanced efficiency is the result of increase in UV-light absorption sensitivity, the positive-shift as decrease in the band gap of Nd³⁺ doped TiO₂ sample and not solely on dye absorption quantity. It results an increased injection driving force of electrons and to improve the

electron injection efficiency from the LUMO of the dye to the TiO₂ conduction band.

5. Conclusion

Nd³⁺ and Dy³⁺ doped TiO₂ were synthesized and their morphological and optical properties were analyzed. The prepared anode materials were utilized to fabricate DSSCs. The Nd³⁺ doped TiO₂ exhibited reduced bandgap (2.92 eV), higher absorption of sunlight and enhanced conversion efficiency (5.48%) when the constructed DSSCs were simulated. This shows that the Nd³⁺ doped TiO₂ as suitable anode material superior to Dy³⁺ doped TiO₂ for the construction of DSSCs.

CRedit authorship contribution statement

S. Bharathi Bernadsha: Conceptualization, Methodology, Investigation, Writing - review & editing, Writing - original draft. **V. Anto Feradrick Samson:** Formal analysis, Writing - review & editing. **J. Madhavan:** Supervision. **M. Victor Antony Raj:** Resources, Project administration.

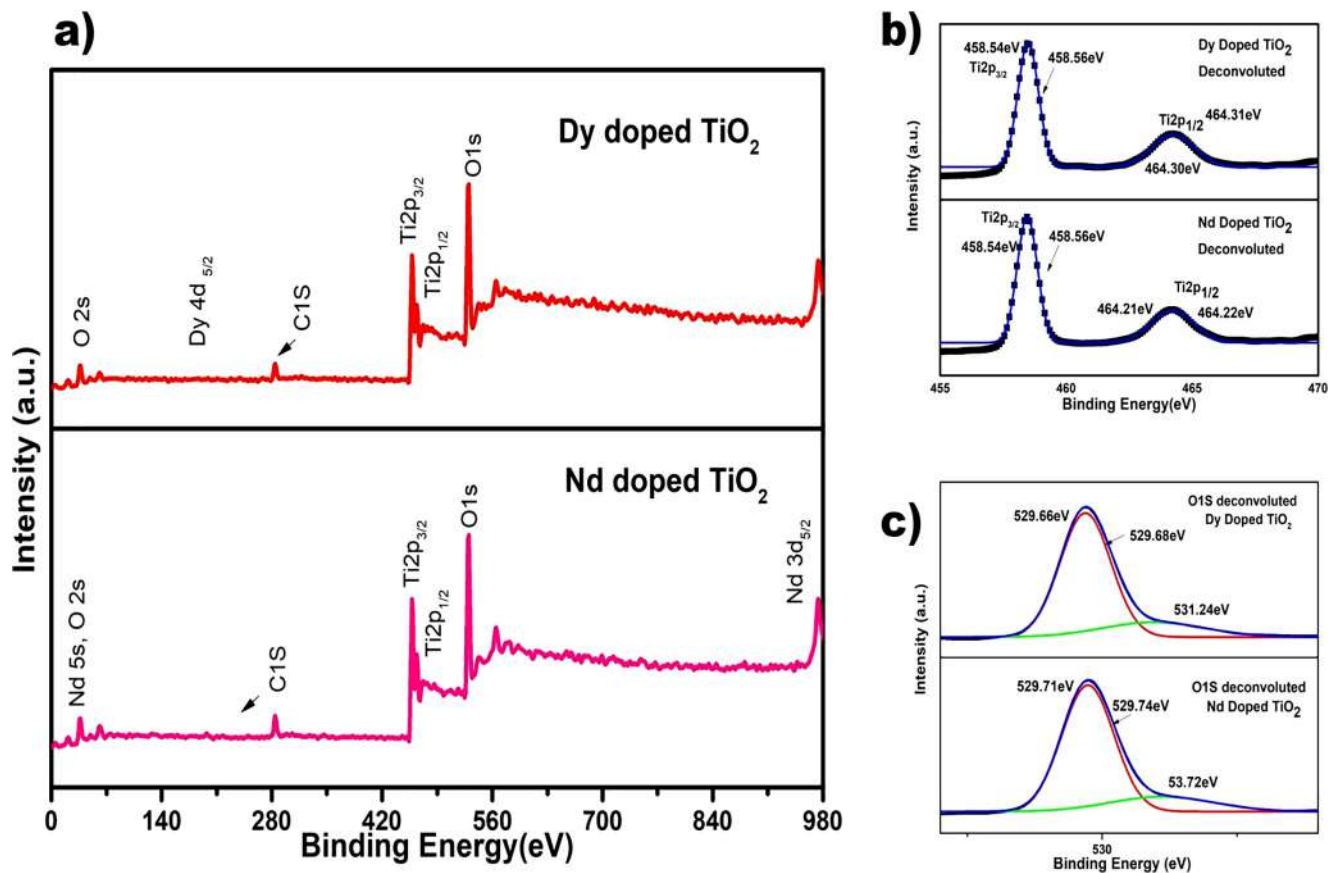


Fig. 3. XPS Spectra of Nd Doped and Dy Doped.

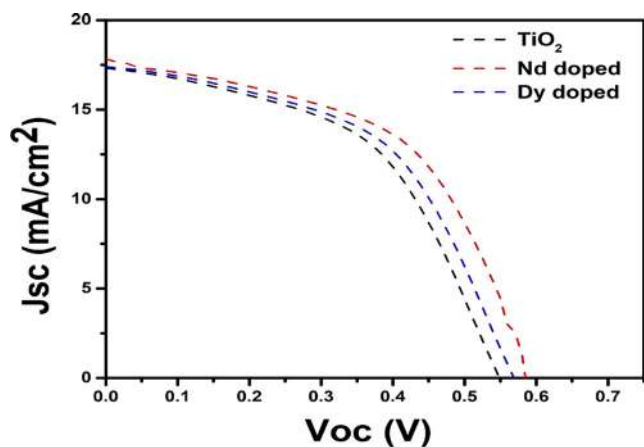


Fig. 4. Current Density – Voltage Curve.

Table 1
Performance of the Dye Sensitized Solar Cells.

Sample	J_{sc} (mA/cm^2)	V_{oc} (V)	Fill Factor (FF)	η (%)
TiO_2	16.91	0.552	0.4494	4.8278
Dy ³⁺ DopedTiO ₂	17.52	0.571	0.4768	5.0885
Nd ³⁺ DopedTiO ₂	17.59	0.589	0.5156	5.4802

Declaration of Competing Interest

The authors declare that they have no known competing financial interests or personal relationships that could have appeared to influence the work reported in this paper.

References

- [1] A. Hagfeldt, G. Boschloo, L. Sun, L. Kloo, H. Pettersson, Dye-sensitized solar cells, *Chem. Rev.* 110 (2010) 6595–6663, <https://doi.org/10.1021/cr900356p>.
- [2] M.A. Green, Y. Hishikawa, W. Warta, E.D. Dunlop, D.H. Levi, J. Hohl-Ebinger, A. W.H. Ho-Baillie, Solar cell efficiency tables (version 50), *Prog. Photovolt.* 25 (2017) 668–676, <https://doi.org/10.1002/pip.2909>.
- [3] M. Grätzel, Photovoltaic and photoelectrochemical conversion of solar energy, *Phil. Trans. R Soc. A* 365 (2007) 993–1005, <https://doi.org/10.1098/rsta.2006.1963>.
- [4] M. Grätzel, Solar energy conversion by dye-sensitized photovoltaic cells, *Inorg. Chem.* 44 (2005) 6841–6851, <https://doi.org/10.1021/ic0508371>.
- [5] <https://srdata.nist.gov/xps/Default.aspx> [accessed on 24th November 2020].
- [6] Z.-L. Liu, Z.-L. Cui, Z.-K. Zhang, Structural phase transformation and UV-vis characterization of Cr doped nanosized titanium dioxide, *Gongneng Cailiao* 36 (2005) 1404–1408, <https://doi.org/10.1016/j.apsusc.2011.01.033>.
- [7] D.O. Klenov, G.N. Kryukova, L.M. Plyasova, Localization of copper atoms in the structure of the ZnO catalyst for methanol synthesis, *J. Mater. Chem.* 8 (7) (1998) 1665–1669, <https://doi.org/10.1039/A802155D>.
- [8] K. Ahmadi, Ali Abdolazadeh Ziabari, K. Mirabbaszadeh, S. Ahmadi, Synthesis of TiO₂ nanotube array thin films and determination of the optical constants using transmittance data, *Superlattices Microstruct.* 77 (2015) 25–34, <https://doi.org/10.1016/j.spmi.2014.10.024>, ISSN 0749-6036.

Analysis of optical and structural properties of Sm³⁺ doped TiO₂: A potential composition for the fabrication of efficient DSSCs

Cite as: AIP Conference Proceedings 2265, 030623 (2020); <https://doi.org/10.1063/5.0016719>
Published Online: 05 November 2020

Bharathi Bernadsha S., Anto Feradrick Samson V., Madhavan J., Victor Antony Raj M., and Prathap. S.



[View Online](#)



[Export Citation](#)



Meet the Next Generation
of Quantum Analyzers

And Join the Launch
Event on November 17th



[Register now](#)



Zurich
Instruments

Analysis of Optical and Structural Properties of Sm^{3+} Doped TiO_2 : A Potential Composition for the Fabrication of Efficient DSSCs

Bharathi Bernadsha S¹, Anto Feradrick Samson V¹, Madhavan J¹, Victor Antony Raj M¹, Prathap. S.^{1, a)}

¹*Department of Physics, Loyola College Chennai-34, India*

^{a)}Corresponding author mic.prathap@gmail.com

Abstract. The Lanthanum series (sm^{3+}) doped semiconducting metal oxide nanoparticles have gained significant attention due to their trustable optical properties. Herewith, TiO_2 and Sm^{3+} doped TiO_2 are prepared by utilizing the facile one-pot hydrothermal method. Structural and morphological studies of the samples are obtained by XRD and HR-TEM. The anatase phase and spherical size morphology of the samples are assured from these above mentioned analyses. From UV analysis it is noted that the band gap decreases (positive shift) due to the doping of Sm^{3+} ions on the surface of TiO_2 . Photo and dark conductivity of both samples linearly increase with applied field which confirms that the positive conductivity of the sample. Comparing to pure TiO_2 , Sm^{3+} doped TiO_2 sample exhibits higher conductivity. Hence, Sm^{3+} doped TiO_2 sample could be a potential photo anode for DSSCs applications.

INTRODUCTION

In this era of technology we human beings most of the times worry about the efficiency than the sustenance. Thus sustainable energy production to replace the depleting fossil fuel and other environmental hazardous fuels we need to identify the suitable material. Exploiting the solar energy, converting it into useful modes and storing them up are some of the laudable choices for the sustainable energy utilization [1,2,3]. This work concentrates on employing the rare earth elements (REEs), especially, Samarium (Sm^{3+}) to influence the structure and morphology of the low cost and efficient TiO_2 . To discern the efficiency of Sm^{3+} doped TiO_2 , its properties are to be investigated to identify its potentiality to be an efficient material to fabricate DSSC as a sustainable energy producer. This present work focuses on the comparative study of structural, optical and photo conducting properties of pure and Sm^{3+} doped TiO_2 nanoparticles.

PREPARATION OF TIO_2 NANOPARTICLES

TiO_2 and (Sm^{3+}) doped TiO_2 was prepared by a facile one-pot hydrothermal method. In briefly, Titanium (IV) isopropoxide and acetic acid taken in the molar ratio of 1:4, after that 20M of distilled water was added drop wise under the magnetic stirring to obtain a transparent solution. Then the obtained solution was transferred into Teflon autoclave and it was kept in 180°C for 24h. The obtained powder was ground in a mortar pestle. The obtained product was calcined at 400°C for 3 hours using a heating rate of 5°C/min to obtain TiO_2 nanoparticles. Similarly Sm^{3+} doped TiO_2 samples were synthesized by adding samarium oxide to above synthesis. The material is characterized by X-ray diffractometer (XRD),HR-SEM, UV-DRS spectrometer and KEITHLY 6517A electrometer.

STRUCTURAL ANALYSIS

Crystallographic structure and morphology of the synthesized sample is characterized by XRD and HR-TEM. Fig.1 shows the XRD pattern of TiO_2 and (Sm^{3+}) doped TiO_2 samples. The XRD pattern of both samples show good crystallinity and the peaks are indexed at $2\theta \approx 25.2^\circ, 37.9^\circ, 48.1^\circ, 54.1^\circ, 54.9^\circ, 62.7^\circ, 68.9^\circ, 70.1^\circ$ and 75.1° should be attributed to the reflections from (101), (004), (200), (105), (211), (204), (116), (220), and (215) planes of anatase phase of TiO_2 [4]. While compared with TiO_2 nanoparticles, (Sm^{3+}) doped TiO_2 sample shows a minimal difference in diffraction angles were observed, indicating that the incorporation of (Sm^{3+}) ion into the TiO_2 phase. The Debye Scherrer equation was used to calculate the average crystallite size is found to be 18.38 nm TiO_2 and 21.62 nm for (Sm^{3+}) TiO_2 doped respectively. Figure 2(a) and (b) display the typical HR-TEM images of as synthesis samples. The figure reveals that the nanoparticles are in spherical in shape. Figure 2(b) indicates that the small amount of doping (Sm^{3+}) ions covers on the TiO_2 surface to form some uneven surface morphology. From HR-TEM results, the particle size is calculated 15.62 nm for TiO_2 and 19.71 nm for (Sm^{3+}) TiO_2 which is in good agreement with XRD results. In conclusion, anchoring of Sm^{3+} ion with TiO_2 NPs has produced an expected stimulus on the crystallite structure and morphology of TiO_2 NPs.

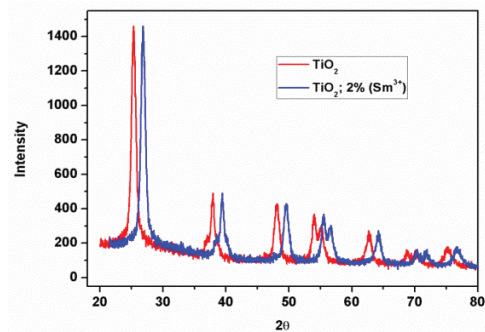


FIGURE : 1 XRD pattern of TiO_2 and (Sm^{3+}) doped TiO_2 samples

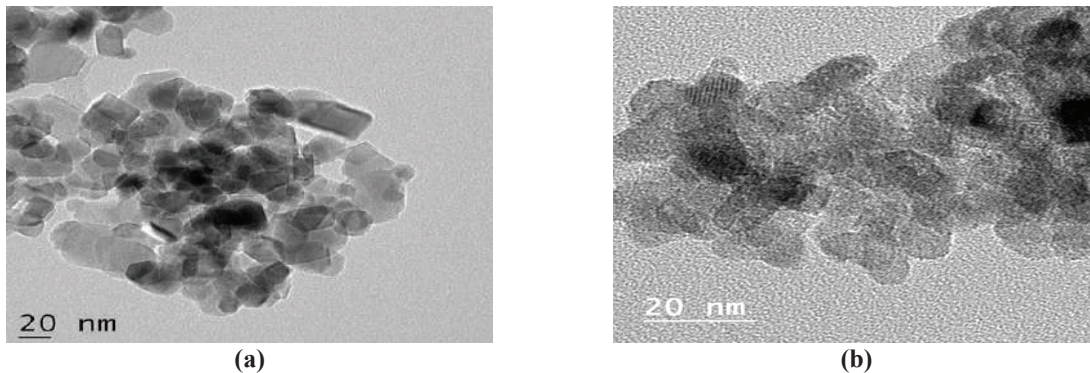


FIGURE: 2 (a) HR-TEM image of TiO_2 and (b) HR-TEM image of (Sm^{3+}) doped TiO_2

UV-ANALYSIS

The UV studies have been measured to examine the optical absorption assets of as synthesized samples. Figure 3 (a) and (b) show the UV absorption spectra of the TiO_2 and (Sm^{3+}) doped TiO_2 samples respectively. It is observed that the spectrum of (Sm^{3+}) doped TiO_2 shifted towards higher wavelengths and an enhancement of visible light absorption due to the doping of (Sm^{3+}) . The extension of light absorption shifted to visible-region compare to pure TiO_2 which indicates that narrowing band gap energy of TiO_2 , which is confirmed by Tauc-Plot function vs the energy of exciting light [5]. The calculated band gaps were 3.04 eV for TiO_2 and 2.98eV for (Sm^{3+}) TiO_2

respectively. The narrowing band gap must be credited to the incorporation of (Sm^{3+}) ion into the TiO_2 surface. The extension of light absorption suggested that the (Sm^{3+}) doped TiO_2 could have higher optical activity.

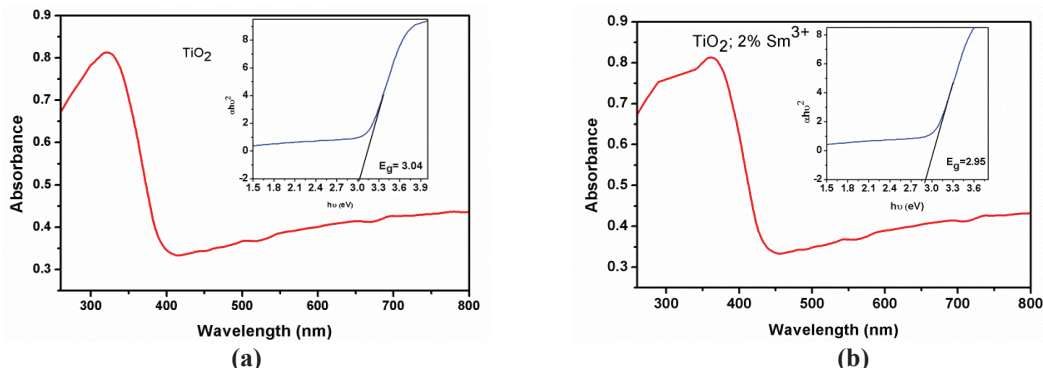


FIGURE: 3(a) UV graph of TiO_2 and (b) (Sm^{3+}) doped TiO_2

PHOTOCONDUCTIVITY STUDIES

Photo conductivity is an essential study to determine the conducting nature and gain or loss of charge carriers within the sample under the presence of light with applied electric current (V) [6]. The conductivity studies of the as synthesized TiO_2 and (Sm^{3+}) doped TiO_2 samples were carried out in the presence and absence of light respectively. Figure 4 (a) and (b) show the dark and photocurrent measurements of the TiO_2 and (Sm^{3+}) doped TiO_2 samples respectively. With an increasing electric field, rise in both photo and dark current of the synthesized samples confirms the ohmic nature positive photoconductivity of the samples. This observed linear increase in current mainly due to photo generation of charge carriers within the sample. The conductivity of the (Sm^{3+}) doped TiO_2 samples exhibits higher conductivity than pure TiO_2 which due to lower bandgap of the material. Since lower band gap materials has transfer of electron from the valence band to the conduction band easier. Therefore as synthesized (Sm^{3+}) doped TiO_2 would be a potential photoanode material for DSSCs

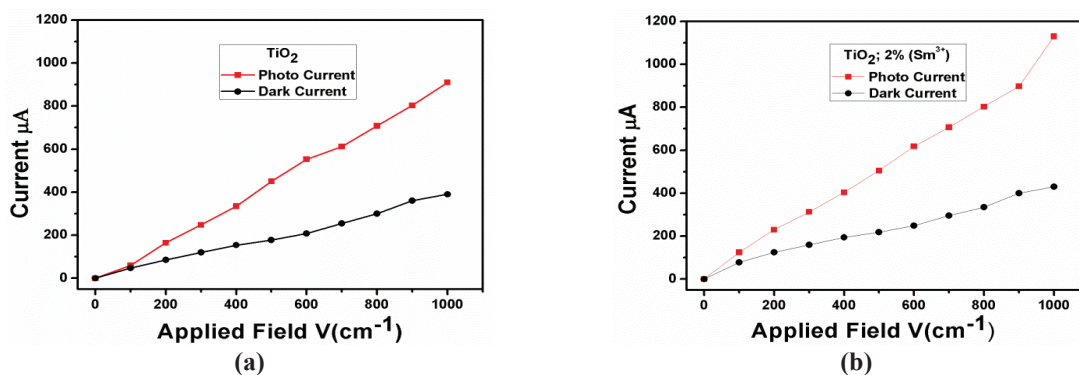


figure: 4 (a) Photo conductivity of TiO_2 and (b) (Sm^{3+}) doped TiO_2

CONCLUSION

In summary, both TiO_2 and (Sm^{3+}) doped TiO_2 nanoparticles are successfully prepared via simple hydrothermal method. XRD analysis exhibits that as-synthesized nanoparticles are good in crystallinity and possess anatase structure. The HR-TEM images exhibit that the nanoparticles are spherical in size morphology and the results are in good agreement with XRD results. The extension of light absorption in the higher wavelengths of Sm^{3+} doped TiO_2

indicates that the samples have higher optical activity. Linear increase in current vs applied field reveals that the samples host positive photoconductivity (positive shift of CB).

REFERENCES

1. Bao, Ruiyu, Runfu Li, Chen Chen, Hua Wu, Jianxin Xia, Chunlin Long, and Hua Li. [Journal of Physics and Chemistry of Solids](#) 126 (2019): 78-84.
2. Zikriya, Mohamed, Y. F. Nadaf, P. Vijai Bharathy, and C. G. Renuka, [Journal of Rare Earths](#) 37, no. 1 (2019): 24-31.
3. Arasi, S. Ezhil, M. Victor Antony Raj, and J. Madhavan. [Journal of Materials Science: Materials in Electronics](#) 29, no. 4 (2018): 3170-3177.
4. Zanatta, A. R., D. Scoca, and F. Alvarez, [Journal of Alloys and Compounds](#) 780 (2019): 491-497.
5. Pugazhendhi, K., Steven D'Almeida, Tenzin Tenkyong, B. Praveen, D. J. Sharmila, and J. Merline Shyla. [Materials Letters](#) 222 (2018): 29-32.
6. Ragu, R., PS Latha Mageshwari, M. Akilan, J. P. Angelena, and S. Jerome Das, [Materials in Electronics](#) 30, no. 2 (2019): 1670-1676.



Design, synthesis novel Pyrazolopyridine derivatives and CREBBP bromodomain inhibitors docking and molecular dynamics

Saamanthi M^{a,*}, Aruna S^a, Girija R^a, D. Vinod^b

^aPG & Research Department of Chemistry, Queen Mary's College, Chennai 60000, India

^bVellore Institute of Technology, Vellore 632014, India

ARTICLE INFO

Article history:

Received 28 December 2020

Received in revised form 2 February 2021

Accepted 12 February 2021

Available online 29 March 2021

Keywords:

Pyrazolopyridine

Anti-cancer

Bromodomains

Molecular dynamics

ABSTRACT

The overall synthetic approach was used to prepare a series of novel compounds pyrazolopyridine. Because of its high efficiency and selectiveness, the combined molecules of anticancer agents have attracted considerable interest. IC50 values were determined against cell line U937, the results obtained have the potential effects against cancer cell line. The cell potency of cell line best compounds 4a IC50 = 62.5 μ M, 5a IC50 = 62.5 μ M, 4b IC50 = 31.2 μ M, 4e IC50 = 31.2 μ M), selectivity, and in vivo. Further, the molecular docking studies discovered that substituted pyrazolo[4,3-c]pyridine derivatives are good anti-cancer activities in the medicinal field. These compounds have potential new frameworks for the advancement of cancer therapy through simpler synthesis and substantial biological activity. In the cancer lines and vivo compound **4f** was shown to be anticancer effect corresponding to antitumor activity of an AML type cancer. Molecular docking with the ligands, the RMSD value was calculated, the protein with the least RMSD was found to be 5KTU screening with 20 small molecules.

© 2020 Elsevier Ltd. All rights reserved.

Selection and peer-review under responsibility of the scientific committee of the International Conference on Mechanical, Electronics and Computer Engineering 2020: Materials Science.

1. Introduction

Worldwide cancer is most commonly diagnosed malignancies leading to deaths [1]. One of the most important methods in the medicine production of the pharmaceutical industry is the chemical modification of biologically active heterocyclic compounds. Pyrazolopyridine is a potent class in heterocyclic compounds which possess a wide spectrum of biological activities [2]. The Bromodomains of CBP/EP300 are targeted in transcriptional regulators factor in human cancer immunotherapy [4]. The BET family is Inhibition of bromodomains is exposed to have probable therapeutic advantage in cancer, inflammation, immunology [5]. Acetyl lysine protein modifications are known as a transcriptional regulation of Bromodomains [6]. Extremely performant inhibitor for and use in cell-based transcriptional applications of CREB binding protein (CBP) bromodomain. Two primary HATs have been used in the gene regulations CBP and p300 (CREBBP or KAT3A or KAT3B) [7]. In Cell biology T cell regulation of the CREBBP/EP300 bromodomains is a major role and T Cells are used in cancer immunotherapy [8]. Post translational change in the function of bromodomains

in protein molecules in acetylated lysine on histones, important function [9]. The CREBBP Bromodomain ligands with cation π interaction are useful tools [10]. Pyrazolopyridines are linked to DNA and prevent cancer cell lines from growing [11]. For non-BET bromodomain have the proteins been used in the HIV and cancer diseases chemical Probes potentially lead to drug discovery [12]. Bromodomains that have the domains are BCPs, HATs and HDAC are effectively used in cancer therapy [13]. BET bromodomain has reflective anticancer and anti-inflammatory in the chemical probes used in biological observed compounds in clinical trials [14].

In human cancer with p53 and acetylation dependent damage and DNA damage, the CREBBP bromodomain binds to KAc382 [15]. The BET family has the schoffed bromodomain BRD2, BRD3, BRD4 are binding specificity very strong and prospective therapeutic benefit [16]. The CBP/p300 bromodomains are used in regulators of cell growth acetyl-lysine protein inhibitor [17]. The oncogenic fusion in leukemia is MOZ acetyl transferees to detect CBP/p300 domain [18,19]. The AML1-ETO fusion protein interacts with p300 and transcription regulates in AML1-ETO aim gene inhibitor of DNA binding [20]. Screening of a small molecular library identifies the compound interaction of p 53 and KAc382-CREBBP at 100 and 50 μ M respectively [21]. The first bromodomain of

* Corresponding author.

E-mail address: samanthishanmugam92@gmail.com (S. M).

BRDT-1 is used to separate the male cell and c-Myc-dependent cancers from the novel men's contraceptives [21]. In BRD4 tumour activation on the in vivo micro-level, tumour and lung growth reductions in chromatin biology and gene transcription in the mice and human BRDs [22]. The creation of a series of CREB-binding protein and bromodomain silico-discovery and the efficacy of antitumor activity is listed below Figs. 1–4.

Molecular docking plays an important role in discovering its affinity and function at its site [23] for the small molecule of its target protein. Molecular dynamics simulations were successfully used to classify biologically active antitumor activity, including inhibition and stability, as a method for medicinal chemistry [24]. In this study microsecond molecular simulation is used to binding site of RVX-208 with bromodomain of BET proteins [25]. Molecular dynamics is ligand design focused on the potential molecule for the CBP bromodomain and high selectivity [26].

2. Result and discussion

In general, the synthesis yields were pretty good and the materials were fairly usable. While the syntheses of most analogues used this general synthesizing path, the Experimental Section may use other methods for particular substitution patterns. The compounds were typically clock purified and their structures determined by the FT-IR, ¹H NMR, ¹³C NMR, mass spectroscopy and elementary analyses. Elements were used to treat the compounds. Claisen-schmidt condensation [27] was used to prepare starting aldehydes, ketones needed for further transformation.

2.1. Synthesis of substituted chalcones

A mixture of substituted aldehydes (0.02 mol) and 1-methyl-4-piperidone (0.01 mol) with 10 percent NaOH and 50 ml ethanol was prepared and the solution of the reaction blend continuously mixed for 15 h at room temperature when the solution was poured to ice cubes to increase precipitation. For draining excess sodium hydroxide from the product **3a(1–10)**. The compound is purified and recrystallized with ethanol.

Synthesis of substituted pyrazolo pyridine derivatives.

Equal moles of substituted chalcone and semicarbazide hydrochloride with 10% sodium hydroxide were refluxed at 80 °C in a heating mantle for 6hrs produced, substituted pyrazolopyridine **4a(1–7)**. All the compounds are purified by recrystallized ethanol.

2.2. Computational details

2.2.1. Docking results

For medicinal chemistry to discover the drug molecule to identify novel drug molecular docking technology. The molecular docking research aims to specify the best relationship between ligand and stable molecules [28]. Twenty ligand structures were

described for docking. Three separate docking programmes, SP Glide, and the XP Glide, Prime MM-GBSA, were used to improve prediction accuracy. These ligands were used as native docking systems for the calculation of docking conformations. In the course of this process, Xscore was accompanied by a molecular docking process, which was effective and accurate in the prediction of protein-linked free energies (Table 1). The study of these effects of docking simulations will reliably predict the activities of the ligand in most binding energy ratings.

Docked ligands 4a, 5a, pyrazolo[4,3-c]pyridine derivatives showed the best range of Docking score, XP Gscore and Binding energy (Table 1).

2.2.2. Molecular dynamics results

Molecular dynamics is now a valuable method to predict the molecular system's normal motion. It explains protein structure and investigates the stability of the compounds. However the large conformational space is more stable at lower simulated temperature [29]. The molecular dynamics simulations time scale is 10–100 nsec with the protein and solvent system good [30]. In drug development, it is a very useful method for the synthesis of new drug molecules with ligand and protein molecule [31]. The findings of the molecular dynamic are suggested to strengthen the polar interactions with the binding site side chain Asn1168. Acetyllysine ligand is in this case a hydrogen bond donor and an acceptor for the MD simulations amide side chain with Asn1168 Tables 2–8.

2.2.3. Protein-Ligand RMSD

The CREBBP binding mode by interaction solvent MD compound simulations. When 1 μs MD runs independently, random speeds are available. Compound 4a root/mean-squared deviation in time series (RMSD) shows binding mode and power, while variations of magnitude in both runs are observed in the MD (Fig. 5).

Additional support for MD simulations in docking and binding is an important component. The study of the interaction motifs on the MD trajectories is used efficiently for the optimization process.

2.3. Biological studies

In order to develop anti-cancer activity, biological trials are used. Nine cancer types derived in the human tumour cell lines: breast, leukaemia, melanoma, lungs, colon, central nervous system, ovarian, kidney, and prostate cancers. Thanks to its high strength and selectance, combined molecular anti-cancer agents are of particular interest. The human cell lines against leukaemia are used for in vitro anti-cancer activities for synthesized compounds. Compound 4a IC₅₀ = 62.5 μg demonstrated a strong efficacy on all the tested drugs, in vitro antitumor testing of the new pyrazolopyridines against leukaemia. Dox for leukaemia cell lines was the standard treatment taken.

3. Experimental

3.1. Materials and methods

Different spectroscopic instruments have confirmed the structure of the prepared compounds. Merck bought all initial supplies. In spectral analysis, IR spectra were detected with potassium bromide pellets for perkin-elmer, ¹H NMR and ¹³C NMR spectra for a 400 MHz spectrometer, while internal ppm chemical changes for TMS were identified. The spectrum was verified by spectral analyses. Mass spectra were reported at 70 eV. Column chromatography was performed on (Merck) silica gel 60 (particle size 0.06 mm–0.20 mm). Thin-layer chromatography with Merck silica gel 60 F254 aluminium sheets tested the purity of the compounds. Spots

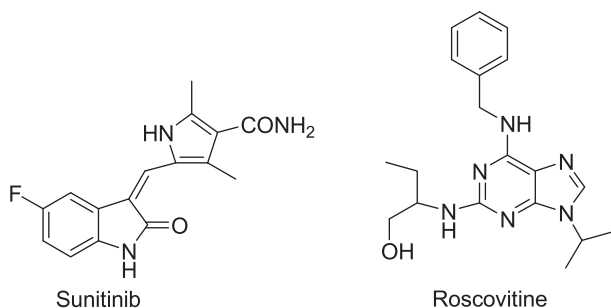


Fig. 1. Potent anticancer compounds.

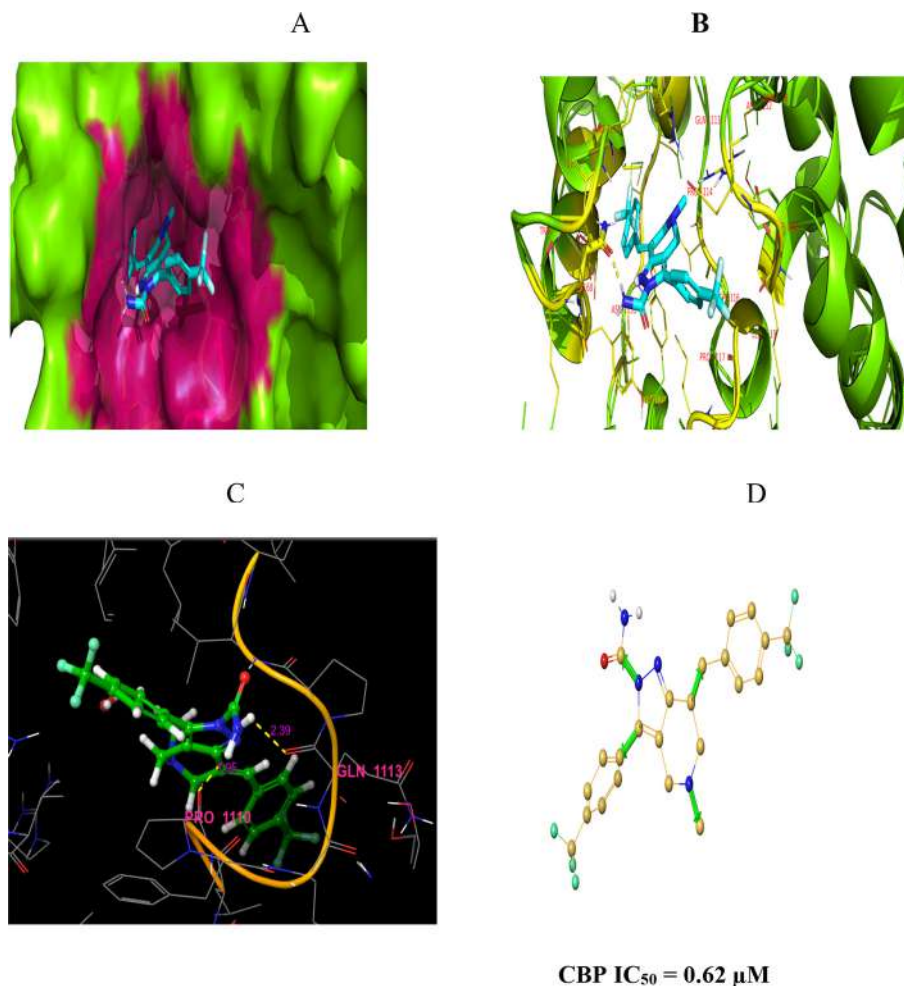


Fig. 2. Schematic representation of 4a in the binding pocket 1abcd, The CBP bromodomain co-crystal structure and D (1.38 Å Resolution; 5KTU PDB Code).

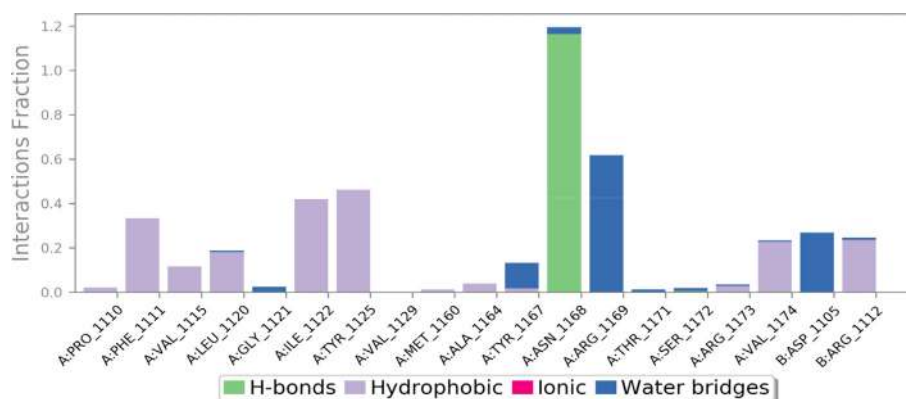


Fig. 3. Lead molecule protein-ligand interaction of compound 4a.

were detected under UV light by their absorption. All compounds prepared in this paper are new and verified with spectral data Figs. 6–12.

3.2. Computational studies

3.2.1. Preparation of ligands

Structures of ligands sketched and saved in SDF format were imported via selecting files. The imported ligands 4a-g, 5a were

set to minimize under force field OPLS3e. Minimization calculations can be performed on all structures of pyrazolo[4,3-c]pyridine derivatives.

3.2.2. Preparation of protein

X-ray crystalline Protein structure 5KTU has been imported into the workspace from the Protein Data Bank (PDB), which is further revised under OPLS3E's force field and amended to eliminate

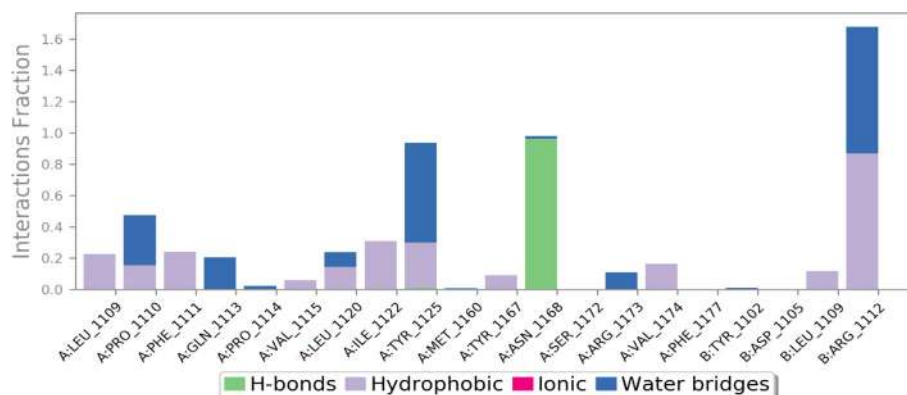


Fig. 4. Co-Crystal 5KTU protein–ligand interaction CREBBP inhibitors.

Table 1

Glide Docking and binding energy scores.

Title	docking score	Glide gscore	Glide emodel	XP GScore	Glide energy	Glide emodel
5KTU	-6.612	-6.612	-6.612	-6.612	-42.057	-59.809
4a	-6.237	-6.237	-6.237	-6.237	-35.312	-49.981
5a	-5.98	-5.98	-5.98	-5.98	-34.8	-49.39
4d	-5.572	-5.572	-5.572	-5.572	-31.043	-47.634
4b	-5.468	-5.468	-5.468	-5.468	-31.746	-40.129
4f	-4.96	-4.96	-4.96	-4.96	-26.952	-39.954
4e	-4.032	-4.032	-4.032	-4.032	-31.793	-45.413
4c	-3.946	-3.946	-3.946	-3.946	-34.717	-48.26

Table 2

Interactions with Amino Acids for the Synthesized Compound against CREBBP Bromodomain.

Compounds	Hydrogen bonding	Hydrophobic interaction	Water bridges
4a	Asn1168	Pro1110, Phe1111, Val 1115, Leu1120, Ile 1122, Tyr 1125, Ala 1164, Val 1174	Gly1121, Tyr1167, Arg1169, Asp1105, Arg 1112
5KTU	Asn1168	Leu1109, Phe1111, Ile1122, Val1175, Leu1120, Tyr1167, Val1174, Leu1109	Gln1113, Tyr1125, Arg1112, Pro1110

Table 3

IC₅₀ of the tested compounds on leukemia cancer.

Compound no	IC ₅₀ (µg /mL)
4a	62.5
4b	31.2
4e	31.2
5b	62.5
Standard-DOX	15.6

Table 4

Anticancer effect of 4a on U937 cell line.

S. No	Concentration (µg/ml)	Dilutions	Absorbance (O.D)	Cell viability (%)
1	1000	Neat	0.624	29.55
2	500	1:1	0.726	34.39
3	250	1:2	0.829	39.27
4	125	1:4	0.928	43.96
5	62.5	1:8	1.039	49.21
6	31.2	1:16	1.150	54.47
7	15.6	1:32	1.261	59.73
8	7.8	1:64	1.352	64.04
9	Cell control	-	2.111	100

unnecessary chains and residues. The results were monitored in the job monitor.

3.2.3. Molecular Docking

For molecular docking, pyrazolo[4,3-c]pyridine are chosen. Both lead compounds displayed strong binding energy, interactions, and lower free energy values, which suggested a more heat-friendly relationship. With regard to Glide docking, the protein preparation Wizard in the Schrodinger suite prepared 5KTU crystal structures. Before docking with the active site determined by the location of the crystal ligand, receptor grids were subsequently created. 5KTU crystal structures, as described in the receptor structure and the position of an active location in the box, were imported into Glide. For grid generatio, the PLS3e force field was used. For docking studies with critical residues, the regular precision (SP) and the extra precision (XP) protocols were set in order to achieve accurate performance. All other parameters were retained as the default value for Prime MM-GBSA.

3.3. Molecular dynamics

The full computational work was carried out with Schrodinger suite (SMDD Suite 2018–2, Schrödinger, LLC, New York, NY, 2018).

Table 5
Anticancer effect of 4b on U937 cell line.

S. No	Concentration ($\mu\text{g/ml}$)	Dilutions	Absorbance (O.D)	Cell Viability (%)
1	1000	Neat	0.667	31.59
2	500	1:1	0.749	35.48
3	250	1:2	0.831	39.36
4	125	1:4	0.912	43.20
5	62.5	1:8	0.994	47.08
6	31.2	1:16	1.118	52.96
7	15.6	1:32	1.200	56.84
8	7.8	1:64	1.282	60.72
9	Cell control	-	2.111	100

Table 6
Anticancer effect of 4e on U937 cell line.

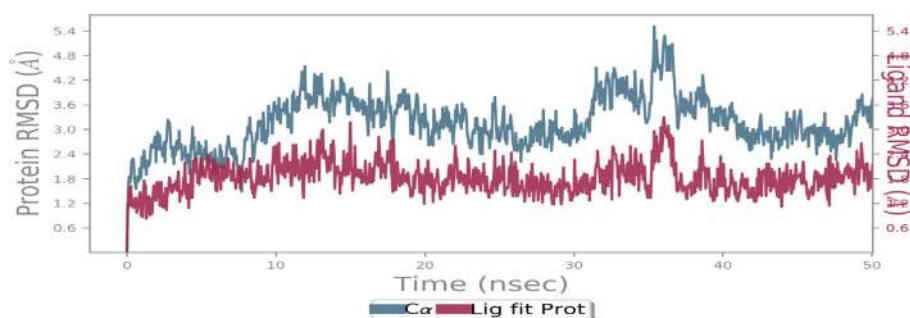
S. No	Concentration ($\mu\text{g/ml}$)	Dilutions	Absorbance (O.D)	Cell Viability (%)
1	1000	Neat	0.665	31.50
2	500	1:1	0.747	35.38
3	250	1:2	0.830	39.31
4	125	1:4	0.926	43.86
5	62.5	1:8	1.002	47.46
6	31.2	1:16	1.103	52.25
7	15.6	1:32	1.201	56.89
8	7.8	1:64	1.497	70.91
9	Cell control	-	2.111	100

Table 7
Anticancer effect of 5a on U937 cell line.

S. No	Concentration ($\mu\text{g/ml}$)	Dilutions	Absorbance (O.D)	Cell Viability (%)
1	1000	Neat	0.626	29.65
2	500	1:1	0.728	34.48
3	250	1:2	0.833	39.45
4	125	1:4	0.934	44.24
5	62.5	1:8	1.051	49.24
6	31.2	1:16	1.168	55.32
7	15.6	1:32	1.285	60.87
8	7.8	1:64	1.382	65.46
9	Cell control	-	2.111	100

Table 8
Anticancer effect of Sample Dox on U937 cell line.

S. No	Concentration ($\mu\text{g/ml}$)	Dilutions	Absorbance (O.D)	Cell viability (%)
1	1000	Neat	0.036	4.77
2	500	1:1	0.095	12.59
3	250	1:2	0.142	18.83
4	125	1:4	0.204	27.05
5	62.5	1:8	0.265	35.14
6	31.2	1:16	0.320	42.44
7	15.6	1:32	0.381	50.53
8	7.8	1:64	0.452	59.94
9	Cell control	-	0.754	100

**Fig. 5.** Various binding modes of lead protein ligand RMSD compound 4a.

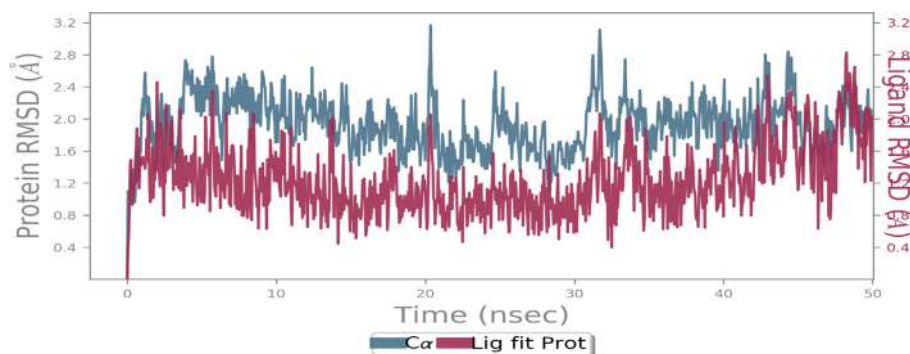


Fig. 6. Structural stability and several modes of binding CREBBP bromodomain with the RMSD co-crystal protein–ligand in 50 ns.

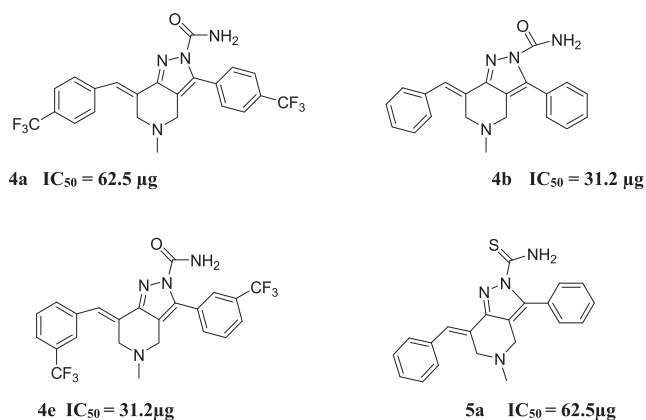


Fig. 7. Pyrazolopyridine cores tested and found potential against U937 Cell line Leukemia inhibition.

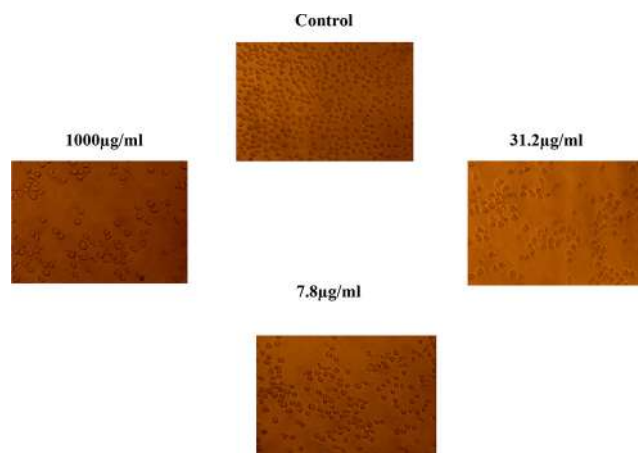


Fig. 9. Pyrazolopyridine Anticancer effect of 4b on U937 cell line.

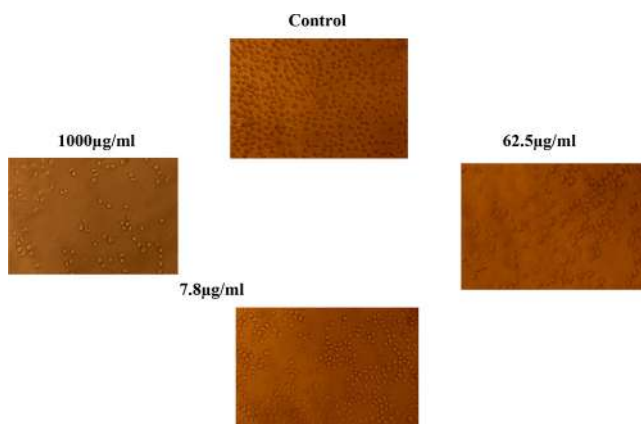


Fig. 8. Pyrazolopyridine Anticancer effect of 4a on U937 cell line.

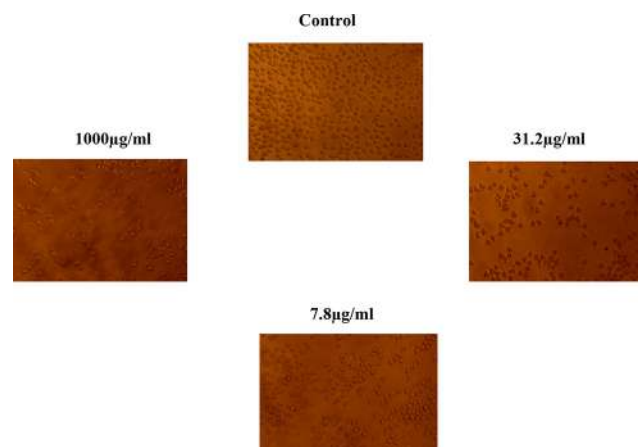


Fig. 10. Pyrazolopyridine Anticancer effect of 4e on U937 cell line.

3.4. Biological testing

3.4.1. In vitro evaluation of the anticancer activity

The NCI protocol mentioned elsewhere has been used to conduct primary anticancer tests. The compounds have been applied at a single level and the cell cultures have been invaded for 24 h. The results for each compound are shown in comparison to untreated control cells as a percent increase (GP-percent). The percentage range of growth among cancer cell lines shows the lowest and the highest percentage.

- (E)-7-(4-(trifluoromethyl)benzylidene)-3-(4-trifluoromethylphenyl)-4,5,6,7-tetrahydro-5-methyl pyrazole[4,3-c]pyridine-2-carboxamide: 4a

Equal moles of chalcone, semicarbazide were treated with 10% sodium hydroxide solution and refluxed for 6hrs at 80 °C mixture (3E,5E)- 3,5-(trifluoromethyl)dibenzylidene –1-methylpiperidin-4-one was treated with semicarbazide with 10% sodium hydroxide were refluxed at 80 °C in a heating mantle for 6hrs produced. Yield : 83%, Yellow solid, 160–161 °C, FTIR (KBr, cm^{-1}) : 3456 (NH₂), 3166 (aromatic C–H), 2281 (CN), 1679 (C = O), 1600 (C = C), 1063 (C–F). ¹H NMR (400 MHz, CDCl₃): δ 2.27 (s, NCH₃), 2.34, (s, NCH₂) 3.81 (s, 2H, CH₂), 7.18–7.26 (m, Aromatic H), 7.65 (NH₂). ¹³C NMR (400 MHz, CDCl₃): δ 20.82, 44.75, 56.33, 125.67, 126.96, 128.71, 130.17, 132.45, 134.00, 136.44, 140.54, 185.20. Mass *m/z* (ESI) : 480.14. Elemental analysis: Calcd % C 57.50, H 3.78, N 11.66, O 3.33, F 23.73. Found C 57.55, H 3.76, N 11.67, O 3.34, F 23.74.

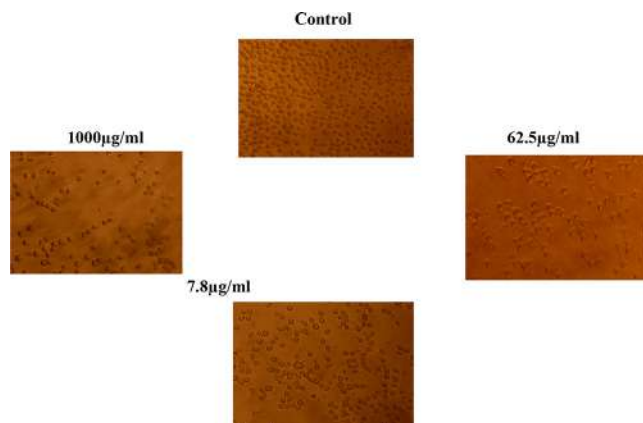


Fig. 11. Pyrazolopyridine Anticancer effect of 5b on U937 cell line.

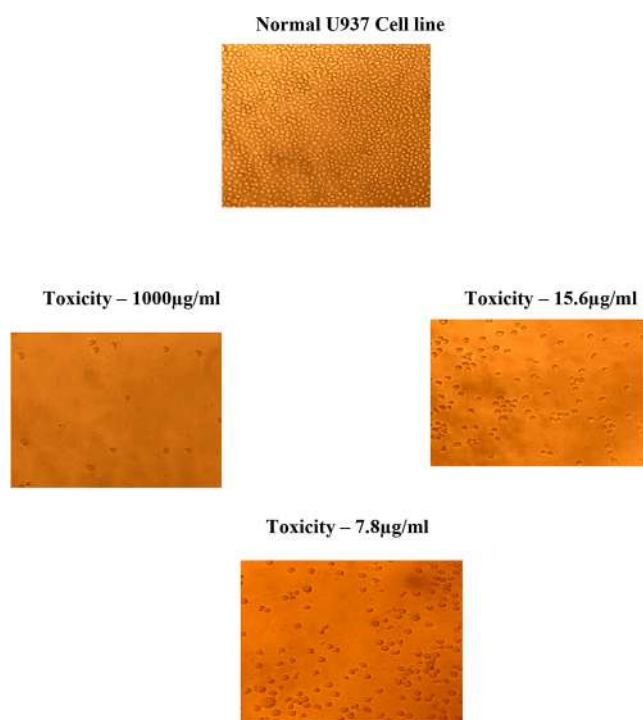


Fig. 12. Anticancer effect of Sample Dox on U937 cell line.

- (E)-7-Benzylidene-4,5,6,7-tetrahydro-5-methyl-3-phenylpyrazole[4,3-c]pyridine-2-carboxamide 4b:

Yield: 87%, Yellow solid ,m.p : 110, FTIR (KBr,cm⁻¹): 3444 (NH₂), 3165 (aromatic C-H), 2235 (CN), 1670 (C = O), 1620 (C = C). ¹H NMR (400 MHz, CDCl₃) : δ 2.27 (s,NCH₃), 3.62 (s,2H, CH₂) 6.9 1 (d,β CH), 7.21–7.48 (m, Aromatic H), 6.0 (NH₂). ¹³C NMR (400 MHz, CDCl₃): δ 43.4, 48.9, 115, 120.2, 126.4, 129.5, 135.2, 156.75. Mass m/z (ESI) : 344.41. Elemental analysis: Calcd % C 73.23, H 5.85, N 16.27, O 4.65. Found C 73.19, H 5.83, N 16.23, O 4.74.

- (E)-7-(4-diethylamino)benzylidene)-3-(4-diethylamino)phenyl-4,5,6,7-tetrahydro-5-methyl pyrazole[4,3-c]pyridine-2-carboxamide 4c

Yield : 83%, Red solid ,m.p: 152–154 °C, FT IR (KBr,cm⁻¹) : 3458 (NH₂), 3288 (aromatic C-H), 2866 (CN), 1685 (C = O), 1600 (C = C). ¹H NMR (400 MHz, CDCl₃) :δ 1.64 (t,2H, CH₃)₂, 2.21 (s,NCH₃), 2.43 (q,6H,N(CH₃)₂), 3.36 (s,2H,CH₂), 6.85 (d,β

CH), 7.07–7.65 (m ,Aromatic H), 7.68 (NH₂). ¹³C NMR (400 MHz,CDCl₃): δ 12.65, 29.71, 44.1, 44.44 ,66.75, 110.57, 122.79, 128.63, 147.25, 147.35, 190.04. Mass m/z (ESI) : 486.31. Elemental analysis : Calcd % C 71.57, H 7.87, N 17.27, O 3.29. Found C 71.60, H 7.84,N 17.30, O 3.28.

- (7E)-4,5,6,7-tetrahydro-5-methyl-7-(E)-3-phenylallylidene)-3-tyrlylpyrazolo[4,3c]pyridine-2-carboxamide 4d

Yield : 85%, Yellow solid, m.p: 182–183 °C, FTIR (KBr,cm⁻¹) : 3468 (NH₂), 3166 (aromatic C-H), 2281 (CN), 1679 (C = O),1600 (C = C). ¹H NMR (400 MHz, CDCl₃) : δ 2.29 (s, NCH₃), 2.39 (s,2H, CH₂)3.78 (s,2H, CH₂) , 6.9 1 (d,β CH), 6.79 (d,δ,CH), 6.25–7.81 (m , Aromatic H), 6.0 (NH₂). ¹³CNMR (400 MHz, CDCl₃):δ 29.70, 43.90, 45.10, 55.41, 113.67, 113.99, 128.37, 130.32, 132.03, 190.02. Mass m/z (ESI) : 396 . . Elemental analysis : Calcd % C 75.73, H 6.10, N 14.13, O 4.04. Found C 75.63, H 6.15, N 14.15, O 4.07.

- (E)-7-(3-(trifluoromethyl)benzylidene)-3-(3-trifluoromethyl)phenyl)-4,5,6,7-tetrahydro-5-methyl pyrazole[4,3-c]pyridine-2-carboxamide 4e

Yield : 87%, Light yellow solid solid, 165–168 °C, FTIR (KBr, cm⁻¹) : 3458 (NH₂), 3166 (aromatic C-H),2281 (CN), 1679 (C = O), 1600 (C = C), 1063 (C-F). ¹H NMR (400 MHz, CDCl₃) : δ 2.27 (s,NCH₃), 3.78 (s,2H, CH₂)3.81 (s,2H, CH₂), 6.9 1 (d,β CH), 6.53–7.40 (m, Aromatic H), 6.0 (NH₂). ¹³C NMR (400 MHz, CDCl₃): δ 20.02, 44.75, 56.23, 125.67, 126.22,130.47, 134.40, 136.44, 140.54, 185.55. Mass m/z (ESI) : 480.14.Elemental analysis: Calcd % C 57.50 ,H 3.78, N 11.66 ,O 3.33, F 23.73. Found C 57.55, H 3.76 ,N 11.67, O 3.34, F 23.74.

- (E)-7-(4-dimethylamino)benzylidene)-3-(4-dimethylamino)phenyl-4,5,6,7-tetrahydro-5-methylpyrazolo[4,3-c]pyridine-2-carboxamide 4f

Yield : 86%, Red solid ,m.p: 148–149 °C, FTIR (KBr,cm⁻¹): 3458 (NH₂), 3165 (aromatic C-H), 2925(CN),1670 (C = O), 1620 (C = C). ¹H NMR (400 MHz, CDCl₃) : δ 2.27 (s,NCH₃), 2.85 (s,6H, N(CH₃)₂),3.62 (s,2H,CH₂), 6.9 1 (d,β CH), 6.65–7.30 (m, Aromatic H), 6.0 (NH₂). ¹³C NMR (400 MHz, CDCl₃) : δ 40.3, 43.4 ,48.9, 115, 120.2, 122.6, 128.9,130.9, 149.6, 189.56.Mass m/z (ESI) : 430.25. Elemental analysis : Calcd % C 69.74, H 7.02, N 19.52, O 3.72. Found C 69.76, H 7.04, N 19.55, O 3.69.

- (E)-7-(4-methoxybenzylidene)-4,5,6,7-tetrahydro-methyl-3-(4-methoxyphenyl)pyrazolo [4,3-c]pyridine-2-carboxamide 4 g

Yield : 84%, Yellow solid ,m.p: 147–149 °C, FTIR (KBr,cm⁻¹) : 3367 (NH₂),3005 (aromatic C-H),2115(CN),1670 (C = O),1607(C = C). ¹HNMR(400 MHz,CDCl₃) : δ 2.27 (s,NCH₃), 3.02 (s,2H,CH₂)3.73 (s,3H,CH₃), 3.81 (s,2H,CH₂), 6.9 1 (d,β CH), 6.81–7.25 (m ,Aromatic H), 6.0 (NH₂). ¹³C NMR(400 MHz,CDCl₃) : δ29.71 ,45.50, 52.47, 62.80, 125.95,126.14, 136.7, 136.23, 137.15,180.00. Mass m/z (ESI) : 404.18. Elemental analysis : Calcd % C 68.30 ,H 5.98, N 13.85,O 11.87.Found C 68.32 , H 5.96, N 13.87 , O 11.85.

- (E)-7-benzylidene-4,5,6,7-tetrahydro-5-methyl-3-phenylpyrazole[4,3-c]pyridine-2-carbothioamide 5a

Equal moles of mixture (3E,5E)- 3,5-dibenzylidene -1-methylpiperidin-4-one are treated with thiosemicarbazide with 10% sodium hydroxide were refluxed at 80 °C in a heating mantle for 6hrs produced 5a . Yield: 77%, Yellow solid ,m.p :119 °C, FTIR (KBr,cm⁻¹): 3440 (NH₂), 3135 (aromatic C-H), 2235 (CN), 1121 (C = S), 1620 (C = C). ¹H NMR (400 MHz,CDCl₃) : δ 2.27 (s,NCH₃), 3.63 (s,2H,CH₂) 6.9 1 (d,β CH), 7.21–7.48 (m ,Aromatic H), 6.1 (NH₂). ¹³C NMR (400 MHz,CDCl₃): δ43.4,48.9,115,120.2,126.4,129.

5,135.2,176.20. Mass m/z (ESI) :360.14. Elemental analysis : Calcd % C 69.97, H 5.59 ,N 15.54 ,O 8.90. Found C 69.99, H 5.57,N 15.56 ,O 8.88.

4. Conclusion

In this section we mentioned the identification of a CBP/EP300 bromodomain inhibitor that is biochemically powerful and in cells with the necessary metabolic stability as an in vivo probe for application. Compounds belonging to this category showed moderate to strong cell line test anti-cancer behaviours. Conventional heating and microwave irradiation prepared the synthesised pyrazolo [4,3-c]pyridine scaffolds. In addition, on all the cell lines tested compound 4a was of interesting effect, while compound 4e was of positive activity on MCF-7 cells. In 4a compounds, cancer treatment is environmentally friendly, safer and cheaper. The aim of this research is to investigate the molecular comparative docking studies of the CREB-binding protein target that is responsible in ligand 4a-5j for cancer. The comparative docking studies were done by "Schrodinger Maestro 12.1". 4a has a better binding score (-6.237 Kcal/mol) than the other standard drugs. The ligand 4e with the Glide score -5.572, shows the binding affinity with the amino acid (AA) residues GLU1113, PRO1110. Hence it has been concluded 4a as a potent inhibitor for CREB-binding protein in Cancer.

Declaration of Competing Interest

The authors declare that they have no known competing financial interests or personal relationships that could have appeared to influence the work reported in this paper.

Acknowledgements

Authors are thankful to Bioinformatics Infrastructure Facility Centre (BIFC), Queen Mary's College, Chennai . I am also thankful to Dr.R.Girija Co-ordinator, BIFC for their guidance and support.

References

- [1] R.L. Siegel, K.D. Miller, A. Jemal, Cancer statistics, *CA Cancer J. Clin.* 67 (2017) 7–30.
- [2] C.M. Bagi, Summary–Cancer cell metastasis session, *J. Musculoskelet. Neuronal Interact.* 2 (2002) 579–580.
- [4] D. Terry, F. Crawford, Anthony Romero, Kwong Wah Lai, Discovery of a Potent and Selective in Vivo Probe (GNE-272) for the Bromodomains of CBP/EP300, *J. Med. Chem.* 59 (2016) 10549–10563.
- [5] Terry D. Crawford, Vickie Tsui, E. Megan Flynn, conformations for BRD4, TAF1 (2), BRD9, and CECR2 bromodomains, *Journal of Medicinal Chemistry*, 2016, 1–40.
- [6] L. Eugene, P. Chekler, J.A. Pellegrino, Transcriptional profiling of a selective CREB binding protein bromodomain inhibitor highlights therapeutic opportunities, *Chem. Biol.* 22 (2015) 1–9.
- [7] M. Delvecchio, J. Gaucher, C. Aguilar-Gurrier, Structure of the p300 catalytic core and implications for chromatin targeting and HAT regulation, *Nat. Struct. Mole. Biol.* 20 (2013) 1040–1047.
- [8] S. Ghosh, A. Taylor, M. Chin, Regulatory T Cell Modulation by CBP/EP300 Bromodomain Inhibition, *Am. Soc. Biochem. Mole. Biol.* (2016) 1–40.
- [9] F. Anthony Romero, A.M. Taylor, T.D. Crawford, Disrupting Acetyl-Lysine Recognition: Progress in the Development of Bromodomain Inhibitors, *J. Med. Chem.* 59 (4) (2016) 1271–1298.
- [10] T.P.C. Rooney, P. Filippakopoulos, A Series of Potent CREBBP bromodomain ligands reveals an induced-Fit Pocket Stabilized by a Cation– π Interaction, *Angew. Chem. Int. Ed.* 53 (2014) 1–6.
- [11] N.S. El-Gohary, M.I. Shaaban, New pyrazolopyridine analogs: Synthesis, antimicrobial, anti-quorum sensing and antitumor screening, *Eur. J. Med. Chem.* 152 (2018) 126–136.
- [12] N.H. Theodoulou, N.C.O. Tomkinson, Progress in the Development of non-BET Bromodomain Chemical Probes, *Chem. Med. Chem.* 11 (2016) 477–487.
- [13] A.F. Hohmann, C.R. Vakoc, A rationale to target the SWI/SNF complex for cancer therapy, *Trends Genet.* 30 (2014) 356–363.
- [14] C.J. Schofield, P.E. Brennan, S. Knapp, S.J. Conway, reviews of BET bromodomain inhibitors and their therapeutic potential, *J. Med. Chem.* 55 (2012) 9393–9413.
- [15] S. Mujtaba, Y. He, L. Zeng, S. Yan, O. Plotnikova, Sachchidanand, Structural mechanism of the bromodomain of the coactivator CBP in p53 transcriptional activation, *Mol. Cell* 13 (2004) 251–263.
- [16] S. Muller, H. Lingard, S. Knapp, Selective targeting of protein interactions mediated by BET bromodomains. *Concepts Case Stud. Chem. Biol.* (2014) 255–307.
- [17] Sarah Picaud1, Oleg Fedorov1, Angeliki Thanasopoulou, Generation of a Selective Small Molecule Inhibitor of the CBP/p300 Bromodomain for Leukemia Therapy, *Cancer Res.* 2015, 75(23), 5106–5119
- [18] T. Katsumoto, N. Yoshida, I. Kitabayashi, Roles of the histone acetyltransferase monocytic leukemia zinc finger protein in normal and malignant hematopoiesis, *Cancer Sci* 99 (2008) 1523–1527.
- [19] Y. Zhang, N. Zeleznik-Le, N. Emmanuel, N. Jayathilaka, J. Chen, P. Strissel, et al., Characterization of genomic breakpoints in MLL and CBP in leukemia patients with t(11;16), *Genes Chromosomes Cancer* 41 (2004) 257–265.
- [20] Y. Zhao, S. Lu, L. Wu, G. Chai, H. Wang, Y. Chen, et al., Acetylation of p53 at lysine 373/382 by the histone deacetylase inhibitor depsipeptide induces expression of p21(Waf1/Cip1), *Mol Cell Biol* 26 (2006) 2782–2790.
- [21] X. Min, A. Unzue, J. Dong, D. Spiliotopoulos, Discovery of CREBBP Bromodomain Inhibitors by High-throughput docking and hit optimization guided by molecular dynamics, *J. Med. Chem.* 59 (4) (2016) 1340–1349.
- [22] Stuart W. J. Ember, Jin-Yi Zhu, Sanne H. Olesen, Acetyl-lysine Binding Site of Bromodomain-Containing Protein 4 (BRD4) Interacts with Diverse Kinase Inhibitors, *ACS Chem. Biol.* 2014, 9, 1160–1171
- [23] R. Sanchez, M.-M. Zhou, The role of human bromodomains in chromatin biology and gene transcription, *Curr. Opin. Drug Discov. Devel.* 12 (5) (2009) 659–665.
- [24] Y. Eryanti, A. Zamri, N. Frimayanti, Synthesis, structure-activity relationship, docking and molecular dynamic simulation of curcumin analogues against HL-60 for Anticancer Agents (Leukemia), *Orient. J. Chem.* 33 (5) (2017) 2164–2172.
- [25] P. Jabbarzadeh, Kaboli1, P. Ismail1, K.-H. Lin, Molecular modeling, dynamics simulations, and binding efficiency of berberine derivatives: A new group of RAF inhibitors for cancer treatment, *PLoS One* 3 (2018) 1–19.
- [26] Q. Wang, Y. Li, X. Jiahui, Y. Wang, Elaine, Selective inhibition mechanism of RVX-208 to the second bromodomain of bromo and extraterminal proteins: insight from microsecond molecular dynamics simulations, *Scientific Rep.* 7 (2017) 1–11.
- [27] L. Batiste, A. Unzue, A. Dolbois, Chemical space expansion of bromodomain ligands guided by in silico Virtual Couplings (AutoCouple), *ACS Cent. Sci.* 4 (2) (2018) 180–188.
- [28] L. Claisen and A. Claparede, Ber., 1881, 14, 2460; J.G. Schmidt, Ber., 1881, 14, 1459; H.O. House, *Modern Synthetic Reactions* (W.A. Benjamin, California, 2nd ed. 1972), 632–639.
- [29] C.A. Lipinski, F. Lombardo, B.W. Dominy, P.J. Feeney, Experimental and computational approaches to estimate solubility and permeability in drug discovery and development settings, *Adv Drug Deliv Rev.* 46 (2001) 3–26.
- [30] K. Alim, B. Lefranc, J.S.-de O. Santos, Design, synthesis, molecular dynamics simulation and functional evaluation of a novel Series of 26RFa Peptide Analogues Containing a Mono- or Polyalkyl Guanidino Arginine Derivative, *J. Med. Chem.* 3 (2018) 1–45.
- [31] M.R. Pitman, R.I. Menz, Methods for protein homology modelling, *Appl. Mycol. Biotechnol.* 6 (2006) 38–59.



Synthesis and biological evaluations of new pyrazole hydrazides as potent anti-microbial agent

Gunasekar S. *, Saamanthi M., Aruna S.

Department of Chemistry, Queen Mary's college, Chennai 600004, Tamil Nadu, India

ARTICLE INFO

Article history:

Received 28 December 2020

Received in revised form 26 January 2021

Accepted 1 February 2021

Available online 27 February 2021

Keyword:

Pyrazole

Hydrazides

Potent anti microbial agents

Heterocycles

Disc diffusion

Biological activity

ABSTRACT

A sequence of pyrazole hydrazides (8a-8r) was synthesized (E)-N-(5-(2-(2-(4-methoxy-2,3-dimethylbenzylidene) hydrazinyl)-2-oxoethyl)-1H-pyrazol-3-yl)-3-(trifluoromethyl) benzamide (8a), and its anti-microbial activities were studied for its in vitro anti-microbial activities against staphylococcus aureus and Escherichia coli and found almost all synthesized molecules are active. Also synthesized molecules were ascertained by ^1H NMR, ^{13}C NMR and mass spectroscopy pyrazole hydrazides was synthesized by dehydration reaction of 2-(3-(5-bromo-2-fluorobenzamido)-1H-pyrazol-5-yl) acetohydrazide (7) with different aldehydes. All the reaction progress were monitored by TLC. Minimum inhibition values of synthesized molecules were studied using Staphylococcus aureus and Escherichia coli and found some of the compounds show good MIC values such as 8 g (24), 8j (23), 8 k (23) as compared to existing drug cefotaxime.

© 2020 Elsevier Ltd. All rights reserved.

Selection and peer-review under responsibility of the scientific committee of the International Conference on Mechanical, Electronics and Computer Engineering 2020: Materials Science.

1. Introduction

Pyrazole molecules are being shows wide variety of biological activities and they have very important role in new drug discovery development due to its biological activities. Also, heterocyclic compounds having pyrazole molecules have extensive variety of biological properties such as anti-microbial, antifungal, anti-tuberculosis, anti-inflammatory, anticonvulsant and anti-cancer activities. Also, it has been found that pyrazole derivatives found their applications as non-steroidal anti-inflammatory drugs clinically. Several natural extracted and chemically synthesized molecules holding pyrazole scaffold shows therapeutic properties. Microbial infections are being increases worldwide, controlling and treating the infections are quite challenge. As extreme case curing of infections such as human immunodeficiency virus (HIV) is not possible. Literature research shows that both hydrazones derivatives as well drugs containing pyrazole derivatives are highly biologically actives against many diseases. Pyrrole and pyrazole derivatives show prominence in medicinal chemistry among the nitrogen containing heterocycles. Especially Pyrazole are scaffold for many drugs such as difenamizole, tepoxalin, distamycin, netropsin etc. possess

therapeutic properties like anti-microbial, antifungal, anti-tuberculosis, anti-inflammatory, anticonvulsant and anti-cancer activities. The nonstop requirement leads to the preparation of pyrazole benzamides; the current research paper put forth the synthesis and biological activities of innovative pyrazole benzamides. In this research innovative pyrazole amide derivatives were synthesized and these derivatives were screened against anti-microbial activities. The molecules of the Pyrazole benzamides was ascertained by ^1H NMR, ^{13}C NMR and LC-MS analysis [Scheme 1](#).

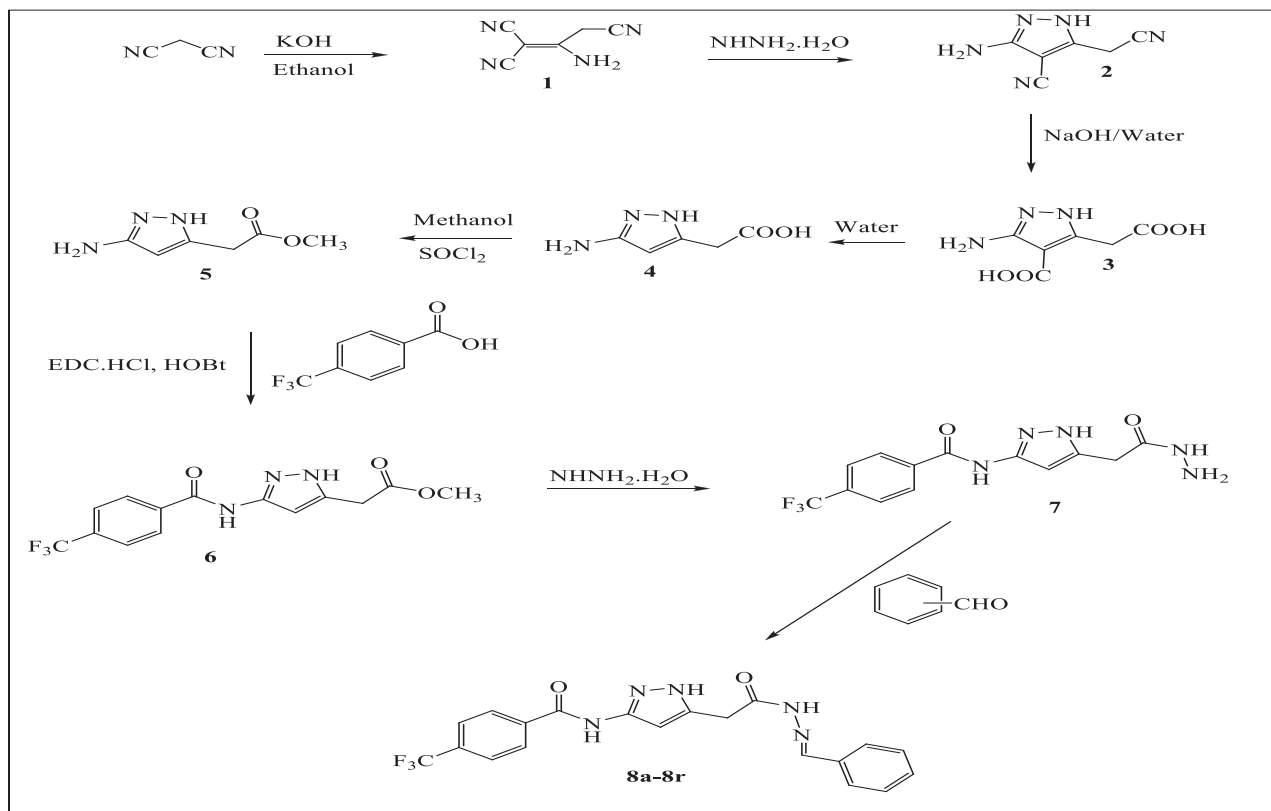
2. Experimental

In an uncorrected open capillary tube melting points were measured. ^1H NMR & ^{13}C NMR were analyzed in BRUKER instrument 400 MHz at Vellore Institute of Technology. LC-MS and IR also studied at the Vellore institute of technology. IUPAC system was followed in the nomenclature of the newly synthesized compounds. The anti-microbial analyses were studied at the Bhat biotech India private limited. All below reactions were checked using TLC.

Synthesis of 2-aminoprop-1-ene-1, 1, 3-tricarbonitrile (1). To a cleaned RBF, charged ethanol (250 mL) and malononitrile (50 g, 0.75 mmol), cooled to 5–10 °C, charged potassium hydroxide (14.025 0.25 mmol) in portions, at 50–55 °C reaction maintained

* Corresponding author.

E-mail addresses: sgsjain@gmail.com, sgsjain@gmail.com (G. S.).



Scheme 1. Synthesis of pyrazole hydrazides (Full scheme).

for 30 min, cooled to 25–30 °C and stirred for 1 h, filtered potassium salt. In an another RBF, charged water (200 mL), pH adjusted to ~3 with concentrated hydrochloric acid and obtained solid was off white solid in color to yield Compound 1; Off white solid and yield 45%; ¹H NMR (400 MHz DMSO *d*₆, δppm): 9.08 (s, 1H), 8.99 (s, 1H), (3.85, 2H) *m/z*: 131.0 [M–H][–].

Synthesis of 3-amino-5-(cyanomethyl)-1H-pyrazole-4-carboxylic acid (3). Compound 2 (35 g, 0.24 mmol) in an aqueous solution of sodium hydroxide (12 M, 60 mL) and refluxed for overnight, at 25–30 °C, pH reduced to ~3 with hydrochloric acid. Under vacuum the obtained solid was dried to get 35 g of compound 3. ¹H NMR (300 MHz DMSO *d*₆, δppm): 11.89 (m, 3H), 5.71 (m, 2H), 3.55 (m, 3H) *m/z*: 186.3 [M + H]⁺.

Synthesis of 2-(3-amino-1H-pyrazol-5-yl) acetic acid (4). In to Compound 3 (28 g, 0.15 mmol) added water (700 mL), temperature increased up to 60 °C for 5 h and evaporated the reaction mixture to dryness, compound 4 resulted as brown solid. ¹H NMR (300 MHz DMSO *d*₆, δppm): 7.30 (m, 1H), 5.25 (s, 1H), 3.30 (s, 2H) mass: 142.3 [M + H]⁺.

Synthesis of Methyl 2-(3-amino-1H-pyrazol-5-yl) acetate hydrochloride (5). To an RBF charged Compound 4 (20 g, 0.14 mmol), methanol (330 mL) and thionyl chloride (54.72 g, 0.45 mmol) at 0–5 °C. For the duration of 4 h, reaction mixture was maintained at 20–25 °C. Observed brown solid and filtered

the solid. ¹H NMR (300 MHz DMSO *d*₆, δppm): 10.72 (m, 3H), 5.91 (s, 1H), 3.8 (s, 2H), 3.63 (s, 3H) *m/z*: 156.2 [M + H]⁺.

Synthesis of 2-(3-(5-bromo-2-fluorobenzamido)-1H-pyrazol-5-yl) acetate (6). In a multi neck round bottom flask, 2-fluoro-5-bromo benzoic acid (15 g, 0.072 mmol), DMF (100 mL) and DIEA (22 g, 0.16 mmol) was mixed and obtained clear solution, further it cooled to 0 °C and added EDC.HCl (20 g, 0.10 mmol) and HOBt (13.57 g, 0.10 mmol) followed by compound 5 (amine) 13.79 g, 0.072 mmol, after the addition the mass temperature was raised to 30 ± 5 °C for 30 min. Reaction was terminated by adding water and desired molecule was extracted with ethyl acetate and it was further evaporated completely under vacuum and added *n*-hexane to the crude and filtered to have methyl 2-(3-(5-bromo-2-fluorobenzamido)-1H-pyrazol-5-yl)acetate (Compound 6) 12 g, Color of the compound is brown solid with 75% yield, ¹H NMR (400 MHz DMSO *d*₆, δppm): 12.42–12.37 (d, 1H), 11.48–11.29 (d, 1H), 11.06–11.02 (d, 1H), 8.5–8.39 (d, 1H), 8.18–8.15 (t, 2H), 7.87–7.85 (d, 2H), 7.68–7.64 (t, 1H), 6.92–6.90 (d, 1H).

2-(3-(5-bromo-2-fluorobenzamido)-1H-pyrazol-5-yl) acetohydrazide (7). To compound 6 (11 g, 0.030 mmol) added hydrazine hydrate (20 g, 0.62 mmol), stirred for 30–45 min at 30–35 °C and found Off white precipitate and it was filtered to get compound 7 VII. Color of the solid is brown with 90% yield. ¹H NMR (400 MHz DMSO *d*₆, δppm): 12.25 (s, 1H) 10.81 (s, 1H), 9.23 (s, 1H), 7.69–7.50 (m, 3H), 6.46 (s, 1H), 4.20 (s, 2H), 3.40 (d, 4H); *m/z*: 356.7 [M + H]⁺.

Over-all procedure to synthesis title molecules (8a-r). To a homogeneous solution of compound VII (500 mg, 0.0014 mol) in ethanol was added aldehyde (0.0014 mol) and catalytic amount of acetic was stirred for 3 h at 75–78 °C, cooled to 20–25 °C. It was Observed solid formation and it was filtered; bed wash was given with ethyl alcohol to remove unreacted starting material.

(E)-N-(5-(2-(2-(4-methoxy-2,3-dimethylbenzylidene)hydrazinyl)-2-oxoethyl)-1H-pyrazol-3-yl)-3-(trifluoromethyl)benzamide (8a). Off white solid. MP 177–181 °C. Yield: 69%. IR (KBr, cm^{-1}): 3258 (NH), 1644 (C=O); ^1H NMR (400 MHz DMSO d_6 , δ ppm): 12.42–12.37 (d, 1H), 11.48–11.29 (d, 1H), 11.06–11.02 (d, 1H), 8.5–8.39 (d, 1H), 8.18–8.15 (t, 2H), 7.87–7.85 (d, 2H), 7.68–7.64 (t, 1H), 6.92–6.90 (d, 1H), 6.61–6.57 (d, 1H), 4.02 (s, 1H), 3.81 (s, 3H), 3.60 (s, 1H), 2.3 (s, 3H), 2.12 (s, 3H); ^{13}C NMR (DMSO d_6 , δ ppm) 21.5, 30.66, 39.75, 40.17, 40.38, 40.59, 97.29, 97.49, 123.03, 125, 128, 129, 131, 135, 137, 138, 140, 144, 147, 163, 165, 171 m/z: 474.10 [M + H]⁺.

(E)-N-(5-(2-(2-(4-bromo-3,5-dimethoxybenzylidene)hydrazinyl)-2-oxoethyl)-1H-pyrazol-3-yl)-3-(trifluoromethyl)benzamide (8b). Pale brown solid. MP 188–191 °C. Yield: 66%. IR (KBr, cm^{-1}): 3258 (NH), 1644 (C=O); ^1H NMR (400 MHz DMSO d_6 , δ ppm): 12.39 (s, 1H), 11.75–11.66 (d, 1H), 11.03 (s, 1H), 8.21–8.14 (q, 2H), 7.98 (s, 2H), 7.87–7.85 (d, 2H), 7.28–7.27 (d, 2H), 6.60 (s, 1H), 4.06–3.64 (d, 2H), 3.94–3.89 (t, 6H); ^{13}C NMR (DMSO d_6 , δ ppm) 30, 39, 40, 97, 119, 120, 124, 125, 128, 129, 131, 135, 137, 138, 140, 144, 147, 158, 160, 161, 165, 171 MS m/z : 555.70 [M + H]⁺.

(E)-N-(5-(2-(2-(2-methoxybenzylidene)hydrazinyl)-2-oxoethyl)-1H-pyrazol-3-yl)-3-(trifluoromethyl)benzamide (8c). Off white solid. MP 212–215 °C. Yield: 70%. IR (KBr, cm^{-1}): 3310 (NH), 1676 (C=O); ^1H NMR (400 MHz DMSO d_6 , δ ppm): 12.41–12.36 (d, 1H), 11.65–11.47 (d, 1H), 11.04–11.01 (d, 1H), 8.57–8.37 (d, 1H), 8.14–8.15 (d, 2H), 7.89–7.85 (t, 3H), 7.43–7.39 (q, 1H), 7.11–7.09 (d, 2H) 7.09–7.0 (t, 1H) 6.61–6.57 (s, 1H), 4.06–3.60 (d, 2H), 3.86–3.85 (d, 3H); ^{13}C NMR (DMSO d_6 , δ ppm) 30, 32, 39, 40, 69, 97, 115, 122, 125, 126, 127, 128, 131, 137, 138, 143, 147, 160, 163, 164, 170 MS m/z : 446.60 [M + H]⁺.

(E)-N-(5-(2-(2-(2,5-dichloro-4-methylbenzylidene)hydrazinyl)-2-oxoethyl)-1H-pyrazol-3-yl)-3-(trifluoromethyl)benzamide (8d). Pale pink solid. MP 177–179 °C. Yields: 59%. IR (KBr, cm^{-1}): 3305 (NH), 1672 (C=O); ^1H NMR (400 MHz DMSO d_6 , δ ppm): 12.42–12.33 (d, 1H), 11.86–11.73 (d, 1H), 11.06–11.02 (d, 1H), 8.40–8.27 (d, 1H), 8.23–8.15 (t, 2H), 7.87–7.85 (d, 2H), 7.42 (s, 2H), 6.62–6.56 (s, 1H), 4.00–3.60 (d, 2H), 2.33 (s, 3H); ^{13}C NMR (DMSO d_6 , δ ppm) 40, 41, 97, 120, 126, 126, 128, 130, 132, 135, 139, 141, 144, 159, 161, 162 MS m/z : 497.70 [M + H]⁺.

(E)-N-(5-(2-(2-(3,5-dichlorobenzylidene)hydrazinyl)-2-oxoethyl)-1H-pyrazol-3-yl)-3-(trifluoromethyl)benzamide (8e). Off white powder. MP 199–201 °C. Yield: 63%. ^1H NMR (400 MHz DMSO d_6 , δ ppm): 12.33 (s, 1H), 11.91–11.73 (d, 1H), 11.06–11.03 (d, 1H), 8.18–8.15 (t, 3H), 7.98 (s, 2H), 7.87–7.75 (m, 2H), 7.68–7.64 (m, 1H) 6.54D (s, 1H), 4.07–3.64 (d, 2H); ^{13}C NMR (DMSO d_6 , δ ppm) 21.5, 30.66, 32, 39, 40, 97, 123, 125, 128, 129, 131, 135, m/z: 483.80 [M + H]⁺.

(E)-N-(5-(2-(2-(4-hydroxy-3,5-dimethoxybenzylidene)hydrazinyl)-2-oxoethyl)-1H-pyrazol-3-yl)-3-(trifluoromethyl)benzamide (8f). Pale pink solid. MP 200–203 °C. percentage of Yield: 70%. ^1H NMR (400 MHz DMSO d_6 , δ ppm): 12.19 (s, 1H), 11.50–11.40 (d, 1H), 11.06–11.03 (d, 1H), 8.91–8.85 (d, 1H), 8.17–8.09 (t, 2H), 7.89–7.85 (t, 2H), 6.97 (s, 2H), 6.58 (s, 1H), 4.00–3.60 (d, 2H), 3.85–3.81 (t, 6H); ^{13}C NMR (DMSO d_6 , δ ppm) 21, 30, 32, 39, 40, 56, 97, 104, 107, 123, 124, 125, 127, 128, 129, 131, 137, 138, 142, 144, 147, 148, 163, 164, 170, 172 MS m/z : 491.80 [M + H]⁺.

(E)-N-(5-(2-(2-(2,3-dichlorobenzylidene)hydrazinyl)-2-oxoethyl)-1H-pyrazol-3-yl)-3-(trifluoromethyl)benzamide (8g). Off white crystal. MP 211–213 °C. Yield: 58%. ^1H NMR (400 MHz DMSO d_6 , δ ppm): 12.29–12.25 (d, 1H), 11.98–11.79 (d, 1H), 11.08–11.04 (d, 1H), 8.64–8.44 (d, 1H), 8.18–8.15 (t, 2H), 8.03–8.01 (d, 1H) 7.88–7.85 (t, 2H), 7.72–7.71 (d, 1H) 7.47–7.43 (t, 1H) 6.58 (s, 1H), 4.07–3.64 (d, 2H); ^{13}C NMR (DMSO d_6 , δ ppm) 21, 30,

32, 39, 40, 97, 123, 125, 128, 129, 131, 135, 137, 138, 140, 144, 147, 163, 165, 171, 172 MS m/z : 483.90 [M + H]⁺

(E)-N-(5-(2-(2-(4-nitrobenzylidene)hydrazinyl)-2-oxoethyl)-1H-pyrazol-3-yl)-3-(trifluoromethyl)benzamide (8h) Brown solid. MP 203–204 °C. Yield: 66%. IR (KBr, cm^{-1}): 3258 (NH), 1644 (C=O); ^1H NMR (400 MHz DMSO d_6 , δ ppm): 12.42–12.39 (d, 1H), 11.95–11.82 (d, 1H), 11.05–11.02 (d, 1H), 8.39–8.27 (m, 2H), 8.18–8.13 (q, 3H), 8.01–7.97 (t, 3H) 7.87–7.85 (d, 2H), 6.62–6.58 (s, 1H), 4.10–3.33 (d, 2H); ^{13}C NMR (DMSO d_6 , δ ppm) 30.66, 32, 39, 40, 97, 120, 123, 125, 128, 129, 131, 132, 138, 140, 141, 144, 148, 163, 165, 171 MS m/z : 460.90 [M + H]⁺

(E)-N-(5-(2-(2-(2-hydroxy-5-nitrobenzylidene)hydrazinyl)-2-oxoethyl)-1H-pyrazol-3-yl)-3-(trifluoromethyl)benzamide (8i). Brown solid. MP 180–183 °C. Yield: 57%. ^1H NMR (400 MHz DMSO d_6 , δ ppm): 12.43–12.37 (d, 1H), 12.20–12.16 (d, 1H), 11.66 (s, 1H), 11.05–11.02 (d, 2H) 8.58–8.56 (q, 2H), 8.18–8.14 (q, 3H), 7.87–7.85 (d, 2H), 7.13–7.08 (m, 1H) 6.63–6.58 (s, 1H), 4.09 (s, 1H)–3.67 (s, 1H); ^{13}C NMR (DMSO d_6 , δ ppm) 30, 32, 39, 40, 97, 117, 120, 121, 123, 124, 125, 126, 128, 129, 131, 138, 140, 144, 162, 163, 165, 170 MS m/z : 476.90 [M + H]⁺.

(E)-N-(5-(2-(2-((6-chloropyridin-3-yl)methylene)hydrazinyl)-2-oxoethyl)-1H-pyrazol-3-yl)-3-(trifluoromethyl)benzamide (8j). Pale gray solid. MP 216–217 °C. Yield: 69%. ^1H NMR (400 MHz DMSO d_6 , δ ppm): 12.43–12.39 (d, 1H), 11.89–11.75 (d, 1H), 11.05–11.02 (d, 2H) 8.72–8.69 (d, 1H), 8.28–8.22 (m, 1H), 8.18–8.15 (t, 3H) 7.87–7.85 (d, 2H), 7.61–7.59 (d, 1H) 6.62–6.57 (s, 1H), 4.07–3.65 (d, 2H); ^{13}C NMR (DMSO d_6 , δ ppm) 30, 32, 39, 40, 97, 120, 123, 124, 125, 128, 129, 130, 131, 137, 138, 139, 143, 147, 149, 151, 163, 165, 171 MS m/z : 450.80 [M + H]⁺.

(E)-N-(5-(2-(2-((2-methoxypyrimidin-5-yl)methylene)hydrazinyl)-2-oxoethyl)-1H-pyrazol-3-yl)-3-(trifluoromethyl)benzamide (8k). Off white fluppy powder. MP 190–193 °C. Yield: 69%. ^1H NMR (400 MHz DMSO d_6 , δ ppm): 12.39 (s, 1H), 11.78–11.65 (d, 1H), 11.04–11.01 (d, 2H) 8.98–8.88 (d, 2H), 8.24–7.85 (m, 5H), 6.61–6.56 (s, 1H), 4.04–3.6 (d, 2H) 3.97 (s, 3H); ^{13}C NMR (DMSO d_6 , δ ppm) 30, 39, 40, 55, 97, 120, 123, 125, 128, 129, 131, 138, 142, 158, 163, 165, 171 MS m/z : 448.00 [M + H]⁺.

(E)-N-(5-(2-(2-(4-hydroxybenzylidene)hydrazinyl)-2-oxoethyl)-1H-pyrazol-3-yl)-3-(trifluoromethyl)benzamide (8l). Pale brown solid. MP 196–198 °C. Yield: 62%. IR (KBr, cm^{-1}): ^1H NMR (400 MHz DMSO d_6 , δ ppm): 12.40–12.36 (d, 1H), 11.45–11.31 (d, 1H), 11.05–11.02 (d, 2H), 9.92 (s, 1H), 8.17–8.15 (q, 2H), 8.11 (s, 1H) 7.92–7.85 (t, 2H), 7.77–7.75 (d, 2H), 6.83–6.81 (d, 2H), 6.60–6.56 (s, 1H), 4.01–3.359 (d, 2H) ^{13}C NMR (DMSO d_6 , δ ppm) 30, 32, 39, 40, 97, 116, 122, 125, 126, 129, 131, 132, 138, 144, 147, 159, 163, 164, 170 MS m/z : 431.90 [M + H]⁺.

(E)-N-(5-(2-(2-((2-bromopyridin-4-yl)methylene)hydrazinyl)-2-oxoethyl)-1H-pyrazol-3-yl)-3-(trifluoromethyl)benzamide (8m) Off white solid. MP 212–215 °C. Yield: 61%. ^1H NMR (400 MHz DMSO d_6 , δ ppm): 12.40 (s, 1H), 11.92 (s, 1H), 11.04 (s, 1H), 8.44–8.43 (d, 1H), 8.18–8.15 (t, 3H) 7.98–7.94 (d, 1H), 7.89–7.86 (t, 2H), 7.76–7.72 (q, 1H) 6.58 (s, 1H), 4.10–3.367 (d, 2H) ^{13}C NMR (DMSO d_6 , δ ppm) 30, 39, 40, 97, 120, 122, 125, 126, 129, 131, 132, 138, 139, 142, 143, 145, 151, 163, 165, 171 MS m/z : 495.90 [M + H]⁺.

(E)-N-(5-(2-(2-(5-chloro-2-methoxybenzylidene)hydrazinyl)-2-oxoethyl)-1H-pyrazol-3-yl)-3-(trifluoromethyl)benzamide (8n). white crystal. MP 190–193 °C. Yield: 69%. ^1H NMR (400 MHz DMSO d_6 , δ ppm): 12.18 (s, 1H), 11.75–11.55 (d, 1H), 11.04–11.01 (d, 1H) (s, 1H), 11.04 (s, 1H), 8.49–8.29 (d, 1H), 8.16–8.14 (t, 2H) 7.85–7.81 (t, 3H), 7.46–7.42 (m, 1H), 7.15–7.12 (q, 1H) 6.56–6.53 (d, 1H), 4.05–3.359 (d, 2H), 3.86 (s, 3H); ^{13}C NMR (DMSO d_6 , δ ppm) 21, 30, 32, 38, 39, 40, 56, 96, 113, 114, 123, 124, 126, 127, 130, 131, 133, 136, 137, 140, 146, 155, 156, 162, 164, 170 MS m/z : 479.90 [M + H]⁺.

(E)-N-(5-(2-(2-(4-(benzyloxy)benzylidene)hydrazinyl)-2-oxoethyl)-1H-pyrazol-3-yl)-3-(trifluoromethyl)benzamide **8(o)**. Brown powder. MP 182–185 °C. Yield: 57%. ¹H NMR (400 MHz DMSO *d*₆, δppm): 12.42–12.36 (d, 1H), 11.92–11.54 (d, 1H), 11.05–11.01 (d, 1H), 10.72 (s, 1H), 8.41–8.32 (d, 1H), 8.17–8.15 (t, 2H), 7.87–7.85 (d, 2H), 7.36–7.35 (d, 1H), 7.25–7.24 (d, 1H), 7.06–7.04 (m, 1H), 6.62–6.57 (d, 1H), 4.04–3.65 (d, 2H), 3.85–3.83 (d, 3H); ¹³C NMR (DMSO *d*₆, δppm) 30, 32, 39, 40, 69, 115, 118, 122, 125, 126, 127, 128, 129, 131, 137, 138, 143, 147, 160, 163, 164, 170 MS *m/z*: 521.90 [M + H]⁺.

(E)-N-(5-(2-(2-(3,4-dimethoxybenzylidene)hydrazinyl)-2-oxoethyl)-1H-pyrazol-3-yl)-3-(trifluoromethyl)benzamide **8(p)**. Pale pink solid. MP 170–173 °C. Yield: 70%. ¹H NMR (400 MHz DMSO *d*₆, δppm): 12.41–12.38 (d, 1H), 11.53–11.41 (d, 1H), 11.05–11.02 (d, 1H), 8.18–8.15 (t, 2H), 7.94 (s, 1H), 7.87–7.85 (d, 2H), 7.33–7.30 (t, 1H), 7.21–7.17 (m, 1H), 7.03–6.99 (d, 1H), 6.61–6.60 (d, 1H), 4.04–3.61 (d, 2H), 3.87–3.80 (m, 6H); ¹³C NMR (DMSO *d*₆, δppm) 31, 32, 39, 40, 56, 97, 113, 116, 120, 122, 123, 125, 126, 129, 131, 136, 138, 139, 145, 146, 147, 149, 163, 165, 170 MS *m/z*: 475.80 [M + H]⁺.

(E)-N-(5-(2-(2-(5-bromo-2-nitrobenzylidene)hydrazinyl)-2-oxoethyl)-1H-pyrazol-3-yl)-3-(trifluoromethyl)benzamide **8(q)**. yellowish brown solid. MP 178–181 °C. Yield: 69%. ¹H NMR (400 MHz DMSO *d*₆, δppm): 12.41–12.36 (d, 1H), 12.02–11.84 (d, 1H), 11.03–11.00 (d, 1H), 8.56 (s, 2H), 8.29–8.28 (t, 2H), 8.16–8.14 (d, 2H), 7.99–7.97 (d, 2H), 7.86–7.84 (d, 2H), 6.61–6.56 (d, 1H), 4.04–3.65 (d, 2H), ¹³C NMR (DMSO *d*₆, δppm) 30, 32, 39, 40, 97, 120, 123, 125, 127, 128, 129, 130, 131, 132, 136, 138, 141, 147, 148, 163, 165, 171.

(E)-N-(5-(2-(2-(5-chloro-2-hydroxy-3-methoxybenzylidene)hydrazinyl)-2-oxoethyl)-1H-pyrazol-3-yl)-3-(trifluoromethyl)benzamide **8(r)**. white to off white powder. MP 192–193 °C. Yield: 65%. ¹H NMR (400 MHz DMSO *d*₆, δppm): 12.41–12.38 (d, 1H), 11.53–11.41 (d, 1H), 11.05–11.02 (d, 1H), 8.18–8.15 (t, 2H), 7.94 (s, 1H), 7.87–7.85 (d, 2H), 7.33–7.30 (t, 1H), 7.21–7.17 (m, 1H), 7.03–6.99 (d, 1H), 6.61–6.60 (d, 1H), 4.04–3.61 (d, 2H), 3.87–3.80 (m, 6H); ¹³C NMR (DMSO *d*₆, δppm) 21, 30, 32, 39, 40, 97, 118, 122, 125, 126, 128, 129, 131, 132, 134, 137, 138, 139, 142, 146, 163, 165, 171, 172 MS *m/z*: 495.90 [M + H]⁺.

3. Results and discussion

3.1. Chemistry

Reaction of malononitrile in the presence of potassium hydroxide and ethanol at 25–30 °C to yield Compound 1, it was treated

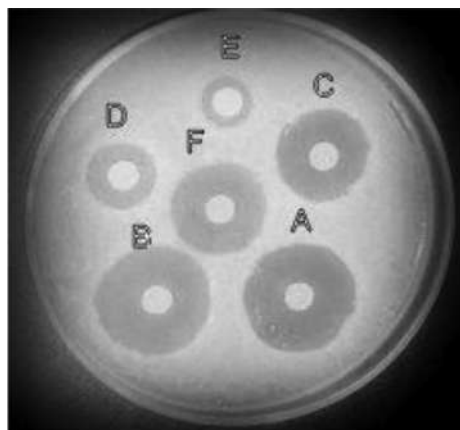


Fig. 1. 8a to 8f.

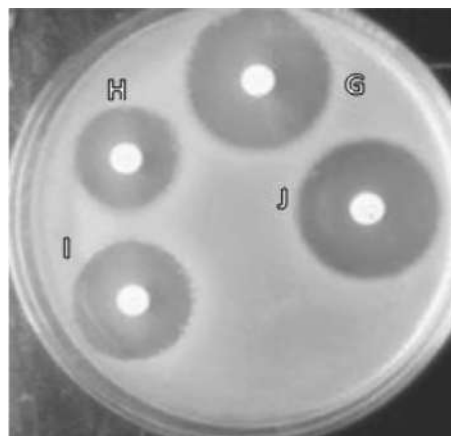


Fig. 2. 8g to 8j.

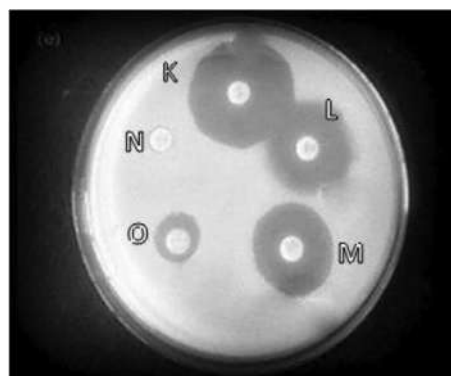


Fig. 3. 8k to 8o.

Table 1
Antimicrobial activity results of 8a–8r.

Compound	R	Minimum inhibition concentration (MIC)	
		Staphylococcus aureus	Escherichia coli
8a	2,3-methyl-4-methoxy	17	20
8b	3,5-methoxy-4-bromo	19	20
8c	2-methoxy	19	19
8d	2,6-dichloro-4-methyl	18	18
8e	3,5-dichloro	15	17
8f	3,5-dimethoxy-4-hydroxy	21	18
8g	2,3-dichloro	24	20
8h	4-nitro	23	18
8i	2-hydroxy-5-nitro	22	16
8j	6-chloro-nicotine	23	16
8k	2-methoxy-5-pyrimidine	23	17
8l	4-hydroxy	20	18
8m	2-bromo-pyridine	20	18
8n	5-Chloro-2-methoxy	14	18
8o	4-benzyloxy	11	17
8p	3,4-dimethoxy	20	16
8q	4-bromo-2-nitro	20	15
8r	5-Chloro-2-hydroxy-3-methoxy	20	16
Cefotaxime		28	26

with hydrazine hydrate at 25–30 °C for 1 h to have compound 2. Compound 2 was stirred with aq. sodium hydroxide solution at 95–100 °C for 24 h to get compound 3. To Compound 3, added water and at 50–55 °C and maintained for 5 to 6 h. TLC was used as tool for reaction monitoring. Reaction mixture concentrated till

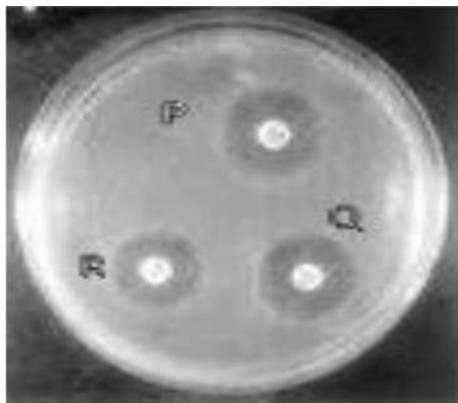


Fig. 4. 8p to 8r.

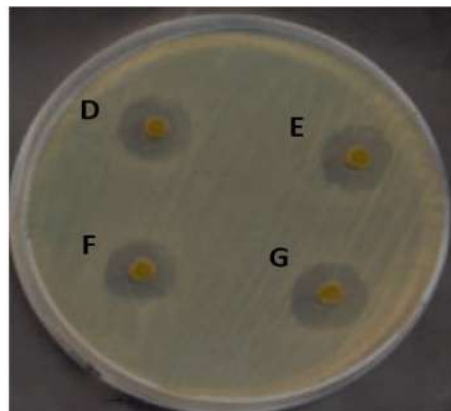


Fig. 7. 8d to 8g.



Fig. 5. Negative control.

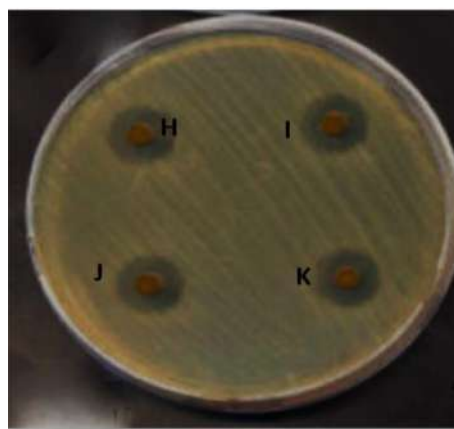


Fig. 8. 8h to 8k.

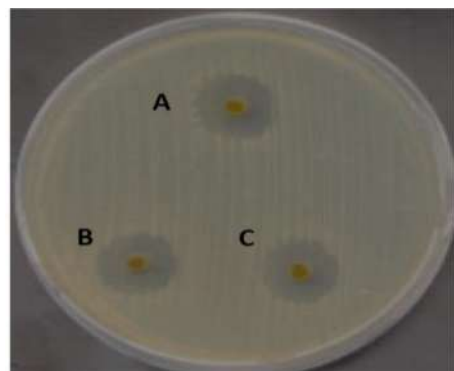


Fig. 6. 8a to 8c.

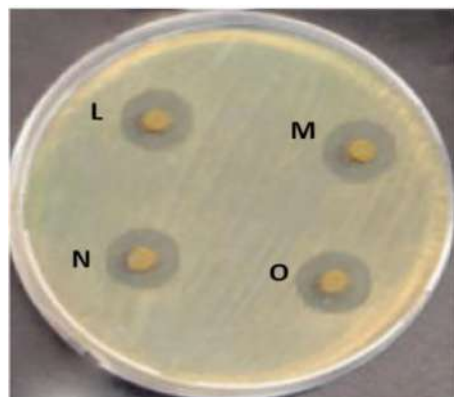


Fig. 9. 8l to 8o.

dryness to obtain compound 4. To Compound 4 added methanol followed by thionyl chloride at 5–10 °C for 1 h, obtained solid filtered to have compound 5. Compound 5 is the key starting material or key raw material for the preparation of target molecules. The isolated solids in each step (compound 1 to 5) were ascertained by ¹H NMR and mass spectroscopy. In an RBF, Carboxylic acid, DMF added and found clear solution, to that further added DIEA, and EDC. HCl & HOBt followed by compound 5 and stirred for 4 h at 30 ± 5 °C, the reaction diluted with H₂O and ethyl acetate. The organic layer was separated, till dryness it was concentrated under reduced pressure. Crude was triturate with n-Hexane to yield Compound 6. Compound 6 in ethanol at 25–30 °C was added hydrazine hydrate slowly, after the addition of hydrazine hydrate,

stirred for 0.5 h, terminated the reaction using water to have Compound 7. Compound 7 is the scaffold molecule for the preparation of hydrazides. The compound 7 were treated with different aldehydes in ethanol to obtain different hydrazides but some reactions were not completed hence added few drops of acetic acid to drive the reaction for completion. The obtained solids were filtered and washed with ethanol to remove unreacted aldehydes. All the hydrazides were obtained as solid material.

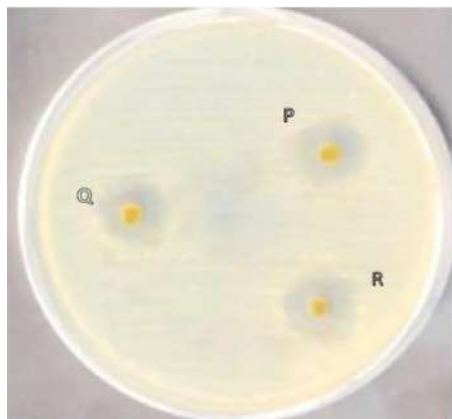


Fig. 10. 8p to 8r.

Structure of all new molecules was ascertained by Proton NMR, carbon NMR and LC-MS. Total synthetic scheme of pyrazole hydrazides mentioned below (Scheme1)

3.2. Antimicrobial screening

The antimicrobial screening of the prepared molecules was tested by disk diffusion method against different strains. From the result it was found that almost all the prepared molecules were shows varying degrees of inhibition against tested microorganisms.

Weigh approximately 29.77-gram SCDA medium HIMEDIA catalogue number (GMH011) mix it properly till dissolve completely after dissolution rest of the purified water. Sterilize the Media, allow to cool till 40 °C to 45 °C then pour each plates 15 to 20 mL allow to solidify. The microbial cultures were spread over sterile plates and Incubated at 30–35 °C for twenty-four hours then synthesized molecules are applied and incubate 30–35 °C 24 to 48 h and read the result. Cefotaxime (0.05 mg) and ampicillin (0.05 mg) were also impregnated on to the disc, air dried and used as positive control the plate was incubated at the suitable temperature (37 °C for bacteria and 25 °C for fungi) and the growth inhibition was measured. The obtained results of anti-microbial activities were tabulated in the Table 1.

Biological activities of synthesized molecule from 8a to 8r were shown inhibition against tested microorganism using staphylococcus aureus and Escherichia coli. The pictures are presented in Figs. 1–10.

4. Conclusion

Almost all the synthesized molecules of pyrazole benzamides shown antimicrobial activities.

CRedit authorship contribution statement

Gunasekar S.: Conceptualization, Data curation, Formal analysis, Investigation, Methodology, Project administration, Resources, Validation, Writing - original draft, Writing - review & editing. **Saamathi M.:** Data curation. **Aruna S.:** Formal analysis, Project administration, Software handling.

Declaration of Competing Interest

The authors declare that they have no known competing financial interests or personal relationships that could have appeared to influence the work reported in this paper.

Acknowledgments

We are grateful to Vellore institute of technology for IR, ¹H NMR, ¹³C NMR and mass spectroscopy studies. Also thankful to the department of molecular diagnostic, Bhat biotech India private limited.

Further Reading

- [1] D. Kumar, Vikramjeet Judge, Rakesh Narang, Sonia Sangwan, Erik De Clercq, Jan Balzarini, Balasubramanian Narasimhan, Eur. J. Med. Chem. 45 (2010) 2806–2816.
- [2] V. Kumar, A. Kumar, Shalabh Sharma, Netra Pal Singh, Ind. J. Chem. 50B (2011) 1496–1503.
- [3] K. Bajaj, V.K. Srivatsava, I. Ahsok Kumar, Ind. J. Chem. 42 (2003) 1149–1155.
- [4] M. Mittelbach, Monatsh. Chem. 116 (1985) 689–692.
- [5] B.E. Love, J. Ren, Org. Prep. Proced. Int. 31 (1999) 399–405.
- [6] V. Koteswara Rao, S. Subbha reddy, B. Sathesh Krishna, Green Chem. Lett. Rev. 3 (2010) 217–223.
- [7] Swayansiddha Tripathy, Viswajanani J. Sattigeri, S.K. Sahu, Int. J. Chem. Pharmaceut. Rev. Res. 1 (2015) 6–9.
- [8] Manisha R. Bhosle, Dayanand Kawale, D. Khillare, Amarsinh R. Dehmukh, Chem. Biol. Interface 7 (2017) 245–254.
- [9] J.C. Sheehan, P.A. Cruickshank, G.L. Boshart, J. Org. Chem. 26 (1961) 2525.
- [10] Shiori, Tet. Lett. 37 (1996) 2261.
- [11] C.A.G.N. Montalbetti, V. Falque, Tetrahedron 61 (2005) 10827–10852.
- [12] Paul J. Erdman, Jimmy L. Gosse, Jamey A. Jacobson, David E. Lewis, Synth. Commun. 34 (2004) 1163–1171.
- [13] S. Tumkevicius, V. Yakubkene, P. Vainilavicius, Chem. Heterocycl. Compd. 35 (1999) 1334–1336.
- [14] Ahmad Shaabani, Sayyed Emad Hoosahmand, Mol. Divers. 22 (2018) 207–224.
- [15] R.A. Carboni, D.D. Coffman, E.G. Howard, J. Am. Chem. Soc 80 (1958) 2838–2840.
- [16] M. Green, D.M. Throp, J. Chem. Soc. B. Phys. Org. (1967) 1067.
- [17] Maria E. Due-Hansen, Sunil K. Pandey, Elisabeth Christiansen, Rikke Andersen, Steffen V.F. Hansen, Trond Ulvan, Org. Biomol. Chem. 14 (2016) 430–433.
- [18] Vimal Bhat, S.D. Samant, Suhas Pednekar, Lett. Organ. Chem. 14 (2017) 764–768.
- [19] Eric Valeur, Mark Bradle, Chem. Soc. Rev. 38 (2009) 606–631.
- [20] Moustafa A. Gouda, Maged A. Berghot, E. Ghada, Abd El-Ghani, El-Galil M. Abd Khalil, J. Heterocycl. Chem. 55 (2018) 1935–1941.

Chief Editor

Dr. M. Sadik Batcha

Advisory Editor

Dr. N. Chandra Segaran

Editorial Board

Dr. MAM. Rameez

Dr. Jeyaraman

Dr.A. Ekambaram

Dr. G. Stephen

Dr. S. Chitra

Dr. S.Senthamizh Pavai

Dr. A. Shunmughom Pillai

Dr. P. Jeyakrishnan

Dr. Seetha Lakshmi

Dr. S. Easwaran

Dr. Kumara Selva

Dr. Ganesan Ambedkar

Dr. Krishanan

Dr. Kumar

Dr. S. Kalpana

Dr. T. Vishnukumaran

Dr. M. N. Rajesh

Dr. Govindaraj

Dr. Uma Devi

Dr. Senthil Prakash

Dr. Pon. Kathiresan

Dr. S. Vignesh Ananth

Dr.M. Arunachalam

Dr. S. Bharathi Prakash

நவீனத் தமிழாய்வு

(பன்னாட்டுப் பன்முகத் தமிழ் ஆய்வு)

Journal of

Modern Thamizh Research

(A Quarterly International Multilateral Thamizh Journal)

Arts and Humanities (all), Language
Literature and Literary Theory, Tamil
UGC Care Listed (Group-I) Journal

சிறப்பிதழ் :
இணையவழிக் பன்னாட்டுக் கருத்தரங்கம்-2020
தமிழ்த்துறை
தொன்போஸ்கோ கல்லூரி,
ஏலகிரிமலை, தமிழ்நாடு. இந்தியா

காலந்தோறும் தமிழ் இலக்கியங்களின் வரலாறும் புதுமைச் சிந்தனைகளும்

சிறப்பிதழ் ஆசிரியர்கள்

Special Issue Editors

முனைவர் **அ. குமார்**
தமிழ்த்துறைத்தலைவர்
தொன்போஸ்கோ கல்லூரி, ஏலகிரிமலை

திருமதி. **வே. செல்வி**
தமிழ்த்துறைத்தலைவர்
ஆதா மாளிக் கலை மற்றும் அறிவியல் கல்லூரி,
முதுயாளைமயம்



Published by

RAJA PUBLICATIONS
10, (Upstair), Ibrahim Nagar, Khajamalai,
Tiruchirappalli - 620 023, Thamizh Nadu, India.
Mobile : +91-9600535241
website : rajapublications.com

11 பகுதி-1
Part -1

1. வே. செல்வி	பெண்ணிய இலக்கிய வரலாறும் புதுமைச் சிந்தனைகளும்	1-5
2. ஞா. சஜாதா	சங்க இலக்கிய வரலாறும் புதுமைச் சிந்தனைகளும்	6-9
3. பொ. இரவந்திரன்	மலைபடுகடாமில் ஜவ்வாது மலை பழங்குடிகளின் வேளாண்மைப் பொருட்கள்	10-13
4. அ. தேவி	வீதிநாடகத்தின் தோற்றமும் வளர்ச்சியும்	14-18
5. அ. அமுதா	கவிஞர் வைரமுத்து கவிதைகளில் நாட்டுப்புறப்பாடல்களின் தாக்கம்	19-26
6. எ.ஆன்	இரட்சணிய யாத்திரிகத்தில் அறக்கோட்பாடுகள்	27-31
7. சி.அருள் எம்மக்கேல் செல்வி	கவித்தொகையில் அறவுணர்வுச் சிந்தனைகள்	32-39
8. பெ. அருணகிரி	தமிழ் நாடக வரலாற்றில் நாட்டுப்புறக் கூறுகள்	40-46
9. அ. குமார்	தலித் இலக்கியத்தின் போக்கும் புதுமைச் சிந்தனைகளும்	47-52
10. ஏ. தன்ராஜ்	அண்ணாவின வரலாற்றுக் கவிதைகள் வலியுறுத்தும் புதுமை வாசிப்பு முறைகள்	53-58
11. ச. தேவி	அர்த்தசாத்திரம் - பதினெண்கீழ்க்கணக்கு அறநூல்கள் (ஆண், பெண் - ஒரு பொதுநிலை ஆய்வு)	59-62
12. சீனு. தண்டபாணி	பதிற்றுப்பத்தில் மகளிர் மட்டும்!	63-68
13. ஜா. ஜெயக்குமார்	குழந்தை இலக்கியத்திற்கு கவிமணியின் பங்களிப்பு	69-74
14. கோ. கவிதா	காலந்தோறும் தூது இலக்கியத்தின் வளர்ச்சியும் புதுமையும்	75-78
15. ஜா.லாலி ஏதேஸ்	சடங்குகள் - நம்பிக்கைகள்	79-83
16. நா. குமாரி & கு. நீத்தியா	சூர்யகாந்தனின் செம்மண் இலக்கியப் படைப்புகளும் விளிம்புநிலை மனிதர்களும்	84-91
17. க. சசிகலா	ஆசாரக்கோவை உணர்த்தும் மருத்துவச் சிந்தனையும் தற்கால நடைமுறையும்	92-96
18. ஜெ.கீதா	சமூகத்தில் பெண்ணியத்தைப் பற்றிய புதுமைச் சிந்தனைகள்	97-102
19. இர.கீதா	நற்றிணையில் வினை எச்சப்பொருள்	103-106
20. இரா.கோமதி	குறுந்தொகையும் உவமைகள் குறித்த புதுமைச்சிந்தனைகளும்	107-112
21. க. கோவிந்தராஜி	நவீன நாடகத்தின் வளர்ச்சி	113-116
22. ஜெயசி ரோஸ் மேரி.அ	தொல்காப்பிய உரை மரபில் பூங்கா செய்த புதுமை	117-121
23. இரா.கீதா & மா.ஜனகர்	அறுஇலக்கியத்தில் மருந்தியல் சிந்தனைகள்	122-125
24. ஜா.ஜாஸ்மின் ஜெபா & ஜா.லாலி ஏதேஸ்	பாடல் அமைப்புமுறையில் தொகையும் - பாட்டும்	126-129
25. ப. ஜீன்றோஸ்	ஈழத்து மக்களின் புலம்பெயர் வாழ்க்கை	130-132
26. தே. ஜீவிதா	சமூக கட்டமைப்பில் அம்பை	133-136
27. மா. ஜெயக்குமார்	திருவாசகத்தில் மும்மலங்கள்	137-140
28. க. ஜெயலட்சுமி	தமிழ் நாவலின் தோற்றமும் வளர்ச்சியும்	141-145
29. T.N. ஜெயந்தி & முனைவர் கோ. சாந்தி	இரட்டைக் காப்பியங்கள் காட்டும் அரசியல்	146-151
30. ஜே.ஜி. ஜோனெஜெபமலர்	முன்றாம் பாலினஇலக்கிய வரலாறும் புதுமைச் சிந்தனைகளும்	152-158
31. காமராஜ் .ச	தமிழ் மலையாள வடமொழிகளில் பிரமாண்ட புராணம் ஓர் ஆய்வு	159-164
32. பெ.கண்ணதாசன்	ஒப்பாரிப் பாடல்களில் பெண் உளவியல் சிக்கல்கள்	165-169
34. சா.கருணாகரன்	சங்கத் தமிழர்களின் அறம் குறித்த வலியுறுத்தல்கள்	170-175
35. ச. கவிதா	பாரதியாரின் படைப்புகளில் புதுமைச் சிந்தனைகள்	176-178
36. செ.கிளறா டெல்பின் ஜடா & நா. ரா. ஷிபஜா	திருநங்கை என்றொரு பாலினம்	179-183
37. நா. கிருஷ்ணராஜ்	பாரதி கண்ட அக்கினிக் குஞ்சு	184-187
38. ப. கோடித்துரை	விவேக சிந்தாமணியில் புதுமைச்சிந்தனைகள்	188-191
39. கிஸ்னவேணி விவானந்தராசா	கூத்து எழுத்துப் பிரதிகளின் வளர்ச்சிப்போக்கும் அவற்றின் பாதுகாப்பு	192-198
40. பி. பாலசுப்பிரமணியன்	சங்க இலக்கியத்தில் மகட்போக்கியத் தாய்க்கூற்றுப் பாடல்கள்: கட்டமைப்பும் ஆய்வுத் தேவையும்	199-204
41. த.லதா	நாலடியாரில் அறம் பற்றிய சிந்தனைகள்	205-209
42. க.லதா & கோ. சாந்தி	முல்லைப்பாட்டில் பழந்தமிழர் வாழ்வியல் கூறுகள்	210-214
43. ஏ.மா.கவிதா	சங்க இலக்கியத்தில் பெண்கள்	215-218
44. MANISH KUMAR	PATRIARCHY AND WOMEN'S SUBORDINATION IN THE HISTORY OF CLASSICAL TAMIL AND SANSKRIT LITERATURE: A SELECT STUDY	219-224
45. ரா. மேரி ஜான்சி & ஏ. ராணி	குமரி மாவட்ட கடற்கரையின் இயற்கை அரண்களான மணற்குன்றுகள் சிதைவினால் ஏற்படும் பாதிப்புகள்	225-227
46. வை. கோகனாம்பாள்	வெ. இறையன்புலின் படைப்பாளுமை	228-231
47. வெ.முரளிதரன்	திருமுறைகள் கூறும் சைவ சமயக் கோட்பாடுகள்	232-236
48. ரா. நாகேந்திரன்	வரலாற்று நோக்கில் வெட்சித்திணை ஓர் ஆய்வு	237-243
49. பி. அனிதா	தமிழ் இலக்கியங்களில் கல்வி வரலாறும் புதுமையும்	244-248
50. பேரா.மு. பத்மநாபன்	குமரகுருபரர் இலக்கியங்களில் அறம்	249-252
51. ரெ.பத்மாவதி	குட்டிரேவதியின் 'முலைகள்' கவிதையில் பெண் உணர்வு	253-256
52. சா.பவித்ரா & நா.குமாரி	சிறார் கதைகளில் விழியன் கையாளும் உத்திகள்	257-260
53. பீ. பெரியசாமி	சங்க இலக்கியத்தில் மருதநில மக்களின் உணவுகள்	261-268
54. ம.சத்தியபாமா	மதுரை கலம்பகத்தில் மெய்ப்பாடுகள்	269-272
55. A.Pirashanth	நாடக எழுத்துருக்கள் ஊடாக மேற்கிளம்பும் நாடக மொழியும் அதன் பரிணாமங்களும்	273-279
56. வ.புங்கொடி	திருமந்திரத்தில் பல்துறை சிந்தனைகள்	280-284
57. அ.பிரசில்லா	நிலம் பூத்து மலர்ந்த நாள் நாவலில் அறமும் மறமும்	285-289
58. இல. பூர்ணிமா ஜோதி	சமையலறைக் கலயங்கள் நாவலில் பெண்ணியச் சிந்தனைகள்	290-294
59. கி. ப்ரியா மகேசுவரி	அண்ணாவின நாடகங்களில் புதுமைச் சிந்தனைகள்	295-300

ஒப்பாரிப் பாடல்களில் பெண் உளவியல் சிக்கல்கள்

பெ.கண்ணதாசன்

பகுதி நேர முனைவர் பட்ட ஆய்வாளர்
அரசு ஆடவர் கலைக் கல்லூரி, கிருட்டிணகிரி

ஆய்வுச் சுருக்கம்

ஒப்பாரிப்பாடல்களில் பெண் உளவியல் சிக்கல்கள் என்னும் பொருண்மையில் அமைந்த இவ்வாய்வுக் கட்டுரை, தொல்காப்பியம், சங்க இலக்கியங்கள், அற இலக்கியங்கள் ஆகியவற்றின் வழியில் நின்று, குழந்தைப்பேறு இல்லாத பெண்களின் உளவியல் சிக்கல்கள், விதவைப்பெண்ணின் உளவியல் சிக்கல்கள், வரதட்சணைக் கொடுமையால் பாதிக்கப்பட்ட பெண்களின் உளவியல் சிக்கல்கள் ஆகிய உட்தலைப்புகளில் ஆராயப்பட உள்ளது.

முன்னுரை

எதார்த்த வாழ்விற்கு இலக்கணம் கூறும் நாட்டுப்புற இலக்கியங்களை மிகைப்படுத்துதல் இல்லாத உள்ளத்தின் வெளிப்பாடு. சிந்தனைகளற்ற உணர்ச்சியின் உந்துதல், இலக்கண விதிமுறைகளற்ற இயல்பான வாழ்வியல் கருவூலம் எனப் பலவாறு சொல்லிச்செல்லலாம். அதிலும், குறிப்பாக நாட்டுப்புற பாடல்கள் வாழ்வியல் அனுபவம் பெற்ற அனைவருள்ளும் சிந்தனை முயற்சியின்றிச் சிறப்பாய் பிறக்கும் தன்மை கொண்டவைகள். வாழ்வியல் பற்றிய நுண்ணிய அறிவும், பரந்துபட்ட அனுபவமும் பெற்ற மூத்தோர்களுக்கு மனித மனத்தை ஆழமாக ஆராய்ந்து தெளியும் பக்குவம் உண்டு. இன்று பல்வேறு துறைகள் பற்றிய சிந்தனைகளை மனித மனம் ஆட்கொண்டுள்ளது. அன்று மனிதனிடம் மேலோங்கியது மனிதனைப் பற்றிய சிந்தனை மட்டும் தான். மனிதனைப் பற்றிய சிந்தனையே பல்வேறு துறைகளுக்கு வழிவகுத்தது.

மனிதனைப் பற்றிய சிந்தனை மனித மனத்தினை அறியும் வேட்கை கொண்டது. அவ்வாறு தான் அறிந்த மனத்தினை பிறருக்கு அறிவிக்கும் நோக்காக பழந்தமிழின மூத்தோர்கள் பாடிய பாடல்களே நாட்டுப்புற பாடல்களாகும். மனித மனத்தினை அறியும் அறிவை உளவியல் அறிவு எனக் கோட்பாட்டாளர்கள் கூறியுள்ளனர். நாட்டுப்புற பிறலக்கியங்கள், சங்க இலக்கியங்கள் என அனைத்து வகைப்பட்ட இலக்கியங்களிலும் உளவியல் சிந்தனைகள் மிகுந்திருந்தாலும், ஒப்பாரிப்பாடல்கள் உணர்த்தும் உளவியல் சிந்தனைகளில், வாழ்வியல் சிக்கல்கள் மிகுந்திருக்கின்ற தன்மையால் அவற்றை ஆராய்வதை இக்கட்டுரை நோக்கமாகக் கொண்டுள்ளது.

பெண் மையமான உளவியல் சிக்கல்கள் நாட்டுப்புறப்பாடல்களில் மிகுந்து காணப்படுகின்றன. “பல்வேறு சமூகக் காரணங்களால் வெளியிடத் தயங்கி, ஒடுக்கப்பட்ட அல்லது நசுக்கப்பட்ட ஆசைகள், தீக்க முடியாத முரண்கள், கலங்கடித்த இறந்தகால நினைவுகள் முதலியவை எல்லாம் சேர்ந்துதான் இந்த நனவிலி மனத்தை உருவாக்குகின்றன”¹ என்கின்ற .:பிராய்டின் கூற்றிற்கு ஏற்றாற்போல், பல்வேறு வாழ்வியல் சிக்கல்களைப் பெண்களைப் பெண்ணுலகம் ஏற்றிருப்பதை ஒப்பாரிப்பாடல்கள் வழி நாம் அறியலாம். எனவேதான், தொல்காப்பி இலக்கணமும், சங்க இலக்கியங்கள் முதலான இலக்கியங்களும் உளவியல் சிந்தனை மிக்கதாகப் படைக்கப்பட்டுள்ளன.

உள்ளத்தின் உணர்வுகள் உடலின்வழி உணர்ச்சிகளாக வெளிப்படும் போக்கை,

“நகையே அழகை இளிவரல் மருட்கை
அச்சம் பெருமிதம் வெகுளி உவகையென்று
அப்பால் எட்டாம் மெய்ப்பாடு என்ப.”²
(தொல்.பொருள்.247)

எட்டுவகையான மெய்ப்பாடுகள் எனத்
தொல்காப்பியர் குறிப்பிடுவது உளவியல்
போக்கிற்குரிய பதிவாகவும்,

“அற்றைத் திங்கள் அவ்வெண் நிலவில்
எந்தையும் உடையேம் எம்குன்றும்
பிறர்கொளார்
இற்றைத் திங்கள் இவ்வெண் நிலவில்
வென்றெறி முரசின் வேந்தர்எம்
குன்றும் கொண்டார்யாம் எந்தையு மிலமே.”³
(புறம்-112)

ஆண்களைச் சார்ந்தே தன் வாழ்வியல்
தேவைகளைப் பெரும்பான்மையாக
அமைத்துக்கொண்ட சமூக அமைப்பிற்கு
உட்பட்டவர்கள் பெண்ணினத்தார்.
இவ்வாழ்க்கைக்கு முந்தைய காலத்தில்
தந்தையைச் சார்ந்தும், இவ்வாழ்க்கையில்
இணைந்த பின்னர் கணவனைச் சார்ந்தும், முதிர்ந்த
பருவத்தில் பெற்றெடுத்த ஆண் பிள்ளைகளைச்
சார்ந்தும் வாழ்ந்து வருபவர்கள் பெண்கள் என்ற
போக்கு சமூகத்தில் நின்று நிலைத்திருந்த காலம்
சங்ககாலம். அத்தகையசூழலில் தந்தையைச்
சார்ந்து வாழ்ந்து வாழ்ந்துவந்த பெண்களுக்கு
தந்தையின் இழப்பு மனத்துயரை
மிகுதிப்படுத்தியுள்ளது. மேலும், தந்தையிடம்
இருந்த சொத்துப் பகைவரால்
அபகரித்துக்கொள்ளப்பட்டு, தமது வாழ்வாரத்தை
முழுமையாக இழந்துவிட்ட பெண்களின்,
வாழ்வதற்கு வழியற்ற, ஆதரவிற்கு துணையற்ற
நிலையினை எடுத்துரைக்கும் இப்பாடல், உளவியல்
சிக்கல்களுக்குரிய பதிவாகவும் விளங்குவதை
அறியலாம். ஒப்பாரிப்பாடல்கள் வெளிப்படுத்தும்
இவ்வாறான பெண் உளவியல் சிக்கல்களைக்
கீழே காண்போம்.

குழந்தைப் பேறு இல்லாத பெண்ணின்
உளவியல் சிக்கல்கள்.

பெருவதற்கரிய செல்வங்களில்
தலையாய செல்வமாகக் குழந்தைப் பேறு

போற்றப்படுகிறது. இவ்வாழ்க்கையில் இணைந்த
இருவரிடமும், உறவினர்களும், இந்த சமூகமும்
எதிர்நோக்கிக் காத்திருப்பது குழந்தைப்
பேற்றையேயாகும். இந்த குழந்தைப்பேற்றின்
வழியே அவர்களுடைய சமூக மதிப்பின்
தீர்மானிக்கப்படுகிறது. குழந்தைப்பேறுடைய
தம்பதிகளை உயர்த்தியும், குழந்தைச்செல்வமற்ற
தம்பதிகளைத் தாழ்த்தியும் மதிப்பிடுகின்ற வழக்கம்
இருக்கின்ற காரணத்தினாலே தான் சங்க
இலக்கியங்கள் குழந்தைச் செல்வத்தின்
இன்றியமையாமையை வலியுறுத்துகின்றன
சான்றாக,

“படைப்புப்பல படைத்துப் பலரோடு
உண்ணும்
உடைபெருஞ்செல்வர் ஆயினும்
மயக்குறு மக்களை இல்லோர்க்குப்
பயக்குறை இல்லை- தாம் வாழும் நாளே.”⁴
(புறம் - 188)

எல்லா வளங்களையும் உடையவராய் பலரோடு
இருந்து உண்ணும் மிகப் பெரும் செல்வர்
ஆனாலும், சிறிய சிறிய அடிகளை எடுத்துவைத்து
சின்ன கைகளை நீட்டி கலத்தில் இட்டும் தொட்டும்
கவ்வியும் பிசைந்தும், நெய்விட்ட உணவை
உடம்பில் சிதறியும் பார்ப்போர்க்கு இனிமையாக
மயக்கம் தருகின்ற குழந்தைகளை
இல்லாதவர்களுக்குத் தமது வாழ்நாள்
பயனுடையதாக இருக்காது என்று கூறுவதன் வழி
ஒருவருடைய பிறவிப்பயன் அவர் பெறுகின்ற
குழந்தைச்செல்வத்தின் வழியே பூர்த்தியடைகின்றது
என்பதை அறியலாம்.

குழந்தையைப் பெற்றெடுப்பதற்கும், பெற
இயலாததற்கும் ஆண் பெண் ஆகிய இருவருடைய
உடல் அமைப்புகளும் காரணமாகும் என்பது
உருத்துவ உண்மையாகும். ஆயினும், “பெண்ணை
மருத்துவ உண்மையாகும். ஆயினும்,” பெண்ணை
வீட்டு வேலைக்குரியவளாகவும், அந்த வேலைக்குச்
சம்பளம் ஏதும் பெறாதவளாகவும், ஆண்களை
வெளிவேலைக்கு உரியவர்களாகவும், சம்பாதித்து
வீட்டையும் மனைவியையும் காப்பாற்றுபவர்களாகவும்
வேலைப்பிரிவினை என்கிற உத்தி மூலம் ஆணாதிக்க
சாதிக்க முடிந்தது,⁵ என்ற கூற்றிற்கேற்ப, ஆண்
குடும்பத்திற்குத் தேவையான பொருளாதாரத்தை

நவீனத் தமிழாய்வு (பன்னாட்டுப் பன்முகத் தமிழ் களாண்டு ஆய்விதழ்) அக்டோபர் 31-நவம்பர் 01, 2020 - சிறப்பிதழ் (ISSN 2321-984X)
Modern Tamizh Research (A Quarterly International Multilateral Tamizh Journal) October 31, November 01, 2020 - Special Issue (ISSN : 2321-984X)

காந்தோறும் தமிழ் இலக்கியங்களின் வரலாறும் புதுமைச் சிந்தனைகளும், இணையவழித் பன்னாட்டுக் கருத்தரங்கம்-2020

தமிழ்த்துறை, தொன்போஸ்கோ கல்லூரி, ஏலகிரிமலை, தமிழ்நாடு, இந்தியா

சுட்டித்தருவதாலேயே அவனுடைய குறைகளைச் சமூகம் பொறுத்துக்கொண்டும், அவனுடைய குறைக்கும் சேர்த்து பெண்ணே பொறுப்பேற்க வேண்டிய சூழலும் இச்சமூகக் கட்டமைப்பால் உருவாகியுள்ளது. மொத்தத்தில் ஆண்களின் பணி பொருளாதார உற்பத்தி சார்ந்தும், பெண்களின் பணி மனித மறு உற்பத்தி சார்ந்தும் கட்டமைக்கப்பட்டுள்ள நிலையில், குழந்தைச்செல்வம் இல்லாத ஒரு பெண் சமூகம் தனக்கு வழங்கிய மனவலியை புறந்தள்ளி, குழந்தைப்பேறு இல்லாமலுக்கு தனக்குக் கணவான அமைந்த ஆண்தான் காரணம் என்பதை முதலில் பதிவு செய்கிறாள். அடுத்து தனக்கு குழந்தைச் செல்வத்தை தர இயலாத ஒருவனுக்குத் தன்னை மணம்முடித்துக் கொடுத்தன் மூலம் பெற்றோர்கள் செய்த தவறைச் சுட்டிக்காட்டுகிறாள்.

கணவனின் குறையும், பெற்றோர்கள் செய்த தவறும் நிலைத்திருக்க, அதனை மறைத்து தன் மீது பழிசமத்தும் இச்சமூகத்தைக் கண்டு மனவேதனை கொள்ளும் ஒரு பெண்ணின் புலம்பல்,

“பத்து மலைக்கப்பால பாலர் வயக்காடு
பத்துக்குறி செங்காடு
பாலே மயக்கத்திலே பன்னீரும்
போதையிலே
என்னப் பெத்த அம்மா - என்ன
பாத்து விதை ஊணிருந்தா
நான் பக்கப் படந்திருப்பேன்
படர்ந்தோடிக் காச்சிருப்பேன்
நீ வச்சப் பாங்கிருந்து வாழ்ந்திருப்பேன்.....
நீங்க பாலே மயக்குத்திலே பன்னீரும்
போதையிலே
பாத்து விதை ஊணாமா.....
அம்மா நான் பக்கப் படரலம்மா
படர்ந்தோடிக் காய்கலம்மா-இந்த நாட்டிலே
நான் பாங்கிருந்து வாழலம்மா....”6

என்ற பாடலின் வழி வெளிப்படுவதைக் காணலாம். விதவைப் பெண்ணின் உளவியல் சிக்கல்கள் அழகிய ஆடையும், அணிகலன்களும் சேர்ந்த வெளித்தோற்றம் ஒருவருக்கு

நேர்மறையான சிந்தனைகளை மனதிற்குள் தோற்றுவிக்கும் என்பது உளவியல் உண்மை. அதன் அடிப்படையில் பெண்கள் தங்களை அழகிய ஆடைகளாலும், அணிகலன்களாலும் அழகுபடுத்திக் கொள்கின்ற வழக்கத்தைக் கொண்டிருக்கின்றனர். குடும்பத்தை நன்முறையில் நடத்தவும், பெற்றெடுத்த குழந்தைகளை நல்வழிகாட்டி வளர்க்கவும், சமூகச் செயல்பாட்டில் தன்னை இணைத்துக் கொள்ளவும், பொது இடங்களுக்கு இயல்பாகச் சென்று வரவும் ஒருவருக்கு வெளித்தோற்றம் விரும்புகின்ற வகையில் அமைதல் வேண்டும். இல்லைபெனில் அவர்களுக்குள் தாழ்வு மனப்பான்மையும், எதிர்மறைச் சிந்தனைகளும் வளர்வதற்கு வாய்ப்பை ஏற்படுத்திவிடும். இதுவே, பின்னாளில் அவர்களுக்கு உளவியல் சார்ந்த சிக்கல்களை உருவாக்கி வாழ்வியலை சிதைத்துவிடும். எனவேதான் சங்ககாலம் தொட்டு பெண்கள் ஒப்பனை செய்துகொள்வதை உயர்வாகப் போற்றினர்.

பெண்களுக்குரிய உரிமைகள் மறுக்கப்பட்ட நீதி நூல்கள் காலத்திலும் இல்லற வாழ்வு தலைக்கப் பெண்கள்தாம் காரணம் என்று கருத்தப்பட்டது. ஆவதும் பெண்ணால் அழிவதும் பெண்ணால் என்ற கொள்கை தமிழகத்தில் நீண்ட காலமாக உண்டு. அன்பும், அறிவும், நற்பண்பும் திறமையும் உடைய பெண்களால்தான் குடும்பங்கள் சிறப்படையும் என்பதை,

“மாண்ட மனையாளை இல்லாதான்
இல்லகம்
காண்டற்கு அரியதுஓர் காடு”7 (நாலடி-361)

மனையாள் இல்லாதவன் வீடு சுகுகாட்டிற்கு ஈடானது என்பதை விளக்கும் மேற்கண்ட பாடலின் வழி குடும்பத்தை வழிநடத்துவதற்குப் பெண்களின் இன்றியமையாமையை உணரமுடிகிறது. அப்படிப்பட்ட பெண்கள் கணவனை இழக்கும்போது அவளுடைய ஆடைகள் மாற்றப்பட்டு, அணிகலன்கள் நீக்கப்பட்டு, சுப நிகழ்ச்சிகளில் ஒதுக்கி ஓரங்கட்டப்பட்டு, சமூகத்தில் விலக்கி வைக்கும்போது

அவள் அளவும் மனவேதனையை உளவியல் சிக்கல்களாக வ்யாசிப் பாடல்கள் பதிவு செய்கிறது

“இன்னைக்கி வளவிக் கார செட்டிமகன்
வளவி வளவினு வருவான் தெருவீதி
என்னப் பெத்த தாயாரு இருந்திட்டா
வளவிக்கட செட்டிமகன்
இன்னைக்கி வளவி வளவினு
என்னோட வளவுக்கே வாங்கலெங்கும்
நான் பெத்த பொன்னு மகளுக்கு
வண்ண கைக்கேத்த வளவிகளே
சொல்லும்போம்
அம்மா இன்னைக்கி வளவி அறுக்கும்
கையாள்
நாங்கள் வளவி எடுக்கலம்மா
நீ பெத்த செல்லமக வயசல அறுத்தேனே
இன்னைக்கு வளவிபோட்டா
தோசமின்னான்...”

கணவனை இழந்த பெண்கள் பூ, பொட்டு, வளையல், தாலி முதலிய அணிகலன்களை இழக்க வேண்டும் என்பதை இப்பாடல் மூலம் அறிகிறோம்.

வரதட்சணைக் கொடுமையும் - உளவியல் சிக்கல்களும்

ஒன்றானும் இரண்டானும் ஆவும் ஆனேறும் வாங்கிக் கொண்டு கன்னியை அலங்கரித்துத் தீ முன்னர்க் கொடுத்தல், தலைவிக்குப் பொன்பூட்டிச் சுற்றத்தார்க்கும் வேண்டுவன கொடுத்துக் கொள்வது ஆகிய ஆரிடம் அகரம் என்கின்ற வடவர்களுக்குரிய மணத்தில் பகமாடு அல்லது காளைமாட்டினையும், பொன் முதலிய பொருட்களையும் பெண்ணின் பொற்றோர்களுக்குக் கொடுத்துவிட்டு, மாட்டிற்கும் பொருளுக்கும் ஈடாகப் பெண்ணைப் பெற்றுக்கொள்கின்ற வழக்கம் வடநாட்டு திருமண முறைகளில் பின்பற்றப்படுவதை அகப்பொருள் விளக்கம் தெளிவாக எடுத்துரைக்கிறது.

இம் முறையிலான திருமணங்கள் பெண்களை ஓர் உயிராக மதிப்பிடுவதைத்

தவிர்த்து, ஒரு பொருளாக மதிப்பிட்டு வடிவத்தை எடுத்துரைக்கின்றது. பெண் என்பவள் ஆண்கள் பயன்பாட்டுப் பொருள் என்கின்ற அளவிற்கு ஆணின் கட்டளையை ஏற்றுச் செயல்படக்கூடியவள் என்ற அடிப்படையிலும் மதிப்பிடப்படுகிறாள். இது ஆணாதிக்கத்தின் உச்ச நிலையினையும் பெண்ணடிமைத் தனத்தின் நீட்சியையும் வெளிப்படுத்துகின்றது. இருக்கு, யகர், சாபம், அதர்வணம் ஆகிய நான்கு வேதங்களுடைய இதனையே கற்பித்துத் தருகின்றன.

வடவர் மணங்கள் இவ்வாறு இருக்க தமிழர்களின் திருமண முறைகளில் பெண் வீட்டாரிடமிருந்து வரதட்சணை பெற்றுக்கொண்டு திருமணம் செய்து கொள்ளும் வழக்கம் இன்றும் நின்று நிலவுகின்றது. குடும்ப பொருளாதார மந்தநிலை காரணமாக வரதட்சணை கொடுக்க முடியாத சூழலில், அப்பெண் என்றும் திருமணம் நடைபெறாமல் முதிர்கன்னியாக வாழவேண்டும் திருணம் முடித்தபின்னர் வரதட்சணை கேட்டு பெண்ணைக் கொடுமைப்படுத்துவது, பெண்வீட்டாரை அச்சுறுத்துவது, கொலைசெய்வது போன்ற கொடிய செயல்களுக்கு ஆண்வர்க்கம் துணைபோகின்ற சமூக எதிர்வினைகளை, கண்களால் கண்டும், ஊடகங்களின் வழி அறிந்தும், இலக்கியங்கள் எடுத்தியம்பியும் அறிந்துள்ளோம்.

அன்பு, கருணை, இறக்கம், உதவும் மனப்பான்மை, மனித உயிர்களின் மீதான மதிப்பு, எதார்த்த வாழ்க்கைமுறை, விட்டுக்கொடுக்கும் மனோபாவம், சகிப்புத்தன்மை, பொறாமையற்ற உள்ளம் ஆகிய நற்பண்புகளுக்கு உரியவர்களாகிய நாட்டுப்புற மக்கள் வாழ்ந்த வாழ்ந்த அந்தக்காலத்திலும் வரதட்சணைக் கொடுமைகள் இருந்ததை,

“இன்னைக்கி ஆத்துக்கு அந்தப்புறம்
என்னப் பெத்த சீமானே
இன்னைக்கி ஆத்தோரம் செம்பருத்தி
அலரோ வெடுச்சிருந்தா
நான் வளத்த கண்ணாமகளுக்கு
கைநிறைய கொடுத்திருந்தா

நான் அல்லி சொடுங்கமாட்டேன்
அரளிப்பூ வாடமாட்டேன்....
நான் வளத்த பொன்னாளுக்குக்
கைநிறையக் கொடுக்காம
நான் அல்லி சொருங்குரேய்யா
அரளிப்பூ வாடுரேய்யா....”

என்னும் பாடல் விவசாயம் பொய்த்துப் போனதால் தன் மகளுக்குக் கொடுக்க வேண்டிய வரதட்சணையைக் கொடுக்கமுடியாத குழல் ஏற்பட்டதையும், அதனால் கணவன் வீட்டாரின் கொடுமைக்குத் தன் மகள் ஆளாததையும் எண்ணி தாய் பாடுவதாக இப்பாடல் அமைந்துள்ளது. மலைகள், நீர், வனங்கள், காடுகள், வயல்கள் முதலியன அழிக்கப்படாமல் செழிப்புற்றிருந்த நாட்டுப்புற வழக்காற்றுக் காலத்திலேயே விவசாயம் பொய்த்துப் போய் மக்கள் வறுமைத் துயருக்கு ஆளான வரலாறு ஒப்பாரிப் பாடல்களில் சொல்லப்பட்டிருப்பதை அறிகையில், இன்றைய விவசாய பெருங்குடி மக்களையும், அவர்களின் வறுமைத் துயரையும் எண்ணி வருந்தவேண்டிய நிலையில் சமூகம் உள்ளது.

மேலும், தாயை இழந்த முதிர்கண்ணியின் புலம்பல், கணவனை இழந்த பெண் பூவையும் பொட்டையும் இழத்தல், விதவைப் பெண்ணின்நிலை, பெற்றோரை இழந்து அண்ணியின் கொடுமைக்கு ஆளான பெண்கள், பெற்றெடுத்த பிள்ளைகளை, உடன்பிறந்த சகோதரர்களை, உற்றார் உறவினர்களை, ஆடுமாடுகளை இழந்தவர்கள் அடைந்த இன்னல்கள் என அனைத்தையும் உளவியல் பார்வையில் ஒப்பாரிப்பாடல்கள் எடுத்துரைத்த விதத்தை இக்கட்டுரையில் ஆய்ந்தறிந்தோம்.

தொகுப்புரை

ஒப்பாரிப்பாடல்களில் பெண் உளவியல் சிக்கல்கள் என்னும் பொருண்மையில் அமைந்த இவ்வாய்வுக் கட்டுரை, தொல்காப்பியம், சங்க இலக்கியங்கள், அற இலக்கியங்கள் ஆகியவற்றின் வழியில் நின்று, குழந்தைப்பேறு இல்லாத பெண்களின் உளவியல் சிக்கல்கள், விதவைப்பெண்ணின் உளவியல் சிக்கல்கள்,

வரதட்சணைக் கொடுமையால் பாதிக்கப்பட்ட பெண்ணின் உளவியல் சிக்கல்கள் ஆகிய உட்தலைப்புகளில் ஆராயப்பட்டுள்ளது.

அடிக்குறிப்புகள்

1. க. பஞ்சாங்கம், இலக்கியமும் திறனாய்வுக் கோட்பாடுகளும், ப.129, இரண்டாம் பதிப்பு. 2016, அன்னம் பதிப்பகம், மனை எண்.1, நிர்மலா நகர், தஞ்சாவூர் - 613 007
2. வ.த. இராமசுப்பிரமணியம் (உ.ஆ), தொல்காப்பியம் - பொருளதிகாரம் மூலமும் உரையும், நூ.எண்.247, முதற்பதிப்பு மார்ச்.2008, பூம்புகார் பதிப்பகம், 127, பிரகாசம் சாலை, சென்னை. 600 108
3. ச.வே. சுப்பிரமணியன் (உ.ஆ) சங்க இலக்கியம், எட்டுத்தொகை, மூலமும் தெளிவுரையும், தொகுதி.3, பா.எண்,112, முதற்பதிப்பு சூன்.21, 2010, மணிவாசகர் பதிப்பகம், 31, சிங்கர்தெரு, பாரிமுனை, சென்னை.800 108.
4. மேலது, பா.எண்.188
5. க. பஞ்சாங்கம், இலக்கியமும் திறனாய்வுக் கோட்பாடுகளும், ப.229, இரண்டாம் பதிப்பு. 2016, அன்னம் பதிப்பகம், மனை எண்.1, நிர்மலா நகர், தஞ்சாவூர் - 613 007
6. கள ஆய்வின் மூலம் தொகுக்கப்பட்டபாடல், பாடியவர் அ. இராசம்மாள், தேவர்மலை, கடவூர் வட்டம், கரூர் மாவட்டம்,
7. ஞா. மாணிக்கவாசகம் (உ.ஆ), நாலடியார், மூலமும் விளக்க உரையும், பா.எண்.361, முதற்பதிப்பு. மே.2009, உமா பதிப்பகம், 18.171, பவளக் காரத் தெரு, மண்ணடி, சென்னை.6009 001
8. கள ஆய்வின் மூலம் தொகுக்கப்பட்ட பாடல், பாடியவர் கல்யாணி, குமாரசுவாமி, வெள்ளியணை வட்டம், கரூர் மாவட்டம்.
9. கள ஆய்வின் மூலம் தொகுக்கப்பட்ட பாடல், பாடியவர் சரவணதேவி, வீரணம்பட்டி, கடவூர் வட்டம், கரூர் மாவட்டம்.

சிறப்பிதழ்
Special Issue

13-15 பங்குனி 2022
26th - 28th March 2021

ISSN : 2321 - 984X

நவீனத் தமிழாய்வு

(பன்னாட்டுப் பன்முகத் தமிழ் ஆய்விதழ்)

Journal of

Modern Thamizh Research

(A Quarterly International Multilateral Thamizh Journal)
Arts and Humanities (all), Language
Literature and Literary Theory, Tamil
UGC Care Listed (Group-I) Journal

சிறப்பிதழ் :
இணையவழிப் பன்னாட்டுக் கருத்தரங்கம் - 2021
தமிழ்த்துறை,
கேரளப் பல்கலைக்கழகம்
காரியவட்டம், திருவனந்தபுரம், கேரளா

பெண் தெய்வங்கள்

சிறப்பிதழ் ஆசிரியர்
Special Issue Editor

முனைவர் ஹெப்சி ரோஸ் மேரி. அ
தமிழ்த்துறைத் தலைவர்



Published by

RAJA PUBLICATIONS
10, (Upstair), Ibrahim Nagar, Khajamalai,
Tiruchirappalli - 620 023, Thamizh Nadu, India.
Mobile : +91-9600535241
website : rajapublications.com

17 பகுதி-1
Part -1

Chief Editor

Dr. M. Sadik Batcha

Advisory Editor

Dr. N. Chandra Segaran

Editorial Board

Dr. MAM. Rameez

Dr. Jeyaraman

Dr. A. Ekambaram

Dr. G. Stephen

Dr. S. Chitra

Dr. S. Senthamizh Pavai

Dr. A. Shunmughom Pillai

Dr. P. Jeyakrishnan

Dr. Seetha Lakshmi

Dr. S. Easwaran

Dr. Kumara Selva

Dr. Ganesan Ambedkar

Dr. Krishanan

Dr. Kumar

Dr. S. Kalpana

Dr. T. Vishnukumaran

Dr. M. N. Rajesh

Dr. Govindaraj

Dr. Uma Devi

Dr. Senthil Prakash

Dr. Pon. Kathiresan

Dr. S. Vignesh Ananth

Dr. M. Arunachalam

Dr. S. Bharathi Prakash

மற்றொன்று:

செம்மொழித் தமிழ்

(பன்னாட்டுப் பன்முகத் தமிழ் காலாண்டு ஆய்விதழ்)

ஜனவரி - மார்ச்

ஏப்ரல் - ஜூன்

ஜூலை - செப்டம்பர்

அக்டோபர் - டிசம்பர்

Journal of

Classical Thamizh

(A Quarterly International Multi lateral Thamizh Journal)

January - March

April - June

July - September

October - December

ISSN:2321-0737

1. அ. ஹெப்சி ரோஸ் மேரி	நாட்டார் பெண்தெய்வ வழிபாட்டில் தோற்றக்கதைக்கூறுகள்	1-7
2. த. விஜயலட்சுமி	கேரளத்தில் கண்ணகி வழிபாடு	8-13
3. அ. பிரசில்லா	புலம் பெயர்ந்தோர் வழிபாடும் சாதியக் கட்டமைப்பும்	14-21
4. லீமா மெட்டில்லா. அ	நாட்டார் நிகழ்த்து கலைகளில் பெண் தெய்வங்கள் (பாலக்காடு மாவட்டம், கேரளம்)	22-28
5. முத்துலெட்சுமி. ச	நாட்டுப்புற தெய்வ வழிப்பாட்டில் செந்திட்டை தேவி	29-33
6. அ. ஏஞ்சல் ராணி	கத்தோலிக்கத் திருச்சபையும் மரியாளும்	34-40
7. த. அஜி	தமிழ்ச் சமூக மரபில் மணிமேகலா தெய்வம்	41-46
8. தி. அல்பா கிரேஸ்	நாட்டுப்புற பெண் தெய்வம் மண்டைக்காடு பகவதி அம்மன்	47-50
9. இ. அல்போன்சாள்	வீரமாமுனிவரின் படைப்புகளில் மரியன்னை	51-56
10. க. அமரேசன்	மக்கள் மரபில் பிடாரி அம்மன் வழிபாடு	57-61
11. தே. அம்சவள்ளி	ஆற்றுப்படையில் பெண் தெய்வங்கள்	62-65
12. மு. அமுதா	பெண் தெய்வங்கள் காட்டும் பக்திநெறி	66-70
13. ற. ஆனந்த மல்லிகா	மாசற்ற மாசாணியம்மன்	71-75
14. க. ஆனந்தராஜன்	பெண்தெய்வ வழிபாட்டில் மதுரை இராக்காயி அம்மன் பெறுமிடம்	76-82
15. செ. ஆனந்தி	தீ பாய்ந்த அம்மன்	83-87
16. க. அன்பழகன்	அம்மன் தோற்றமும் வரலாறும்	88-93
17. செ. அன்பு	"நல்லதங்காள்" என்னும் வாழும் தெய்வம்	94-97
18. கே. எஸ். அன்புகலா	நாவல்களில் பெண்தெய்வச் சித்தரிப்புகள்	98-102
19. யா. ஆரோக்கிய நாயகம்மாள்	கிறித்தவச் சிற்றிலக்கியங்களில் மரியாள்	103-107
20. ப. அருணாதேவி	இலக்கியங்களில் மீவியலாற்றலான அணங்கு வழிபாடு	108-114
21. ஜா. அருள் கனிலா	கிறித்தவர்களின் தாய் அன்னை மரியாள்	115-121
22. இரா. அருள்மொழி	பெண் தெய்வ வழிபாடு	122-126
23. து. அருண்பாண்டியன்	காட்டேரி சிறுதெய்வ வழிபாடும் இறை தத்துவமும்	127-131
24. வே. அருட்பாமணி	சகலமும் நல்கும் ஸம்பக்கர்தேவி அல்லது அரசு காத்த அம்மன் (வழிபாட்டு மரபுகள்)	132-134
25. நீ. பகவதியம்மாள்	வலிகளின் பின்னணியில் வாழ்ந்து சிலையான கருவறைத் தெய்வங்கள்	135-141
26. பி. பாலச்சந்திரன்	சக்தி வடிவத்தின் தத்துவக் கோட்பாடுகள்	142-147
27. அ. பெனிலா ஜாய்	கண்ணகி வழிபாட்டு தொன்மை	148-153
28. பாரதி ராஜா. வே	ஜெயமோகனின் காமரூபினி கதையில் யட்சிகளும், இசக்கிகளும்	154-160
29. மு. பிருந்தாவனம்	தமிழ் இலக்கியங்களில் தாய்த்தெய்வ வழிபாடு	161-165
30. சீ செஞ்சுலட்சுமி	செல்லியம்மன் வழிபாட்டு மரபுகள்	166-171
31. மு. சென்னப்பன்	தமிழரின் களவொழுக்கத்தில் வெறியாட்டு	172-175
32. அ. டெய்சி	நாட்டார் இலக்கியங்களில் பெண் தெய்வமும் வழிபாடும்	176-180
33. க. தேவி	நாட்டார் வழிமரபில் சுயம்புவாகத் தோன்றிய பெண் தெய்வங்கள்	181-185
34. வி. தேவி	சரபேந்திரர் பூபாலக் குறவஞ்சியில் - பெண் தெய்வங்கள்	186-189
35. ந. தனசேகர்	கொல்லிப்பாவை	190-194
36. அ. திவ்யா	பெண் தெய்வ தோற்றக் கதைகள் - பேச்சிப்பாறை பேச்சியம்மன்	195-200
37. கோ. சாந்தமூர்த்தி	தமிழ் இலக்கியங்களில் பெண் தெய்வ வழிபாடு	201-205
38. க.நீ. இளங்கோவன்	செல்லாண்டியம்மன், மதுரகாளியம்மன் வரலாறும் வழிபாடும்	206-210
39. சு. பாத்திமா	தமிழ் - மலையாளப் புதினங்களில் பெண் தெய்வ வழிபாடுகள்	211-217
40. ச. காயத்ரி	திரௌபதியம்மன் பெண் தெய்வ தோற்ற மரபுகள்	218-222
41. ச. கீதா	பெண் தெய்வங்களில் காத்தாயி அம்மன் வழிபாடு	223-228
42. கீதா இராமலிங்கம்	இசக்கியம்மன் வழிபாடு	229-235
43. க. கிரிவாசன்	மதுரகாளியம்மன் வழிபாட்டில் மரபும் புதுமையும்	236-240
44. மா. கோமதி	சித்தர் இலக்கியங்களில் பெண் தெய்வங்கள்	241-245
45. சு. கோமதி அழகு	எண்ணெய்க்காரச்சி அம்மன் வரலாறும் வழிபாடும்	246-252
46. ச. குருஞானாம்பிகா	இருக்கன்குடி மாரியம்மன் ஆலய வழிபாட்டு முறைகள்	253-261
47. செ. லீ. ஹெலன்	தத்துவ நோக்கில் பெண் தெய்வ வழிபாடு	262-266
48. பீ. இலக்கியா	முப்பந்தல் இசக்கியம்மன் தோற்றக் கதையும் தற்போதைய நிலையும்	267-273
49. வி. இளமதி கனகசுந்தரம்	பெண் தெய்வ வழிபாடு மலர்ந்து வந்த பாதை	274-281
50. கு. ஜெயந்தி	அகநூல்களில் முல்லைத்திணையில் பெண்கள்	282-285
51. வெ. ஜெயந்தி & என். விஜயலட்சுமி	இறையருள் நாட்டிய பெண் தெய்வங்கள்	286-290
52. ஜென்ஸிஸ் குமார். மி.	தாய்த்தெய்வ வழிபாட்டில் வளமைசார் கருத்தாக்கங்கள்	291-295
53. ஜென்சி வை.கி	நாட்டார் பெண் தெய்வங்களில் இசக்கியம்மன் வழிபாடு	296-303
54. தா. ஜெயலக்ஷ்மி	சு. தமிழ்ச்செல்வியின் நாவல்களில் பெண் தெய்வ வழிபாட்டு முறைகள்	304-308
55. ஜெ.சா. ஜிஜி கிறிஸ்டோபெல்	நாட்டுப்புற வழிபாட்டில் சப்த கன்னிமார்கள் குறித்தான வழிபாடு	309-314
56. லூ. ஜோன் சில்வியா பிரேமா	பெண் தெய்வ வழிபாட்டு முறைகளும் மரபுகளும்	315-319
57. அ. ஜோதிரவிந்திரன்	பாரதியார் கவிதைகளில் பெண்தெய்வ வழிபாடு	320-324
58. அ. கலைச்செல்வி	கதைப் பாடல்கள் காட்டும் கொலையில் உதித்தப் பெண் தெய்வங்கள்	325-329
59. இரா. கலைச்செல்வி	அழியாப் பெண்ணினத்தின் மீட்சி (அழியா இலங்கை அம்மன்)	330-334
60. கல்பனா. ச & க. கலாவதி	மலசர் பழங்குடியின் மாகாளியம்மன் வழிபாடும் தாய்வழி பண்பாட்டியங்கியலும்	335-340

தமிழரின் களவொழுக்கத்தில் வெறியாட்டு

மு. சென்னப்பன்

முனைவர் பட்ட ஆய்வாளர் (முழுநேரம்), தமிழ்த்துறை,
அரசு கலைக்கல்லூரி, தருமபுரி - 636 705. தமிழ்நாடு, இந்தியா.

ஆய்வுச் சுருக்கம்

பழந்தமிழர் திருமணமாகாத கன்னிப் பெண்களை சூர், அணங்கு மற்றும் முருகப்பெருமானும் துன்புறுத்துவதாக நம்பினர். அதை மெய்பிக்கும்வகையில் பெண் ஒருத்தி களவொழுக்கத்தினால் அவளுடைய உடலில் சில மாற்றங்கள் உண்டாகின்றன. அதற்கான காரணத்தை அறியாமல் அப்பெண்ணின் தாயும் செவிலியும் இந்த நோய் முருகப்பெருமானால் வந்தது என்று எண்ணி முருகனுக்கு தொண்டு செய்யும் வேலனை அழைத்து வெறியாட்டு எடுத்து வழிபாட்டு சடங்குகளைச் செய்து இது தெய்வக் குற்றமெனக் கூறி அதற்கான பரிகாரங்களைச் சொல்லி அதைச் செய்துள்ளதையும், நற்றிணை, குறுந்தொகை, அகநானூறு, கலித்தொகை வெறியாடல் பொருள் பற்றியே ஐங்குறுநூற்றில் வெறிபத்து என ஒரு பத்து அமைந்துள்ளன. இவ்வகையில் சிலப் பாடல்களைக் கொண்டு சங்ககால மக்கள் வாழ்வில் வெறியாட்டு நிகழ்வுகளையும் அதற்கான காரணத்தையும் இக்கட்டுரையில் தெளிவாக ஆராயப்பட்டுள்ளன.

கலைச்சொற்கள்: முருகன், வேலன், பூசாரி, கட்டுவிச்சி, வெறியாட்டு, அணங்கு, செவிலி, நற்றாய், தோழி, தலைவி, களவு, காதல்

முகப்புரை

சங்க காலச் சமுதாயம் பெரிதும் இம்மை வாழ்வின் செம்மையிலும் இன்பத்திலும் நாட்டமுடையதாக இருந்தது. எனினும் மக்கள் தங்கள் வாழ்வும் வளமும் சிறக்கவும் தாங்கள் எண்ணிய வினைகள் இனிதே நிறைவேறவும், மனித சக்திக்கு அப்பாற்பட்ட மற்றொரு சக்தியான தெய்வ சக்தியைப் பண்டைய காலம்

முதல் இன்று வரை இந்த மானிடச் சமூகம் நம்பிக்கையோடு வழிபட்டு வருகின்றன. இந்த தெய்வ வழிபாடு என்பது இறைவனை மனதால் நினைத்து இரு கரங்களால் கூப்பித் தொழுதலே ஆகும். 'வழிபாடு' எனும் சொல் 'தொழுதல்' என்ற பொருளிலேயே பெரும்பாலும் வழங்கப்படுகின்றன.

சங்க கால மக்களின் கடவுள் வழிபாடு என்பது நிலத்தின் தன்மைக்கேற்ப வழிபாட்டு முறைகள் அமைகின்றன. முருகன் வழிபாடு அதன் தொன்மை தொல்காப்பியர் காலம் முதல் 'சேயோன் மேய மைவரை உலகமும்' என்ற தொடர் மூலம் அறிந்துகொள்வதோடு குறிஞ்சி நிலத்துக் கடவுளாகவும் விளங்குகின்றன. புறப்பொருள் நூல்கள் முருகனைப் போர் கடவுளாகக் குறிப்பிடுகின்றன. அகப்பொருள் நூல்கள் முருகனை காதற் கடவுளாகப் பேசப்படுகின்றன. தமிழரின் களவொழுக்கம் பற்றிப் பேசப்படும் இடங்களில் எல்லாம் வேறு கடவுளுக்கு இடமில்லை. முருகனே முதன்மை பெறுகின்றான். பண்டைத் தமிழ் மக்களின் அகவாழ்வு முருகனோடு பின்னிப்பிணைந்துள்ளதையும் வெறியாட்டு நிகழ்வுகளையும் பற்றி ஆராய் வதே இக்கட்டுரையின் நோக்கமாகும்.

மலைக் கடவுள்

சங்க இலக்கியங்கள் முருகனை மலைநிலக் கடவுளாகவே வருணிக்கப்பட்டுள்ளன.

“வான் கோட்டுக் கடவுள்”¹

“பிறங்கு மலை மீமிசைக் கடவுள்”²

இந்த வரிகள் மூலம் முருகன் குன்று, மலைகளில் வாழும் குறிஞ்சிநிலக் கடவுளாக இலக்கண இலக்கியங்கள் வழி உணரமுடிகின்றன.

முருகன் தலங்கள்

திருச்சீரலைவாய், திருவாவிநன் குடி திருப்பரங்குன்றம் ஆகிய மூன்று தலங்கள் பற்றி அகநானூற்றின் வாயிலாக,

“முருகன் நற்போர் நெடுவேள் ஆவி அறுகோட் டியானைப் பொதினி”³

“பல்பொறி மஞ்சை வெல்கோடி உயரிய ஓடியா விழவின் நெடியோன் குன்றம்”⁴

“திருமணி விளக்கின் அலைவாய் செருமுகு சேஎம்”⁵

என்பது அறியமுடிகின்றது.

போர் கடவுள்

குறிஞ்சிலக் கடவுளான முருகனை வீரத்தின் வடிவமாகவும், போர்க்கடவுளாகவும் மக்கள் வழிபடுகின்றனர் என்பதை,

“முருகன் நற்போர்”⁶

“செங்களம் படக்கொன்றவுணர் தேய்த்த”⁷

“போர்வெல் வல்லான்”⁸

இப்பாடல்களின் மூலம் உணரலாம். முருகனைப் பெண் தெய்வங்களோடு தொடர்புபடுத்தி பெரும்பாணாற்றுப்படையில் முருகனைப் ‘பேய் கூத்தாடும் துணங்கையெம் செல்வியின் குழவியெனக்’ கூறுகின்றது. நக்கீரர் திருமுருகாற்றுப்படையில் கொற்றவை சிறுவனாகவும், பழையோள் குழவியாகவும், மலைமகள் மகனாகவும் குறித்துள்ளார்.

வெறியாடல்

களவொழுக்கத்தில் தலைவியின் உடல் மற்றும் நடத்தையில் மாற்றம் ஏற்படுகின்றன. இதனைக் கண்ட செவிலி, நற்றாய் இதற்குக் காரணம் முருகனே என்று முதுபெண்டிர் சொல்படி வெறியாட்டை நிகழ்த்துகின்றனர். வெறியாட்டை நிகழ்த்துபவன் வேலன் என்னும் பூசாரி. வேலன் ஆடுகளம் அமைத்து ஆடுபலி கொடுத்து நெற்பொரி, தினை தூவி முருகனை வழிபட்டு ஆவேசமாக ஆடித் தலைவிக்கு வந்த

மாற்றத்திற்கு முருகன்தான் காரணம் என்று கூறுகின்றான்.

“களவு அலர் ஆயினும் காமம் மெய்ப்படுப்பினும் அளவுமிகத் தோன்றினும் தலைப்பெய்து காணினும்”⁹

என்கிற தொல்காப்பிய நூற்பாவின் மூலம் வெறியாட்டு நிகழ்ச்சியின் தன்மையை அறியமுடிகின்றது.

செவிலித்தாய், தலைவியின் தாய் தலைவியின் மாற்றத்தைக் கண்டு வேலனை அழைத்து வெறியாட்டு மற்றும் குறி சொல்பவளை அழைத்து மக்களின் நோய்க்கான காரணம் கேட்கிறாள். இத்தருணத்தில் தோழி குறிக்கிட்டு மலைத் தலைவனைப் பற்றி கூறுமாறும் கேட்கிறாள்.

“அகவன் மகளே அகவன் மகளே!

மனவுக்கோப் பன்ன நன்னெடுங் கூந்தல்”¹⁰

ஆக, தலைவன் தலைவியின் களவொழுக்கம் வெறியாடல் மூலம் தோழி வெளிப்படுத்துகின்றான்.

தலைவியின் களவு பலரால் அறியப்பட்டு அலர் ஏற்படுகின்றன. காமத்தினால் தலைவியின் உடலில் மாற்றம் நிகழ்கின்றன. இவை முருகனால் வந்தது என்று கட்டுவிச்சி மற்றும் வேலன் மூலமும் குறி பார்த்து வெறியாடல் நிகழ்த்துகின்றனர்.

“கறிவளர் சிலம்பின் கடவுட் பேணி அறியா வேலன்வெறியனெக் கூறும்”¹¹

“பொய்யா மரபின் ஊர்முது வேலன் கழங்குமெய்ப் படுத்துக் கன்னம்தூக்கி”¹²

“மென்தோள் நெகிழ்த்த செல்லல் வேலன் வென்றி நெடுவேள் என்னும் அன்னையும்”¹³

என்ற பாடல்கள் வழியே முருகனால் மகளிர் அணங்குப் பெற்றுள்ளதையும் அறியமுடிகின்றன.

களவொழுக்கத்தில் முருகனைப் பற்றி வரும் இடங்களில் எல்லாம் ‘வெறியாடல்’ என்னும் வழிபாட்டுமுறையே முதன்மை பெறுகின்றன. களவில் ஈடுபட்டிருந்த தலைவி தலைவனைச்

மு. சென்னப்பன்

சந்திக்க முடியாமையால் அவளது உடல் மெலிந்து வாடினாள். இதனை அறியாத தாய் வெறியாடல் என்னும் வழிபாடு செய்ய 'வேலன்' என்னும் முருகப் பூசாரியை வரவழைத்துவிட்டாள். வேலனும் கட்டும் கழங்கம் பார்த்து 'இந்நோய் முருகனால் வந்தது' எனக் கூறி வெறியாடலைத் தொடங்கினான். முருகா! தலைவிக்கு ஏற்பட்டுள்ள நோய் தலைவனால் வந்தது என்று நீ அறிந்திருப்பதால் வேலன் வேண்டினான் என்பதற்காக நீ வருதல் உன் பெருமைக்கு ஏற்றதல்ல. நீ கடவுள் ஆயினும் மடவை' என்று கடிந்துரைக்கின்றான். தோழி,

“கார் நறுங் கடம்பின் கண்ணிகுடி
வேலன் வேண்ட வெறிமனை வந்தோய்
கடவுள் ஆயினும் ஆக
மடவைமன்ற வாழிய முருகே”¹⁴

என்று தலைவியின் காதல் ஒழுக்கத்தை தெரிந்துக் கொள்ளாமல் அவளது தாய் வேலனைக் கொண்டு வெறியாட்டை நிகழ்த்துகின்றான். 'காதல் வாழ்வினை முருகனது விளையாட்டுகளுடன் இயைபுபடுத்துதல் முற்றிலும் ஒரு தமிழ் மரபு' என்கிற கருத்தும் உள்ளம் கொள்ளத்தக்கதாகும் (Dr. N. Subramanian, Sangam Policy, P.36).

வெறியாடல் நிகழ்ச்சி நடத்தப்பட்ட முறைமைக் குறித்து அகநானூறு 22,29-ஆம் பாடல்கள் கூறுகின்றன.

வெறியாடல் நடந்த முறை

வேலன் வெறியாட்டுக் களத்தை அமைத்து வேலுக்கு மாலை அணிவித்து ஆட்டுக்குட்டியைப் பலி கொடுத்துச் சிவந்த திணையை அதன் இரத்தத்துடன் சேர்த்துக் கலந்து தூவி ஒலி எழுப்பி நடு இரவில் முருகனை அழைக்கின்றான். அதன் பின் வெறியாடுகிறான். கழற்காயைத் தன் உடலில் அணிந்து படிமக்கலத்தைத் தூக்கிக் கொண்டு தலைவிக் க வந்திருப்பது முருகணங்கின் குறையே என்று வேலன் கட்டுவதாக.

“நெடுவேட் பேணத் தணிகுவள் இவள்
முதுவாய்ப் பெண்டிர் அதுவாய் கூற”¹⁵

இப்பாடல் மூலம் நாம் உணரமுடிகின்றது. வேலனைப் போன்று வெறியாடலைப் பெண்களும் நடத்தியுள்ளனர். பெண்டிர் தெய்வமுற்று வெறிகொண்டு ஆடியுள்ளதாக,

“வெறிகொள் பாவையிற் பொலிந்தஎன்
அணிதுறந்து
ஆடுமகள் போலப் பெயர்தல்”¹⁶

இப்பாடல் மூலம் உணரமுடிகின்றன.

வெறியாடலில் பெண்கள் நிலை

தலைவியின் காதலை அறியாதத் தாய் வெறியாட்டு நிகழ்த்துவதாகப் பல பாடல்கள் உள்ளன. வெறி, அணங்கு, நோய் என மாறுபட உணர்ந்த பெண்களாக இருந்துள்ளதை,

“அறியாமையின் வெறியென மயங்கி
அன்னையும் அருந்துயர் உழந்தஎன்”¹⁷

இப்பாடல் தாயின் அறியாமை உண்மையாகின்றன. ஐங்குறுநூறு 241:1-2, அகநானூறு 272:13-15. இப்பாடல்கள் தலைவியின் தாயின் அறியாமை பற்றிக் குறிப்பிடுகின்றது.

வெறியாட்டு நிகழ்ந்த நாளன்று இரவில் தலைவன் வந்ததால் தலைவியின் நோய் தீர்ந்ததாக,

“வெறியென உணர்ந்த வேலனோய் மருந்
தறியா னாகுதல் அன்னை காணிய”¹⁸

என்கிற இப்பாடல் உணர்த்துகிறது. ஆனால் வேலனின் வெறியாட்டலால் இந்நோய் தீர்ந்ததாக தலைவியின் தாய் எண்ணுகிறாள். இது தாயின் அறியாமைத் தனத்தைக் காட்டுவதாக அமைந்துள்ளன.

வேலன் வெறியாட்டு செயல்களைக் கண்டு தலைவி, தோழி போன்ற பெண்கள் எள்ளல் நகைப்பதாக உள்ளன.

“வேலன் வேண்ட வெறிமனை வந்தோய்
கடவுள் ஆயினும் ஆக”¹⁹

இதன் மூலம் கடவுளும் அறியாமை உடையவராக உள்ளனர். தலைவியின் காதலை தெரியாதவன் வேலன் என்று இகழப்பட்டதை அறியலாம்.

வெறியாடலில் தாயின் நிலை வேறாகவும், தலைவி, தோழி இவர்களது நிலை வேறாகவும் இருப்பதை அறியமுடிந்தது. ஆம்! தலைவியின் உடல் வேறுபாடு முருகனால் ஏற்பட்டது என்று தாய் எண்ணி வருந்துகின்றாள். ஆனால் தலைவிக்கும் தோழிக்கும் இந்த வேறுபாடு தலைவனால் ஏற்பட்டது என்பதனை வெறியாடல் பாடல்கள் மூலம் அறியமுடிந்தன.

தொகுப்புரை

முருகன் குன்று மலைகளில் வாழும் குறிஞ்சிநிலக் கடவுளாகும். வீரத்தின் வடிவமாகவும் போர்க் கடவுளாகவும் வழிபட்டுள்ளனர். களவொழுக்கத்தில் தலைவிக்கு ஏற்பட்டது காதல் நோய். ஆனால், அதை அறியாமல் தாய், செவிலி ஆகிய இருவரும் இந்த நோய் முருகனால் வந்தது என்று எண்ணி வேலனை அழைத்து வெறியாட்டு நிகழ்த்தியுள்ளனர். அதற்கான வழிபாட்டு சடங்குகளும் பரிகாரங்களும் செய்துள்ளனர். இதைக் கண்ட தலைவியும் தோழியும் இந்த நோய் தலைவன்பால் வந்தது. ஆனால், இவர்கள் செய்யும் நிகழ்வுகளைப் பார்த்து நகைக்கின்றனர். எனவே, இது தாயின் அறியாமையும், தலையின் மீது கொண்ட பற்றுப்பாசத்தையும் காட்டுவதோடு தெய்வக்குற்றம் ஏதாவது நிகழ்ந்துவிடுமோ என்ற அச்ச உணர்வினால் வெறியாட்டு நிகழ்த்தியதின் மூலம் இறை நம்பிக்கையும் உணரமுடிகின்றன.

முடிவுரை

தமிழகத்தில் முருக வழிபாடு என்பது தொன்றுதொட்டு உருவான குலவழிபாடே என்பதற்கு வேலன் வெறியாடலே இதற்குச் சான்றாகும். உயிர்பலியிடல் முருக வழிபாட்டில் இருந்துள்ளது. தலைவி களவு வாழ்க்கையில் இருக்கும்பொழுது இக்களவு தாய்க்கு தெரியாமல் இருந்துள்ளதையும் அறியமுடிகின்றன.

தலைவியின் உடல் வேறுபாடு முருகனால் வந்தது என்று எண்ணி அதைத் தீர்ப்பதற்கு முதுபெண்டிர்கள் வெறியாடல் நிகழ்த்தியதையும் அறிந்துகொள்ளமுடிந்தது. தலைவியின் தாய்க்கு தலைவியின் களவொழுக்கத்தை தோழி அறத்தொடு நின்று வெறியாட்டின் மூலம் தெளிவுப்படுத்தியதும் அறியமுடிந்தன. தெய்வ வழிபாடு என்பது மானிடச் சமூகம் உள்ள வரை பரிணமித்துக் கொண்டுதான் இருக்கும் என்பதுதான் நிதர்சனமான உண்மை.

அடிக்குறிப்புகள்

1. அகநானூறு, பா.348, வரி.7:8.
2. குறிஞ்சிப்பாட்டு, பா.208, வரி.9.
3. அகநானூறு, பா.1.
4. மேலது, பா.149.
5. மேலது, பா.266.
6. மேலது, பா.1:3.
7. குறுந்தொகை, பா.1, வரி.1.
8. கலித்தொகை முல்லை, பா.4, வரி.13-14.
9. தொல்காப்பியம் பொருள் களவு, 1061.
10. குறுந்தொகை, பா.23.
11. ஐங்குறுநூறு, பா.243, வரி.1-2.
12. மேலது, பா.245, வரி.1-3.
13. குறுந்தொகை, பா.111, வரி.1-3.
14. நற்றிணை, பா.14, வரி.34.
15. அகநானூறு, பா.22, வரி.6-10.
16. மேலது, பா.370, வரி.14-16.
17. ஐங்குறுநூறு, பா.242, வரி.1-2.
18. குறுந்தொகை, பா.360.
19. நற்றிணை, பா.34, வரி.9-010.

ஓ